Report to the Texas Coastal Coordination Council: CMP Cycle 14 Suplimental Funding Requests Final Report: Mapping and Coring of the modern Brazos River Delta

Dr. Timothy M. Dellapenna
Joseph Carlin
Department of Marine Sciences, Texas A&M University at Galveston

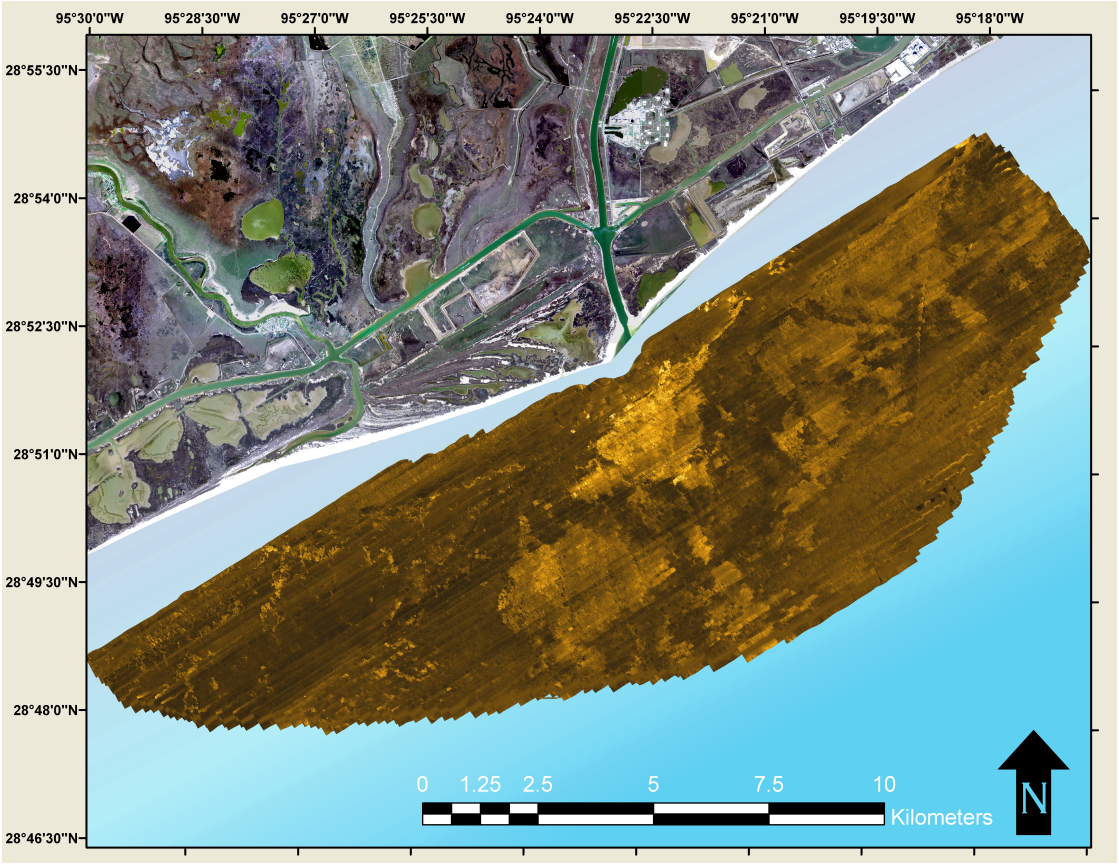

Coastal TEXAS 2020

Galveston

Department of Oceanography
Texas A&M University
College of Geosciences

TABLE OF CONTENTS

1.0 INTRODUCTION

River mouths are the most fundamental element of a deltaic system as they are the dispersal point for terrestrial sediments to the marine environment (Wright 1977). Globally, 10-20 billion metric tons of sediment are transported by rivers to the oceans each year (Milliman and Syvitski 1992). Once in the ocean, the sediment may undergo multiple phases of deposition and resuspension before ultimately finding an area in which it accumulates (Wright and Nittrouer 1995).

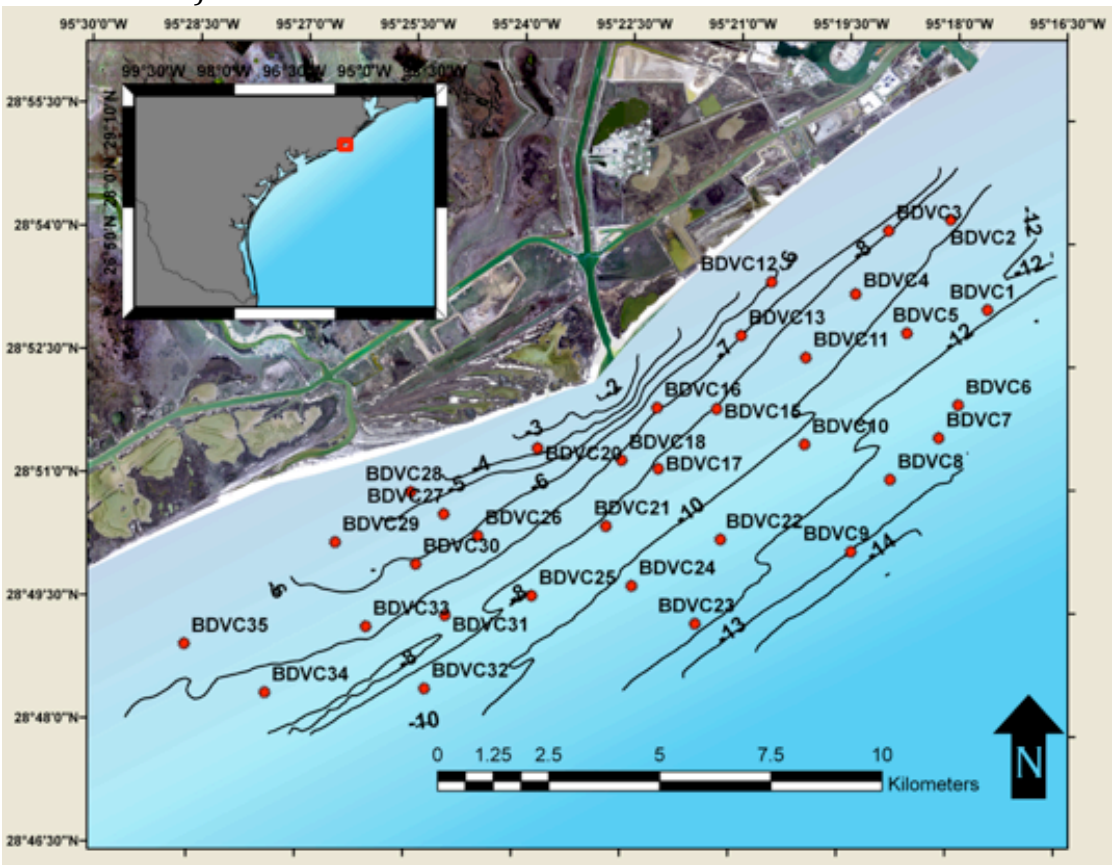

Figure 1: Study area with bathymetric data and core locations. Isobaths are in meters below mean low water.

This report highlights results from a study of the subaqueous delta of the Brazos River and adjacent shelf. The study, performed by the Coastal Geology Lab at Texas A&M University at Galveston, was conducted in 2011 and collected swath bathymetry, side scan sonar data, and sediment cores to investigate the surface and shallow subsurface geology of the study area. In addition, the study also was able to both quantitatively and qualitatively asses the potential sand resources of the Brazos River subaqueous delta.

2.0 BACKGROUND

2.1 Study Area

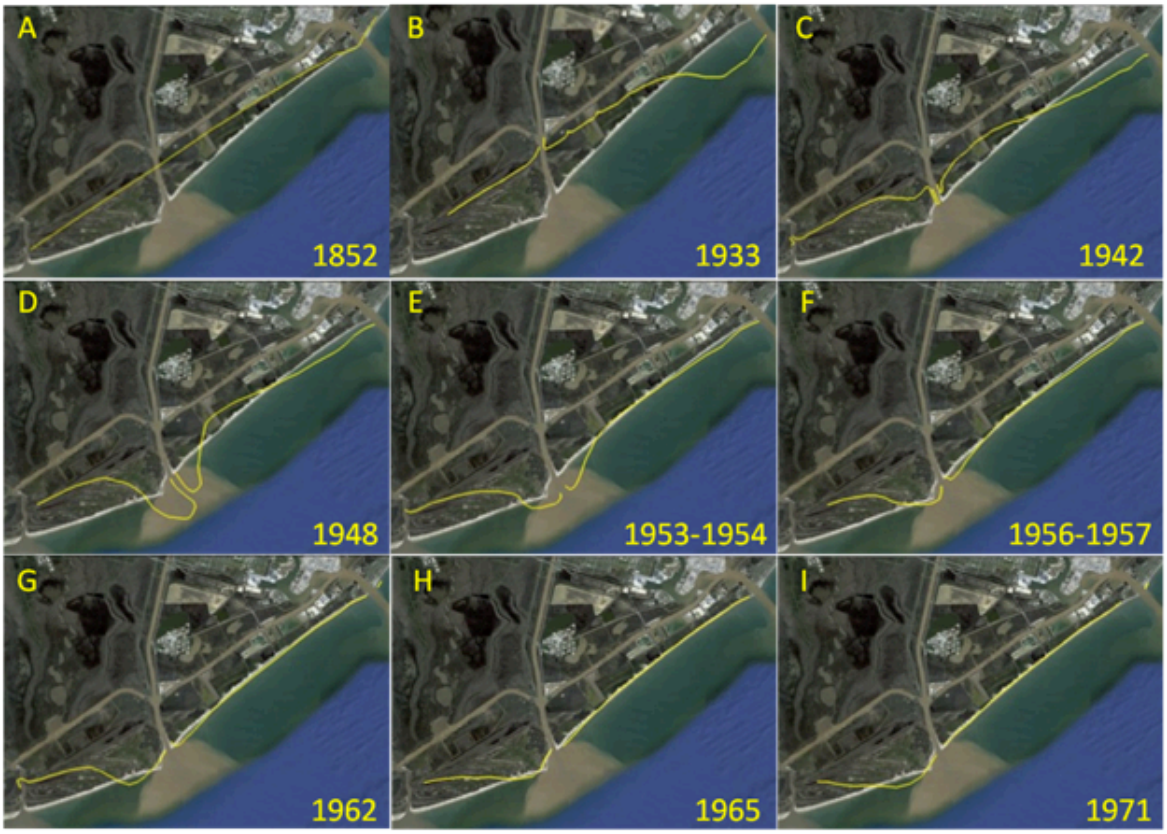

Figure 2: Historic shoreline position compared to 2009 satellite image. Modified from Seelig and Sorenson, 1973 and Google Earth. The 1852 shoreline (A) was prior to construction of the jetties at the old mouth.

The Brazos River is the 11th longest river in the United States with an 118,000 km^2 watershed encompassing areas in northeastern New Mexico and large portions of Texas. It has the highest rate of flow and sediment yield of all Texas rivers (Rodriguez et al. 2000). Estimates of the sediment load for the river range from ~ 10 - 16 Mt/yr with a sediment yield ranging from 88 to 140 t/km^2/yr (Milliman and Syvitski 1992; Syvitski and Saito 2007), where ~ 5 – 10% of this is considered bedload (Syvitski and Saito 2007). These sediments are characterized by their distinctive red color as they are derived from Triassic red beds (Rodriguez et al. 2000).

Within the drainage basin, annual rainfall averages ~ 100 – 125 cm, although large deviations can occur during floods and tropical-storm induced precipitation events which affect the delta area on an average of once every two years (Rodriguez et al. 2000). This is the only river on the Texas coast that consistently drains into the Gulf of Mexico where it forms a 35 km^2 delta of which approximately 70% is subaqueous (Figure 1). The delta is

located on a 130 km wide shelf with a 0.5 m tidal range and 1.1 m mean wave height. These waves generally trend northeast-southwest, approaching the shore in a northwest direction, resulting from predominately southeasterly winds (Rodriguez et al. 2000). As a result net longshore drift is from the east to the west (Seelig and Sorensen 1973). The direction of the longshore drift can fluctuate throughout the year as a function of wave direction, where waves from the southeast and from the south create a westward and eastward flowing longshore drift, respectively (Seelig and Sorensen 1973), and semipermanent surface currents in the northwestern Gulf of Mexico. Most of the year the coastal current in this part of the Gulf of Mexico flows counterclockwise (east to west) from the Mississippi River to the southern Texas coast. This nearshore current is primarily forced by wind stress. Beginning in May wind stress begins to change, causing the current to switch, flowing from South Texas towards the Mississippi River. This direction persists through the summer months, primarily July and August, and by September both the wind stress and currents have returned to a counterclockwise flow (Curray 1960; Nowlin Jr et al. 2005).

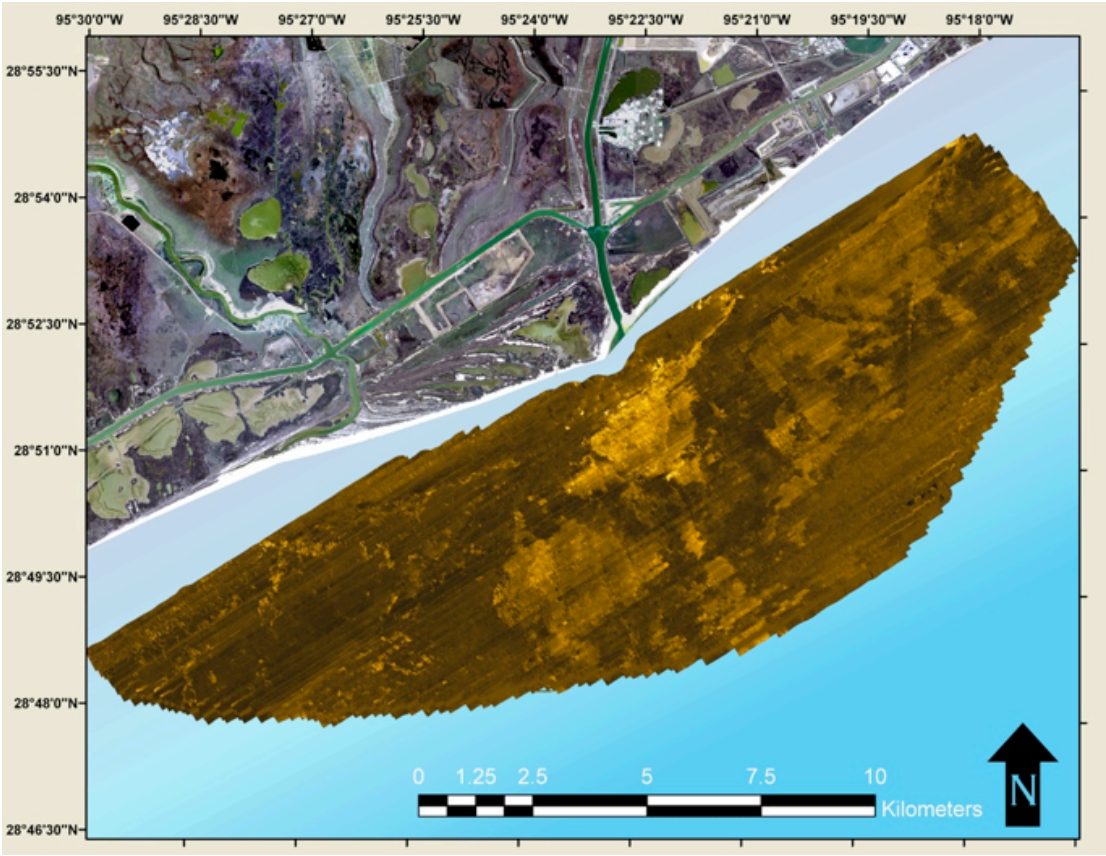

Figure 3: Side scan sonar mosaic, lighter areas correspond to high backscatter.

The prodelta extends from 6 – 15 m water depths, and coastal storm events can significantly affect the delta front environment (Rodriguez et al. 2000). Wave base for this part of the Texas coast is between 8 – 10 m (Siringan and Anderson 1993). Fluvial flood events can lead to progradation of the subaerial delta by creating mouth bars on the western side of the river mouth (Rodriguez et al. 2000), and when these flood events are

preceded by prolonged dry periods, the mouth bars are substantial enough to become welded to the shoreline as a beach ridge (Fraticelli 2006). The Brazos Delta has been described as an asymmetric wave-influenced delta (Bhattacharya and Giosan 2003), which are often found in micro-tidal areas, with a strong net longshore transport, an updrift sand source.

Figure 4: Side scan sonar mosaic with sediment core locations.

The subaerial morphology of the delta is dynamic and well documented. Prior to the diversion of the river mouth, the river entered the Gulf of Mexico through what today is the Freeport Channel. In the early 1820s the Mexican government opened the land adjacent to the river to Anglo-American settlers to establish the first colonies within the watershed, within a few years the entire east bank of the river was occupied by settlers extending over 200 km inland from the Gulf of Mexico (Long tshaonline.org). The U.S. National Ocean Survey conducted a survey of the area in 1852 (Figure 2A). From this survey the Old Brazos Delta (OBD) largely resembled the present day configuration of Modern Brazos Delta (MBD), with an arcuate shape and a slight asymmetry favoring the downdrift lobe. A mouth bar was present at the time of the survey. Jetties were constructed starting in 1881 and completed in 1899, which caused the OBD to prograde approximately 1.6 km seaward

and develop a strong asymmetry to the west (Figure 2B). This asymmetrical deposition resulted from the jetties interrupting the longshore currents, allowing for river derived sediment to rapidly accumulate downdrift of the jetties (Seelig and Sorensen 1973).

In 1929 the river was rerouted to its present location, and the MBD began forming immediately. While the MBD was prograding seaward, the OBD was retreating landward at approximately the same rate (Figure 2C). By 1948 the subaerial MBD had grown almost 2.5 km in less than 2 years reaching its most seaward position, the subaerial delta exhibited a cuspate shape, and at this time the river mouth was deflected 45° eastward as shown in Figure 2D. After 1948, the MBD began to retreat landward, and by 1953 the OBD had returned to its approximate position in 1852 (Figure 2E and F). Hurricane Carla in 1961 made landfall approximately 100 km from the MBD as a category 4 hurricane, and the second most intense hurricane to make landfall on the Texas coast, ninth most on the mainland US as of 2006 (Blake et al. 2007). The storm reworked sediment at the MBD, skewed the shape of the delta to west (Figures 2G-I), and initiated a westward migration of the delta (Seelig and Sorensen 1973). Only a slight asymmetry of the subaerial delta is evident today compared to past configurations in the 1940s and 1950s.

3.0 MATERIAL AND METHODS

3.1 Geophysical Surveys

3.1.1 Survey Design

The Brazos Delta Survey, conducted in February and March of 2011, extended from near the Freeport Jetties in the east to a few kilometers west of the mouth of the San Bernard River. All of the surveying was conducted aboard the NOAA FGBNMS R/V Manta in water depths from the 3 m to 10 m isobath based on NOAA nautical charts. Survey lines were plotted parallel to the shore using Hypack® 2009a Coastal Oceanographic software. Lines spacing was 100 meters giving 200% coverage for the side scan data and approximately 60% coverage for the bathymetry data. Survey data was collected in the WGS 1984 datum and projected into UTM Zone 15 North coordinates. The horizontal and vertical data are in meters. The bathymetric data was corrected to mean low water (MLW) using NOAA tide station 8772447 located at the US Coast Guard station in Freeport, TX located approximately 10 km from the Brazos Delta study area.

3.1.2 Data Collection

Side scan sonar (SSS), and bathymetric data were collected concurrently using a Teledyne Benthos® C3D-LPM High-Resolution Side-Scan Sonar Bathymetric System. This sonar utilizes two transducers operating at a frequency of 200 kHz coupled with a six hydrophone array receiver collect the SSS data, and bathymetric data is computed by the

sonar using the computed Angle of Arrival Transient Imaging (CAATI) algorithm. The sonar was pole-mounted to the bow of the vessel, position of the vessel was determined using a Hemisphere® Vector differential GPS and ship motion data was determined using a SG Brown TSS® DMS3-05 motion reference unit to correct the bathymetric data collected. Sub-bottom data was collected using an Edgetech® 216 Full Spectrum Sub-bottom CHIRP seismic sonar operating on frequencies between 2 and 16 kHz that was towed behind the vessel. Additional sub-bottom data was collected on June 6, 2011 using the R/V Cavalla. Periodic casts with an Odom® Sound Velocity Probe were conducted to collect sound velocity data throughout the water column to also correct bathymetric data. Sonar data was acquired using Hypack® Hysweep 2009a software.

3.1.3 Data Processing

Bathymetric data was processed using Hypack® Hysweep 2009a software, where tidal, ships motion, and sound velocity data were integrated to correct the raw bathymetric soundings. SSS data was processed using Chesapeake Sonar Wiz.Map® software to create and export SSS mosaics (Figure 3).

3.2 Sediment Data

3.2.1 Sediment Core Collection

Sediment cores were collected in September of 2011 aboard the NOAA FGBNMS R/V Manta, a total of 33 cores were collected (Figure 4). The cores were 7.62 cm (3 in) in diameter, and on average 1 m of sediment were recovered. These cores were collected using a pneumatic submersible vibra-core rig deployed off the stern of the vessel. Cores were stored upright and refrigerated until analyzed. Surface sediment grab samples were also collected.

3.2.2 Sediment Analysis

Cores were cut lengthwise, photographed, and visual descriptions of the sediment lithology were recorded. One-half of the core was archived for future reference and one-half processed for water content and grain size analyses. Water content sample data will be used for ancillary analyses. This data is not provided in this report. Cores were sub-sampled for every lithological unit as determined by visual analysis in sections ranging from 1 – 5 cm thick depending on the unit for the length of the core, and placed into labeled whirl-pak bags until analyzed.

Sediments samples were analyzed in the lab for grain size distributions using a Malvern Mastersizer 2000® laser particle diffractometer. Sediment samples were homogenized, and an approximately 3-5 g aliquot was placed in a 100 ml glass jar. Ten milliliters of a 5.5-g/L sodium hexametaphosphate solution was added to the jar as a dispersant. The

sediment with dispersant was sonicated for 30 min. at a temperature of approximately 25°C at a frequency of 40 kHz. After sonication, samples were wet-sieved through a 2 mm sieve into a 250 ml glass jar, and material larger than 2 mm was placed in a pre-weighed aluminum dish, dried for at least 24 hrs, and then weighed. The sample slurry in the 250 ml glass jar was filled with de-ionized water to a volume of exactly 200 ml then placed on a stir plate. While the slurry was stirring, a representative 10 ml aliquot was removed by a pipette and placed in a pre-weighed aluminum dish and dried for at least 24 hours then weighed. After the 10 ml aliquot was removed, the slurry was pipetted into the Malvern Mastersizer 2000® until a pre-determined level of obscuration was reached. At this point the instrument made three measurements and averaged the three results. The instrument determined percent composition of sand, silt and clay of the samples, and from the 10 ml aliquot that was removed and the material excluded during the wet-sieving process the percentage of material greater than 2 mm was calculated. In total the fraction of gravel, sand silt and clay were determined for each sample, as well as the mean grain size of the sand fraction.

4.0 RESULTS

4.1 Bathymetry

The bathymetry of the subaqueous delta shown in Figure 1, shows a distinct asymmetry updrift (east) and downdrift (west) of the river mouth. On the updrift side, isobaths trend parallel to the shoreline and this area exhibits a relatively steep slope for the study site of ~1:625 or on average 0.09°. West of the river mouth, water depths are less compared to the east, and only the 5 m isobath and below trend parallel to the shoreline. Water depths in this area of the subaqueous delta range from 2 m to 10 m below (MLW), with a slope of ~ 1:900 or on average ~0.07°. From Figure 5 the difference in bathymetry between the updrift and downdrift sides of the subaqueous delta is shown. A diversion between the bathymetry data collected and the nautical chart used to plan the survey is evident as the survey area was constrained by the 10 m isobath according to the chart, but soundings in excess of 14 m were collected. This shows that the area has undergone some changes since the publishing of the nautical charts.

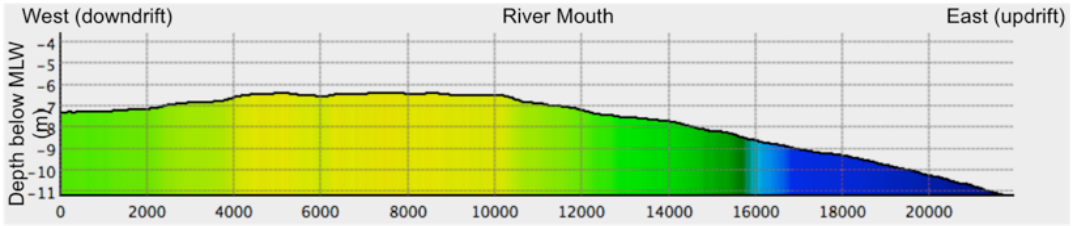

Figure 5: Bathymetric profile across the subaqueous delta from west to east showing the asymmetrical structure. Approximate location of the river mouth is labeled.

4.2 Side Scan Sonar

Results from the SSS showed a similar asymmetry as the bathymetry. The mosaic (Figure 3) shows two distinct lobes with unique backscatter characteristics; the Western Lobe (Figure 6A) dominated by low backscatter (darker colors) with small isolated areas of high backscatter (lighter colors), and the Eastern Lobe (Figure 6B) dominated by large clearly defined high backscatter features. The Western Lobe is much smaller and is a wedge extending from the river mouth in a southwesterly orientation. Most of the mosaic is dominated by the Eastern Lobe, which is primarily seaward and to the east of the river mouth. Two large distinct high backscatter features were observed in the center of the

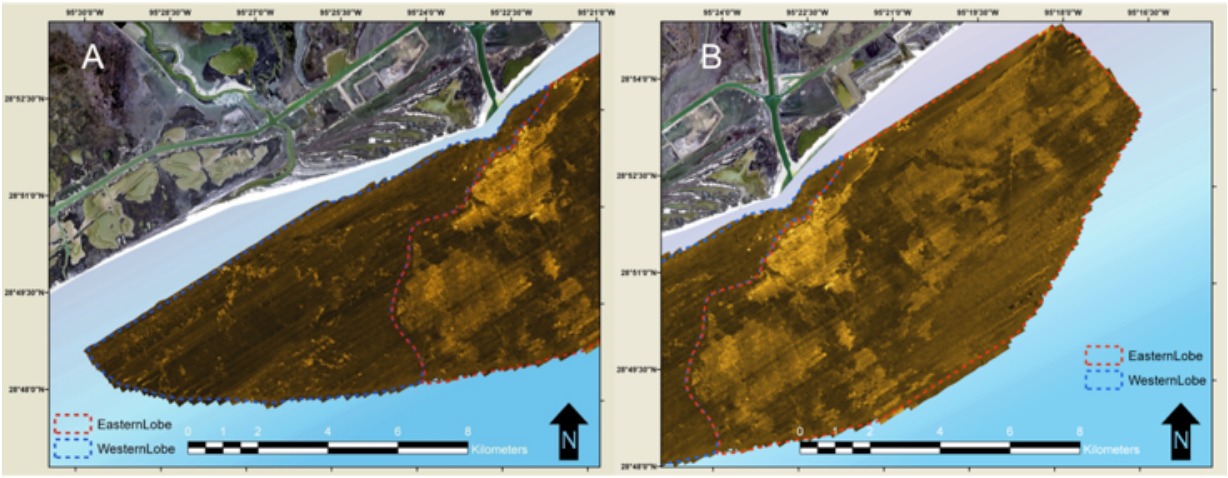

Figure 7: The two lobes of the sub aqueous delta as defined through the SSS data, Western Lobe (A) and Eastern Lobe (B).

survey area. The most dominant of these features (Feature A) is located directly seaward of the river mouth (Figure 7A), encompassing an area of approximately 5 km^2, while the other feature (Feature B) is located approximately 5 km due south (Figure 7B) with an area of ~10 km^2. The western boundary of these features distinguishes the transition between the high backscatter and low backscatter areas of the mosaic. Figure 8A shows the relationship between the features observed in the SSS mosaic and the bathymetric

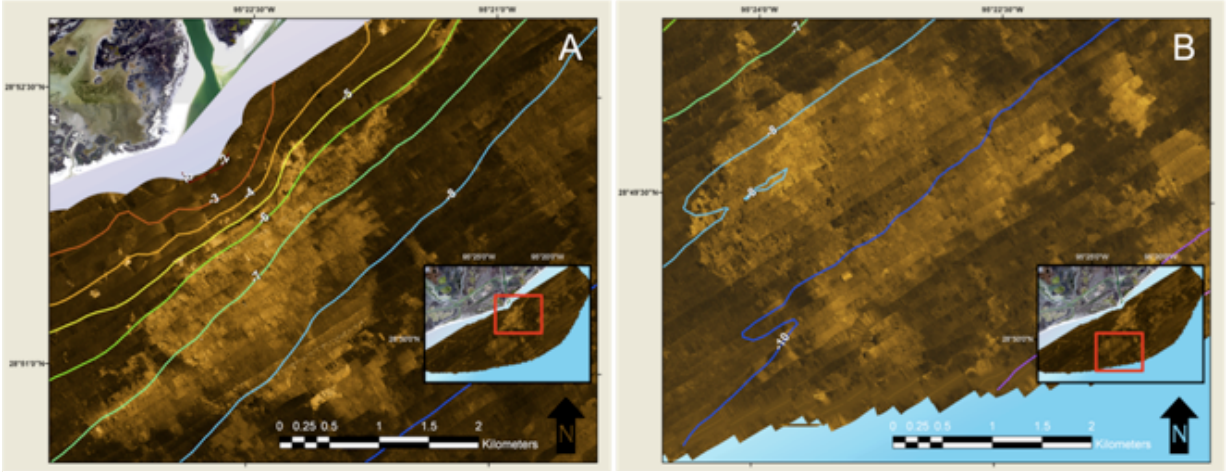

Figure 6: Zoomed image showing prominent high backscatter features from the side scan sonar mosaic, Feature A (left) and Feature B (right), with bathymetric contours.

contours. This figure shows that the high backscatter observed in the eastern section of the study area is confined between water depths between 7 and 12 m. Feature A is bounded by the 5 m isobath directly adjacent to the river mouth, and the 6 m isobath on earthier side (Figure 7). This feature extends to just landward of the 10 m isobath. Feature B is located landward of the 8 m isobath and extends seaward of the 10 m isobath.

4.3 CHIRP

Throughout most of the survey area two prominent sub-bottom intervals are evident (Figure 8). The lowermost, shown in blue, is thickest, and consists of a series of parallel reflectors, relatively tightly spaced, oriented mostly horizontal. The surface of this sequence is a strong reflector oriented subparallel to the seabed. We are interpreting this sequence as the relic clinoform, and sitting directly atop this reflector is the upper sequence in yellow, which we interpret as the modern clinoform, deposited after human interventions to the system. The hard surface reflector between the two clinoforms was the seabed surface not only prior to the time of the river diversion, but also colonization of the catchment and construction of the jetties at the old mouth in the 19th Century. This modern clinoform consists of a series of seaward dipping, parallel to subparallel reflectors. The reflectors in the modern clinoform, updrift of the river mouth, exhibit a greater dip angle than those observed downdrift of the river mouth, however the thickness of this modern clinoform is greater downdrift of the river mouth. In some areas the record of the modern clinoform is obscured by shallow biogenic gas in the sediments. The base of the sub-bottom record is the multiple shown as a solid red line, which obscures the data below.

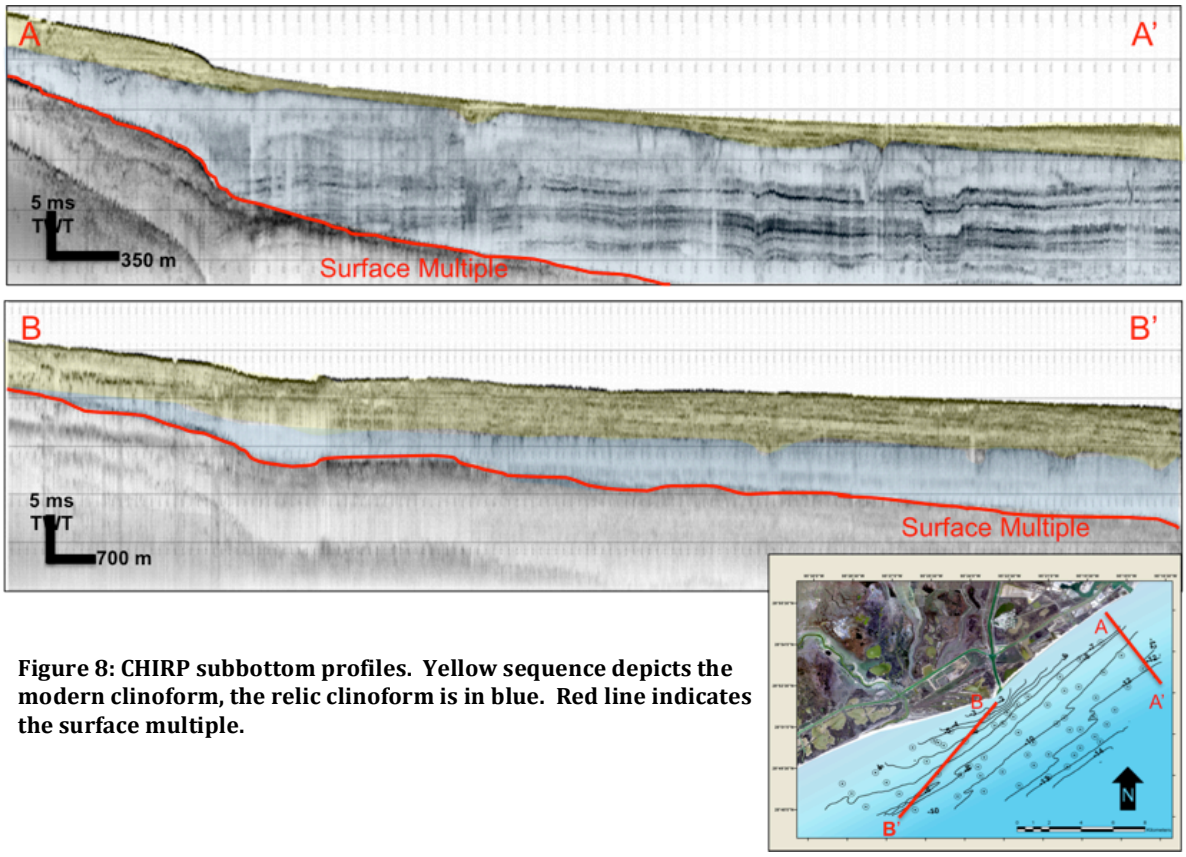

Figure 8: CHIRP subbottom profiles. Yellow sequence depicts the modern clinoform, the relic clinoform is in blue. Red line indicates the surface multiple.

4.4 Sediment Analysis

An example of sediment core results are seen in Figure 9, and a complete record of the results can be found in the appendix. In addition the size fractions that comprise the sediment of Brazos Sub Aqueous Delta, the sediments also can be characterized by unique coloration, which range from grey to red. These changes in color of the sediment layers has been studied previously by Rice et al. in prep, in which they observed the following sediment colors: grey, grey-brown, brown, red-brown and red. These colors were also observed within the cores collected for this project. This allows the sediment from this area to be analyzed for both size and color.

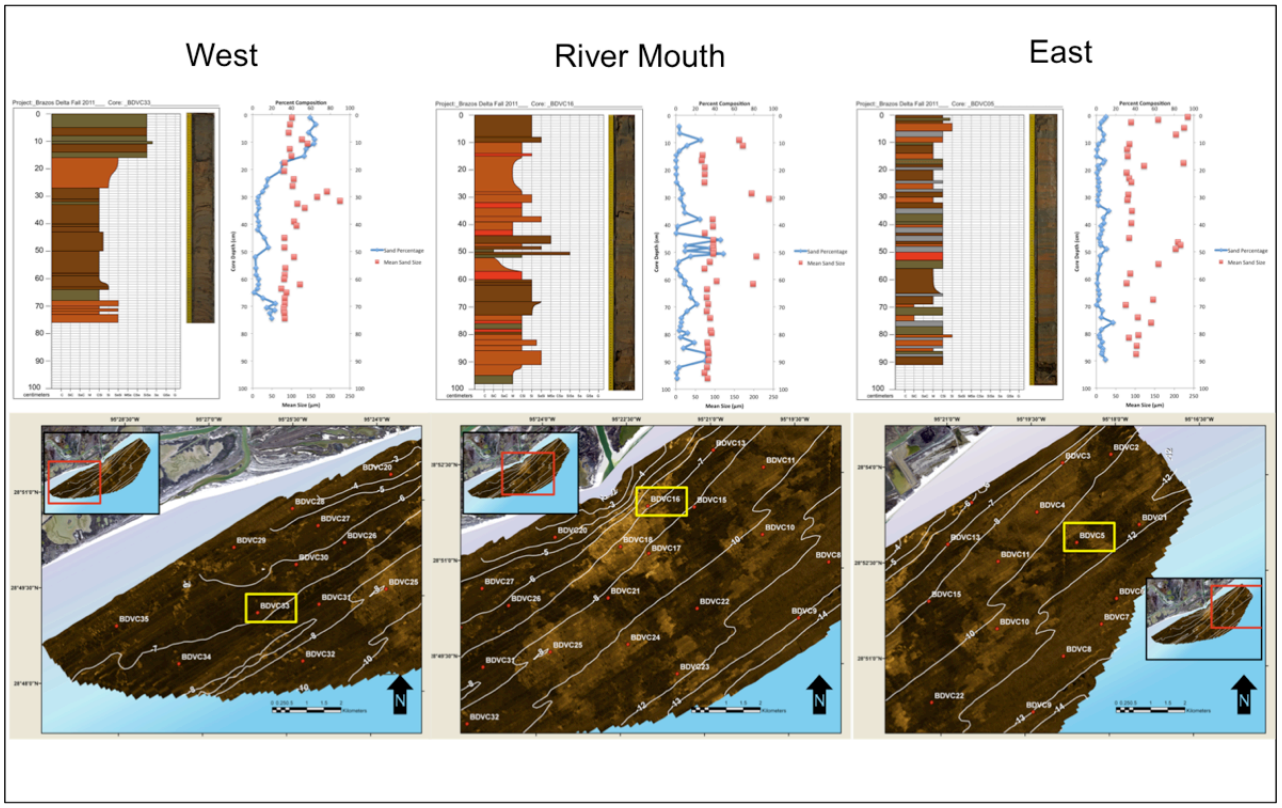

Figure 9: Examples of core data from different regions of the study area. Data includes core description, core photo, and grain size data including percent sand, and the mean size of the sand fraction. For core description key see appendix.

Figure 10B shows the results from the grain size analysis as contours of percent coarse-grained sediment (>63 μm) overlying the SSS mosaic. The surface sediment characteristics were determined from analysis of the surface sediment grab samples, and averaging the results from the upper ~ 5 cm of each core. These results show that most of the coarse grained sediment is found downdrift of the mouth, in areas of low backscatter. Of the three areas where over 80% consisted of coarse-grained sediment, two are located downdrift of the river mouth. With the one area updrift, located within the nearshore zone. The smaller of these depocenters is located approximately 2 km to the southwest of the river mouth, while the larger area is ~10 km to southwest of the river mouth near the seaward extent of the survey. Outside of these depocenters the coarse-grain content of the sediments decrease sharply to less than 20% in some areas. Updrift of the river mouth is largely dominated by sediments consisting of 20% or less coarse-grains, with the exception of the nearshore coarse –grained depocenter mentioned above. Another area with increased coarse-grained content (40% or more) is found in a relatively flat deep water (>12 m) area to the east of the river mouth. Most of the high backscatter areas correspond to fine sediment (<20 % coarse), where Features A and B are completely dominated fine-grained sediment. The coarse fraction increases (20 – 40 %) in the low backscatter area directly east of Feature A, then decreases in the high backscatter area further east.

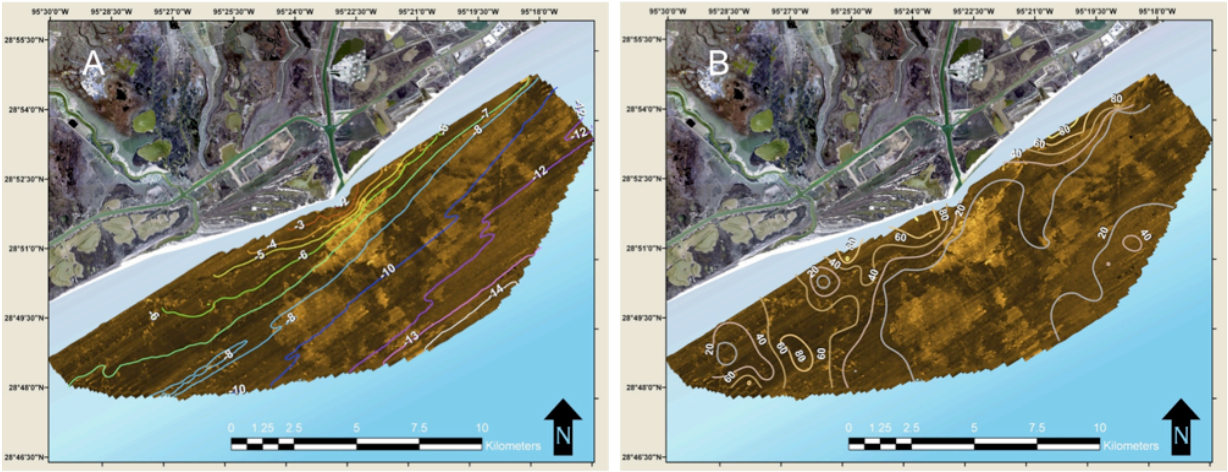

Figure 10: Side scan sonar mosaic with bathymetric contours (A) in meters below mean low water. Side scan sonar mosaic with percentage of coarse-grained (>63μm) surface sediment (B).

Five sediment facies were distinguished based on size distributions from the sediment cores. An example can been seen in Figure 11. Two of the facies were dominated by mud (<63 um, i.e. silt and clay), two were dominated by sand, and one was a transitional facies with mostly mud and some sand.

4.3.1 Facies A:

This facies is dominated by clay particles (< 4 μm) with some silt, usually less than 45 % silt. Sand is usually absent or present in only trace amounts. Observed in less than 3 % of all samples analyzed, this facies was the least common in the study area. It was most frequently observed in an area approximately 5 km directly seaward of the river mouth (Figure 12A).

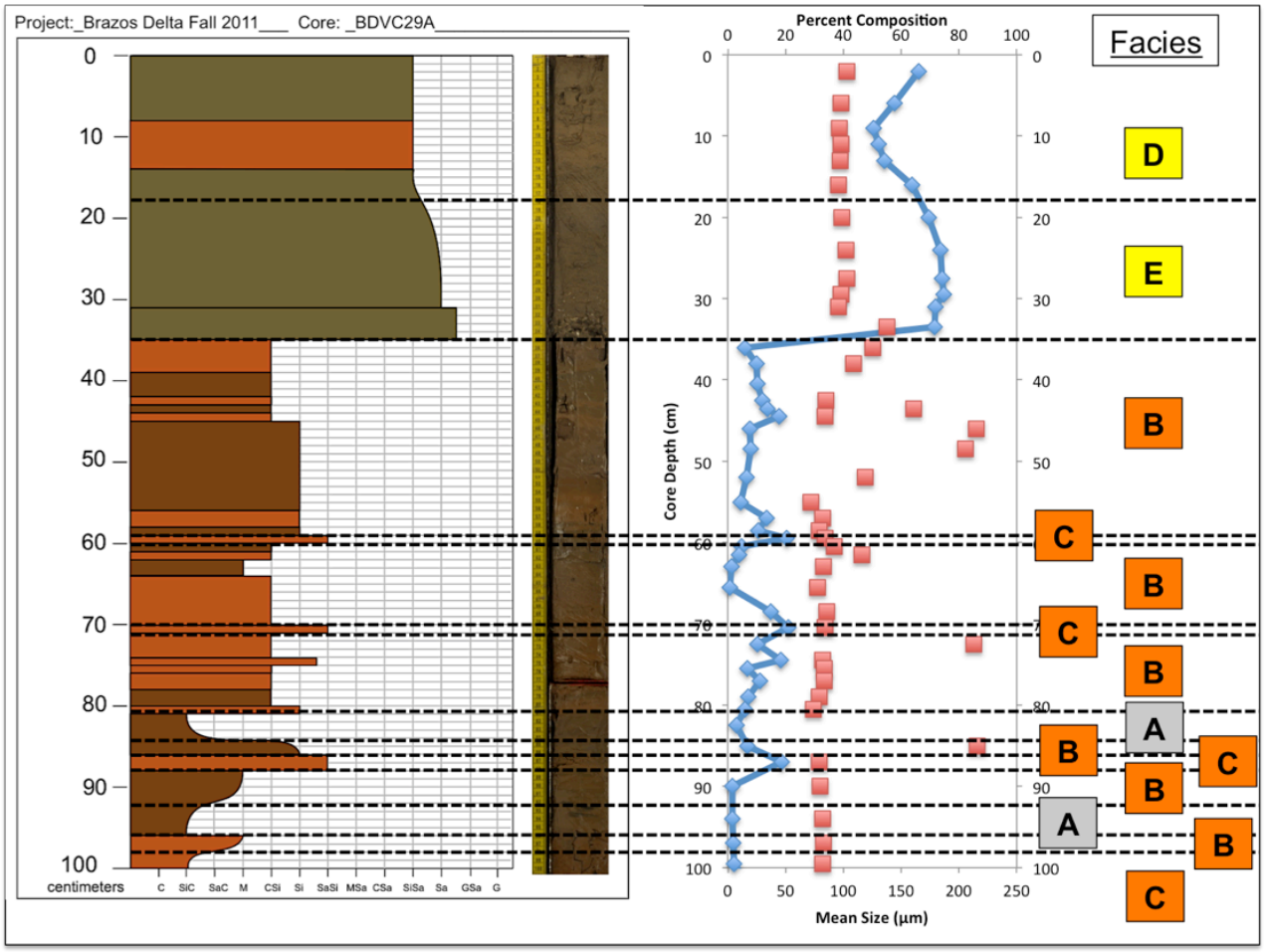

Figure 11: Example of facies distinctions A,B,C,D, and E with core BDVC29.

4.3.2 Facies B:

The most dominant facies, over 80% of all samples analyzed were categorized as Facies B. This facies primarily consisted of sediment dominated by silt, with some clay (45 % or less), but also included sediment that was near equal parts silt and clay, and sediment that was almost exclusively all silt. When sand was present it was usually less than 15 % of the total sediment. This facies was found in all cores, except one, and dominates the study area with

the exception of a nearshore area between the Brazos and San Bernard River mouths (Figure 12B).

4.3.3 Facies C:

The transitional facies, Facies C is dominated by silt, but has a significant fraction of sand (usually less than 45 %). If clay is present it is in a smaller fraction than that of the sand. Over 7 % of all samples analyzed were characterized as Facies C, and it was most observed downdrift of the river mouth in the center or the Western Lobe (Figure 12C).

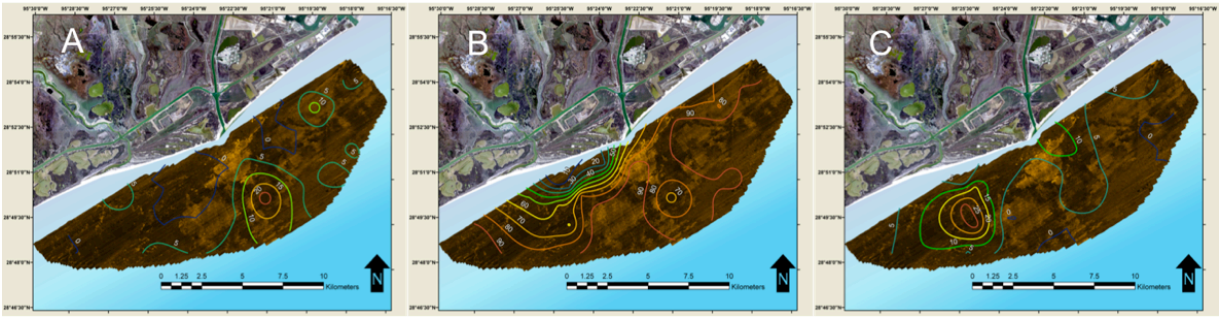

Figure 12: Side scan sonar mosaic with percentage core that is classified as Facies A (A), Facies B (B), and Facies C (C).

4.3.4 Facies D:

The first of the sand facies, Facies D sediment is dominated by sand, but has a significant portion of silt (< 45 %). The clay fraction is absent or negligible. This facies describes nearly 4 % of sediment analyzed. It is primarily found directly downdrift of the river mouth, within the shallower waters of the study area (Figure 13A).

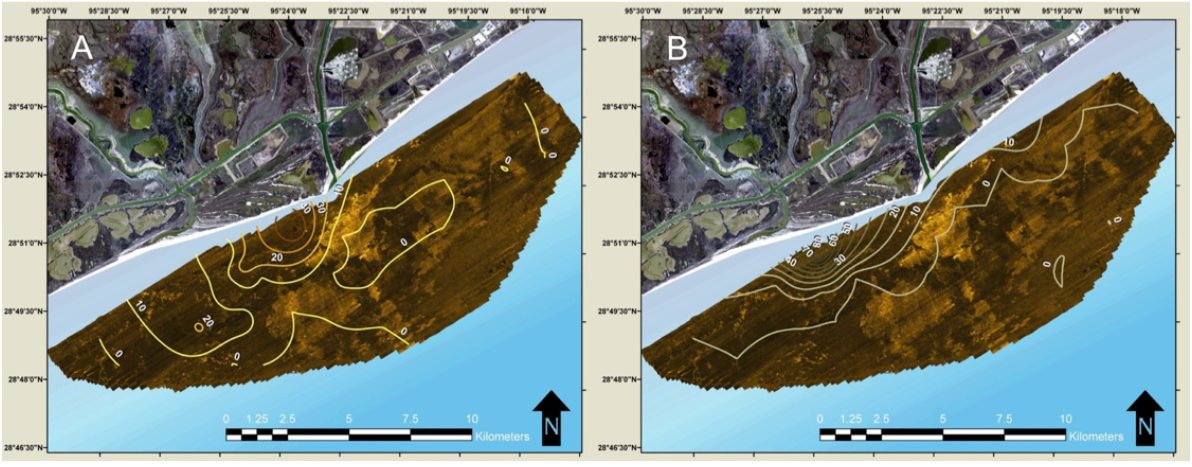

Figure 13: Side scan sonar mosaic with percentage core that is classified as Facies D (A), and Facies E (B).

4.3.5 Facies E:

This facies is almost entirely sand (>70 %), although significant portions of gravel, in the form of shells and shell fragments, within the basal layer of a deposit in some cores. Silt and clay have relatively small fractions, and a little over 3 % of samples analyzed fell into this category. Primarily found downdrift of the river mouth, proximal to the San Bernard, although it was also present in one core in the nearshore area updrift of the river mouth (Figure 13B). From Facies D and Facies E, the sand in this system is primarily found downdrift of the river mouth, in water depths less than 6 m (Figure 14).

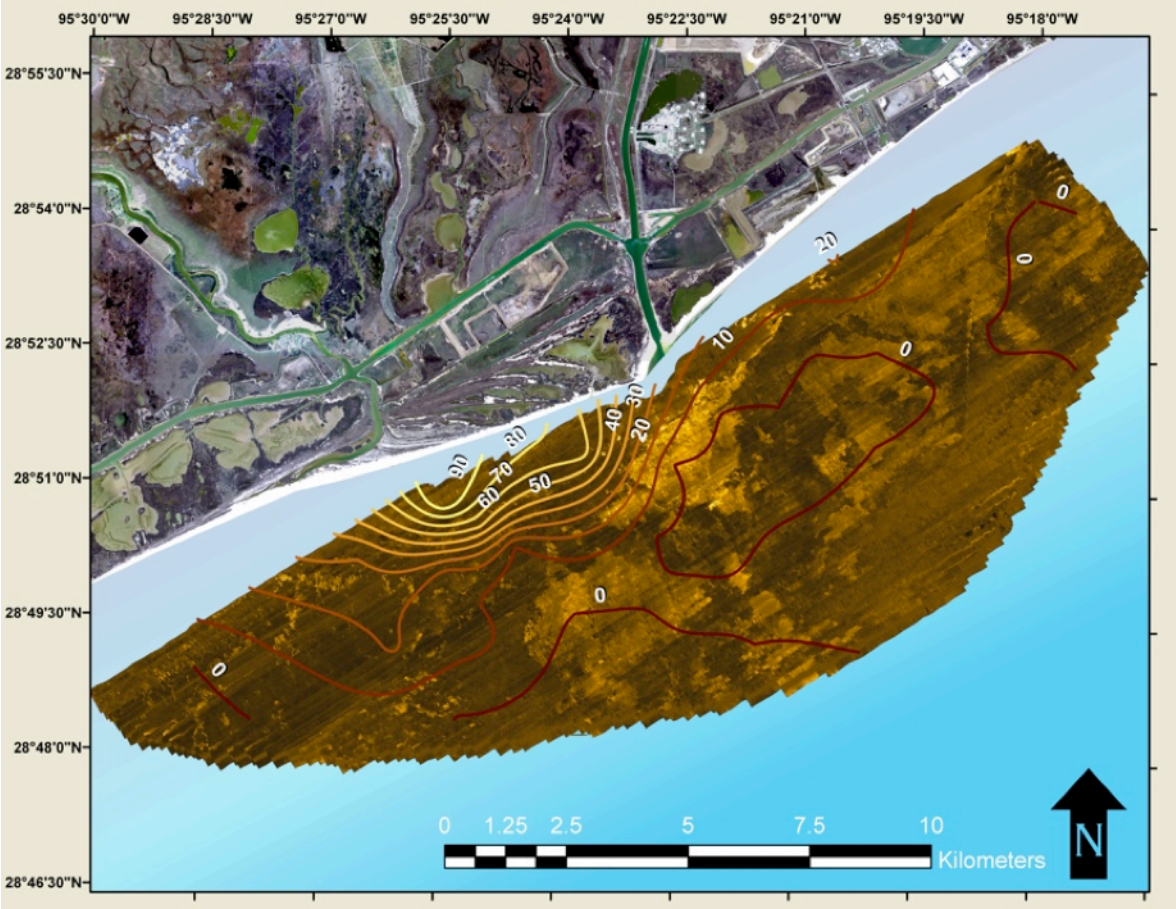

Figure 14: Side scan sonar mosaic with percentage of core that is sandy sediment (Facies D and E).

Results show no definitive relationship exists between sediment color and the size based facies, though some trends are evident (Figure 15). Facies B was the only facies to be observed in all 5 colors with a normal distribution where brown was most observed and red and grey sediment least observed. Red sediment layers were only found in Facies A and B sediments, and grey sediments were only found in Facies B, C and D. The frequency of red-brown sediment decreases as the facies coarsen (From Facies C to E), and Brown

sediment is the dominant or co-dominant color in all of the facies with the exception of Facies D, where grey-brown dominates. Brown sediment dominates the surface sediments of the study area (Figure 16), with the exception of two small areas of red-brown surface sediments in the middle of the Eastern Lobe, and two areas of grey-brown sediment in the middle of the Western Lobe, and in the deepest portion of Eastern Lobe. One core in this deep portion of the eastern lobe did exhibit grey sediment at the surface.

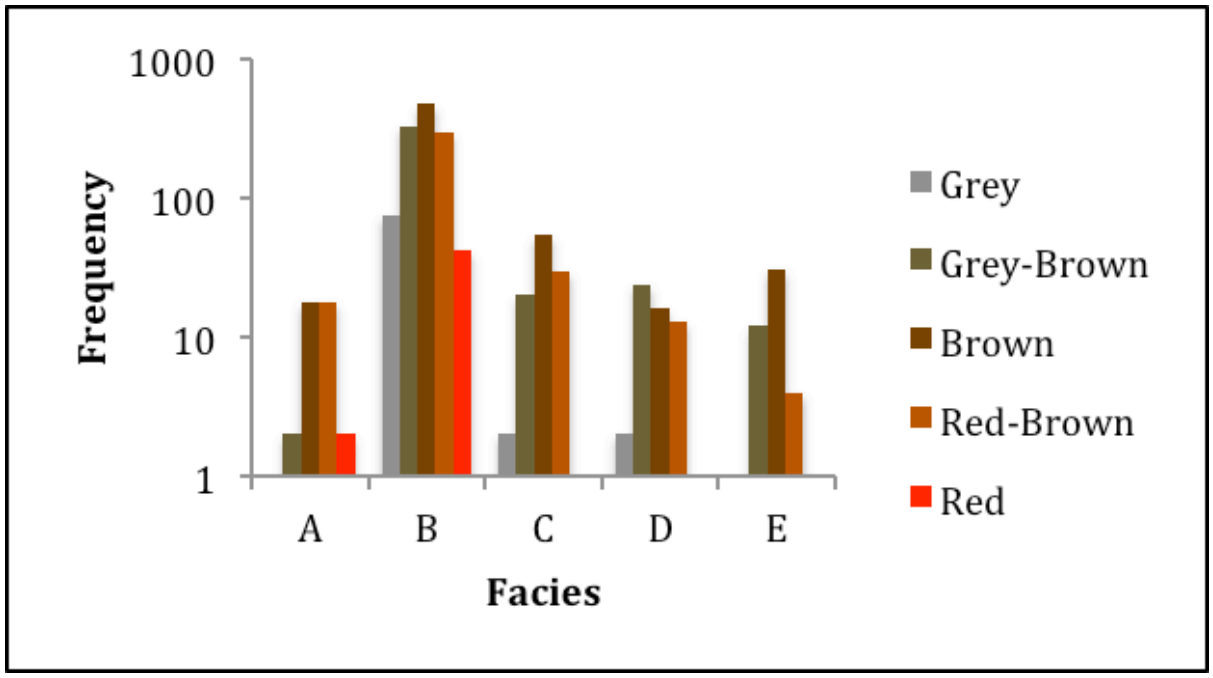

Figure 15: Graph showing the relationship between sediment facies and sediment color from this study.

Figure 17A shows the percentage of the cores that were comprised of either grey or grey-brown sediment. Much of the central portion of the Eastern Lobe had the highest proportion of this grey sediment within the cores, the highest values being in the areas the furthest offshore. The proportion of grey sediments decrease both to the east, towards the Freeport channel and the OBD, and to the west in the Western Lobe. Grey sediment proportions are lowest proximal to the river mouth, and increase downdrift through the Western Lobe.

Brown sediments (Figure 17B) are relatively common throughout the study area, but dominate in the nearshore areas both updrift and down drift of the river mouth. Although directly down drift of the river mouth values are relatively lower. In the Eastern Lobe the percent age of brown sediments in the cores decreases with increasing water depth generally, while much of the Western Lobe cores had over 40 % of brown sediments in the cores.

The percentage of red sediments shown in Figure 17C consists of both red and red-brown sediments within the core. There are three distinct areas where red sediment dominates

or comprise a significant portion of the sediment, one area in the far eastern edge of the study area proximal to the OBD, and two areas extending from the modern river mouth. The smaller of these two areas extends southeastward from the river mouth only a couple of kilometers, while the second extends southwestward, follow the trend of the Western Lobe approximately 5 km.

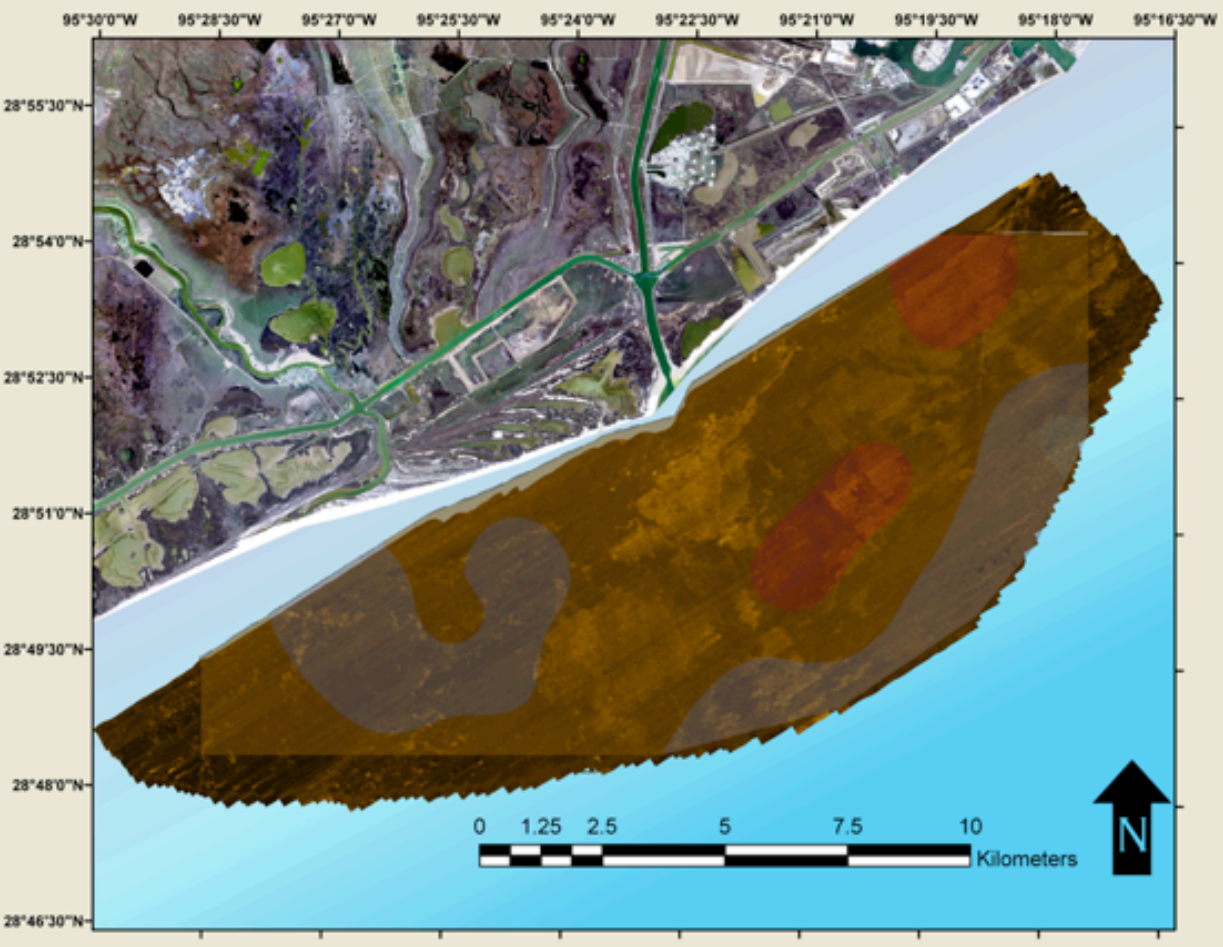

Figure 16: Map showing the color of surface sediment from sediment cores with SSS mosaic underlain.

5.0 DISCUSSION

5.1 Sediment Dynamics

The two lobes defined by the SSS data also exhibit unique sediment characteristics that offer insights into the evolution of the MBD and current the sediment dynamics of this study area. The Eastern lobe of the subaqueous delta comprises much of the survey area

(Figure 6B). With an area in excess of 80 km^2, the Eastern Lobe is approximately two-thirds of the study area. This lobe is delineated on its western boundary by the 5 m and 6 m isobaths that make the boundary of side scan Feature A near the river mouth, and the 20% coarse surface sediment contour. As such, large areas of high backscatter, fine surface sediment and steeper slopes dominate this area. The Eastern Lobe also has higher percentages of Facies A, B, and C within the cores (Figure 12). This lobe has the highest percentages of grey sediments, and the lower percentages of brown and red sediments (Figure 17). In addition to these sediment characteristics the Easter Lobe also shows an increased number of times the color of sediment changes, and the color changes between more colors in the sediment color spectrum (Figure 18).

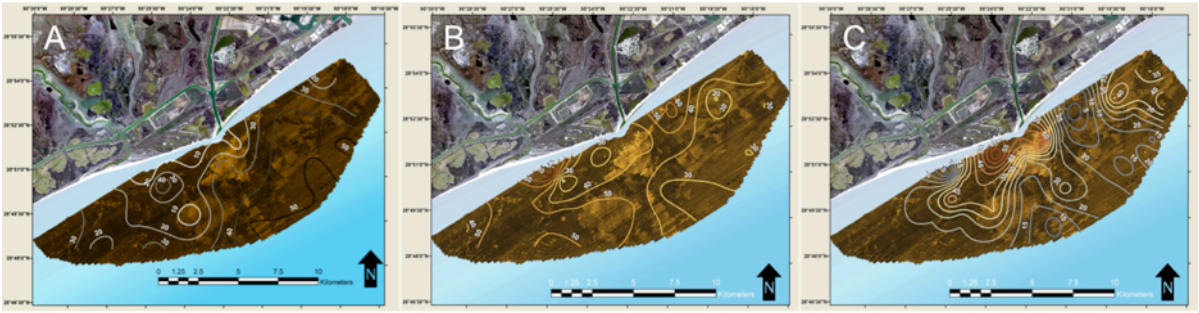

Figure 17: Side scan sonar mosaic with percentage core that is classified as grey sediment which includes grey and grey-brown sediment (A), brown sediment (B), and red sediment including red and red-brown sediment (C).

From this we conclude that the Eastern Lobe consists of predominantly eroded sediment from the OBD. In this sense the high backscatter features are related to erosion, rather that sediment composition. The easternmost potion of the Eastern Lobe has increased red sediment, which is believed to be directly derived from the Brazos River (Rice et al , in prep), and increased changes in sediment color indicating that this sediment in this area is from the OBD. These increasing red trending color changes indicate that this sediment may be derived from river flooding events prior to diversion of the mouth in 1929. Furthermore, given that these cores are on average only 1 m in length, this would suggest that little sediment has accumulated from the modern river mouth in the decades since this erosion. To this point, in the western portion of the Eastern Lobe, between the modern mouth and the OBD dominated area, the sediment is dominantly grey in color with some of the lowest percentages of red sediment for the entire study area. As Figure 2 shows the initial MBD prograded into this area, yet little red sediment was preserved suggesting that the sediment delivered during the initial growth phase of the MBD was eroded.

The Western Lobe of the subaqueous delta occupies one-third of the study area, or approximately 40 km^2 (Figure 6A). This lobe is principally defined by low backscatter, with the absence of the large distinct high backscatter features of the Eastern Lobe. Although small isolated areas of high backscatter are observed. Located directly seaward of the modern river mouth, this lobe extends out in a southwestwardly direction. The slope of this lobe is gentler than the Eastern Lobe, with a maximum depth of approximately 10 m, compared to depths in excess of 14 m in the Eastern Lobe (Figure 6B). Coarse-grained (>63 μm) surface sediment comprises a majority of the surface sediment in this lobe (Figure 10B), Facies C, D, and E, and red and brown sediments dominate the lobe. The

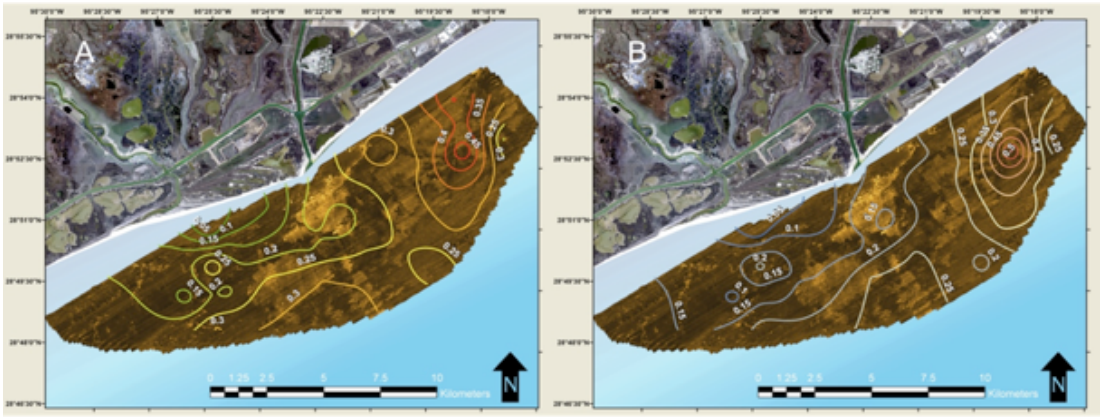

Figure 18: Side scan sonar mosaic with the Color Change Index (A) classifying how frequent the sediment color changes down core increased values indicate more color changes, and the Color Diversity Index (B) classifying not only how frequent the sediment color changes, but also how many different colors are represented in the core. Increased values indicate that the sediment color is changing often and between multiple different colors.

sediment color does not change as much compared to the Eastern Flank, and the when the color does change it primarily fluctuates between brown and red-brown sediments, lacking the color diversity of the Eastern Flank. This Western Lobe represents the active subaqueous lobe. The Western Lobe was activated in 1961 after Hurricane Carla shifted sediments to the west, downdrift of the river mouth (Seelig and Sorensen 1973). From this we conclude that sediment from the river is preferentially dispersed along the Western

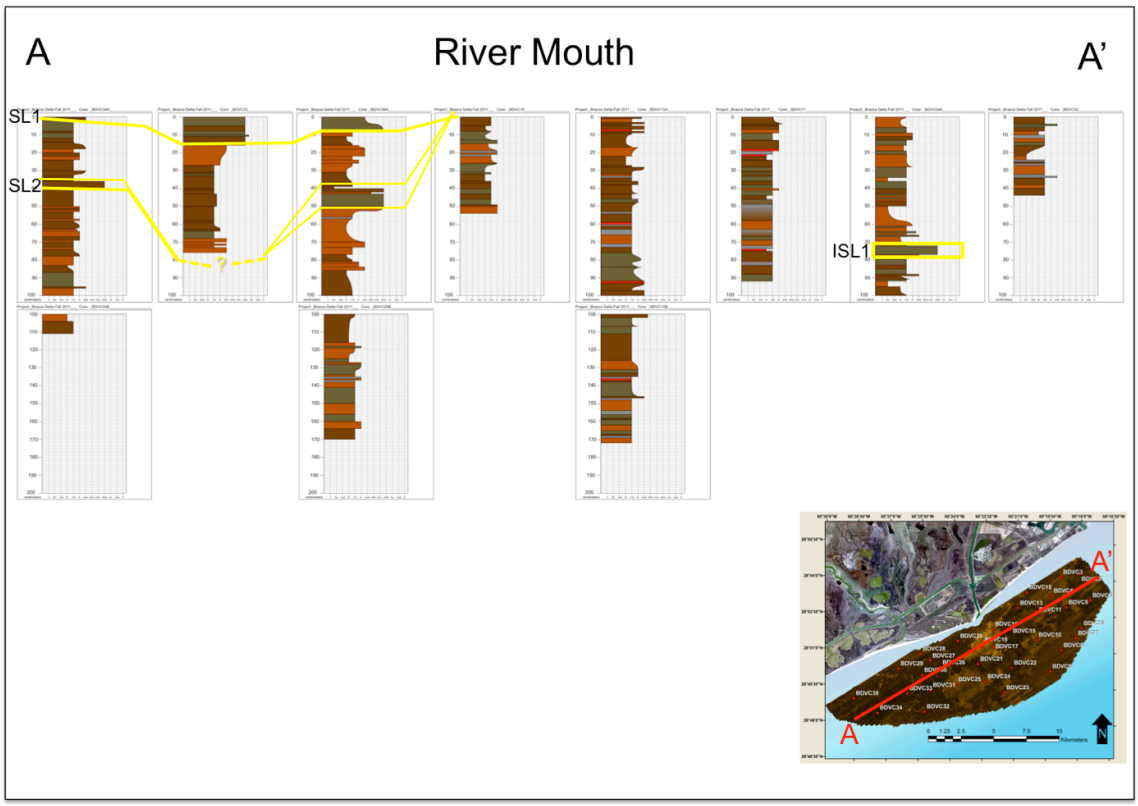

Figure 19: Along shore cross section across the study area. Cross section shows the surface sand layer (SL1), subsurface sand layer (SL2), and an isolated sand layer (ISL1).

Lobe, and the Eastern Lobe is eroding, and sediment is transported either downdrift to the Western Lobe, or across the shelf to deeper water. The sediment accumulating on the Western Lobe is increasingly coarse in the nearshore areas and fines both across the shelf and downdrift of the river mouth.

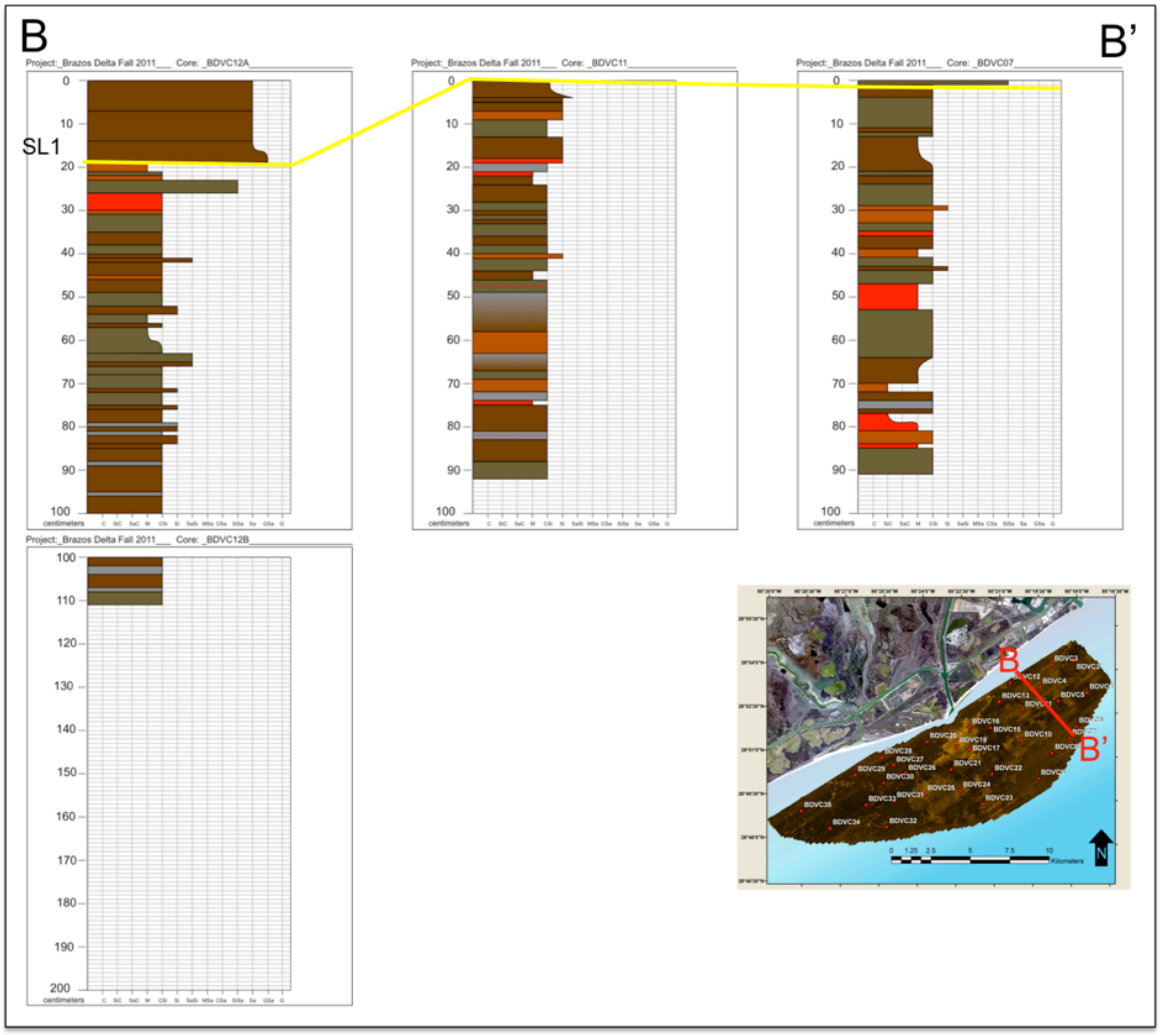

Figure 20: Eastern Lobe cross section. Cross section shows surface sand layer (SL1).

5.2 Sand Resources

The percentage of sandy sediment (Facies D and E) is shown in Figure 14. Though this shows the percentage of sand for the entire core, those areas with the highest percentage, i.e. the Western Lobe, have the thickest sand layer at the surface. This is the most extensive sand layer within the study layer. The cross sections in Figures 19-21 show the surface sand layer (SL1), and a lesser thick subsurface sand layer (SL2) in the Western Lobe in addition to isolated sand layers (ISL1) found in the subsurface of the Eastern Lobe. The thickness of SL1 (Figure 22) exceeds 35 cm at its thickest, and forms 3 distinct nearshore depocenters. The smallest of the three is located updrift of the river mouth with a maximum thickness of 15 cm. Directly downdrift of the river mouth the second of the three

depocenters lies, larger than first with a maximum thickness on the order of 20 cm. The largest sandy depocenter lies just downdrift, extends into the center of the Western Lobe, and reaches the maximum thickness in excess of 35 cm. This sandy sediment has an approximate volume of 5 X 10^8 m^3, or 0.5 km^3. This value includes Facies D, so this value does have some fraction of silty sediment included. In addition, the sand in this sediment is also relatively fine (see core data in appendix). The mean sand size for core BDVC26, which is >35 cm of Facies E sand, has a mean sand size of 120 µm and represents the coarsest of the sand found in any or the cores. All of the rest of the sand in the study area rare has a mean sand size that exceeds 100 µm. For reference, the mean diameter

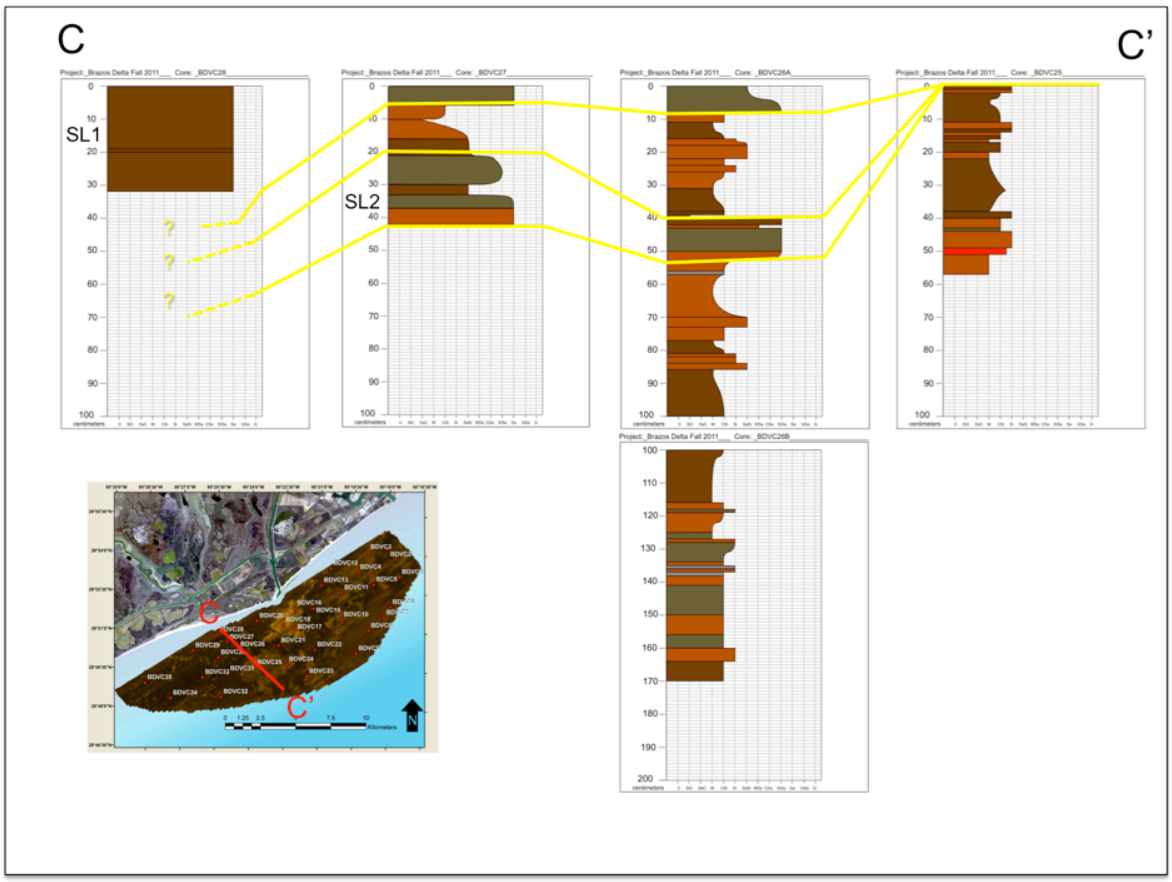

Figure 21: Western Lobe cross section. Cross section show surface sand layer (SL1), and subsurface sand layer (SL2).

(D50) of sand for the beaches of Galveston Island is 120 µm. Previous work off of Galveston found sand of 100 µm mean diameter was unsuitable for beach nourishment (2005 Galveston Island Sand Source Study). Facies E represents ~36% of the sand within the above referenced deposit, this means that of the total sand deposit described above, there is 1.9x10^6 m^3 (2.5 x 10^6 cubic yards) of beach quality sand.

6.0 CONCLUSIONS

In conclusion the subaqueous delta of the Brazos River is a dynamic system. The area exhibits an asymmetry with two distinct subaqueous lobes, the Eastern Lobe dominated by erosion and sediment mass movements, and the Western Lobe dominated by the current deposition and accretion of fluvially derived sediment. Silts dominate these sediments, and form thin layers, on the order of centimeters, characterized by changes in sediment composition and coloring. Sand is present, but dominantly in the near surface layers, to west of the river mouth in water depths less than 8 m, in layers 40 cm or less thick. Although the entire sand deposit contains 5 X 10^6 m^3 (6.54 x 10^6 cubic yards), only 36% or 1.9x10^6 m^3 (2.5 x 10^6 cubic yards) is beach quality >120μm mean diameter (D50). The remainder of this sand generally has a mean diameter of 100 μm (D50), rendering this sand unsuitable for beach nourishment.

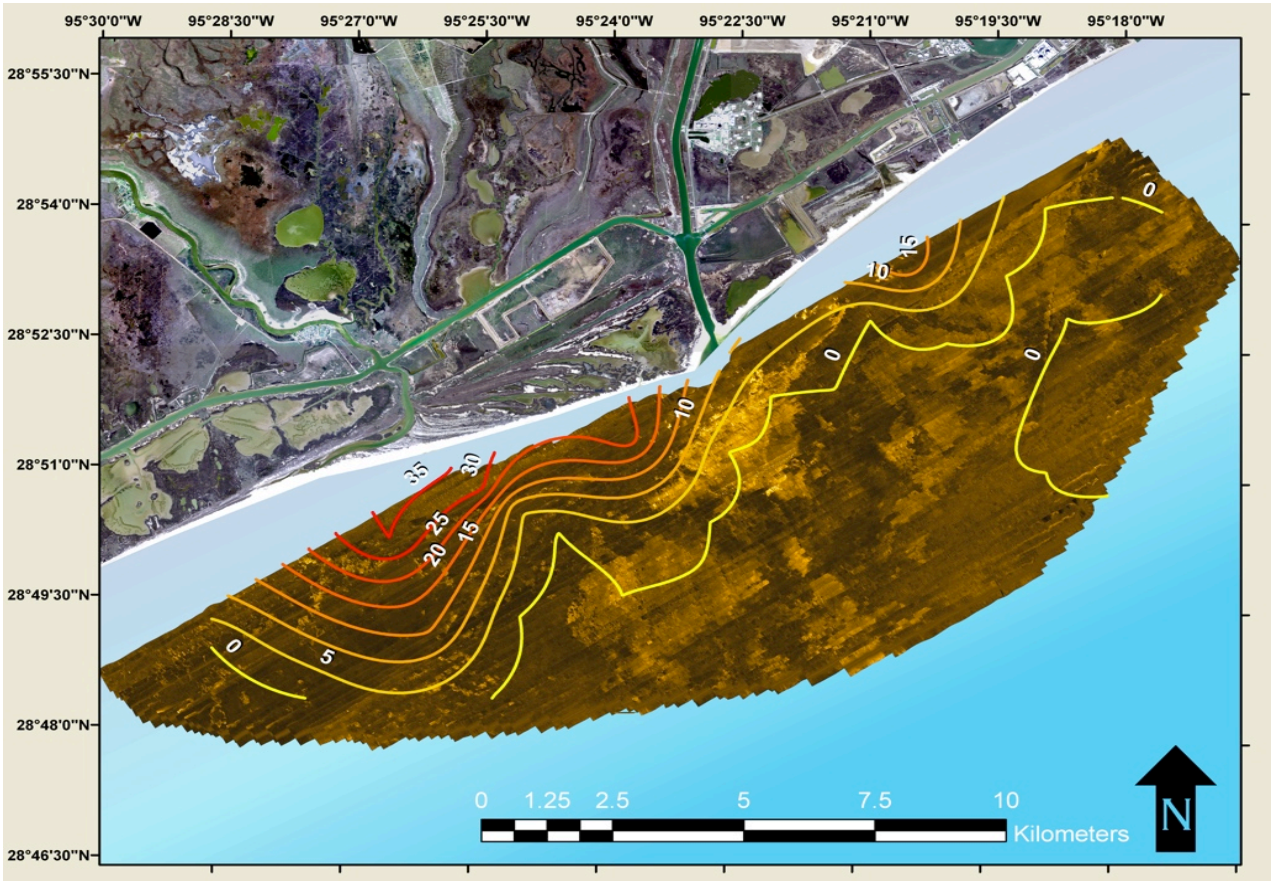

Figure 22: Isopach map of SL1 (Facies D and E) thickness with SSS mosaic. Values are in cm.

7.0 REFERENCES

Bhattacharya, J. P., and L. Giosan. 2003. Wave-influenced deltas: geomorphological implications for facies reconstruction. Sedimentology **50:** 187-210.

Blake, E. S., E. N. Rappaport, and C. W. Landsea. 2007. The Deadliest, Costliest, and Most Intense United States Tropical Cyclones From 1851 to 2006 (And Other Frequently Requested Hurricane Facts). *In* N. H. Center [ed.]. National Weather Service.

Curray, J. R. 1960. Sediments and History of Holocene Transgression, Contiental Shelf, Northwest Gulf of Mexico, p. 221-266. *In* F. P. Shepard, F. B. Phleger and T. H. Van Andel [eds.], Recent Sediments, Northwest Gulf of Mexico: ASymposium Summarizing the Results of Work Carried On in Project 51 of the American Petroleum Institute 1951-1958. The American Association of Petroleum Geologists.

Fraticelli, C. M. 2006. Climate Forcing in a Wave-Dominated Delta: The Effects of Drought–Flood Cycles on Delta Progradation. Journal of Sedimentary Research **76:** 1067-1076.

Long, C. Old Three Hundred. *In* tshaonline.org [ed.], Handbook of Texas Online. Texas State Historical Association.

Milliman, J. D., and J. P. M. Syvitski. 1992. Geomorphic Tectonic Control of Sediment Discharge to the Ocean - the Importance of Small Mountainous Rivers. Journal of Geology **100:** 525-544.

Nowlin Jr, W. D., A. E. Jochens, S. F. Dimarco, R. O. Reid, and M. K. Howard. 2005. Low-Frequency Circulation Over the Texas-Louisiana Continental Shelf, p. 219-240. *In* W. Sturges and A. Lugo-Fernández [eds.], Circulation in the Gulf of Mexico: observations and models: Geophysical monograph series. American Geophysical Union.

Rodriguez, A. B., M. D. Hamilton, and J. B. Anderson. 2000. Facies and Evolution of the Modern Brazos Delta, Texas: Wave vs Flood Influence. Journal of Sedimentary Research **70:** 283-295.

Seelig, W. N., and R. M. Sorensen. 1973. Investigation of Shoreline Changes at Sargent Beach, Texas, p. 153. Texas A&M University Sea Grant

Siringan, F. P., and J. B. Anderson. 1993. Seismic Facies, Architecture, and Evolution of the Bolivar Roads Tidal Inlet Delta Complex, East Texas Gulf-Coast. Journal of Sedimentary Petrology **63:** 794-808.

Syvitski, J. P. M., and Y. Saito. 2007. Morphodynamics of deltas under the influence of humans. Global and Planetary Change **57:** 261-282.

Wright, L. D. 1977. Sediment transport and deposition at river mouths: A synthesis. Geological Society of America Bulletin **88:** 857-868.

Wright, L. D., and C. A. Nittrouer. 1995. Dispersal Of River Sediments In Coastal Seas - 6 Contrasting Cases. Estuaries **18:** 494-508.

Core Description Key

Sediment Grain Size

Clay Dominated

C	"Clay"	Clay comprises more than two-thirds of sediment
SiC	"Silty-Clay"	Clay dominates with silt comprising a significant fraction
SaC	"Sandy-Silt"	Clay dominates with sand comprising a significant fraction

Silt Dominated

CSi	"Clayey-Silt"	Silt dominates with clay comprising a significant fraction
Si	"Silt"	Silt comprises more than two-thirds of sediment
SaSi	"Sandy-Silt"	Silt dominates with sand comprising a significant fraction

Sand Dominated

CSa	"Clayey-Sand"	Sand dominates with clay comprising a significant fraction
SiSa	"Silty-Sand"	Sand dominates with silt comprising a significant fraction
Sa	"Sand"	Sand comprises more than two-thirds of sediment
GSa	"Gravely-Sand"	Sand dominantes with gravel comprising a significant fraction

M	"Mud"	Near equal portions silt and clay with little sand
MSa	"Muddy-Sand"	Near equal portions mud and sand
G	"Gravel"	Gravel comprises more than two-thirds of sediment

Sediment Color Key

Brazos Delta Cores: Observed Color

- Grey
- Grey-Brown
- Brown
- Red-Brown
- Red

Brazos Delta Core: BDVC1

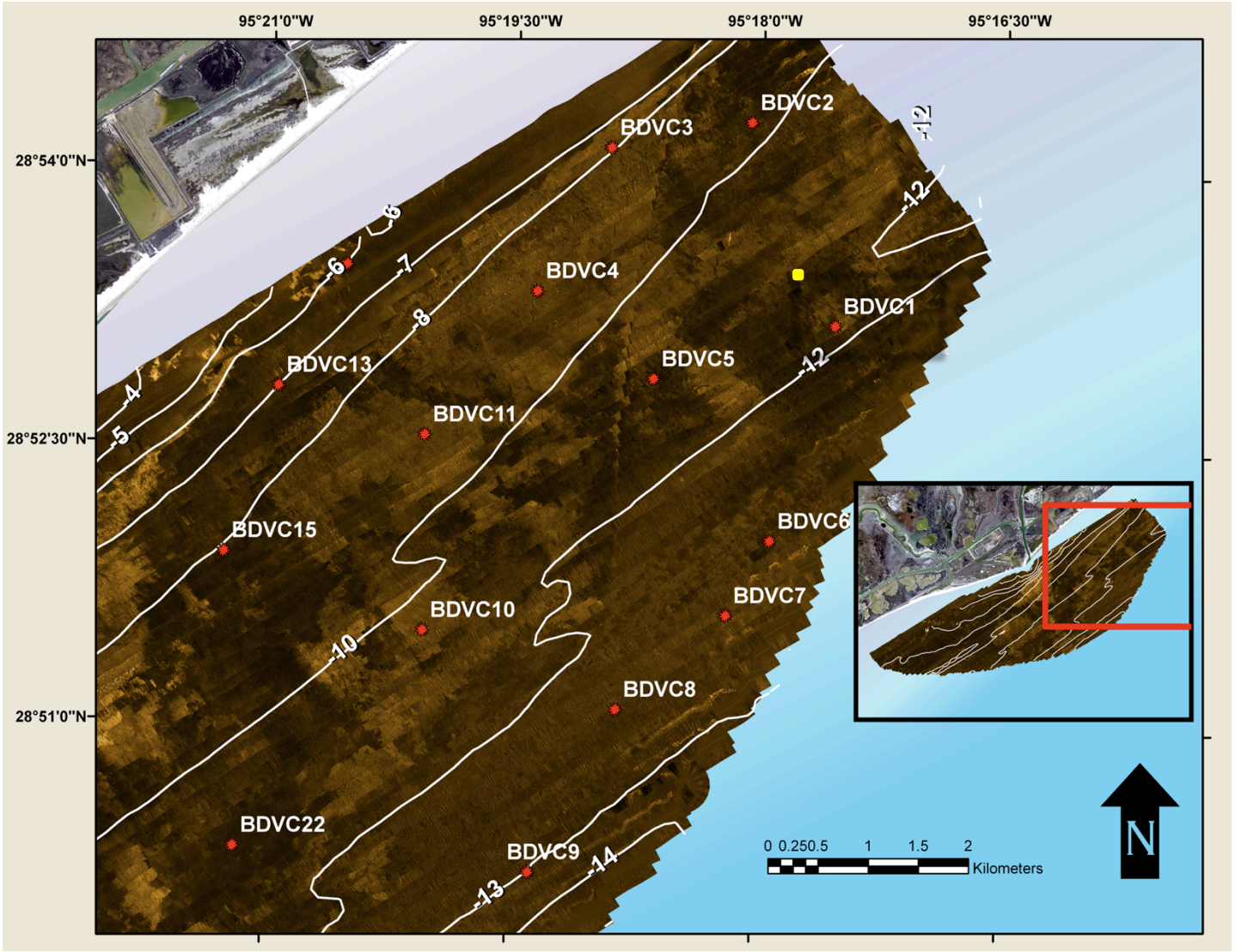

Project:_Brazos Delta Fall 2011___ Core: _BDVC01_____

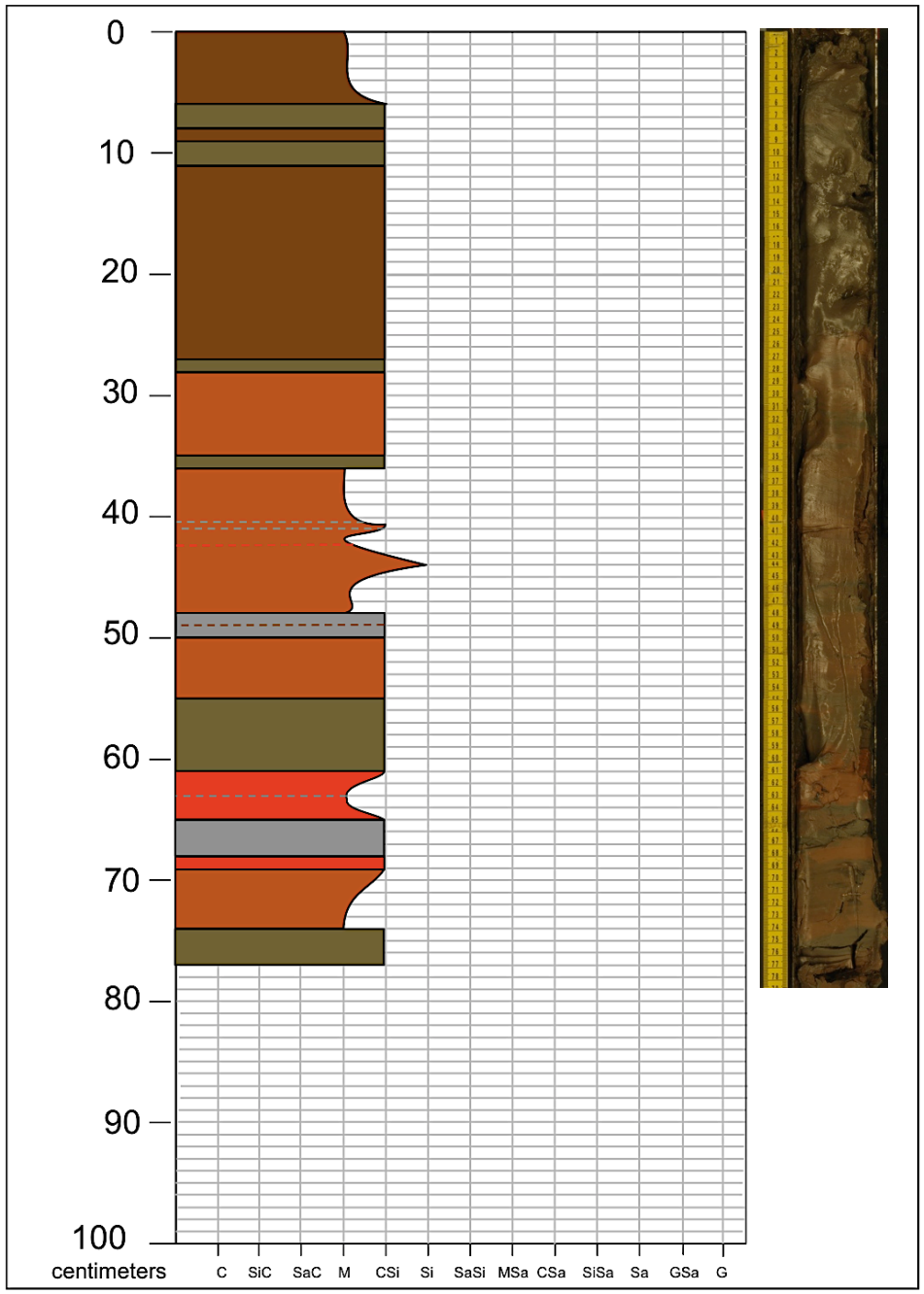

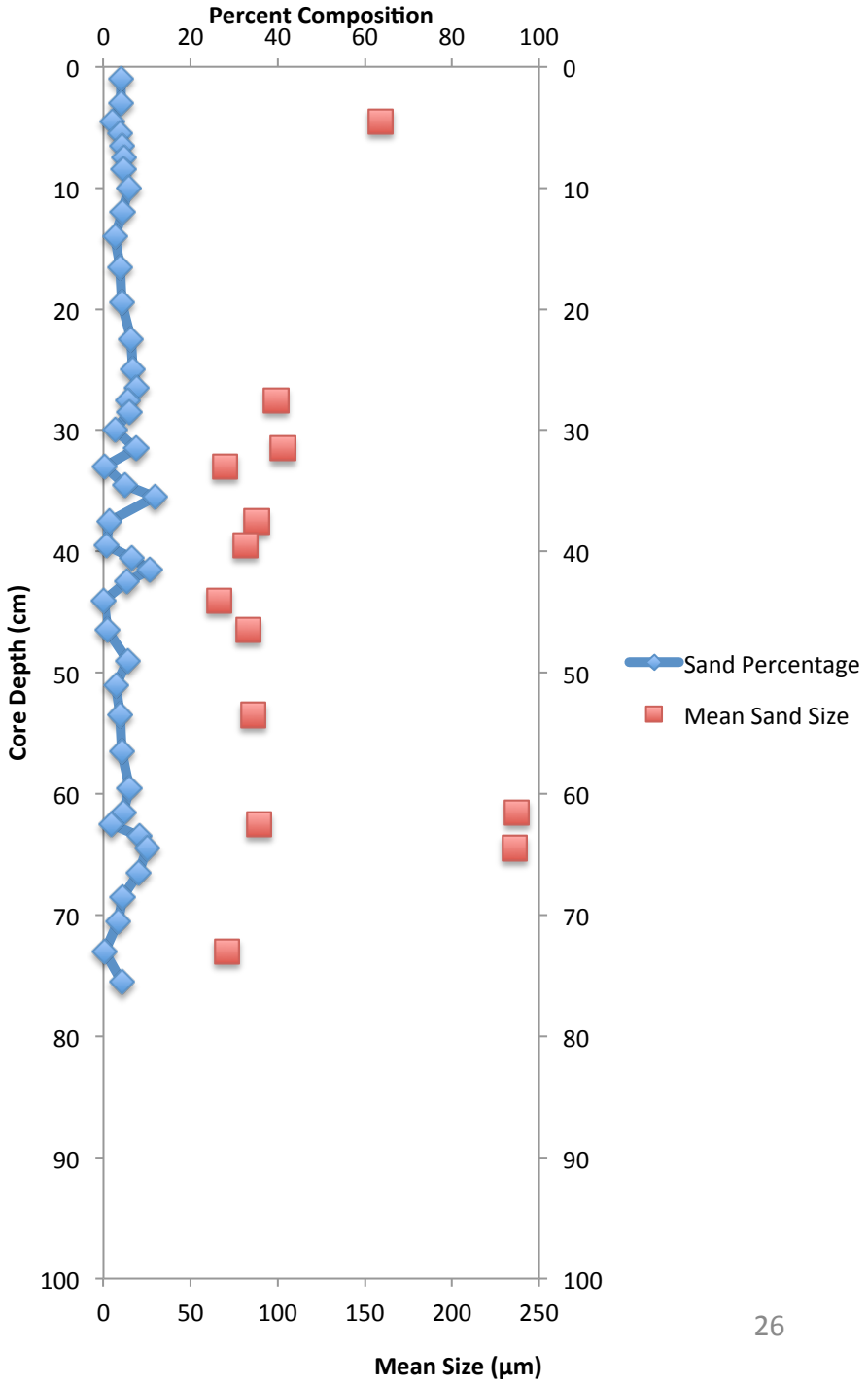

Brazos Delta Core: BDVC2

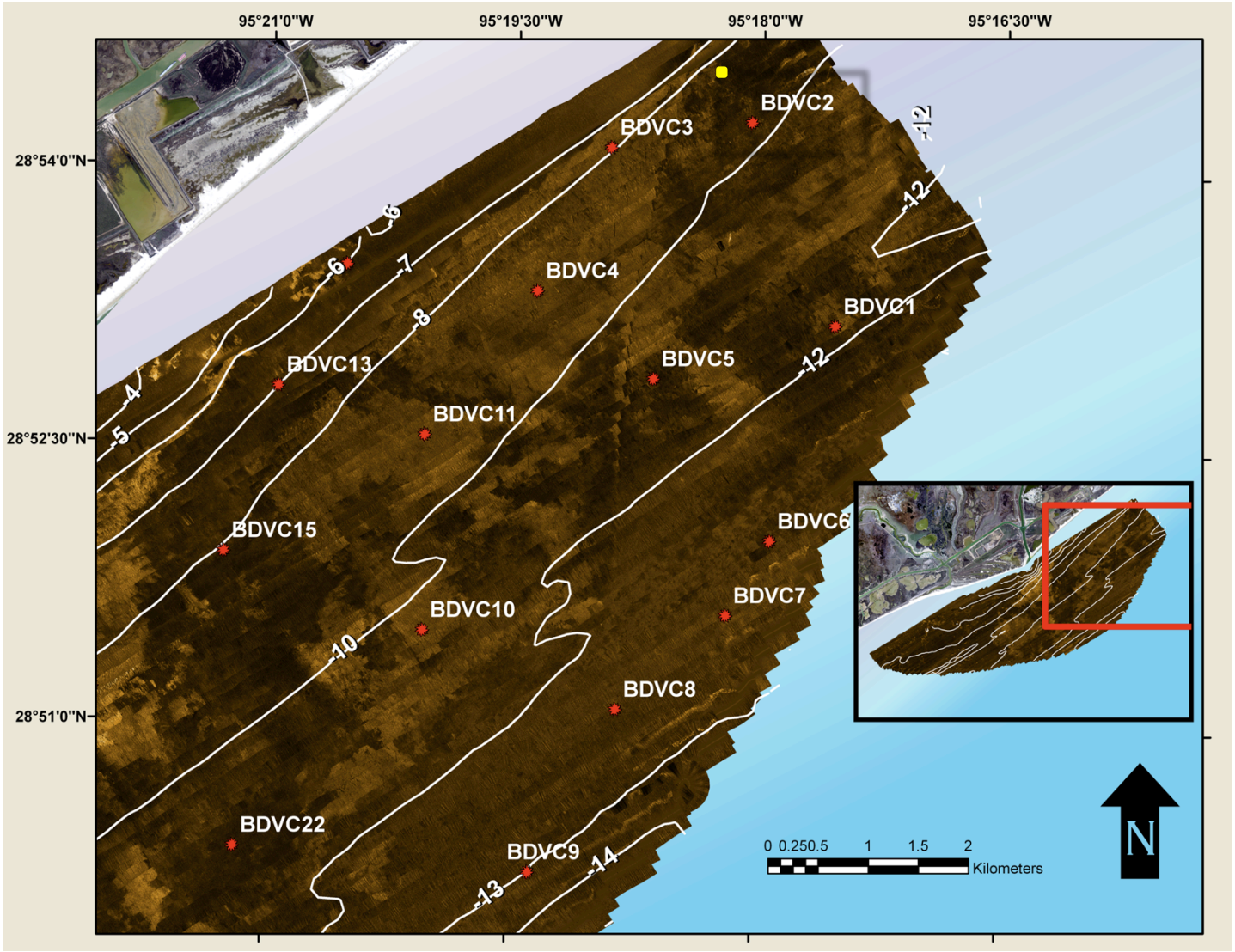

Project:_Brazos Delta Fall 2011___ Core: _BDVC02_____

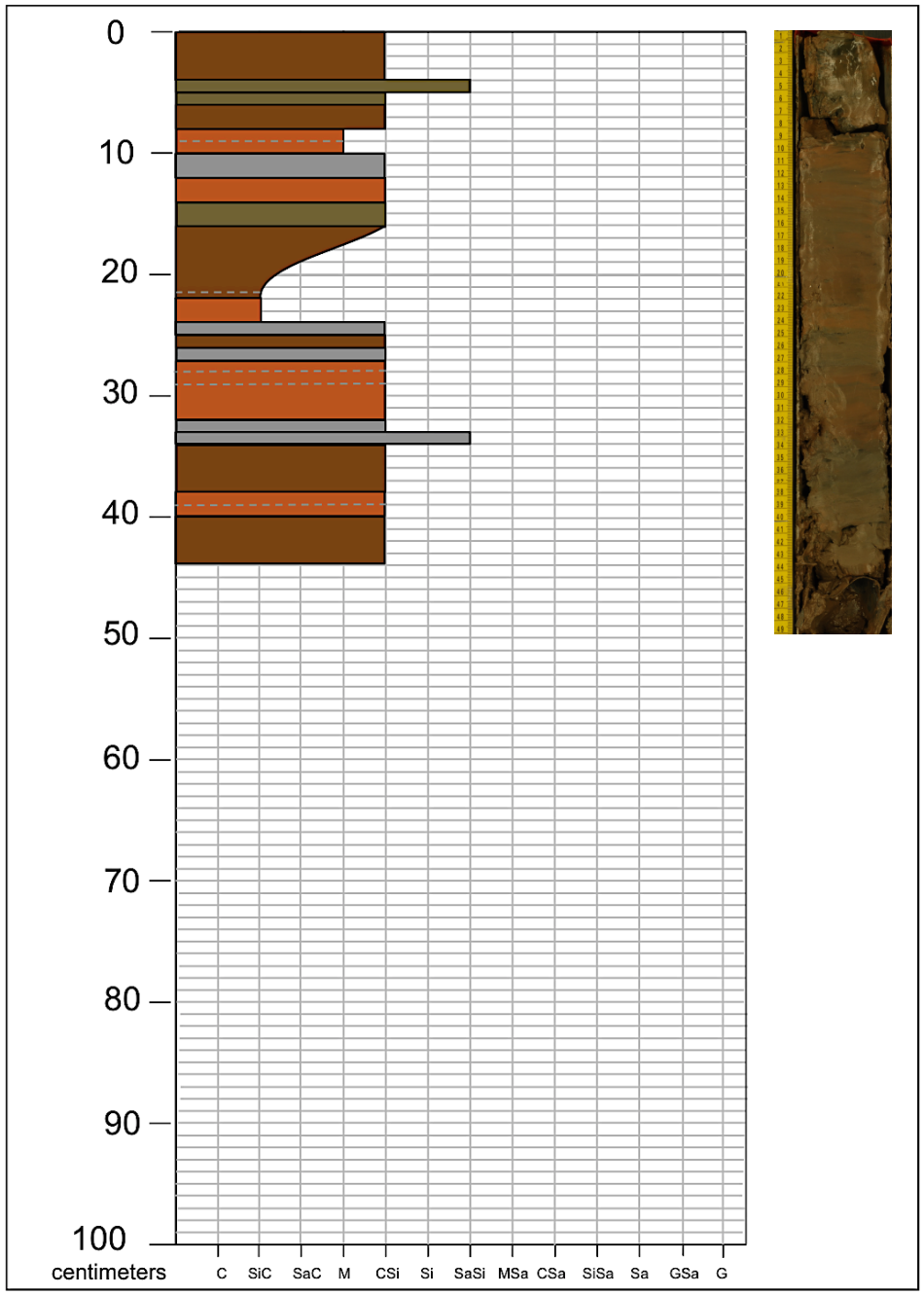

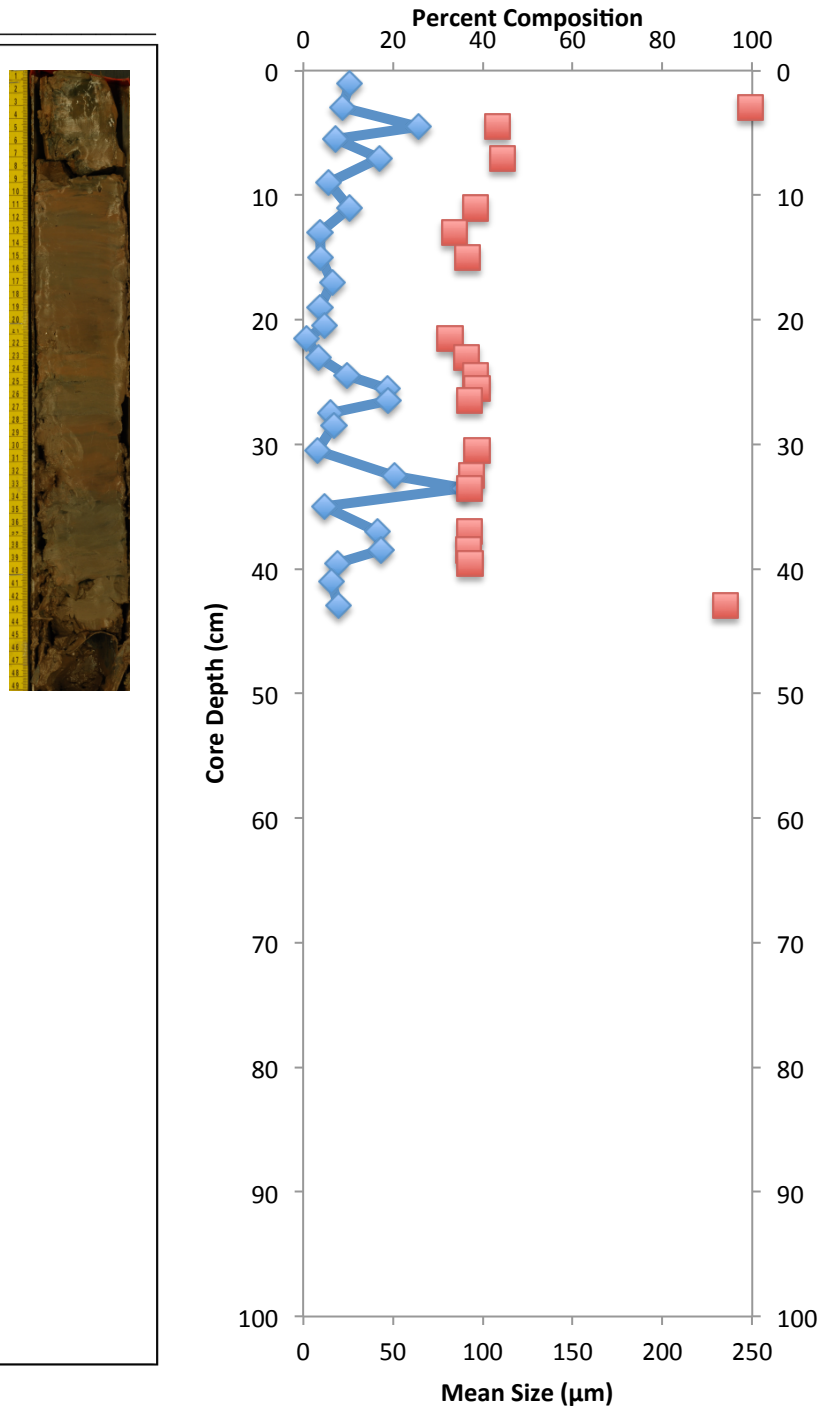

Brazos Delta Core: BDVC3

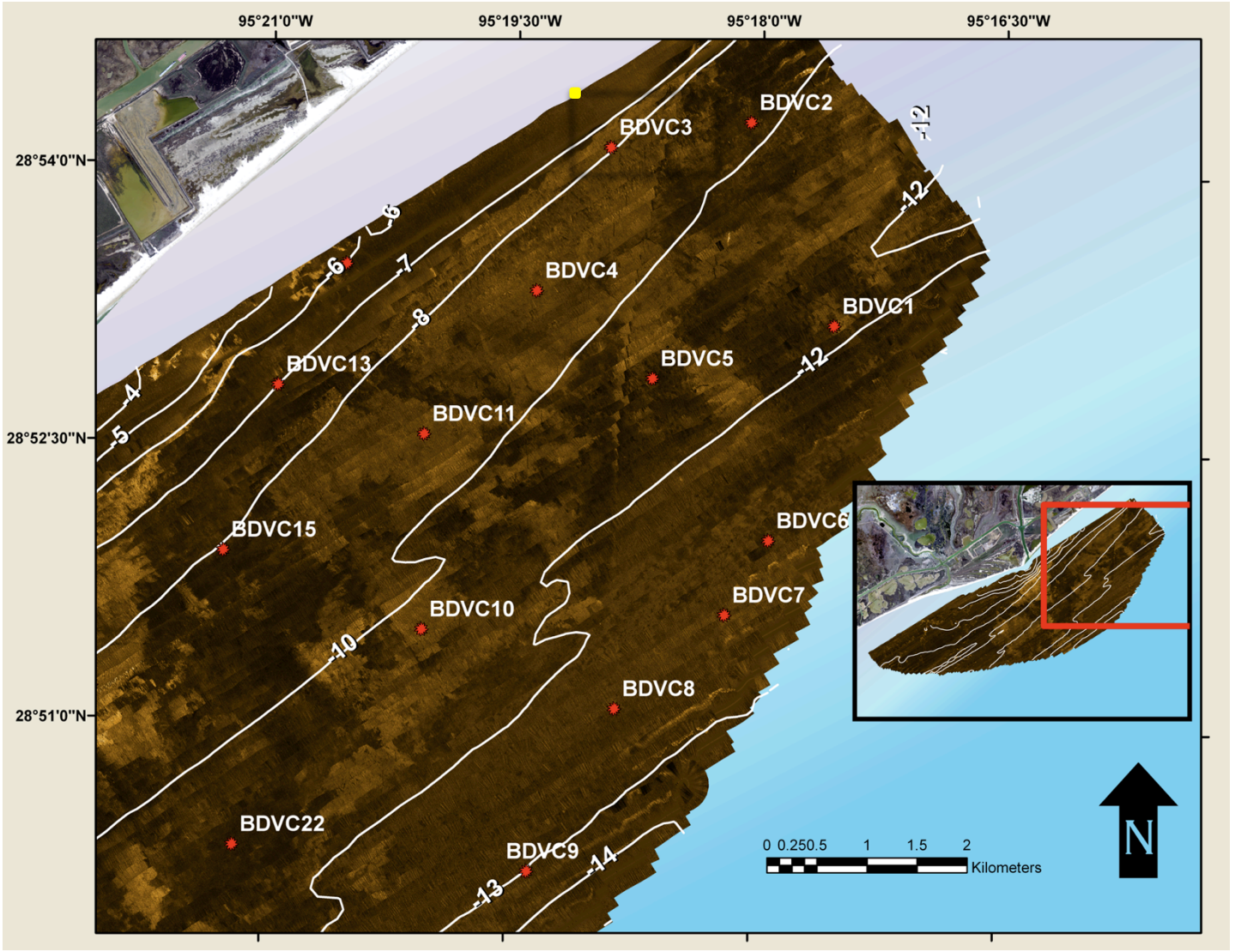

Project:_Brazos Delta Fall 2011___ Core: _BDVC03_____

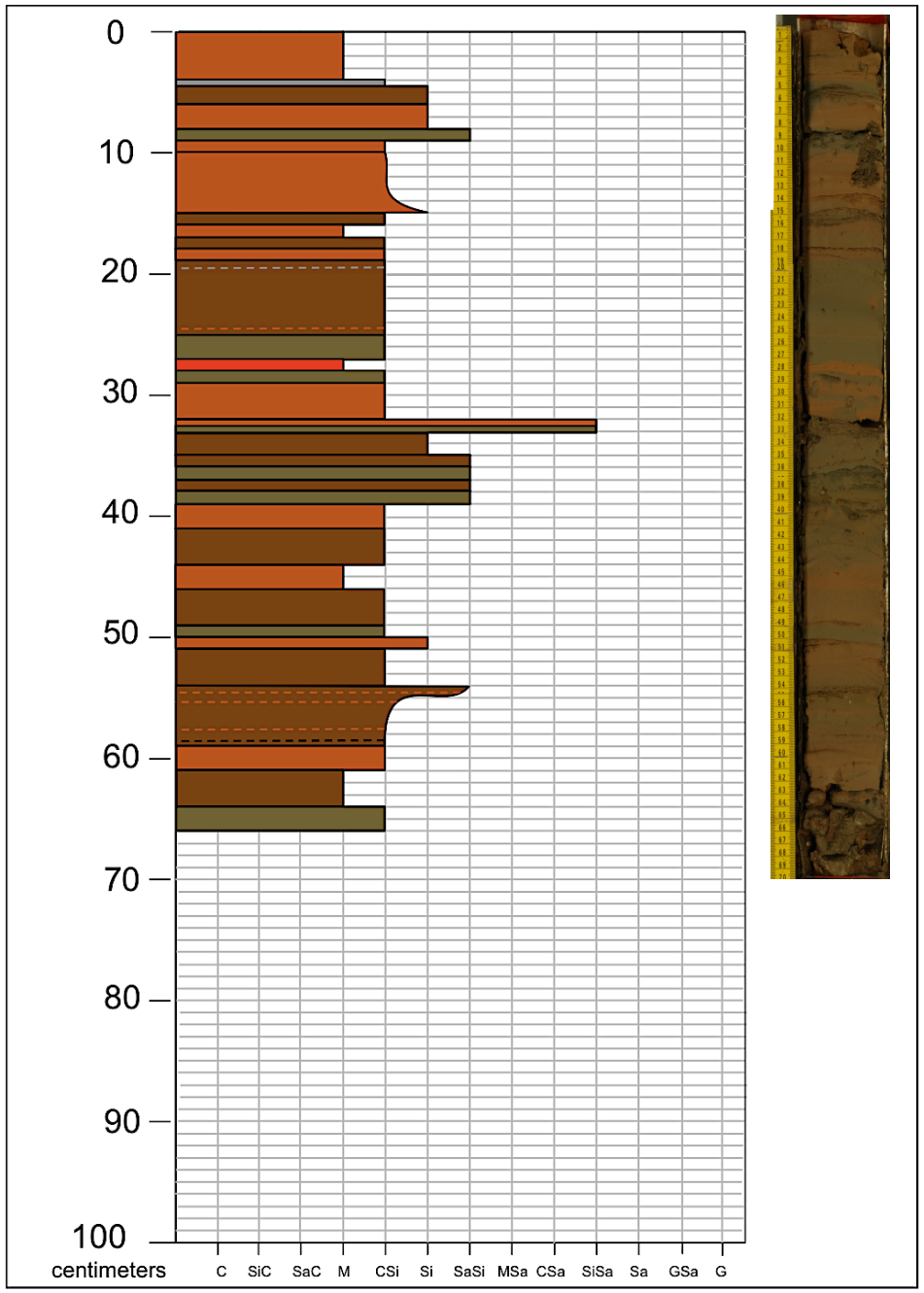

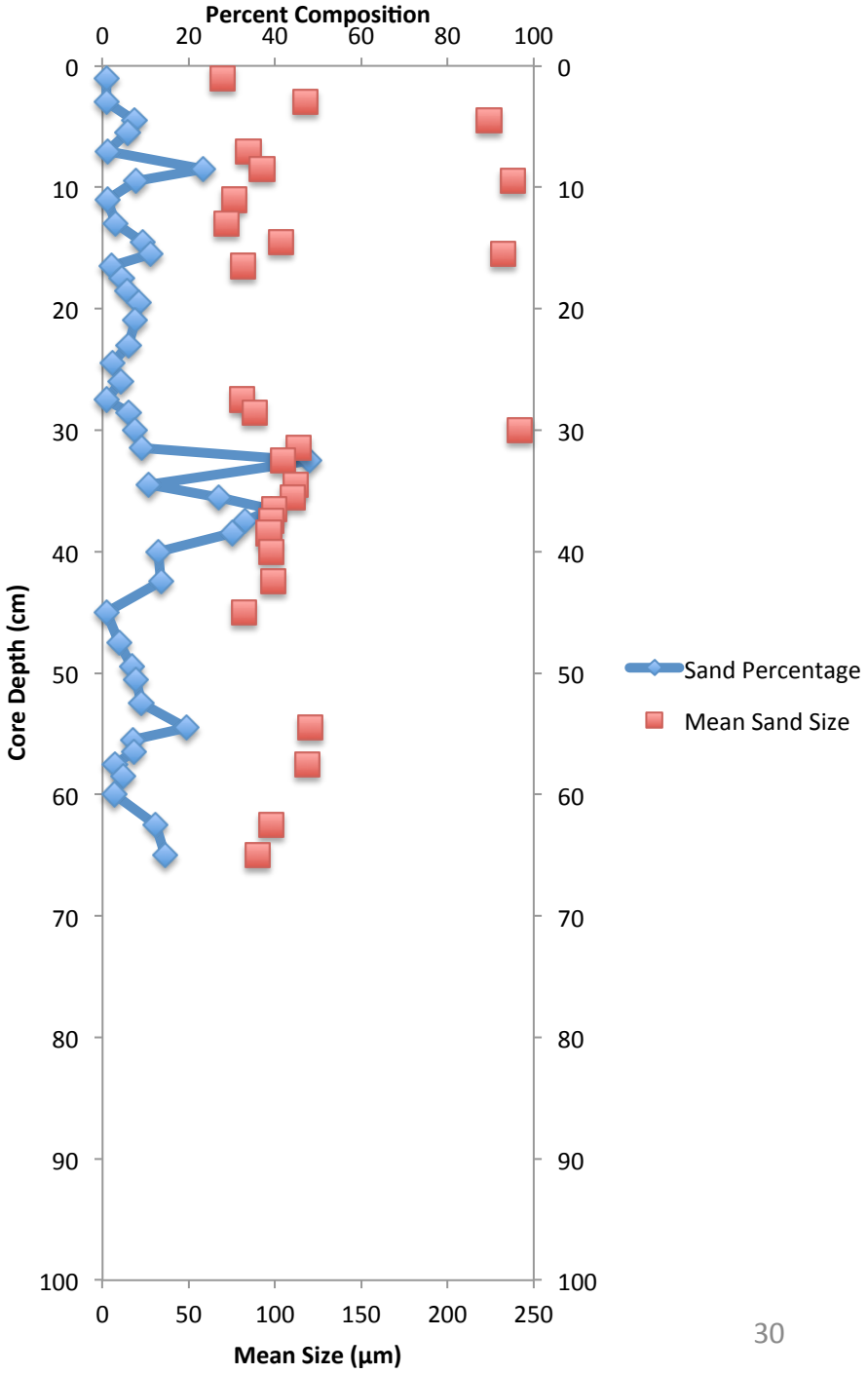

Brazos Delta Core: BDVC4

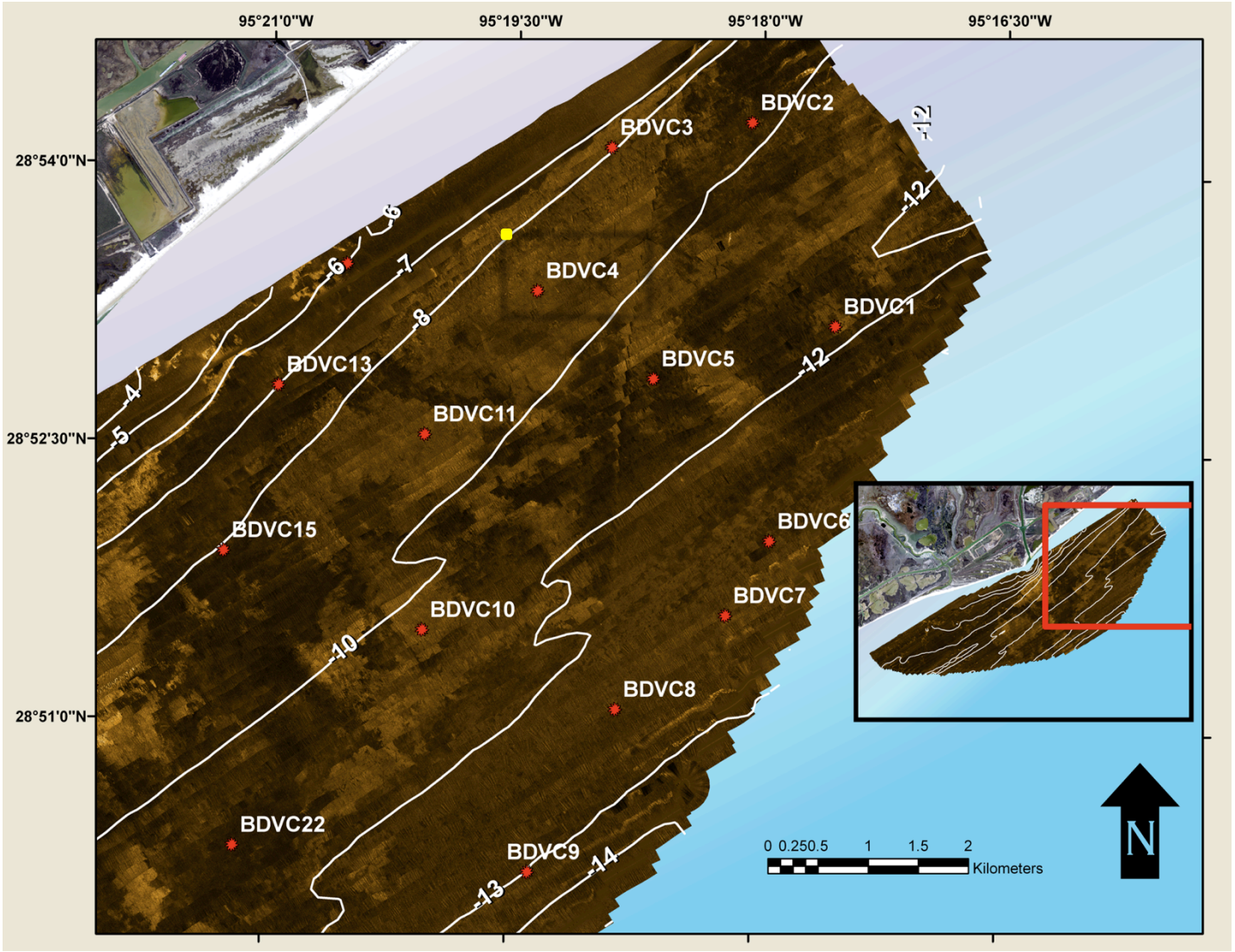

Project:_Brazos Delta Fall 2011___ Core: _BDVC04A_____

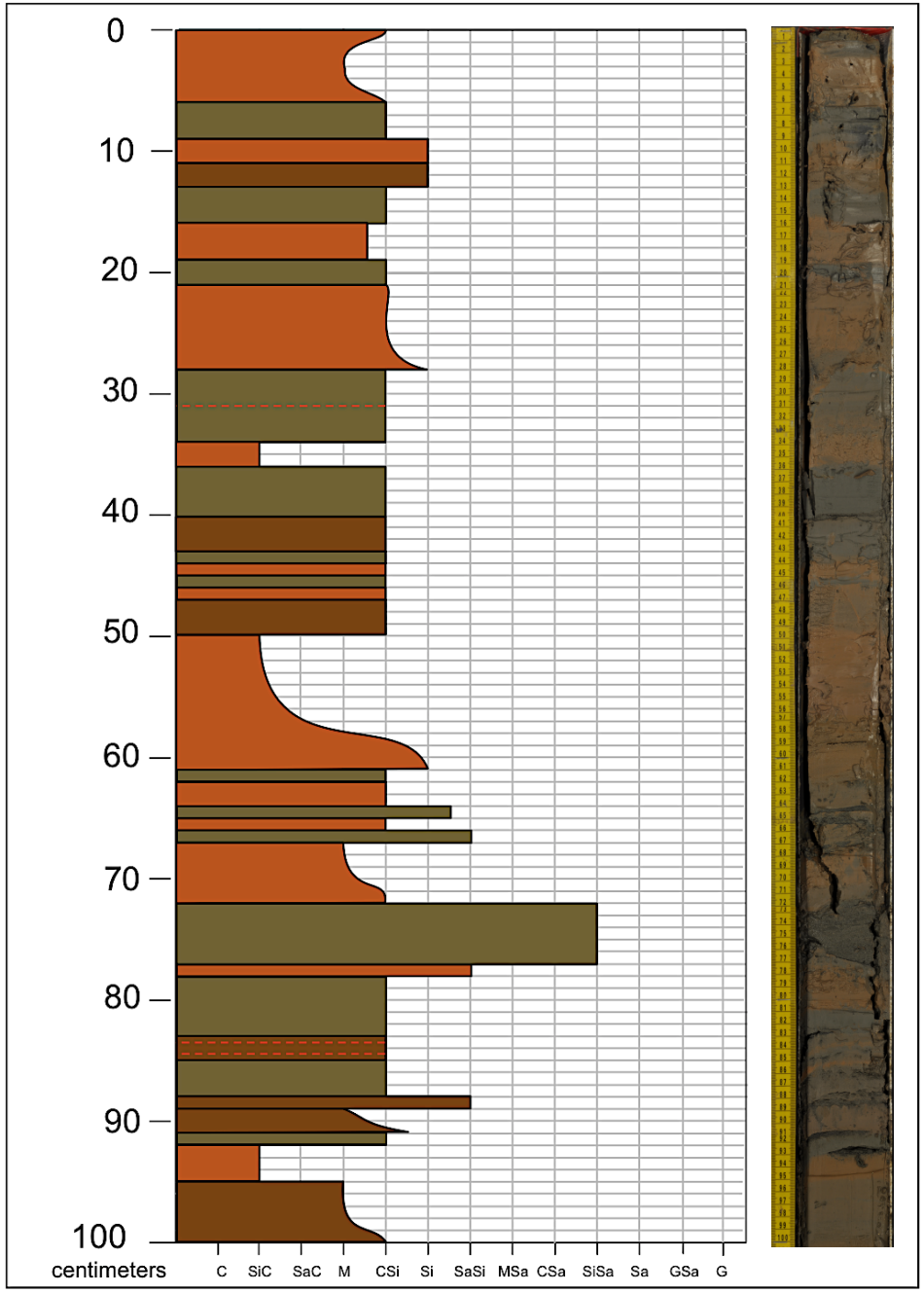

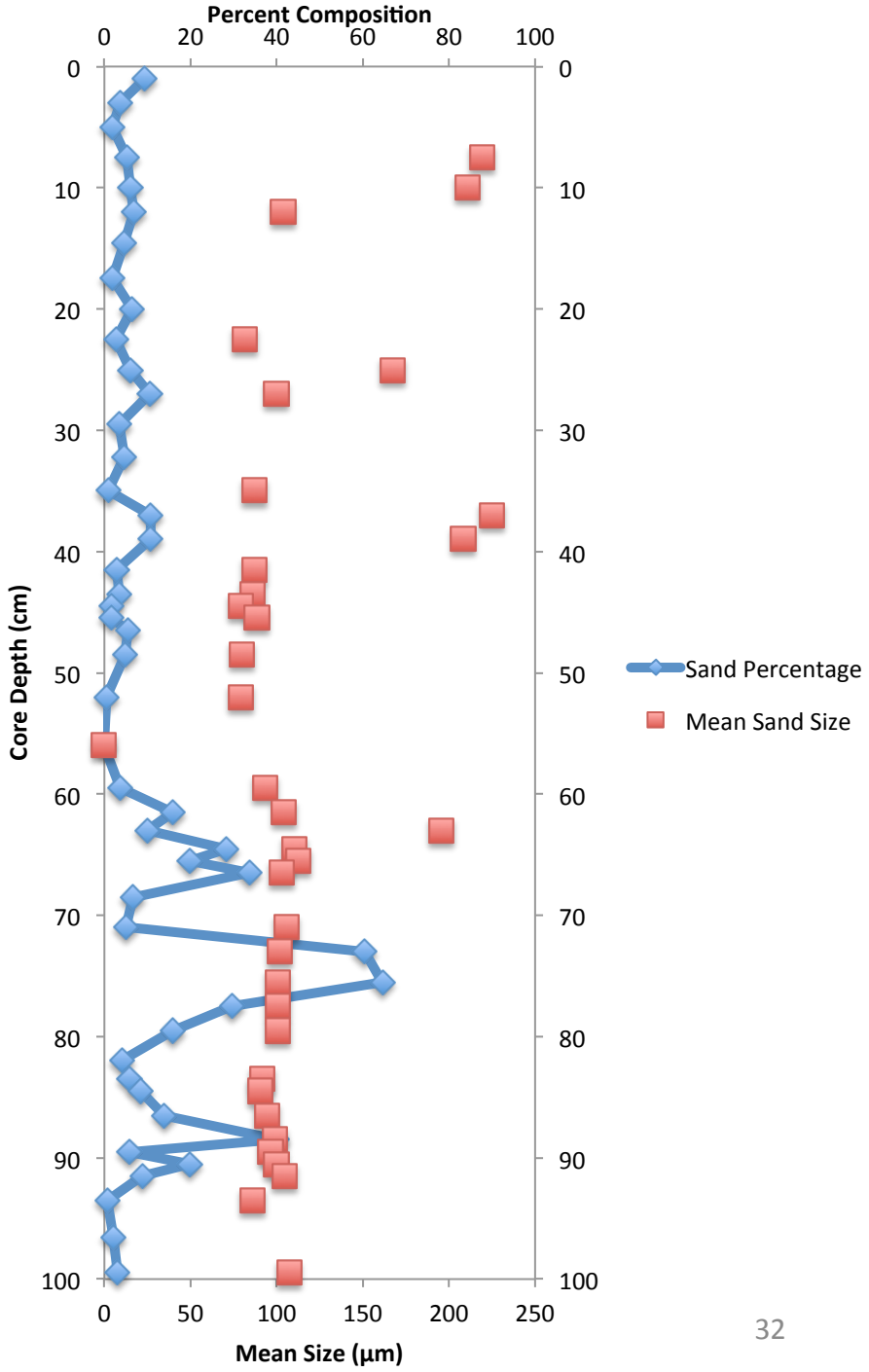

Project:_Brazos Delta Fall 2011___ Core: _BDVC04B_____

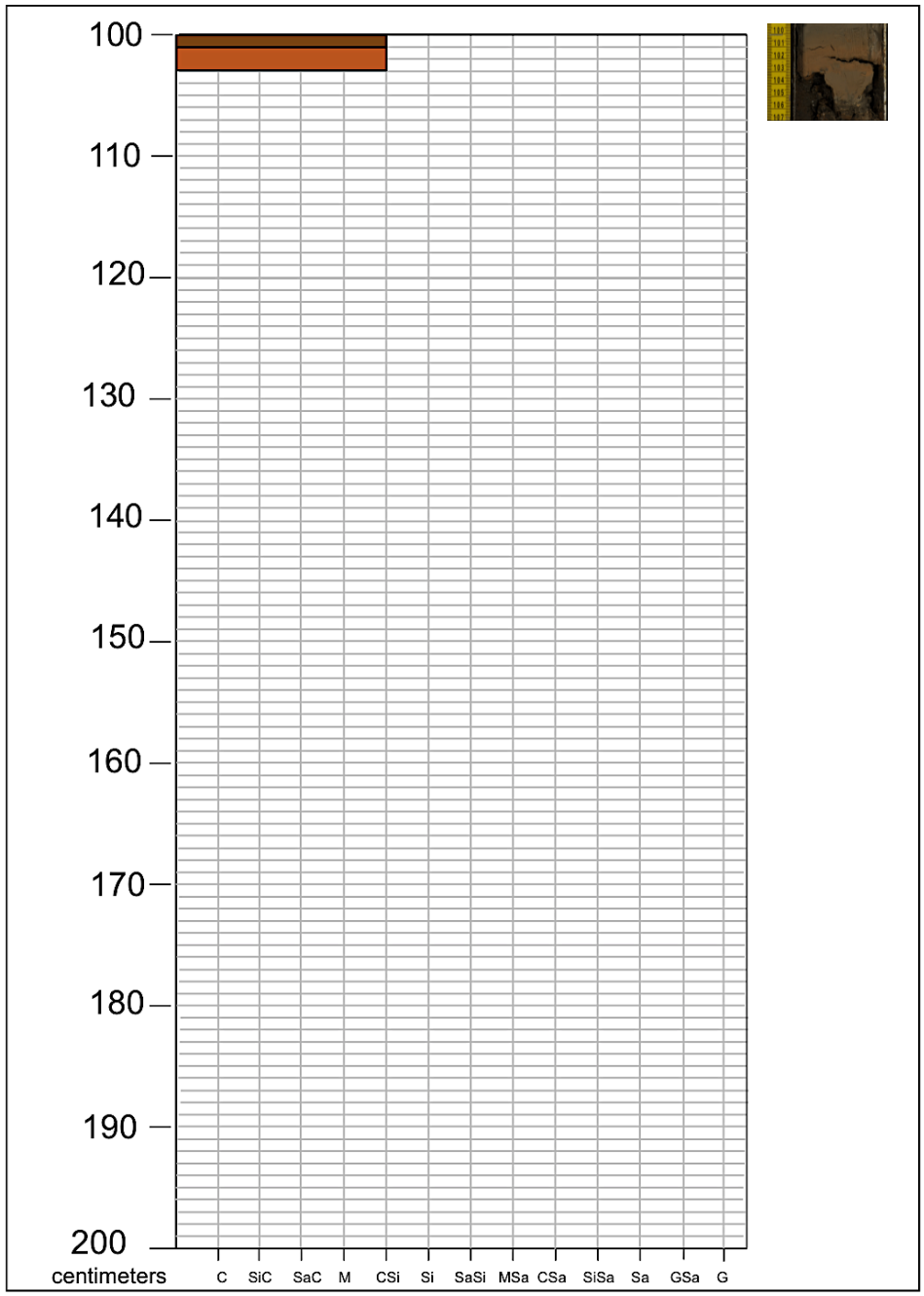

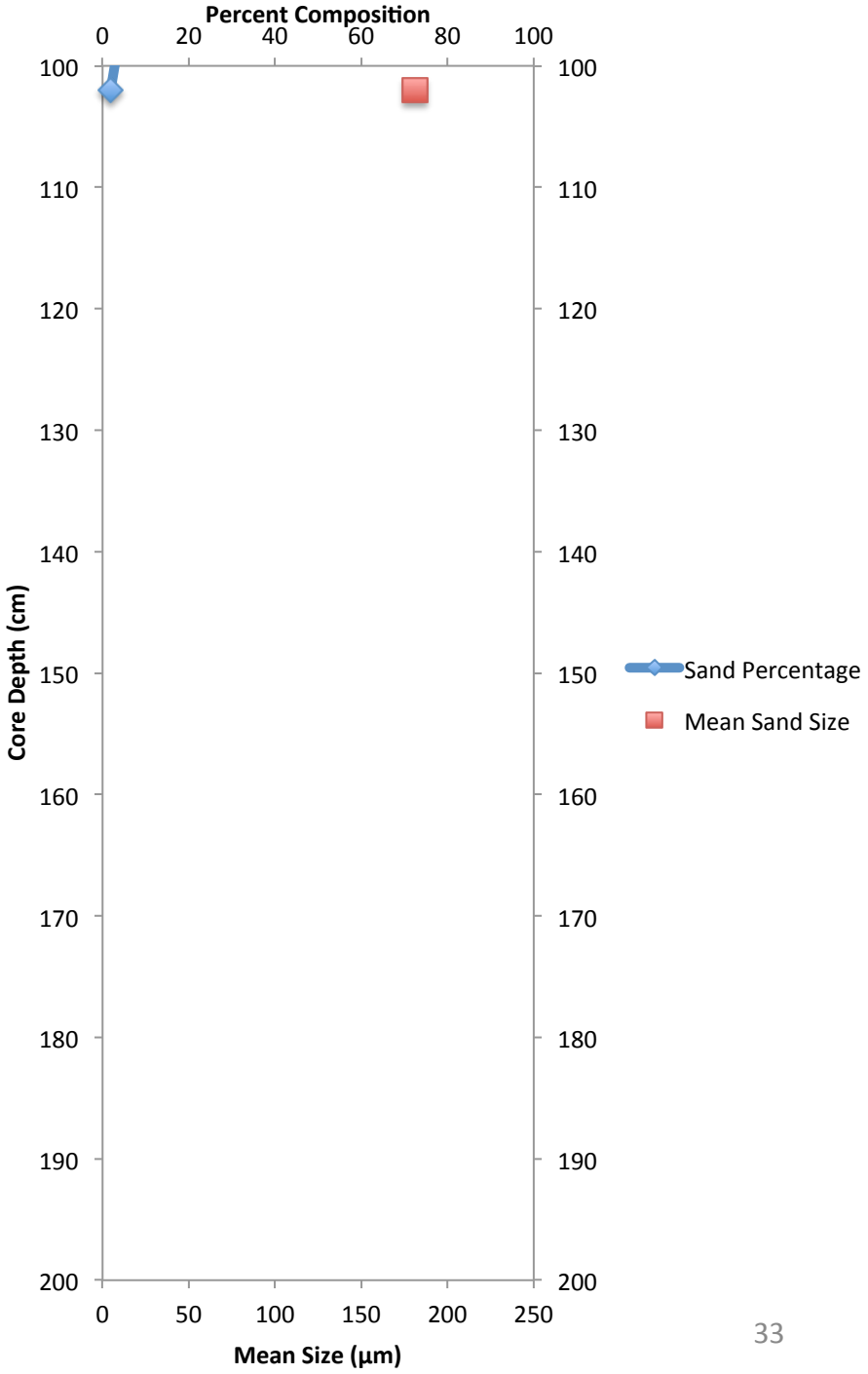

Brazos Delta Core: BDVC5

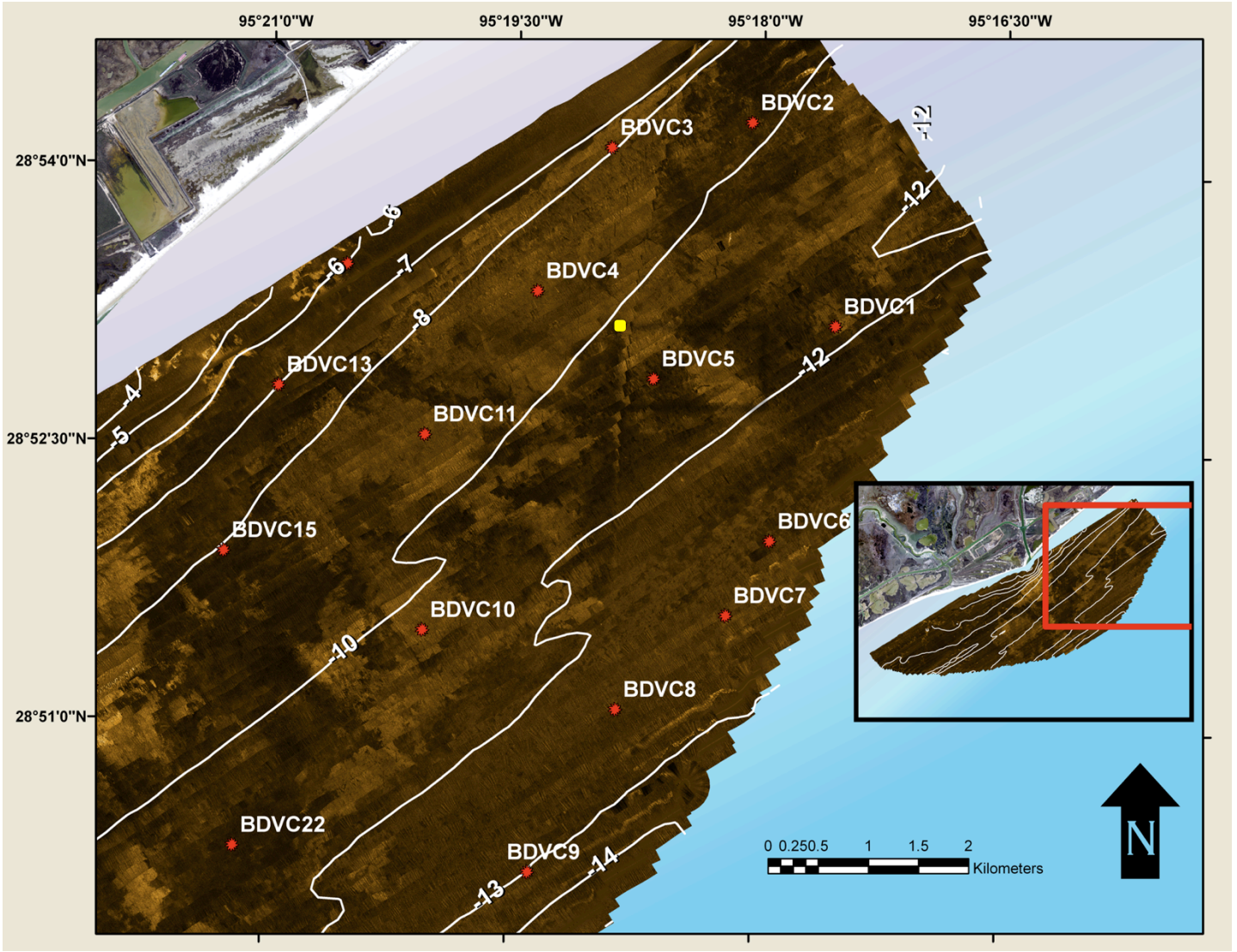

Project:_Brazos Delta Fall 2011___ Core: _BDVC05_____

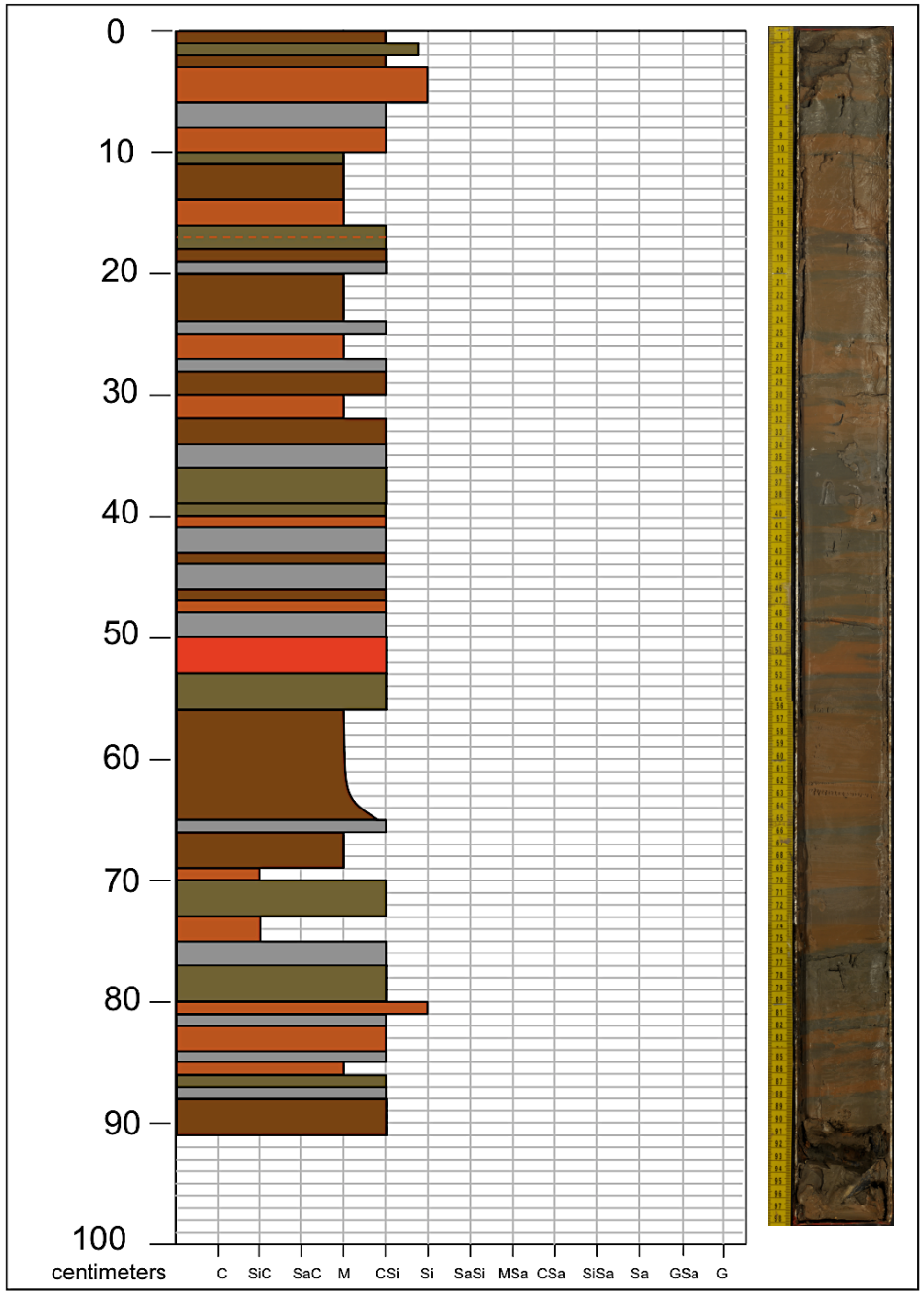

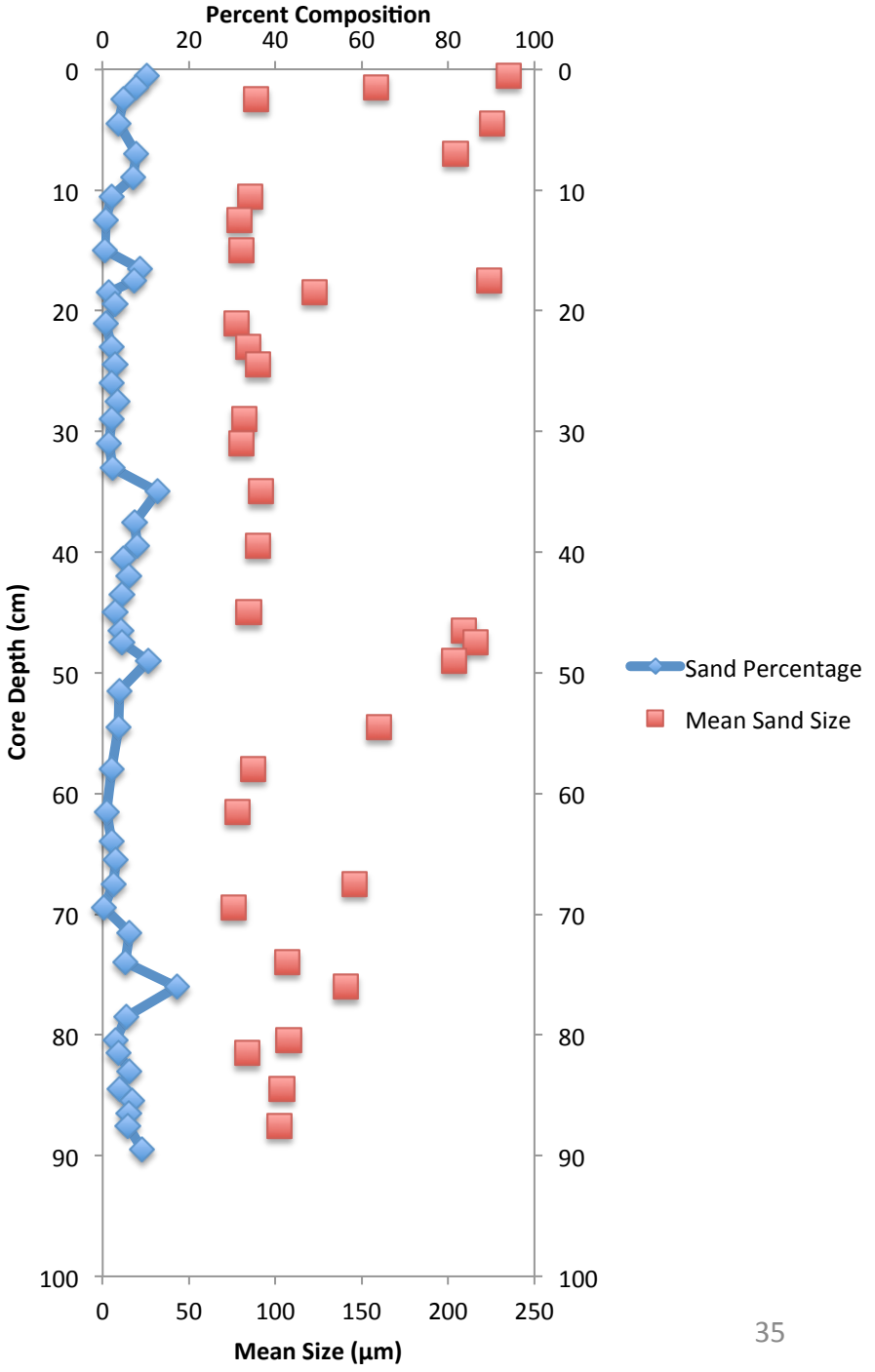

Brazos Delta Core: BDVC6

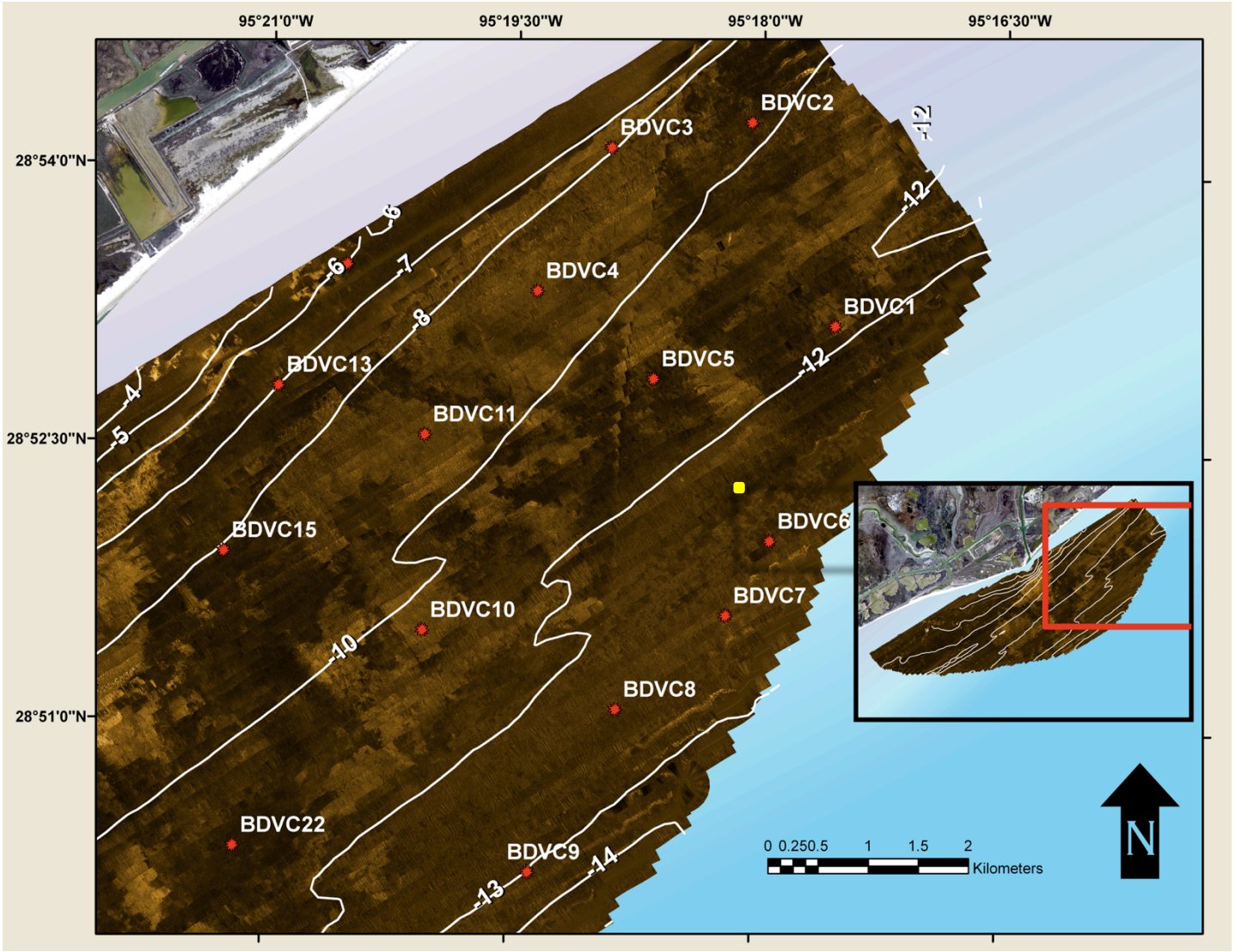

Project:_Brazos Delta Fall 2011___ Core: _BDVC06A_____

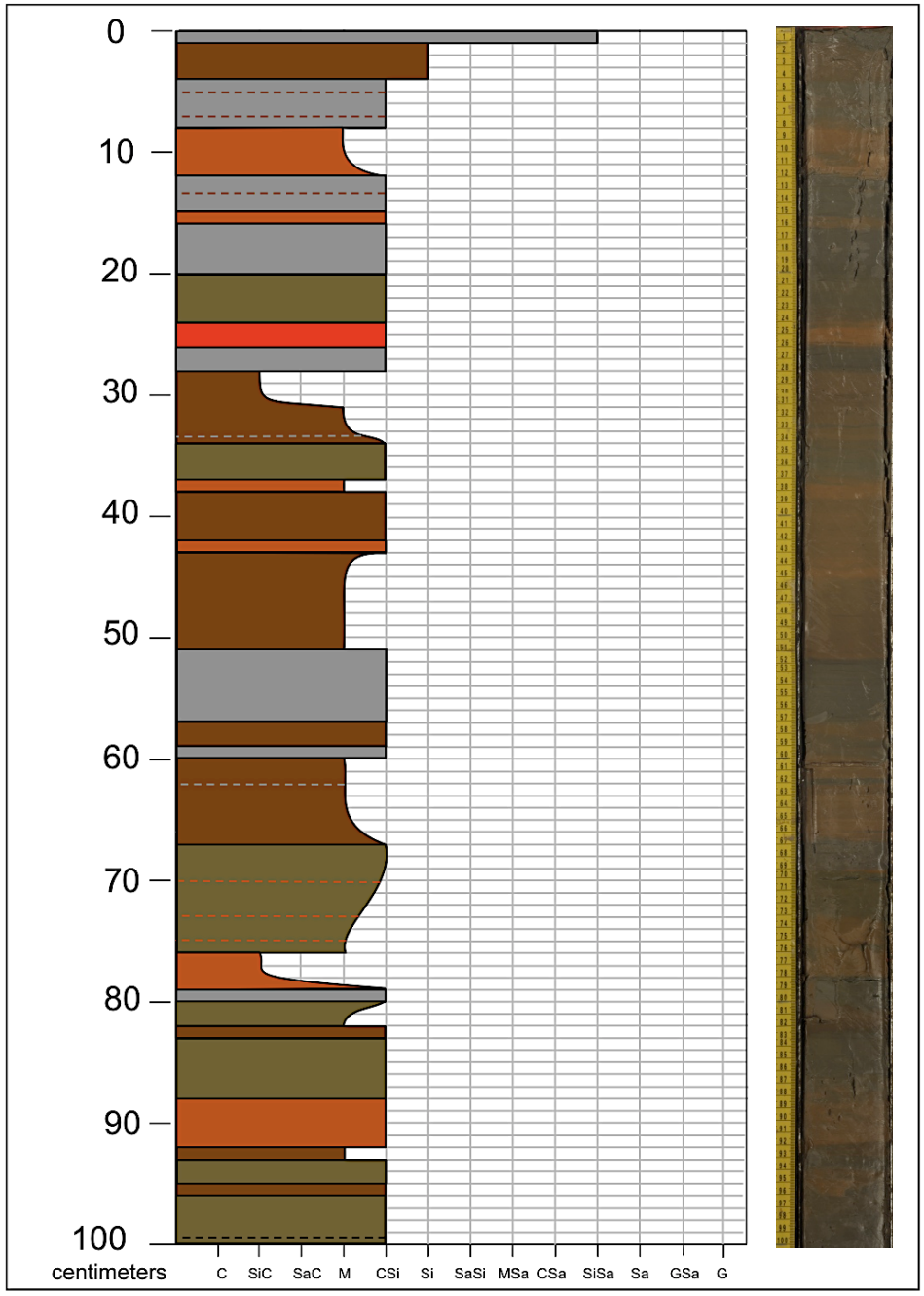

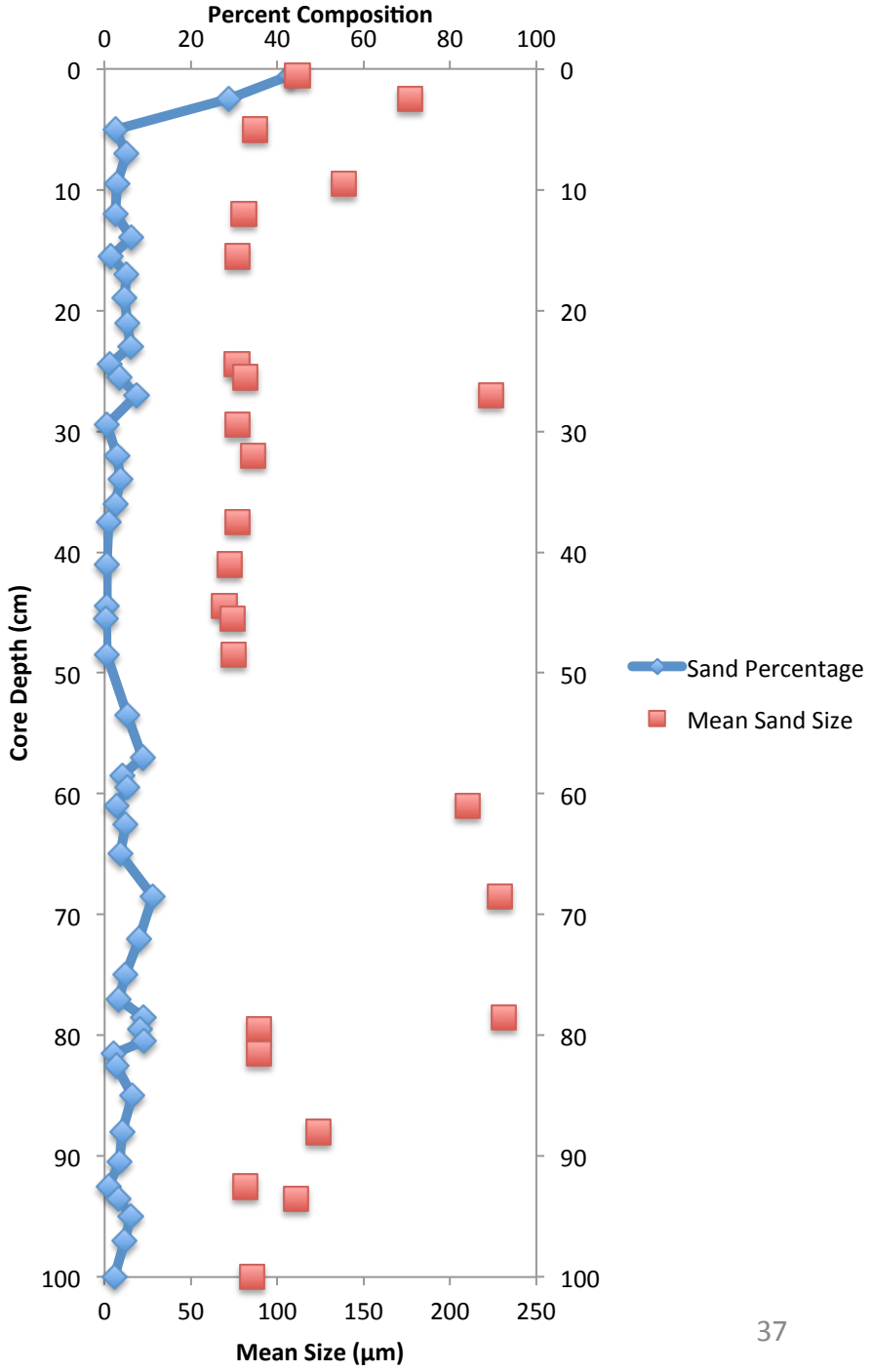

Project:_Brazos Delta Fall 2011___ Core: _BDVC06B_____

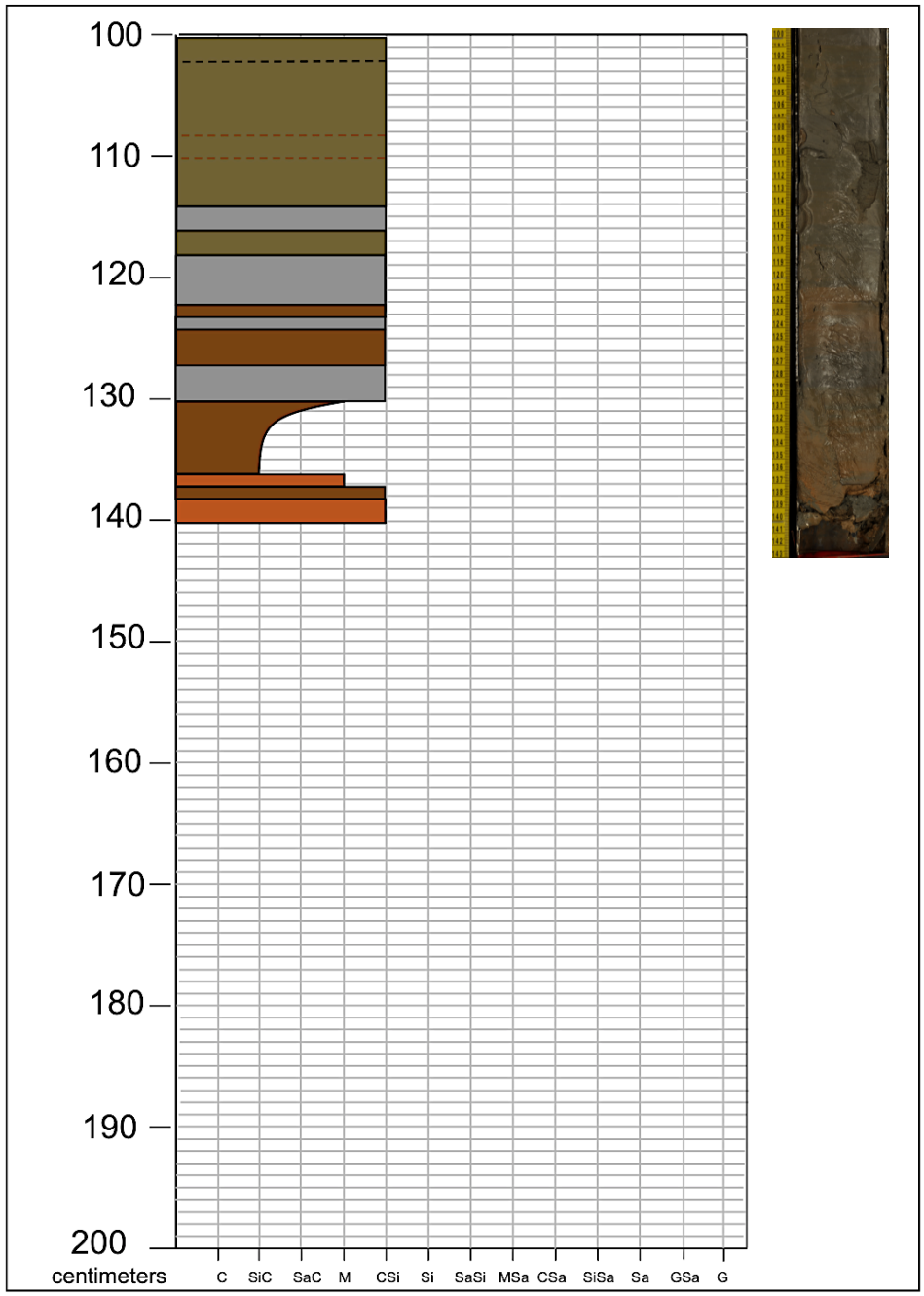

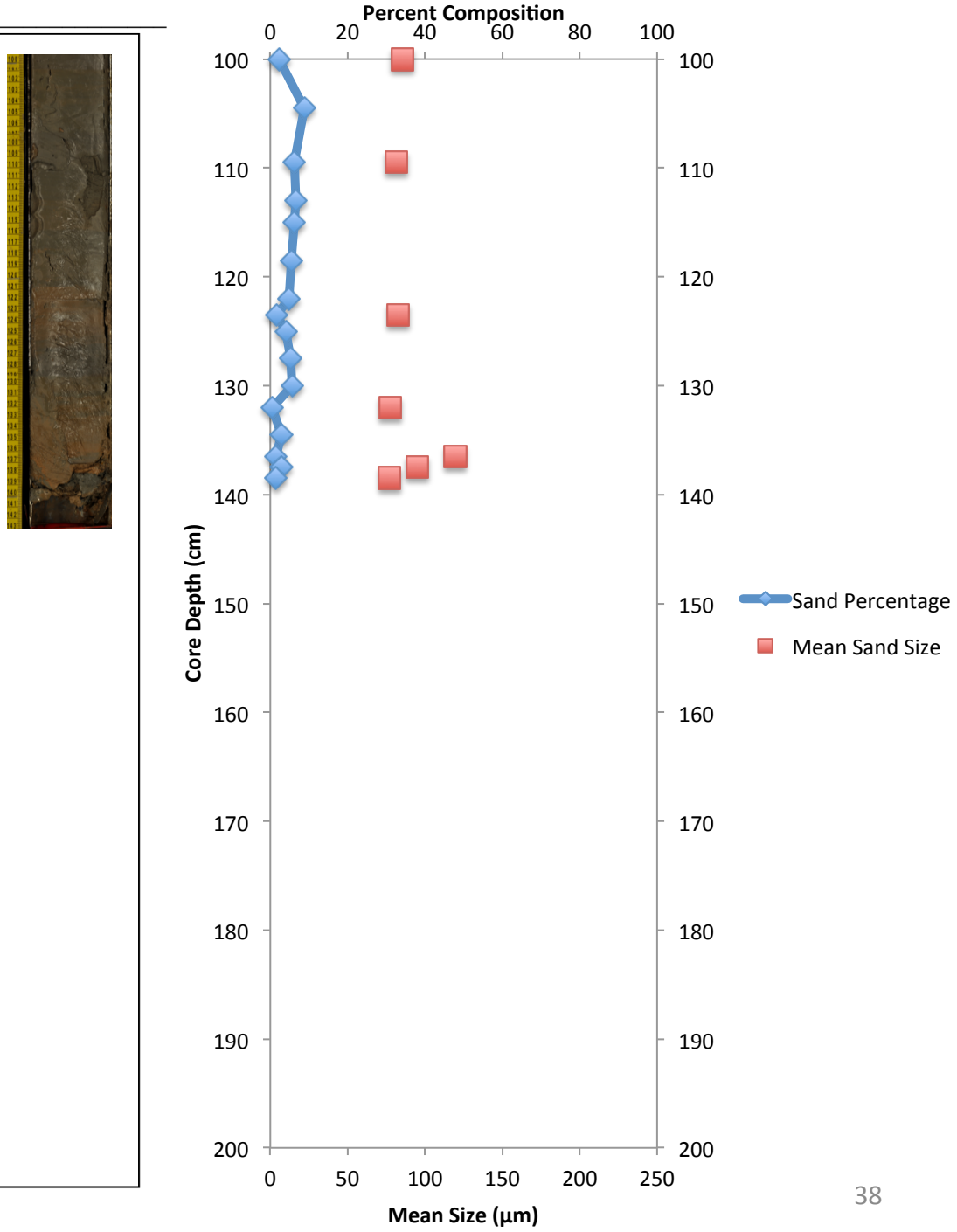

Brazos Delta Core: BDVC7

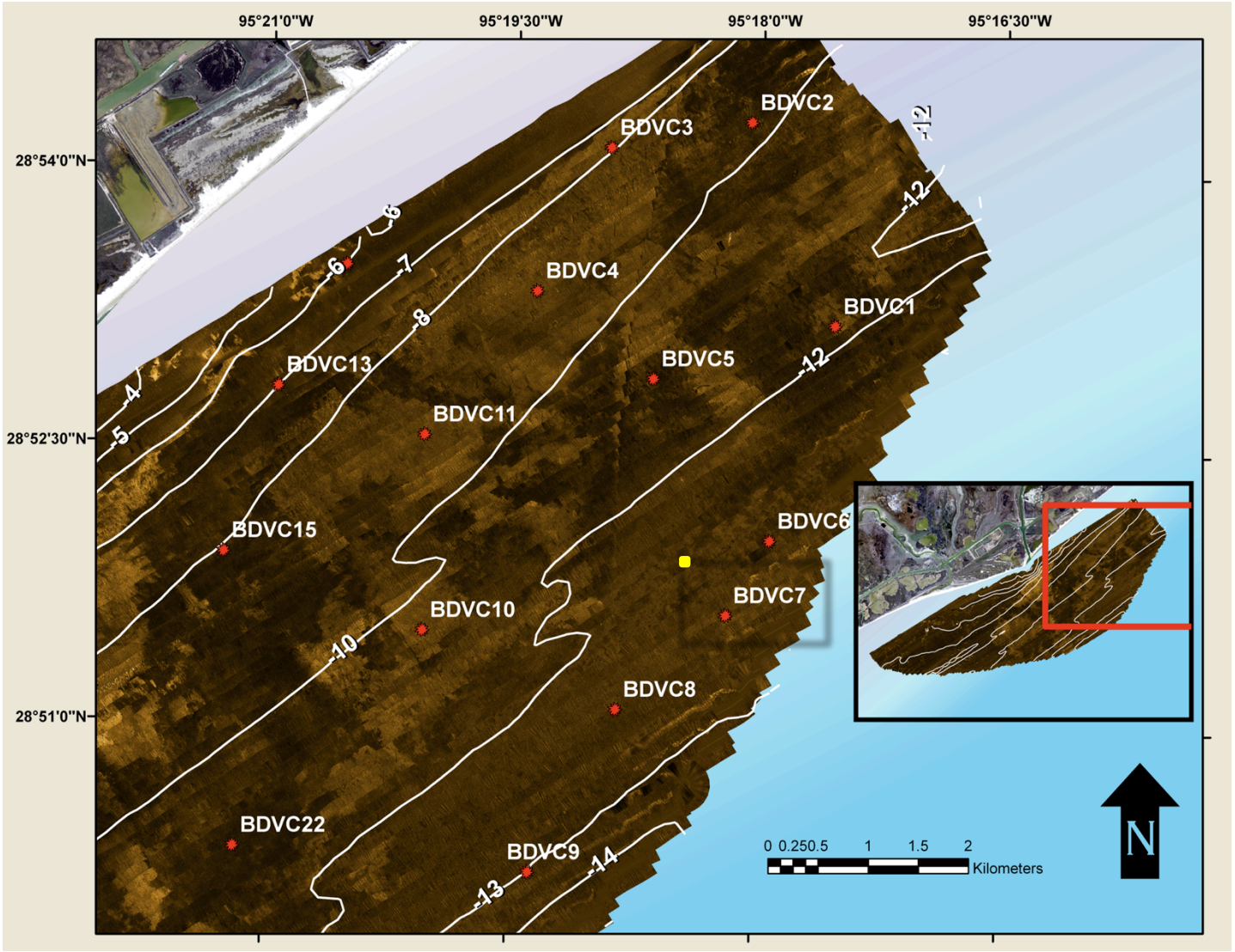

Project:_Brazos Delta Fall 2011___ Core: _BDVC07_____

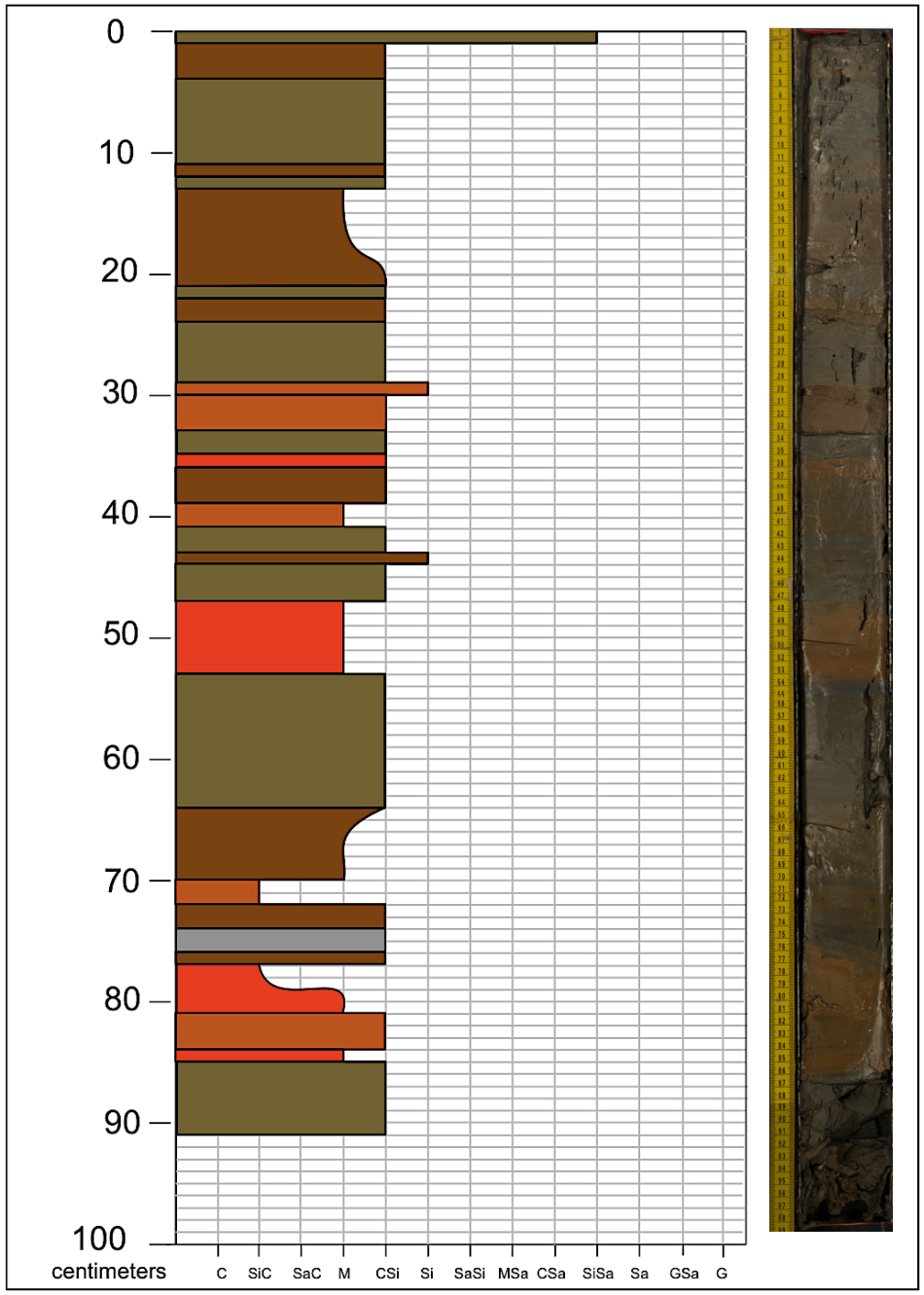

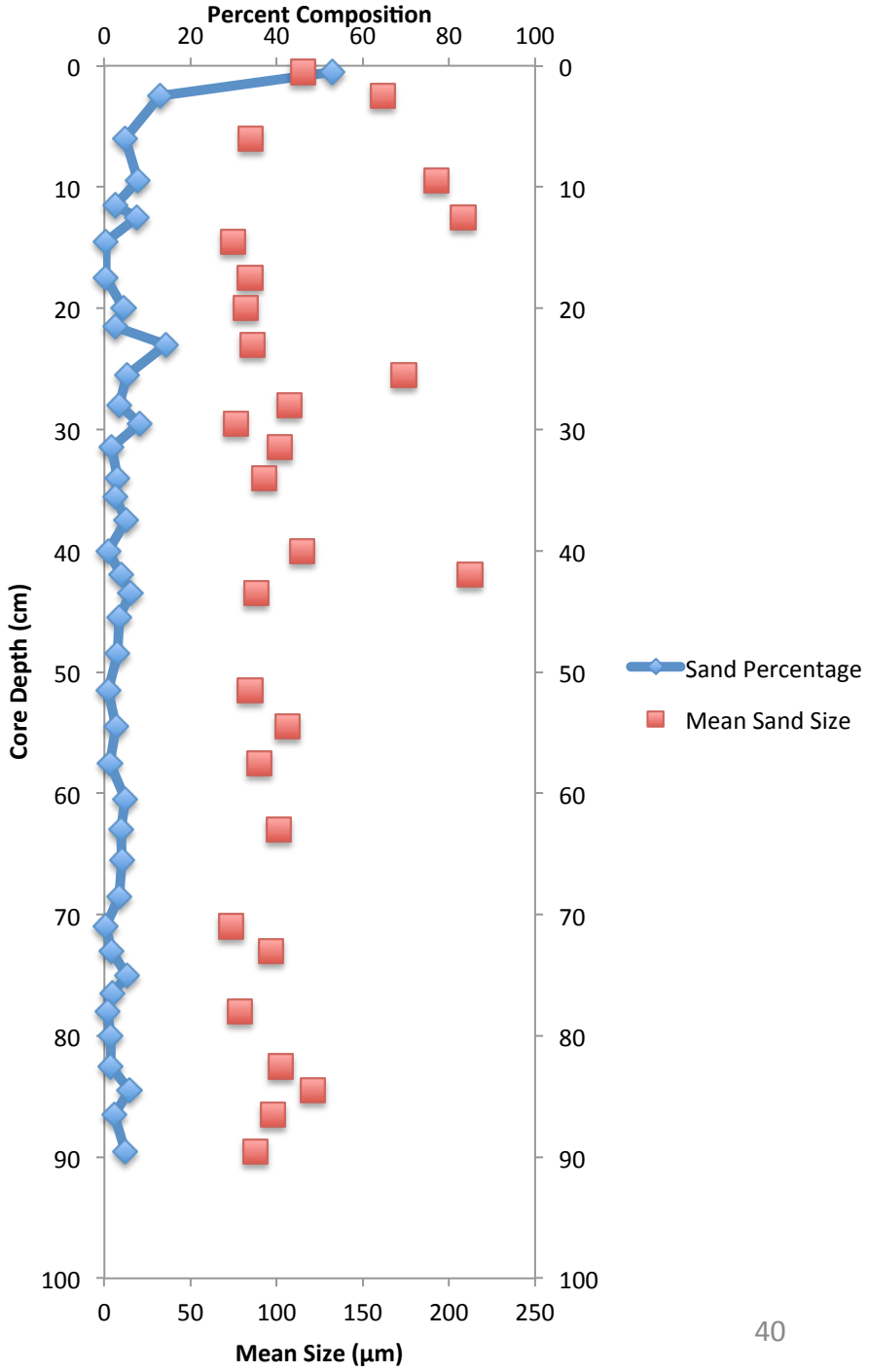

Brazos Delta Core: BDVC8

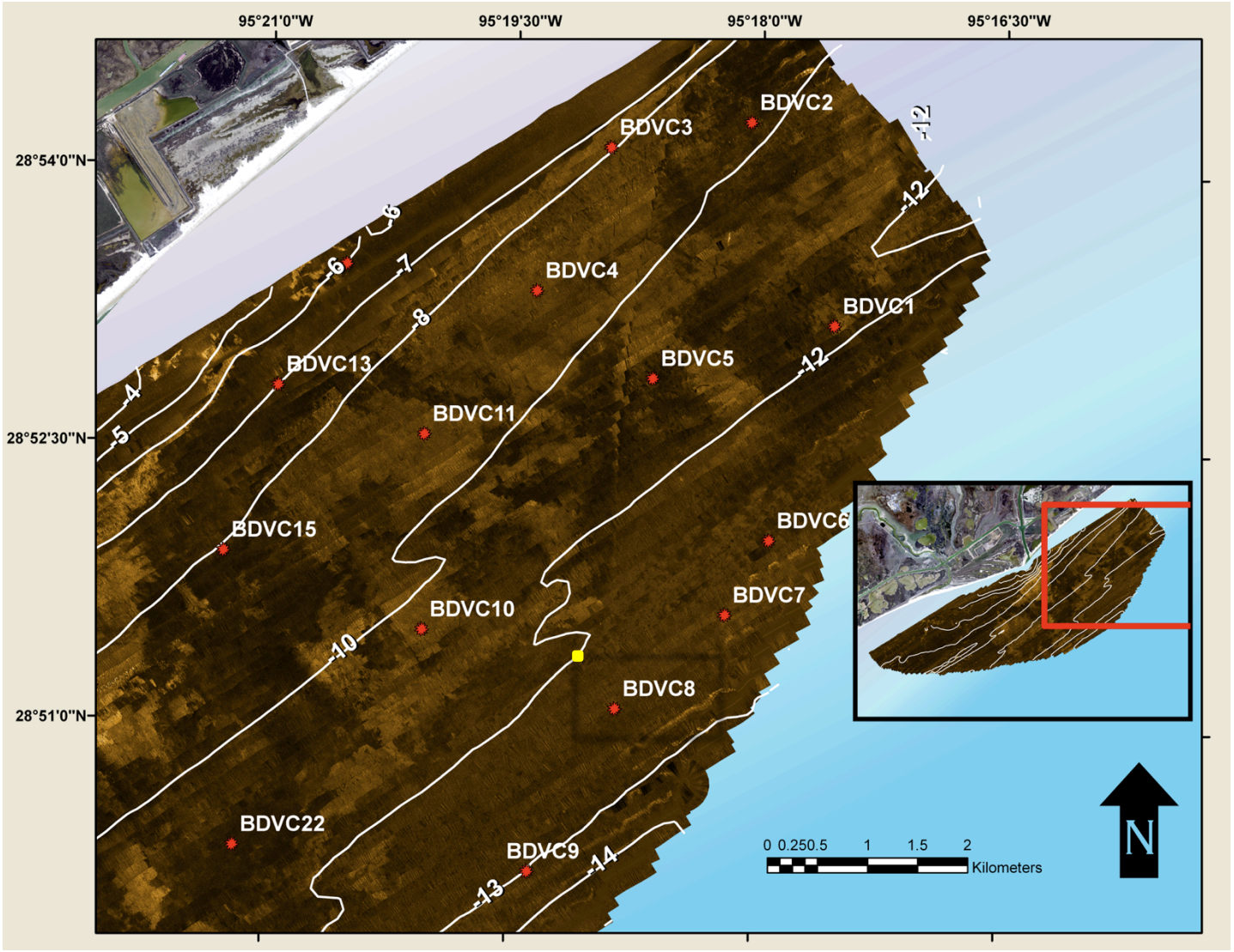

Project:_Brazos Delta Fall 2011___ Core: _BDVC08_____

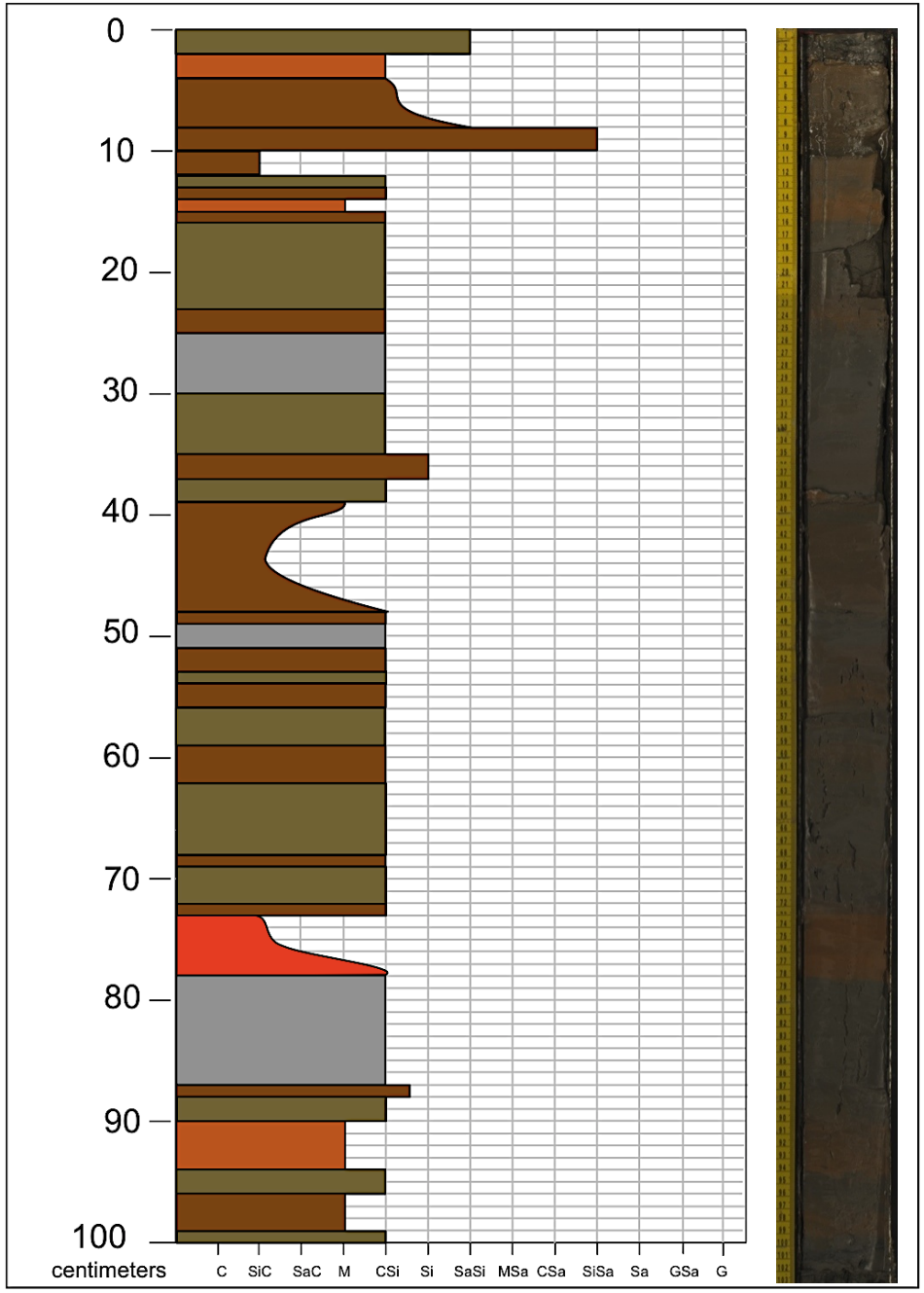

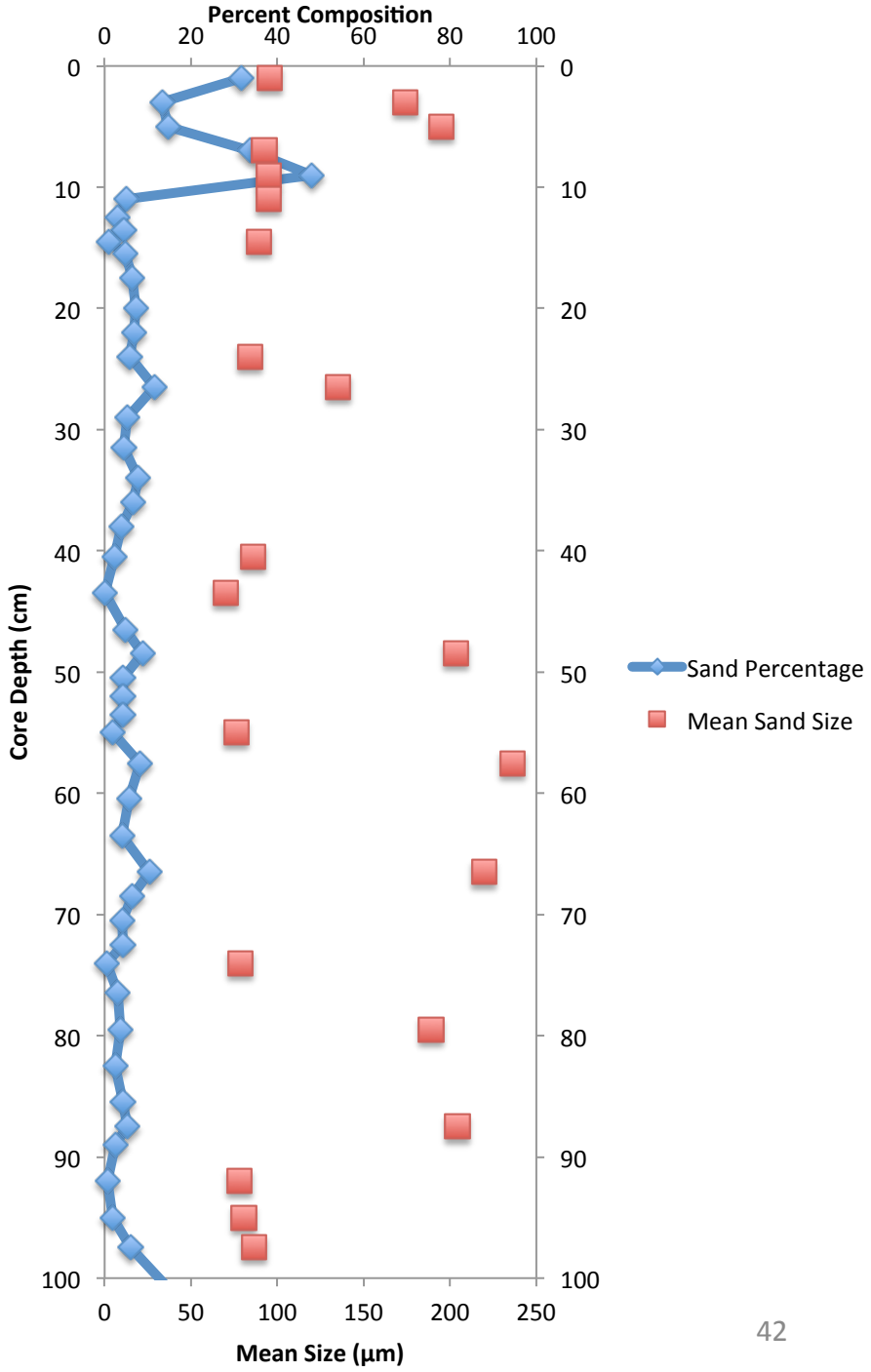

Brazos Delta Core: BDVC9

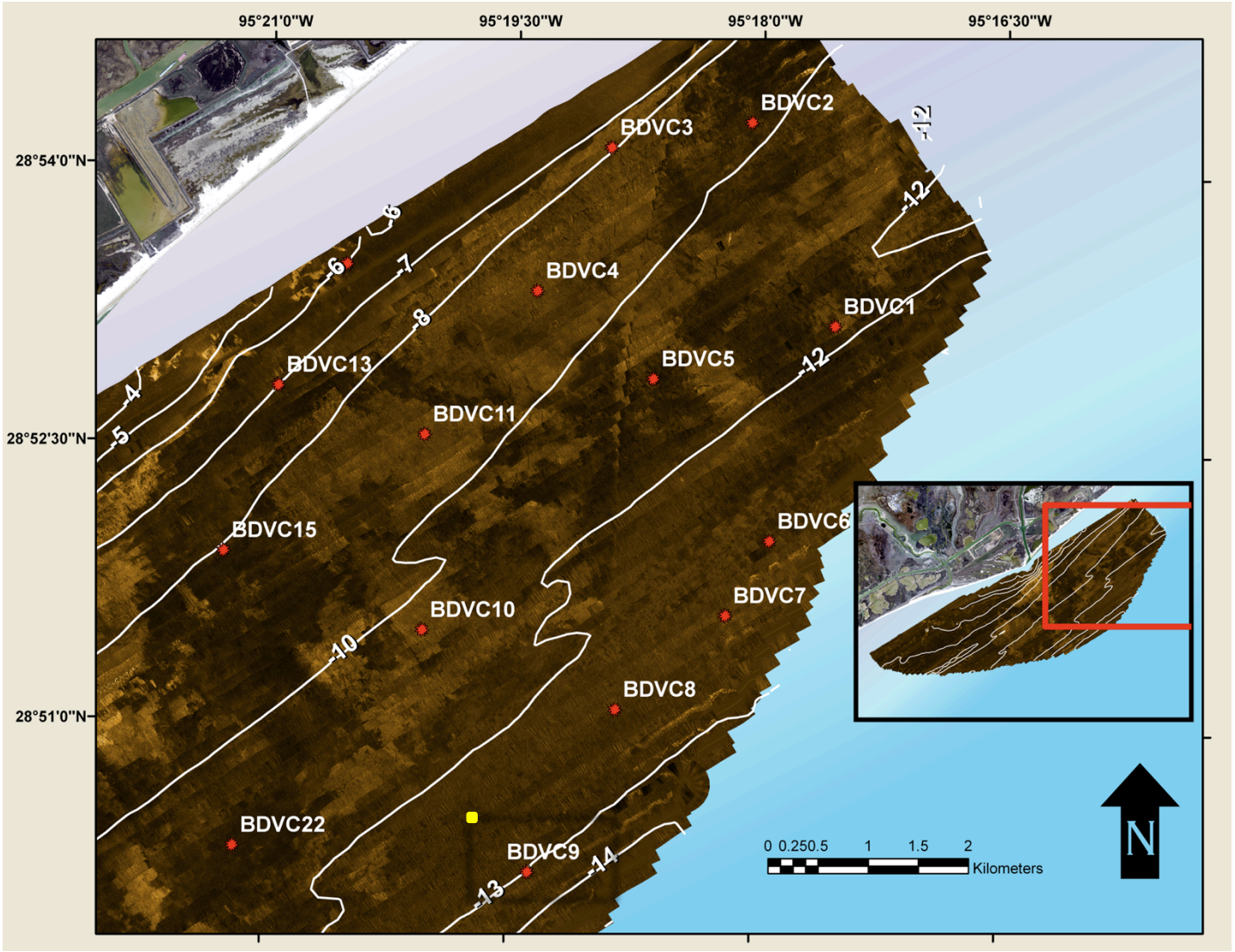

Project:_Brazos Delta Fall 2011___ Core: _BDVC09A_____

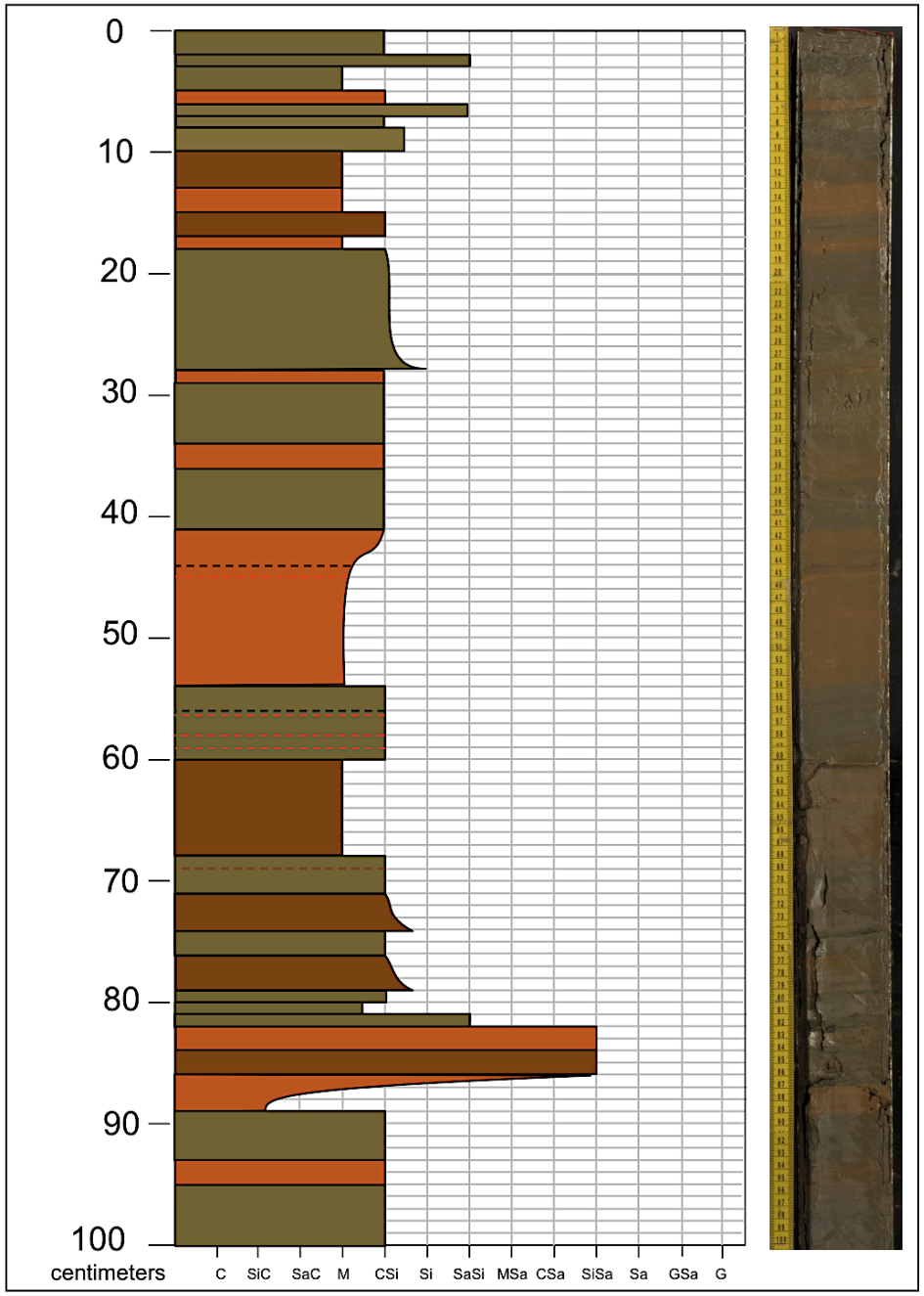

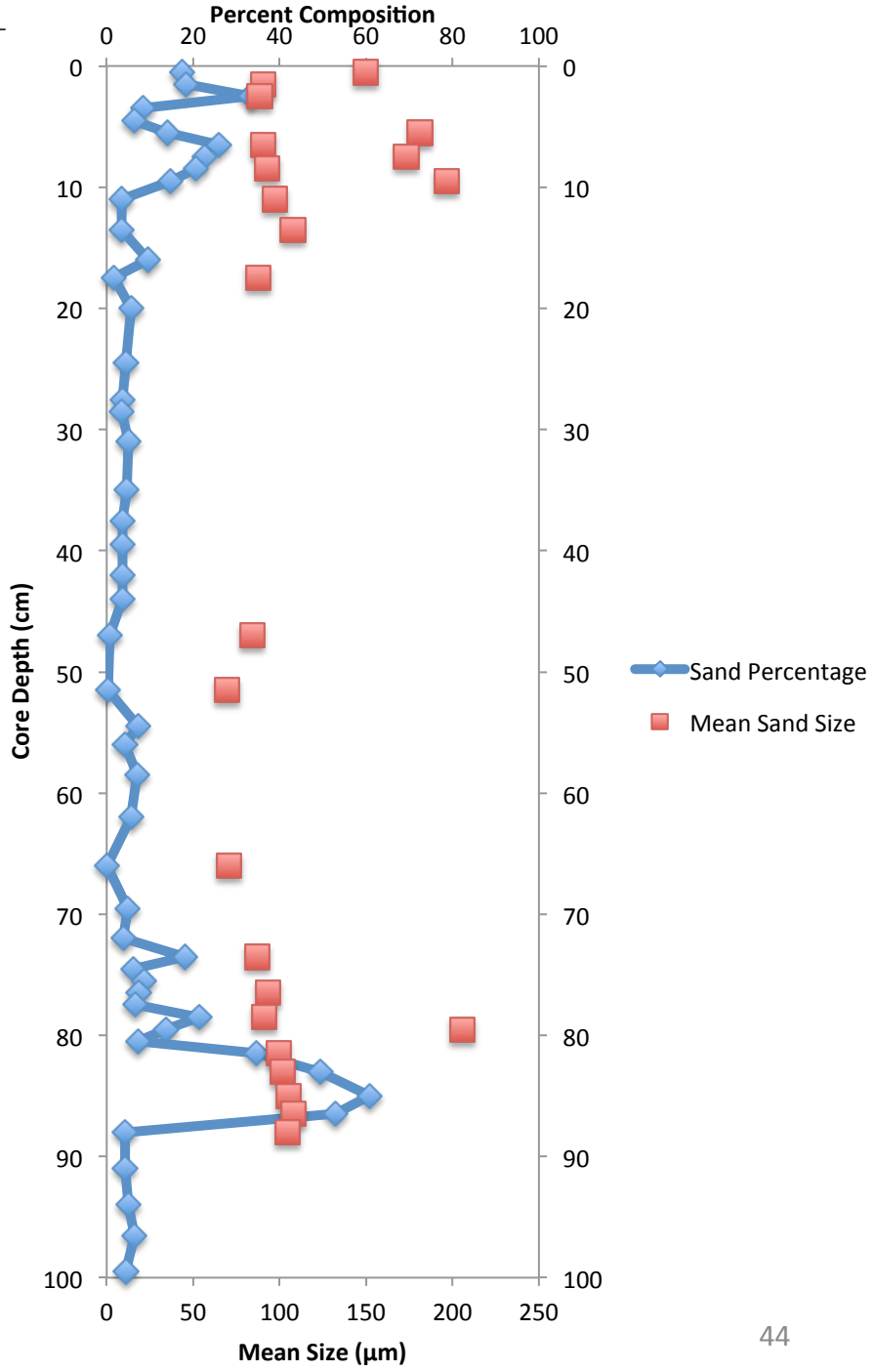

Project:_Brazos Delta Fall 2011___ Core: _BDVC09B_____

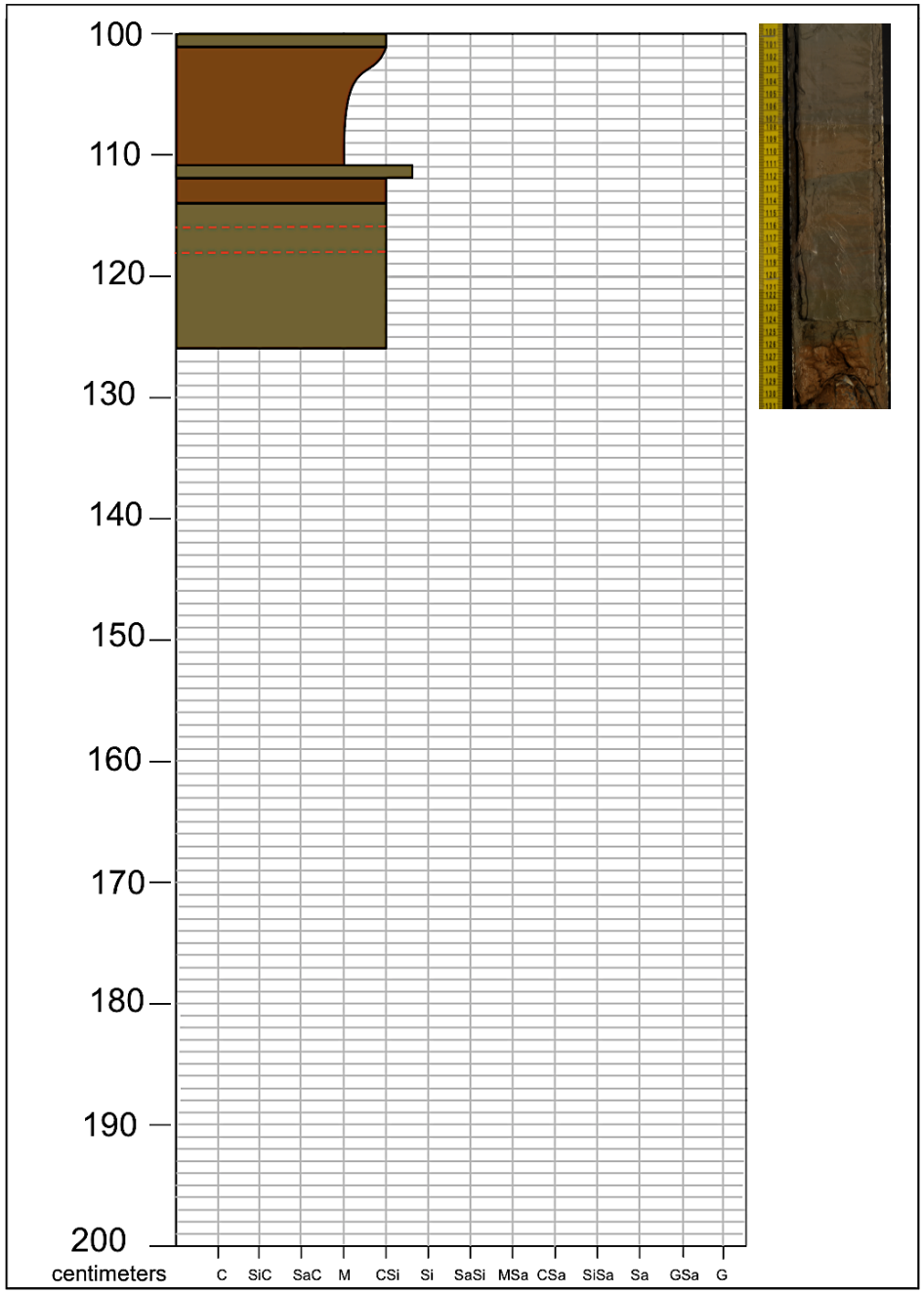

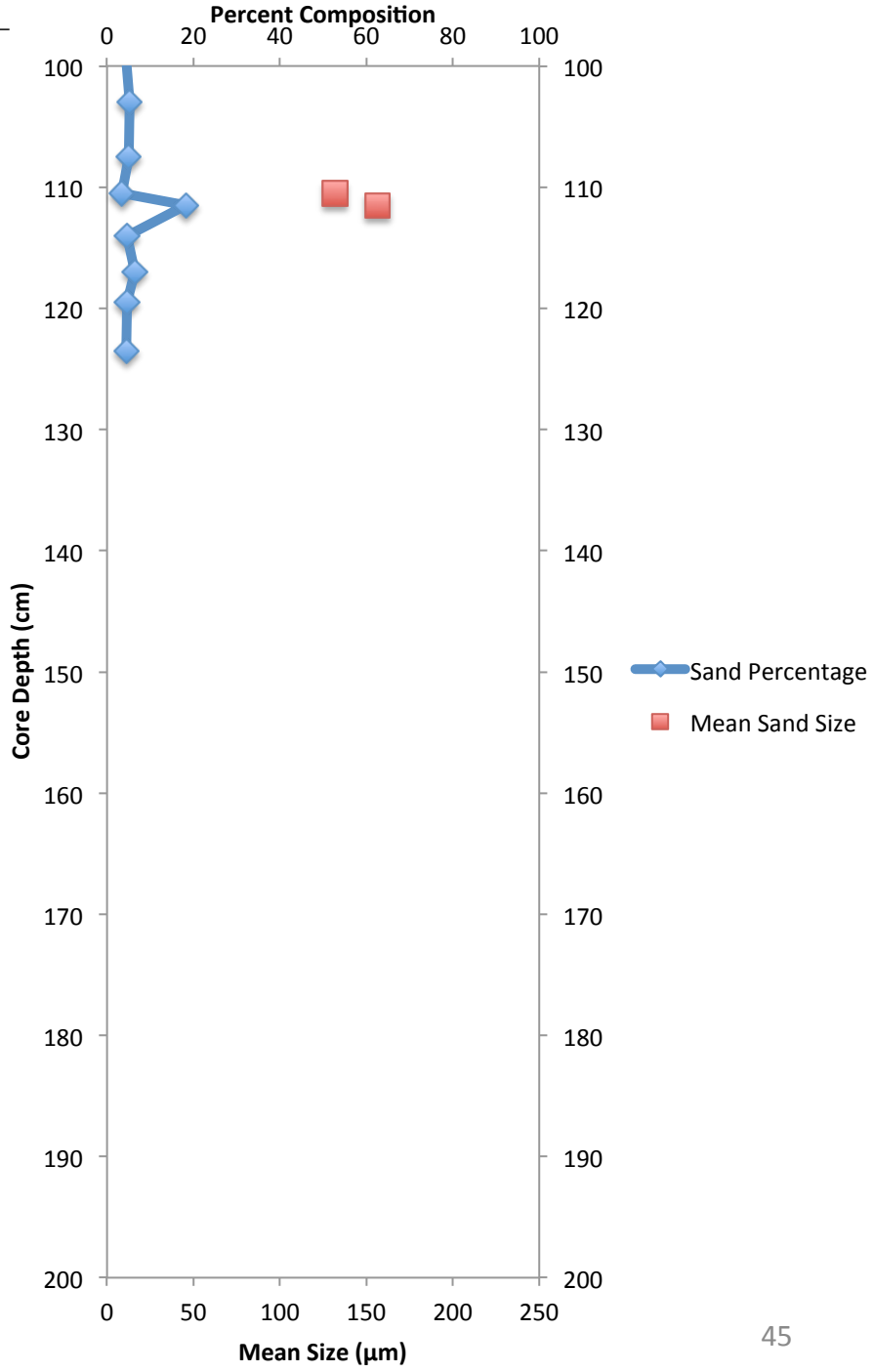

Brazos Delta Core: BDVC10

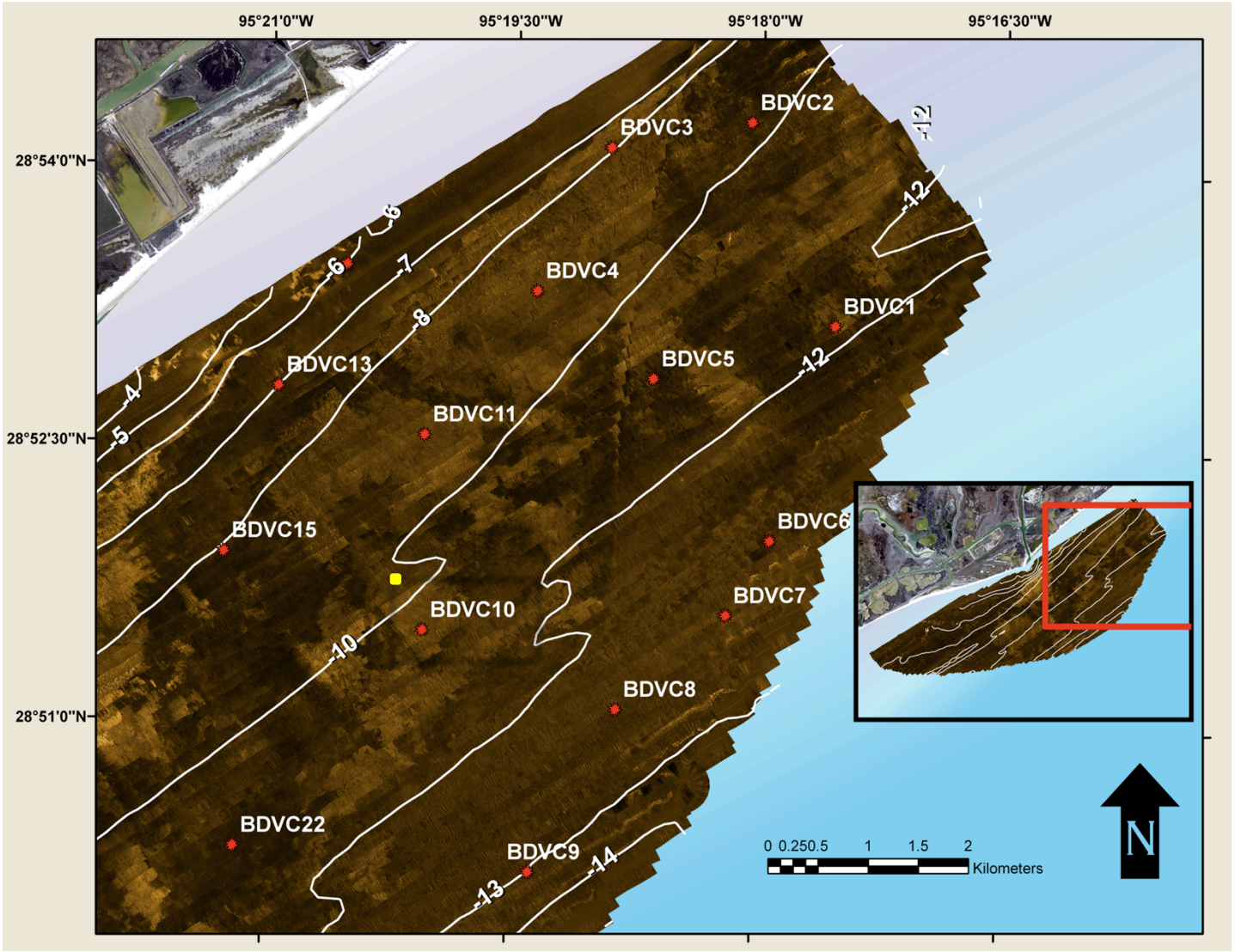

Project:_Brazos Delta Fall 2011___ Core: _BDVC10A_____

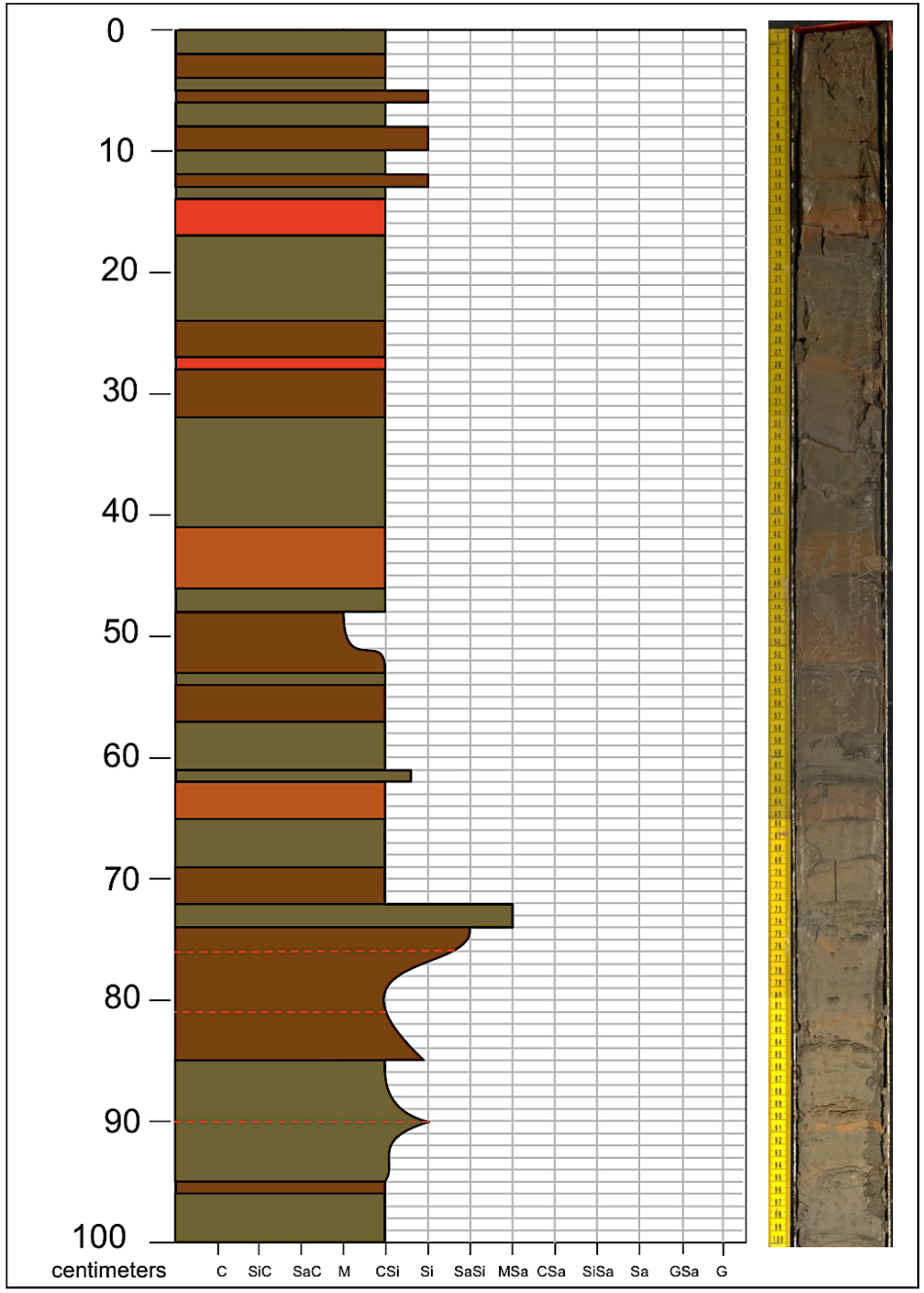

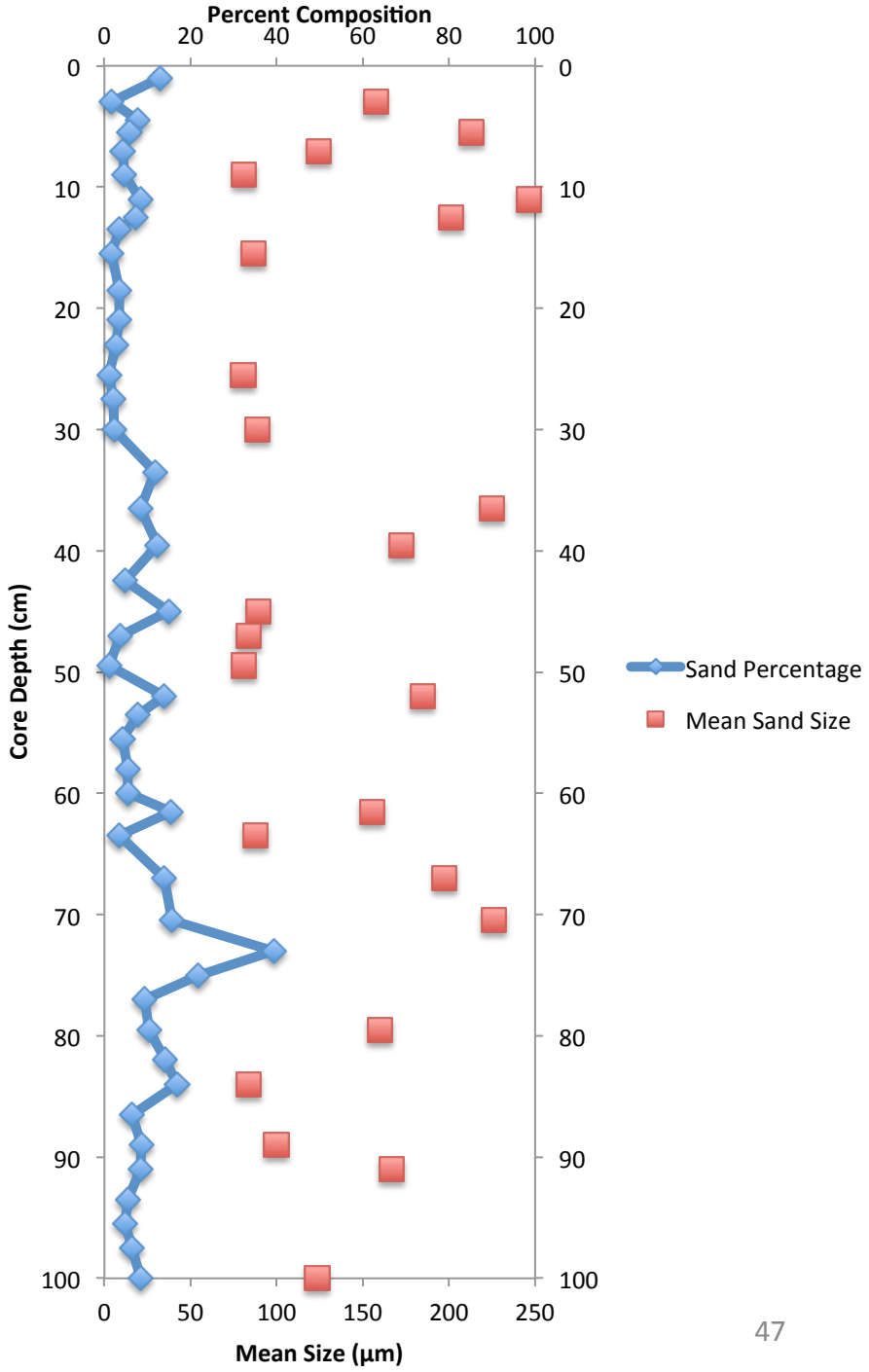

Project:_Brazos Delta Fall 2011___ Core: _BDVC10B_____

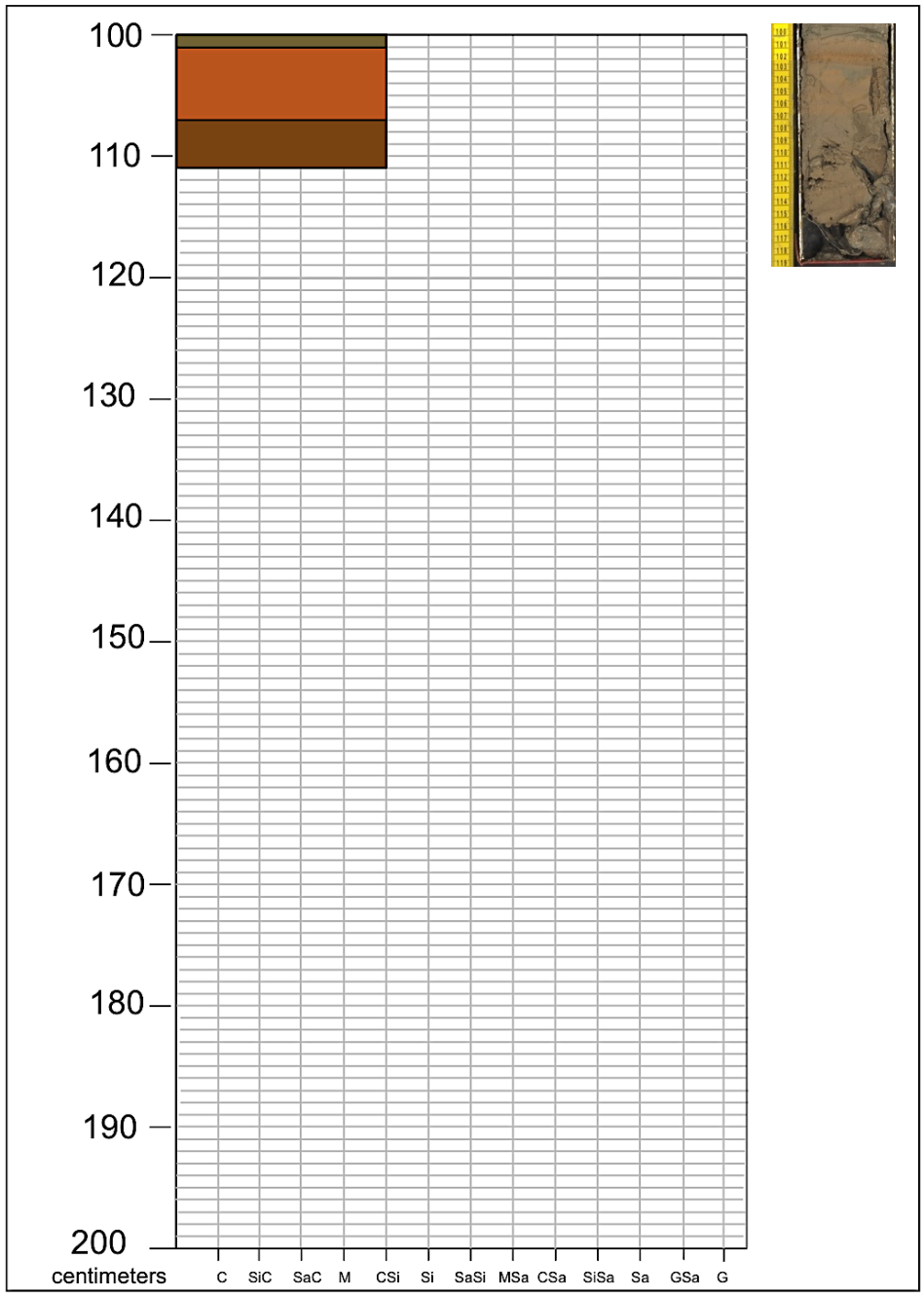

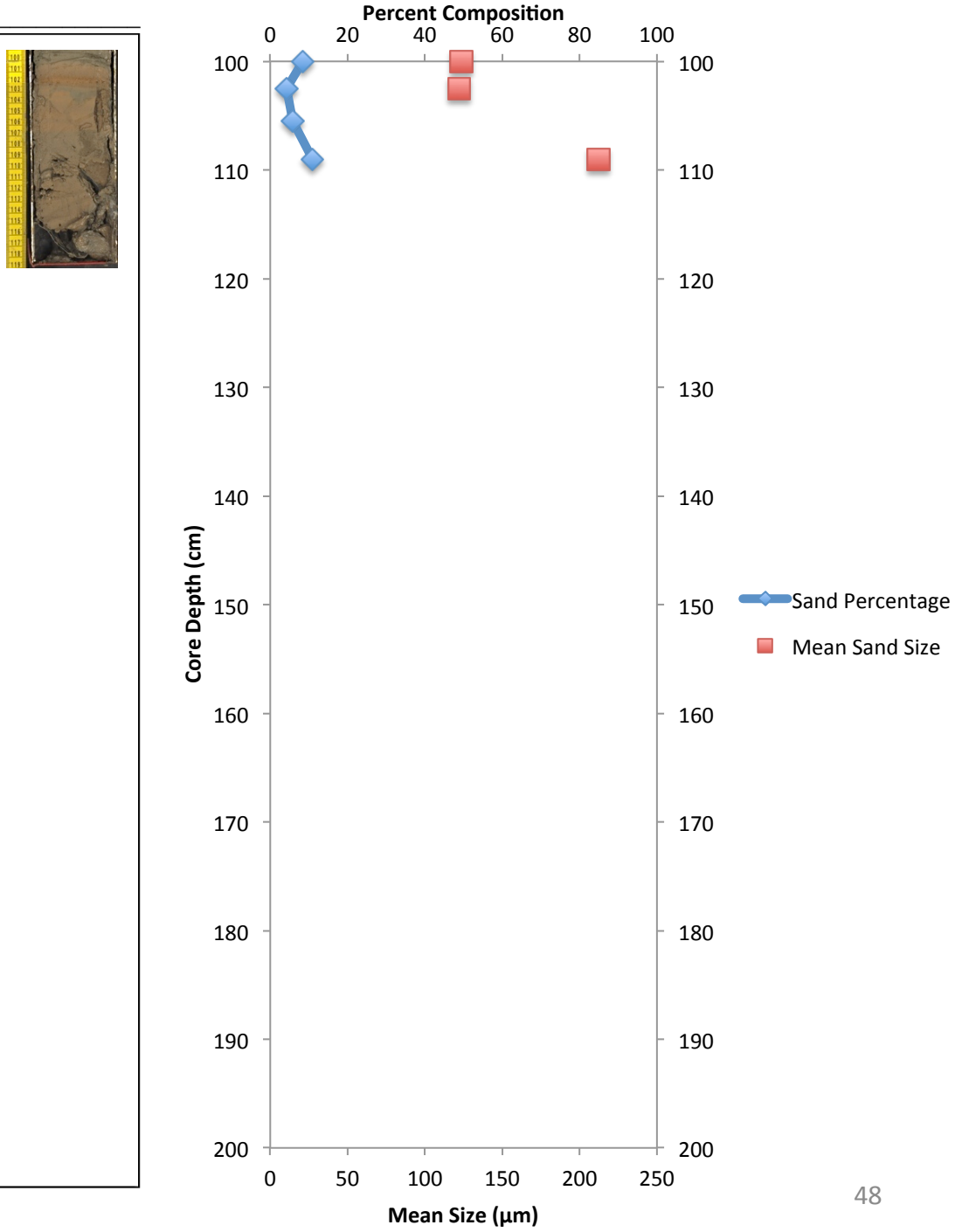

Brazos Delta Core: BDVC11

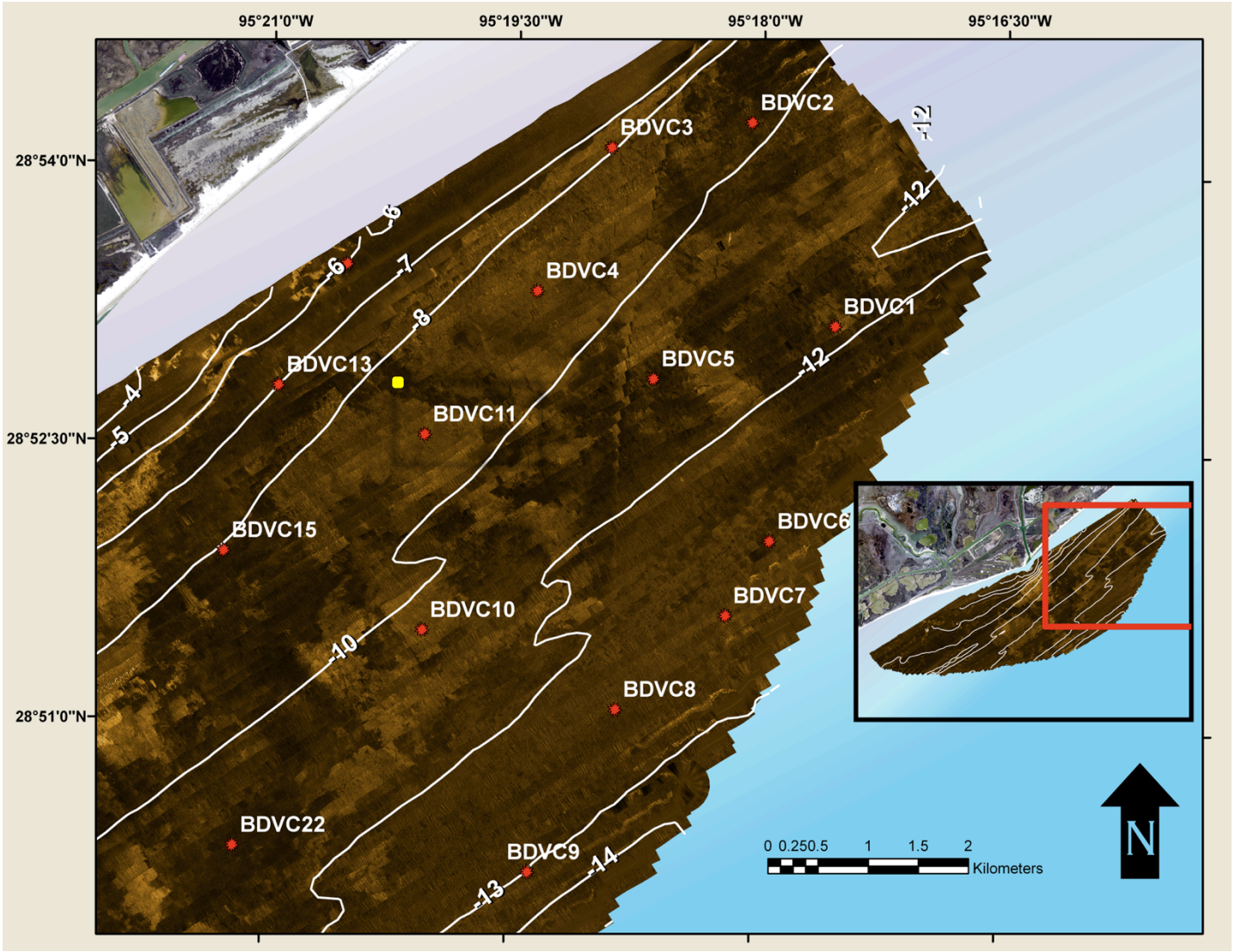

Project:_Brazos Delta Fall 2011___ Core: _BDVC11_____

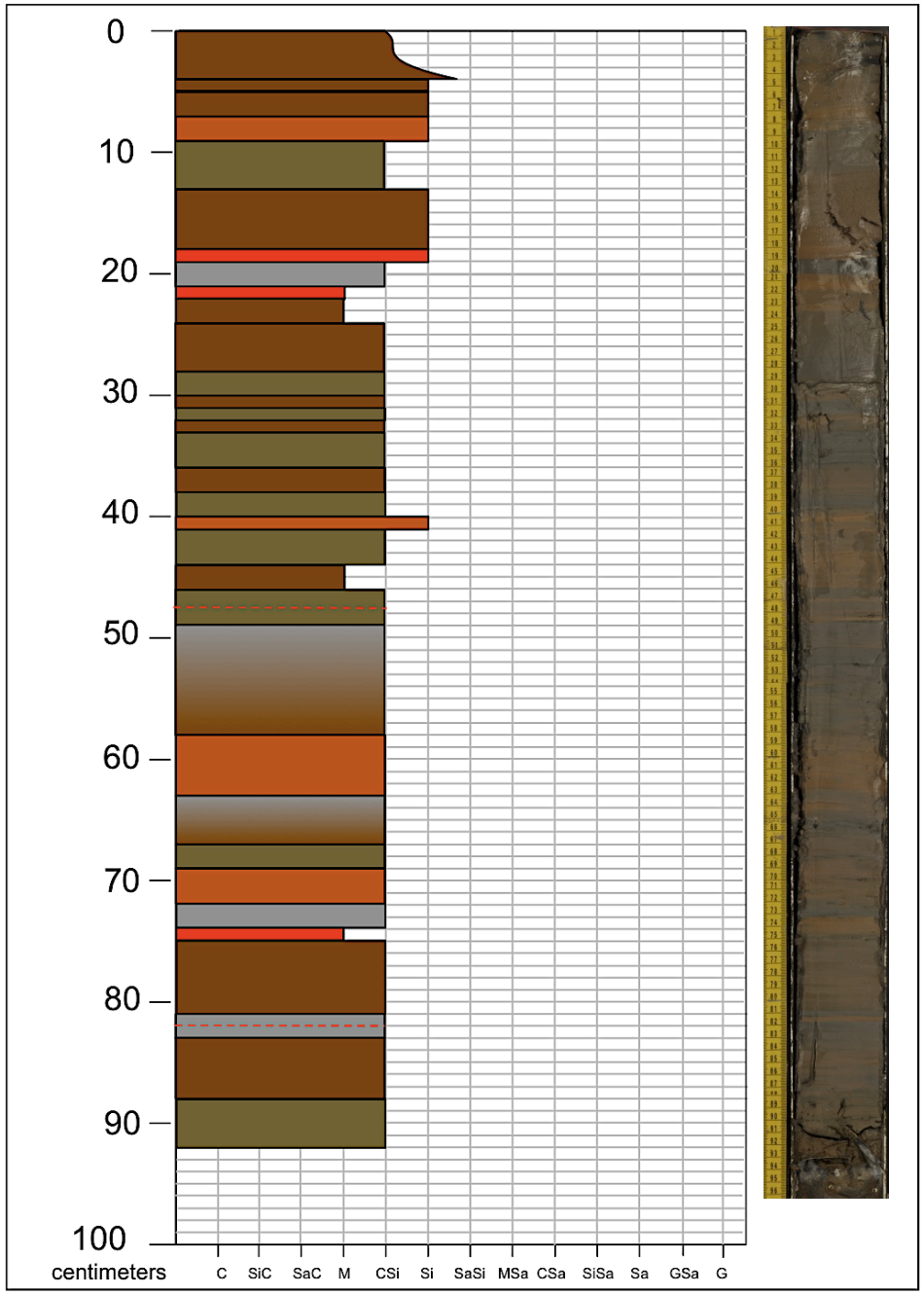

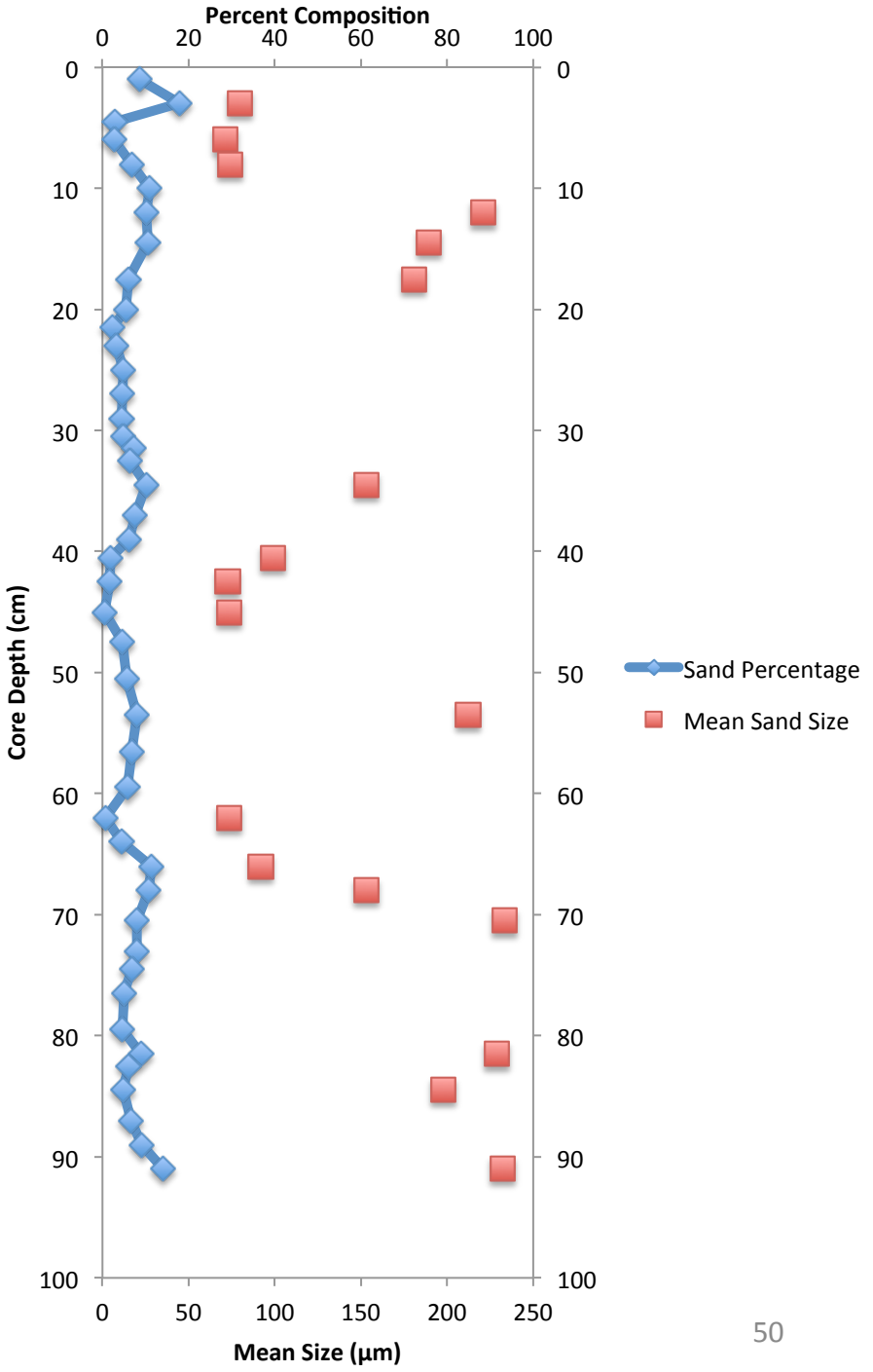

Brazos Delta Core: BDVC12

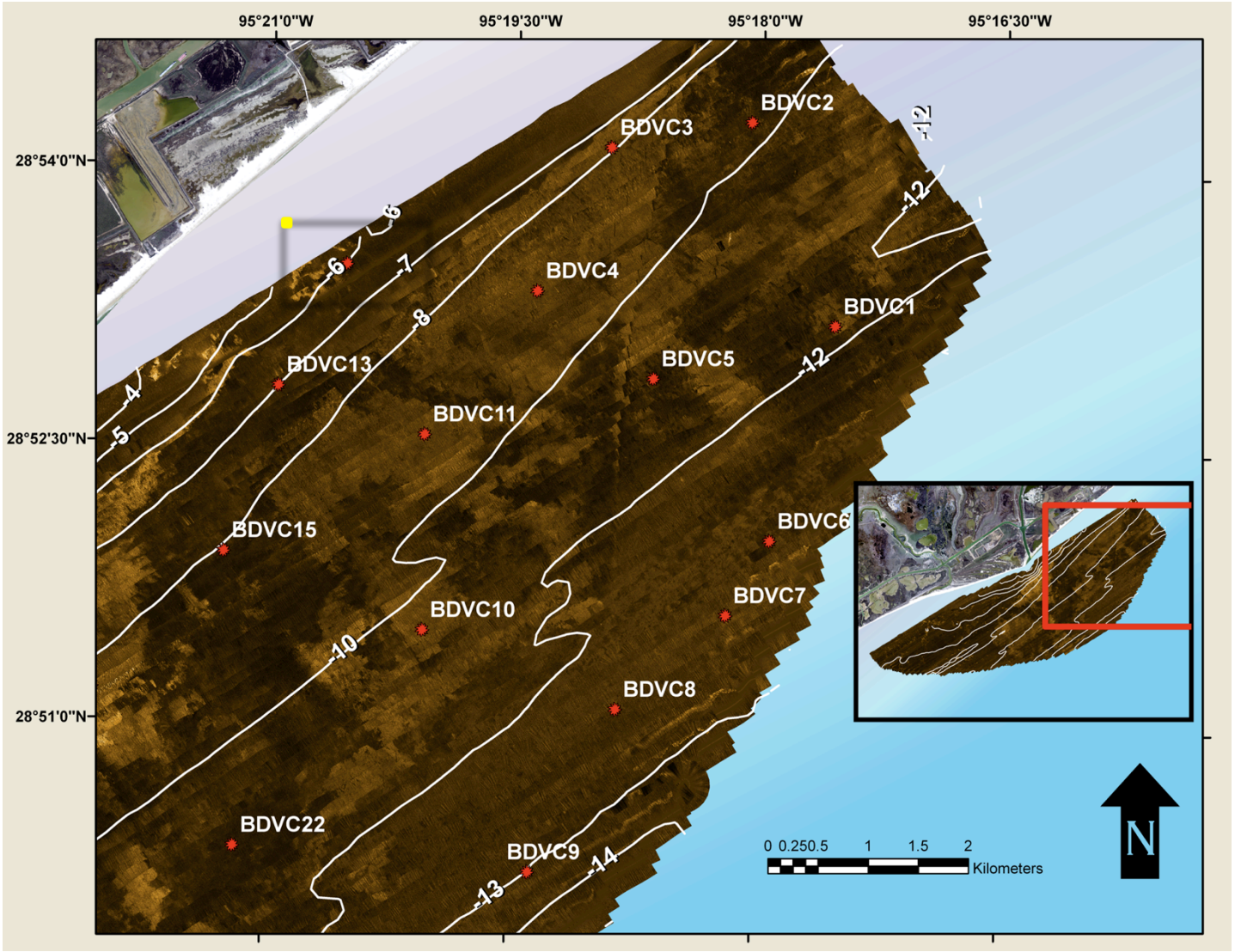

Project:_Brazos Delta Fall 2011___ Core: _BDVC12A_____

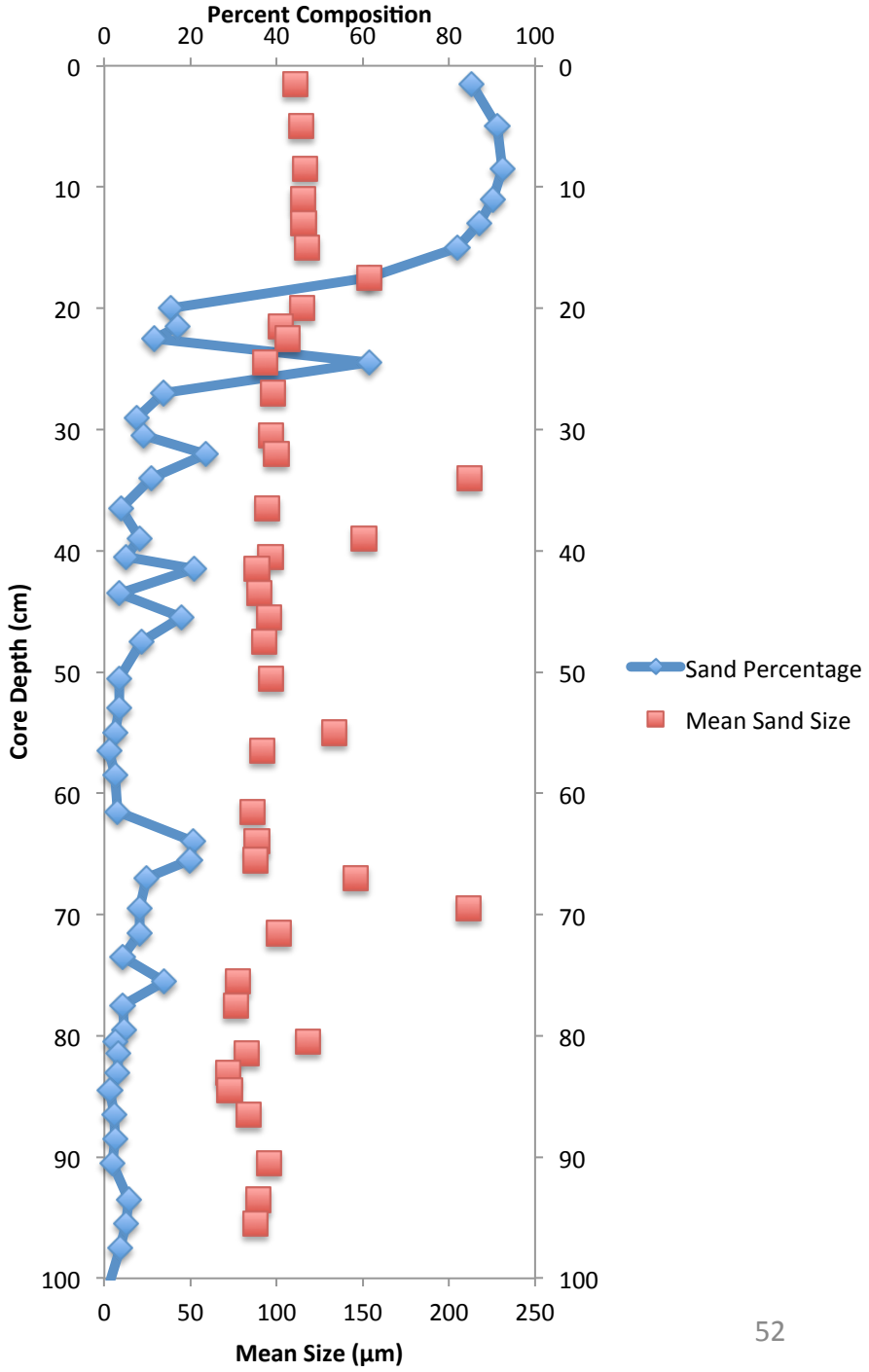

Project:_Brazos Delta Fall 2011___ Core: _BDVC12B_____

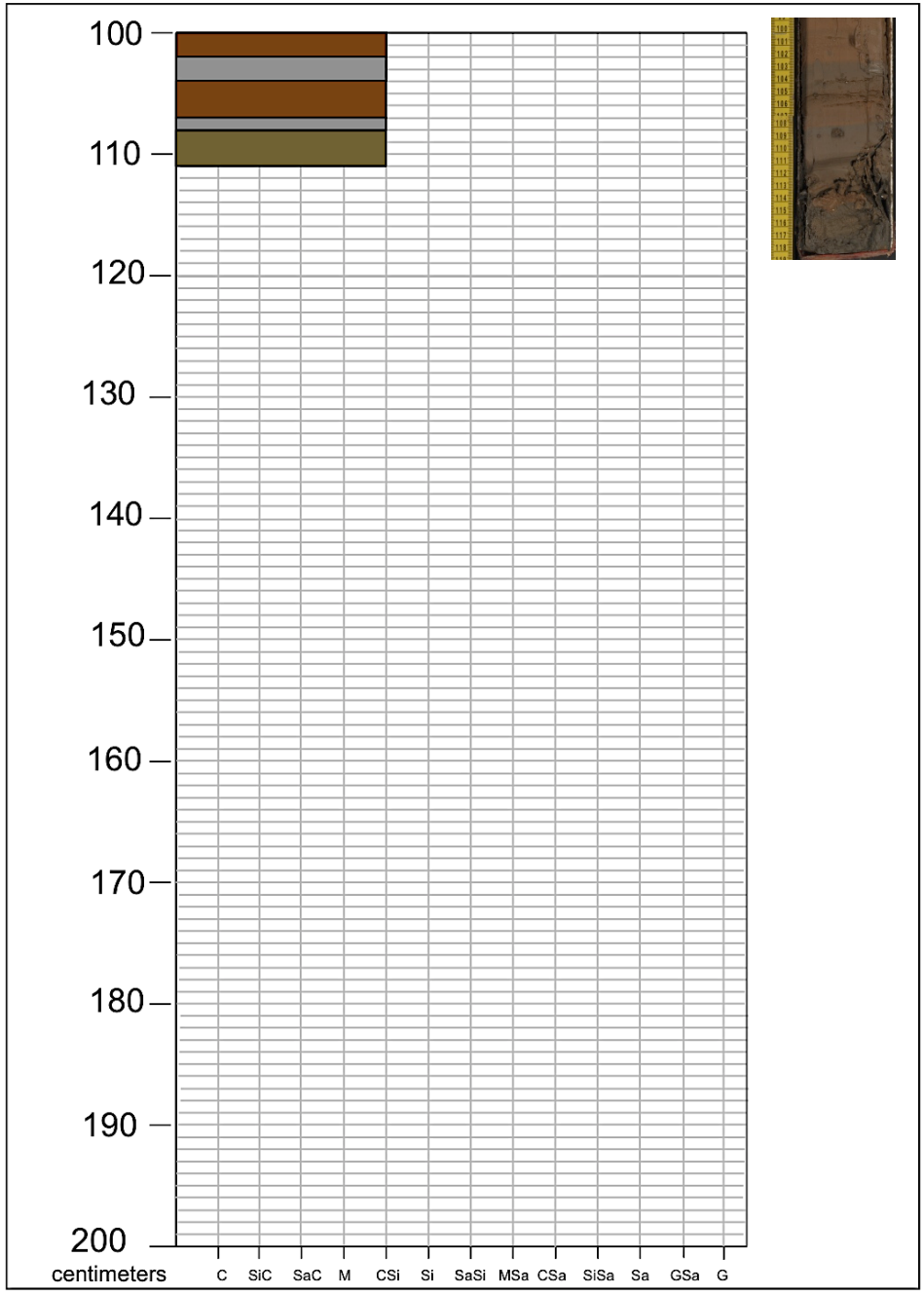

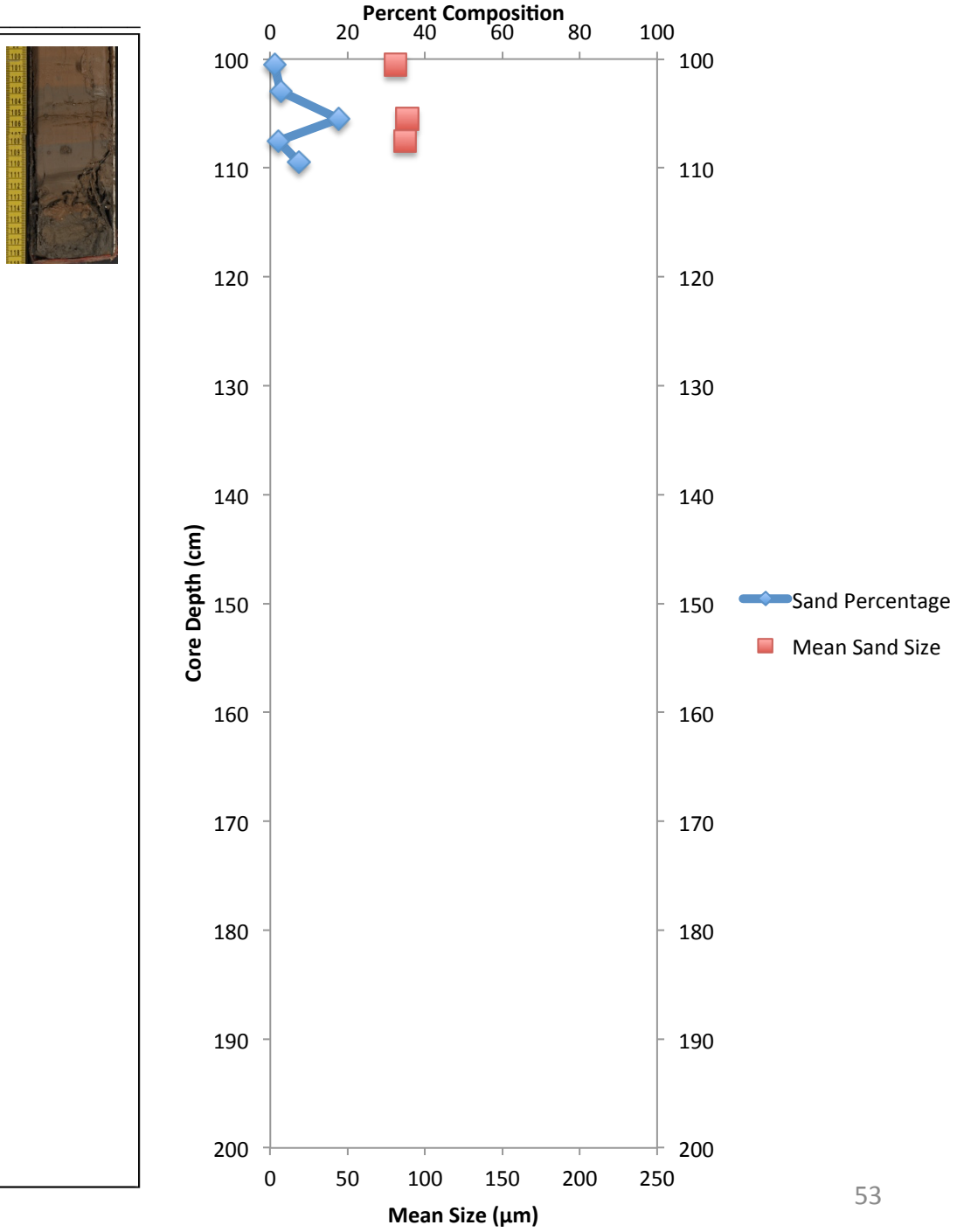

Brazos Delta Core: BDVC13

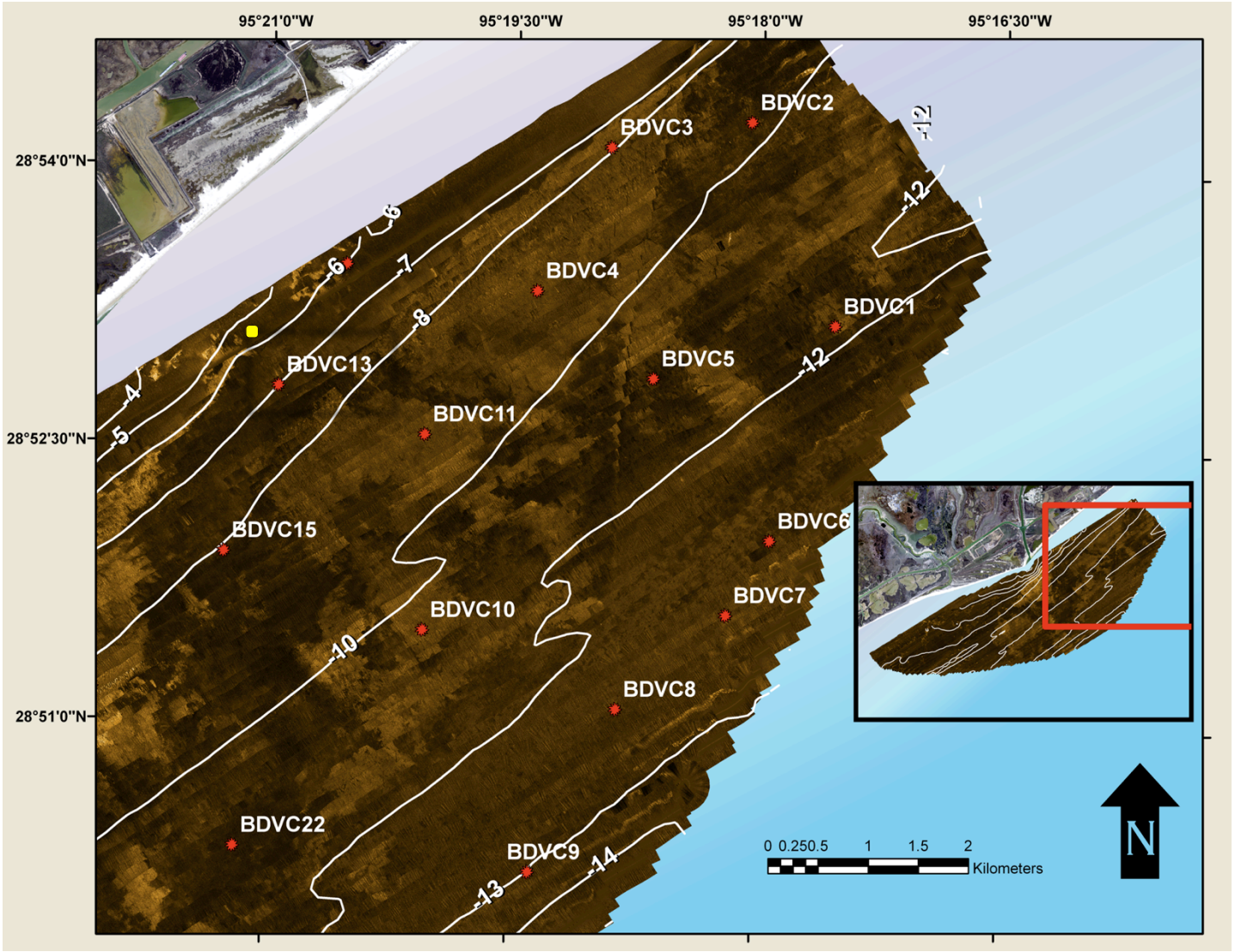

Project:_Brazos Delta Fall 2011___ Core: _BDVC13_____

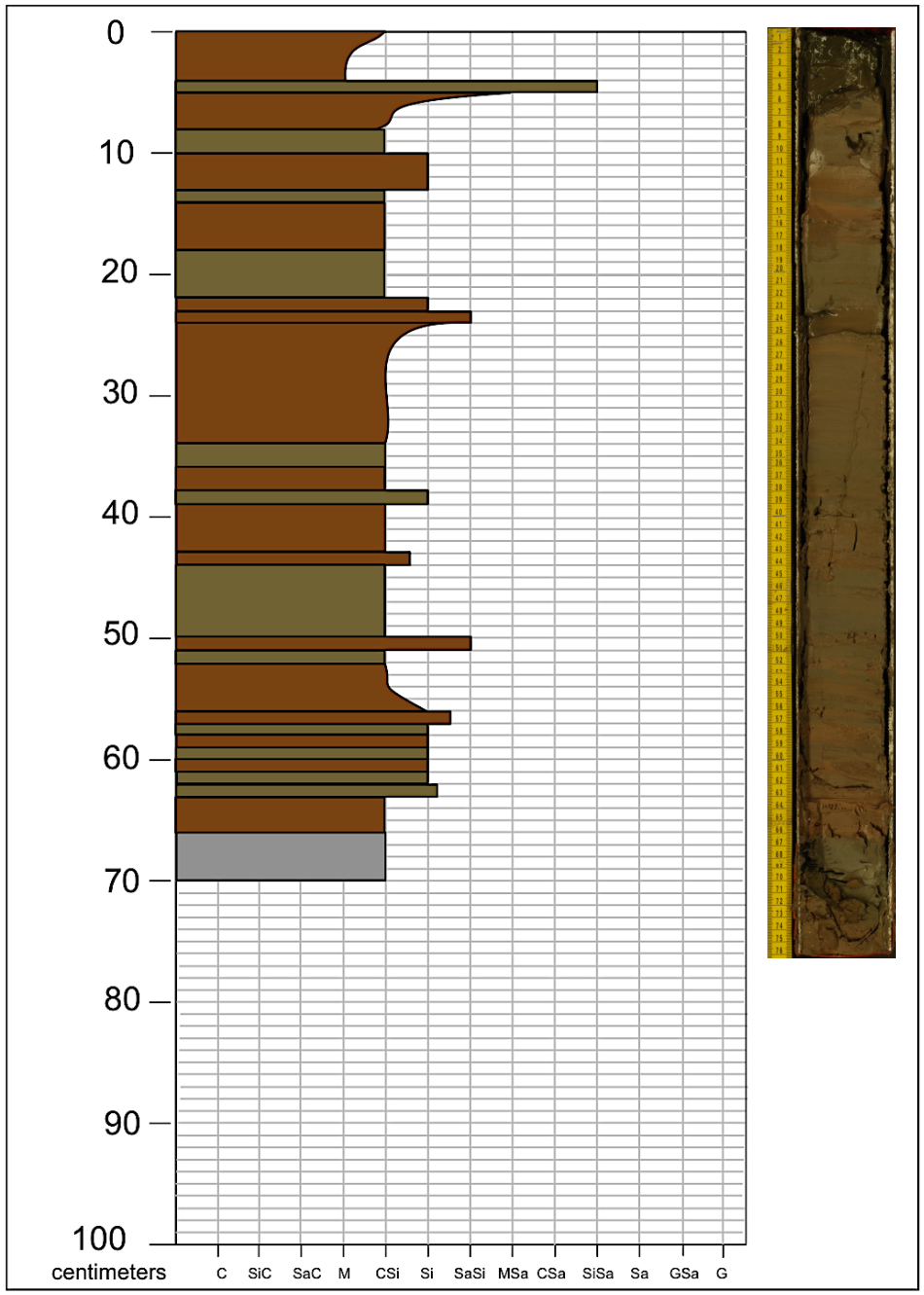

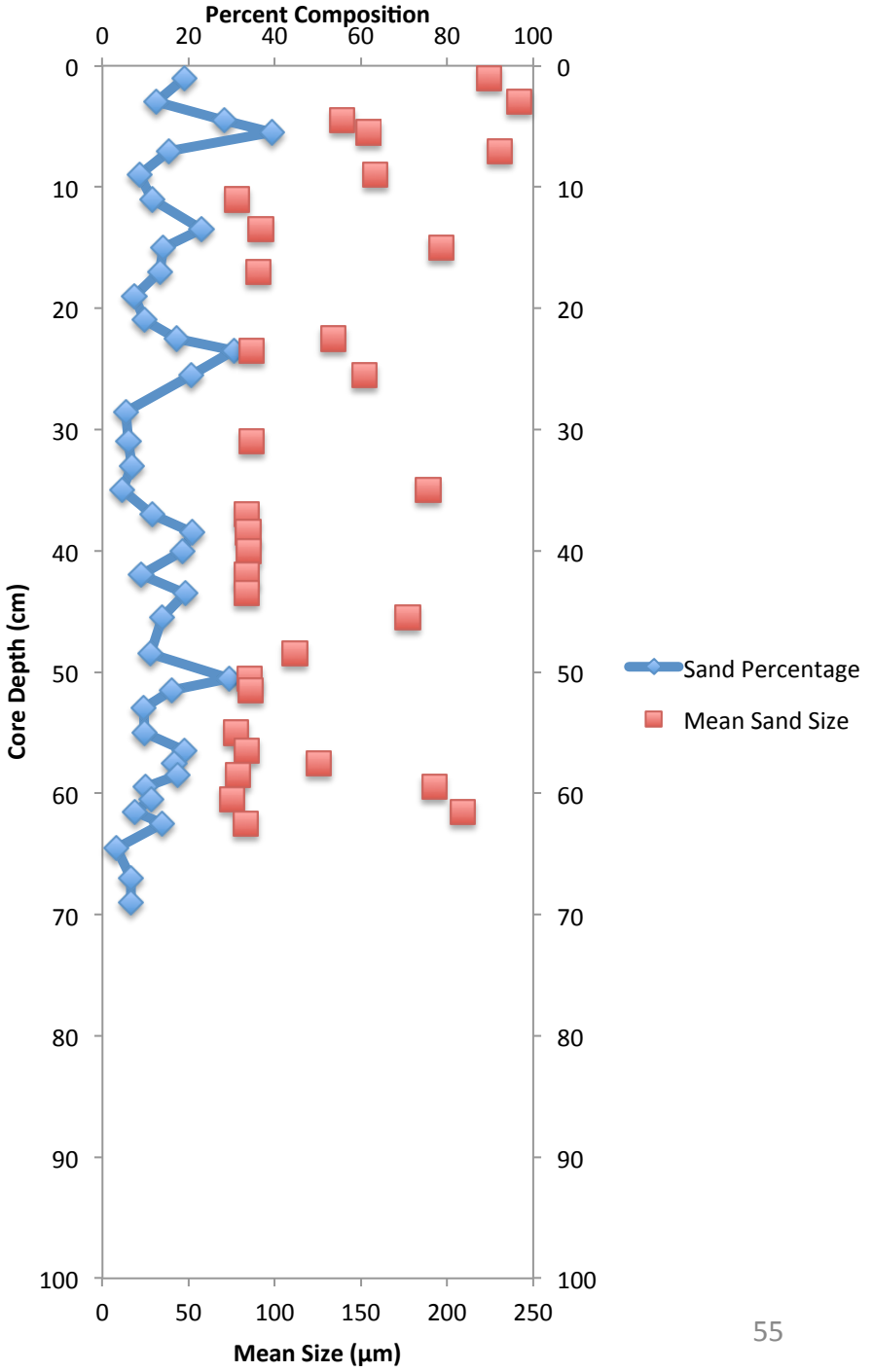

Brazos Delta Core: BDVC15

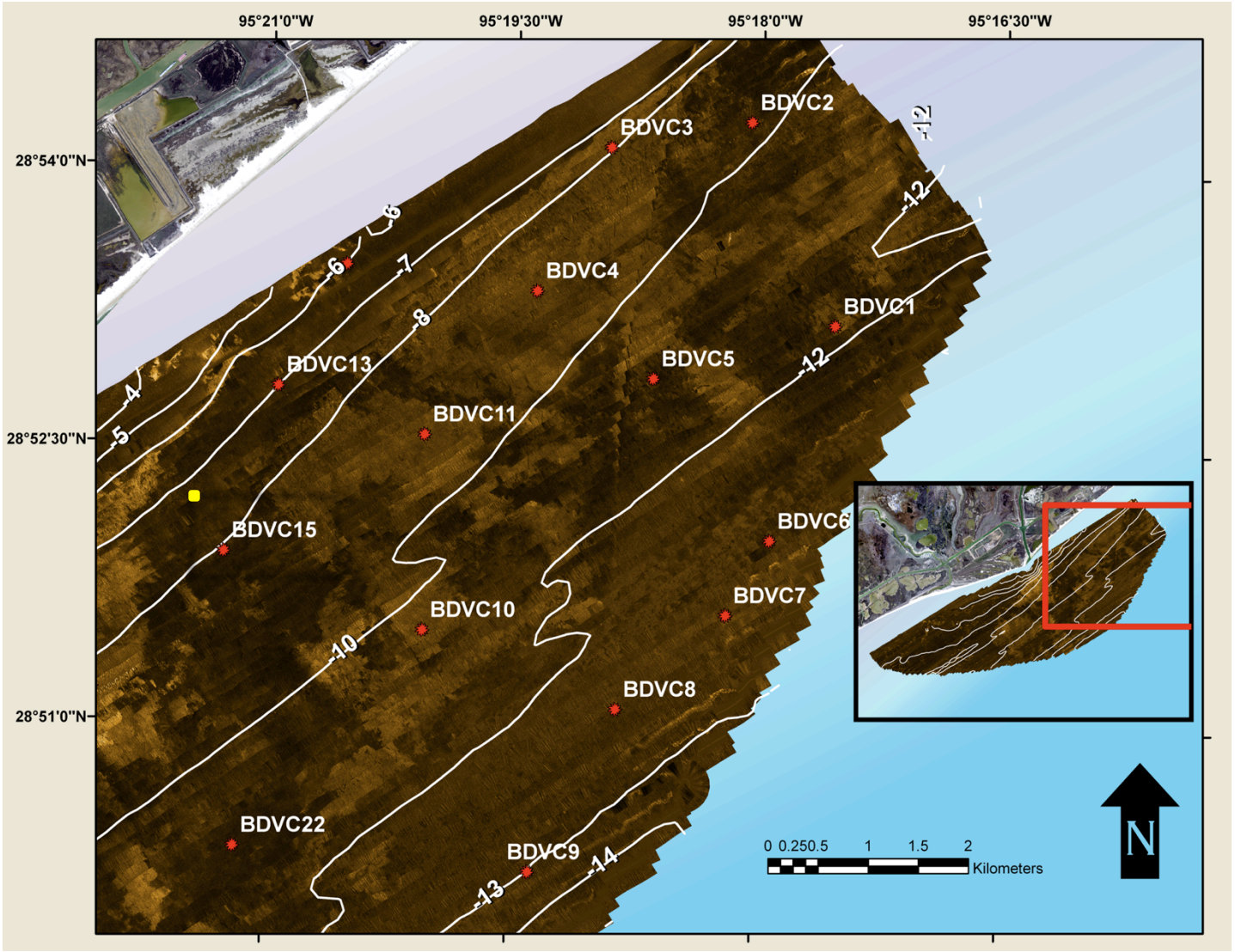

Project:_Brazos Delta Fall 2011___ Core: _BDVC15A_____

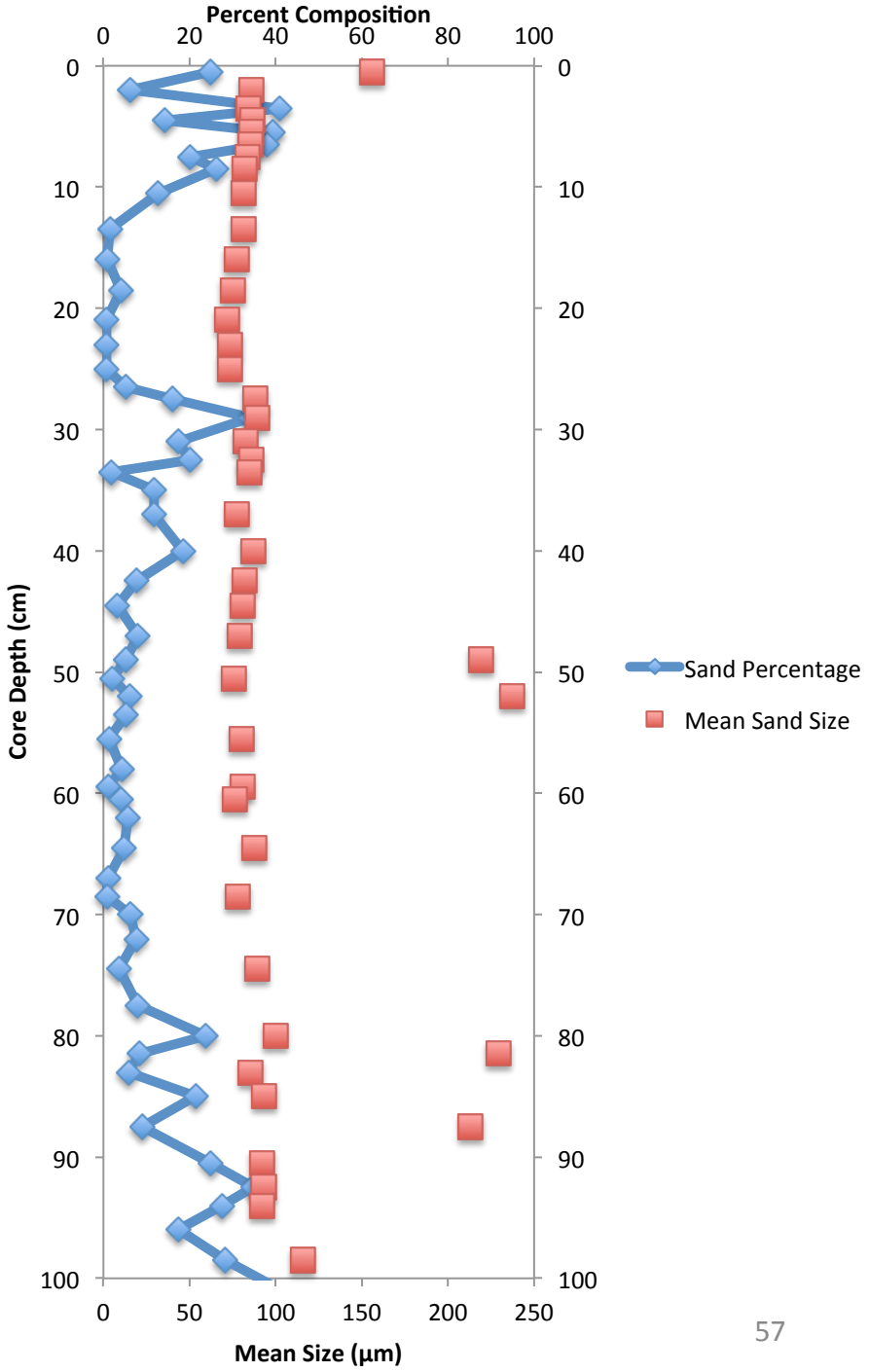

Project:_Brazos Delta Fall 2011___ Core: _BDVC15B_____

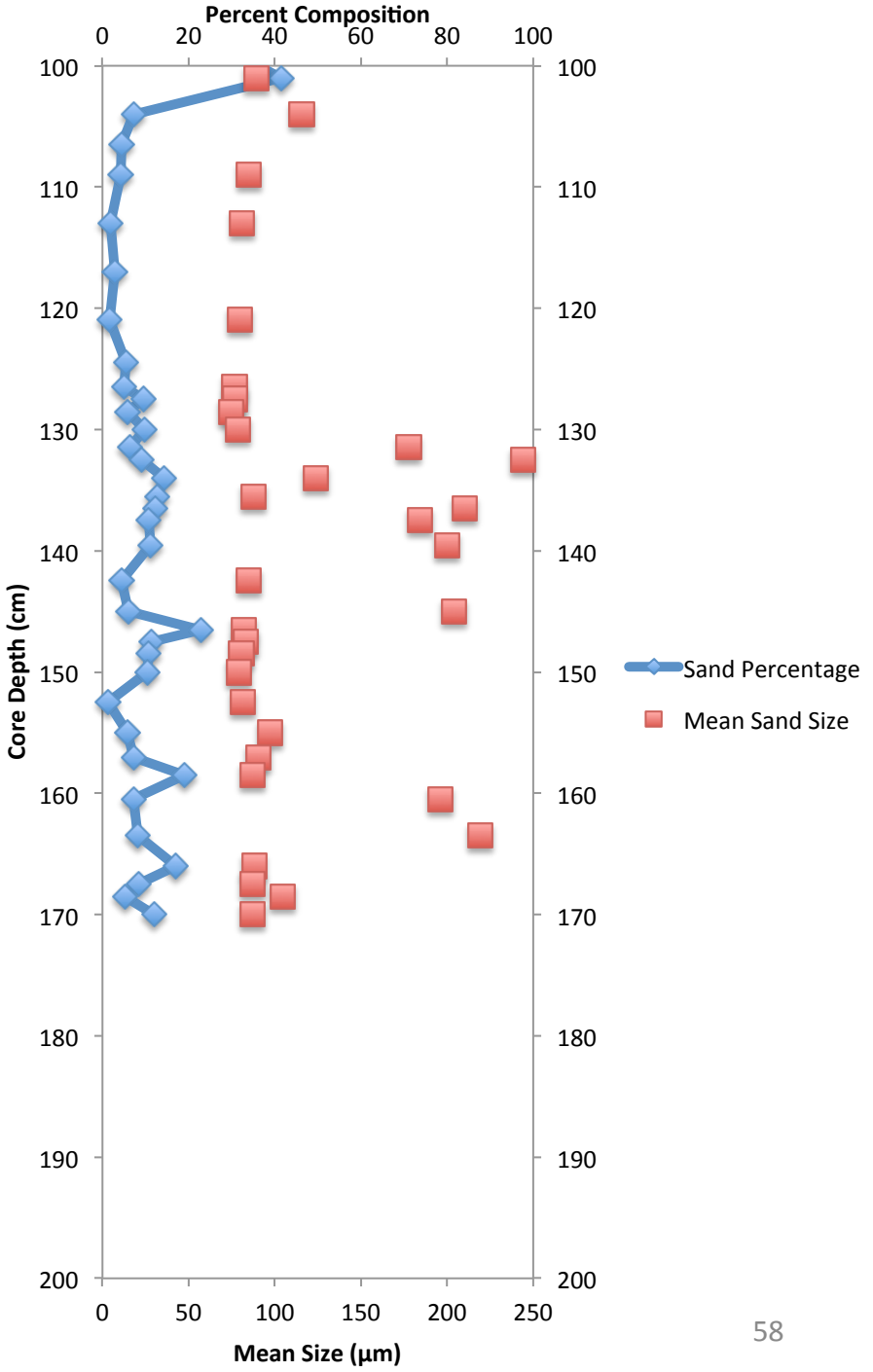

Brazos Delta Core: BDVC16

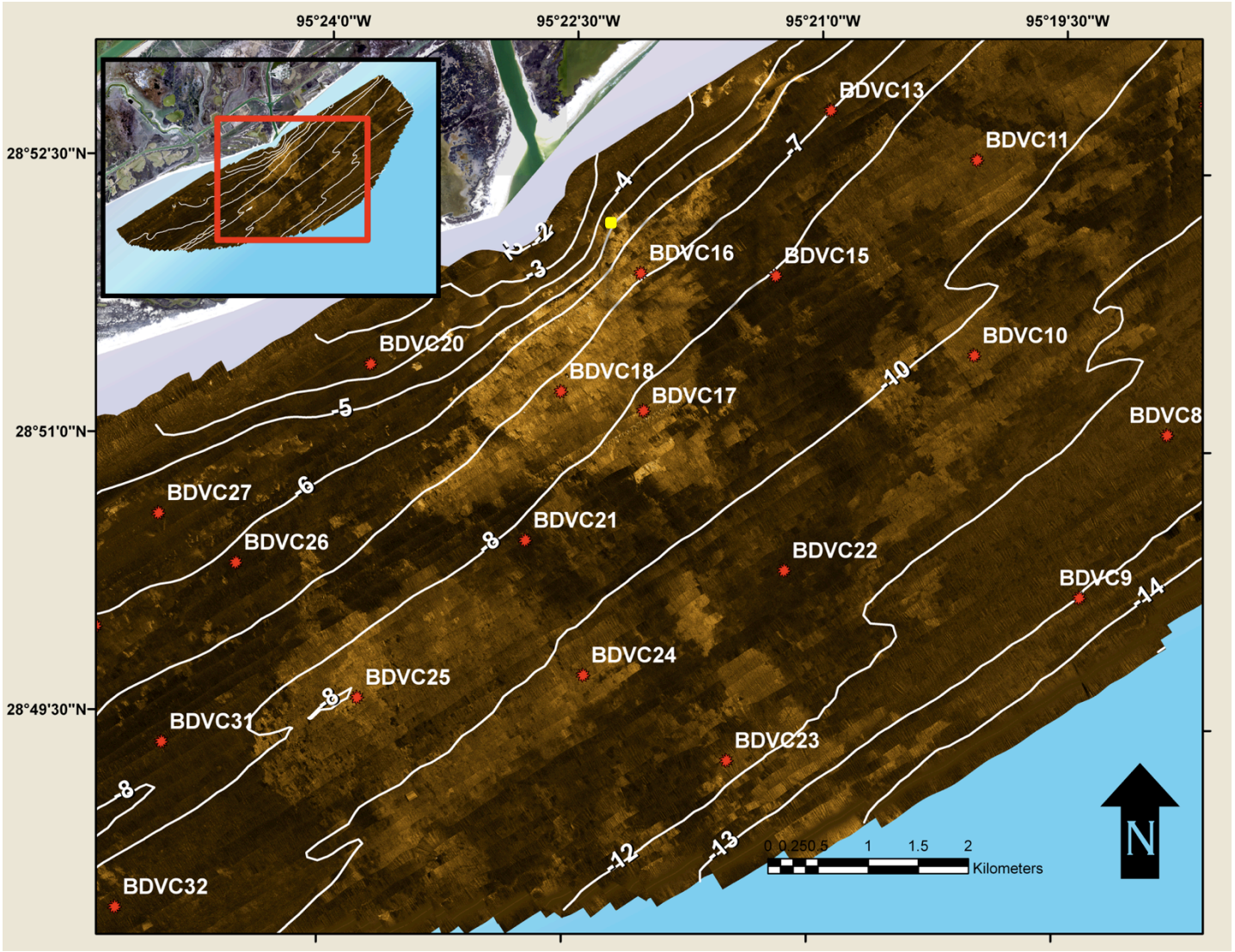

Project:_Brazos Delta Fall 2011___ Core: _BDVC16_____

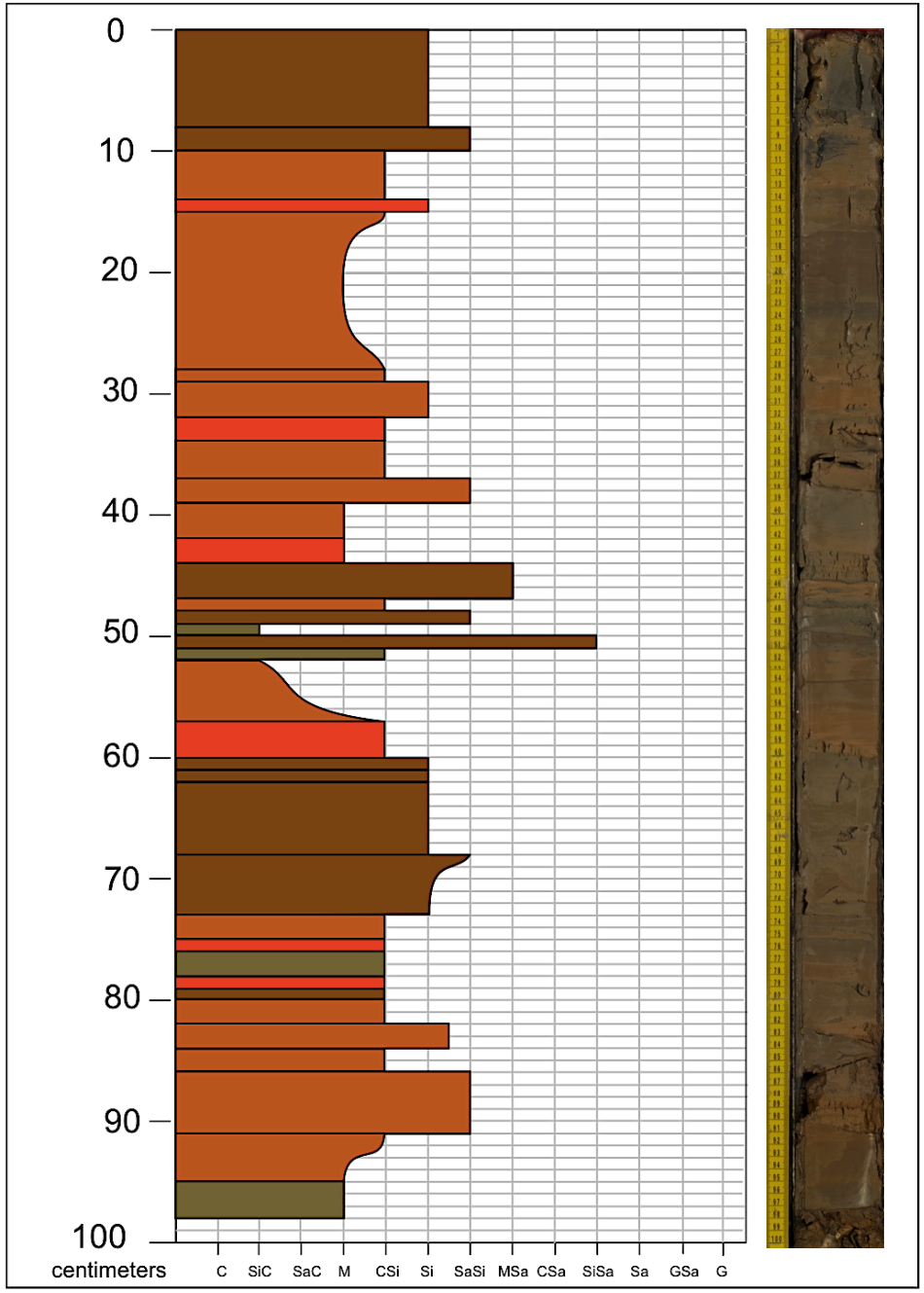

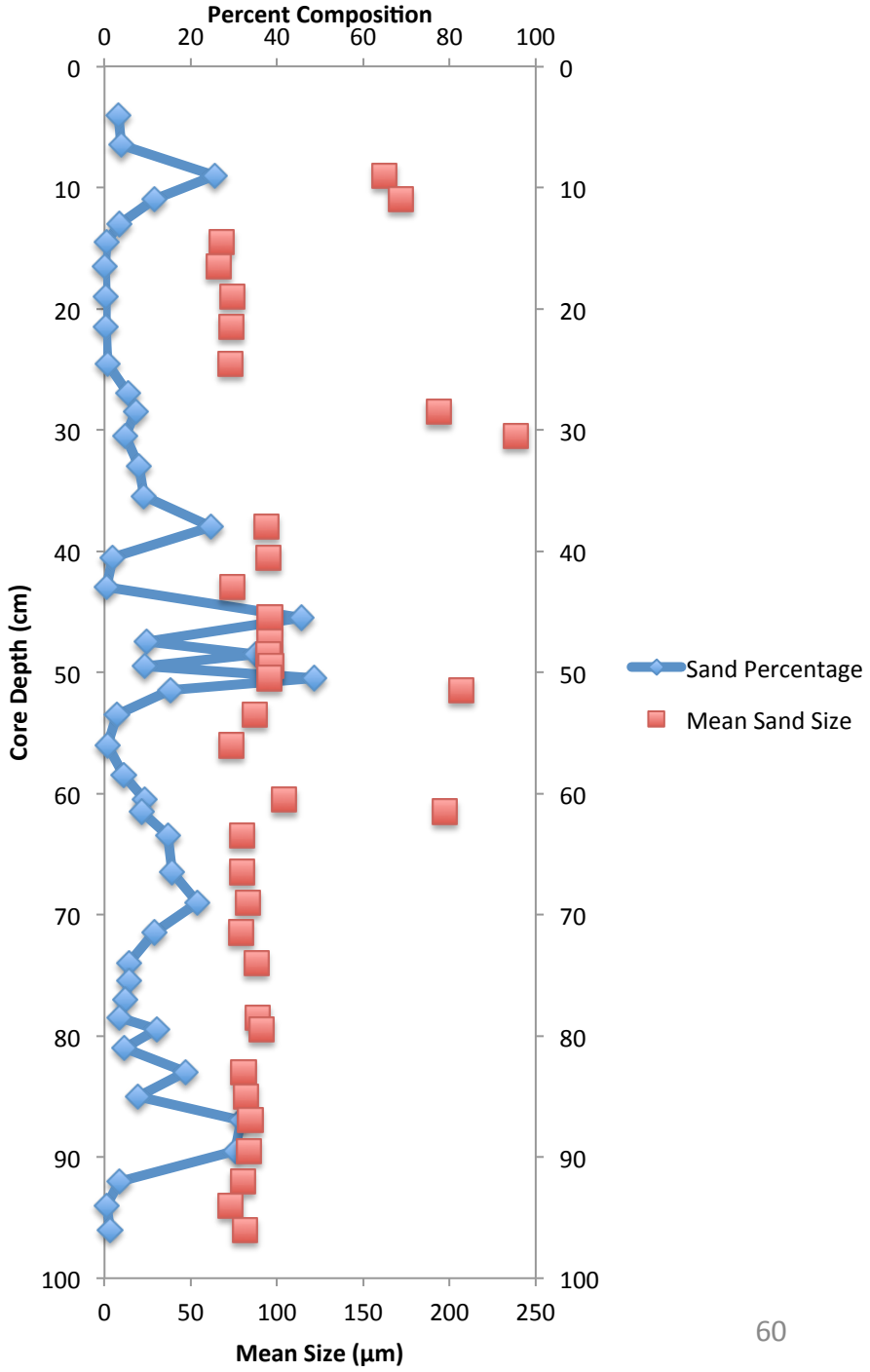

Brazos Delta Core: BDVC17

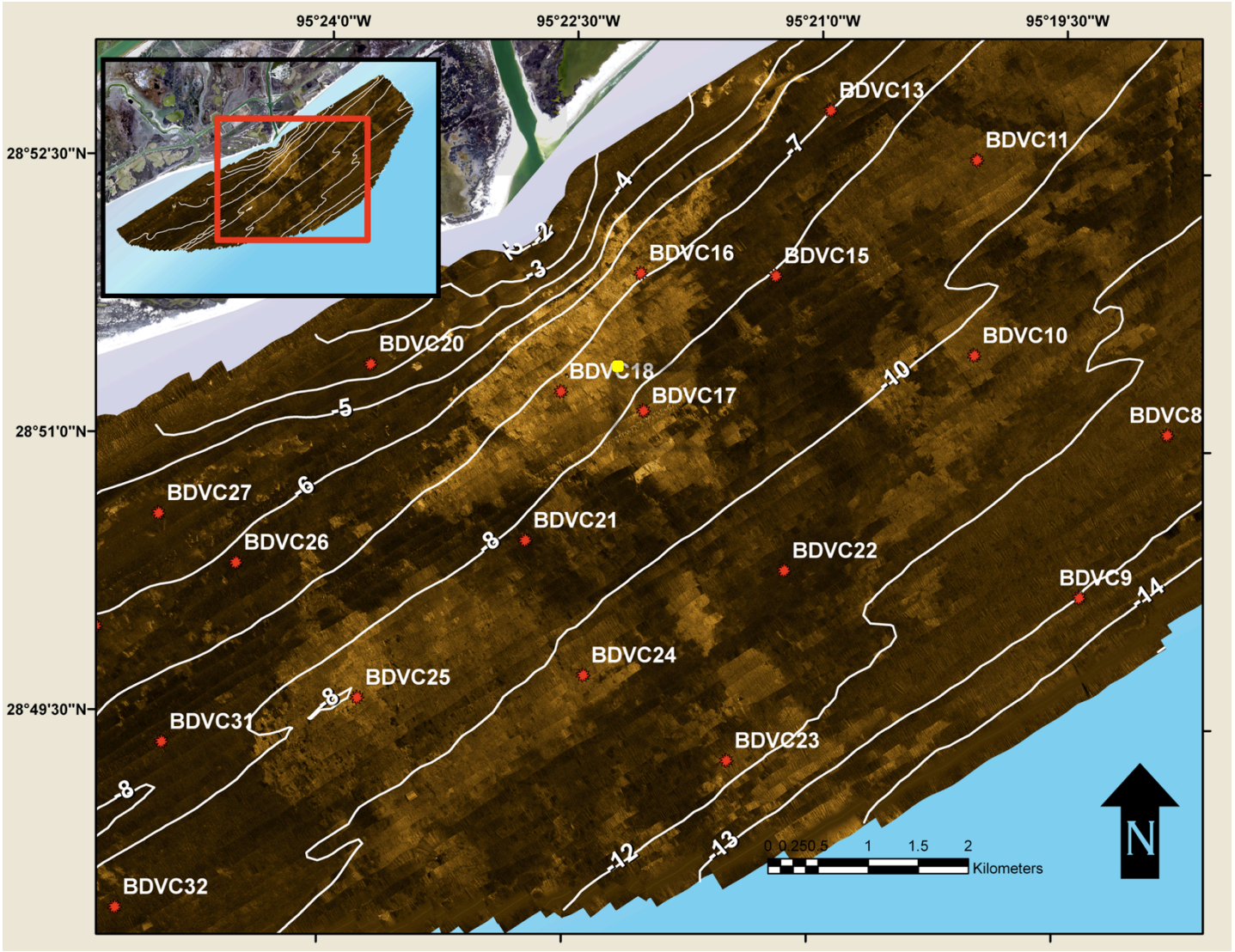

Project:_Brazos Delta Fall 2011___ Core: _BDVC17_____

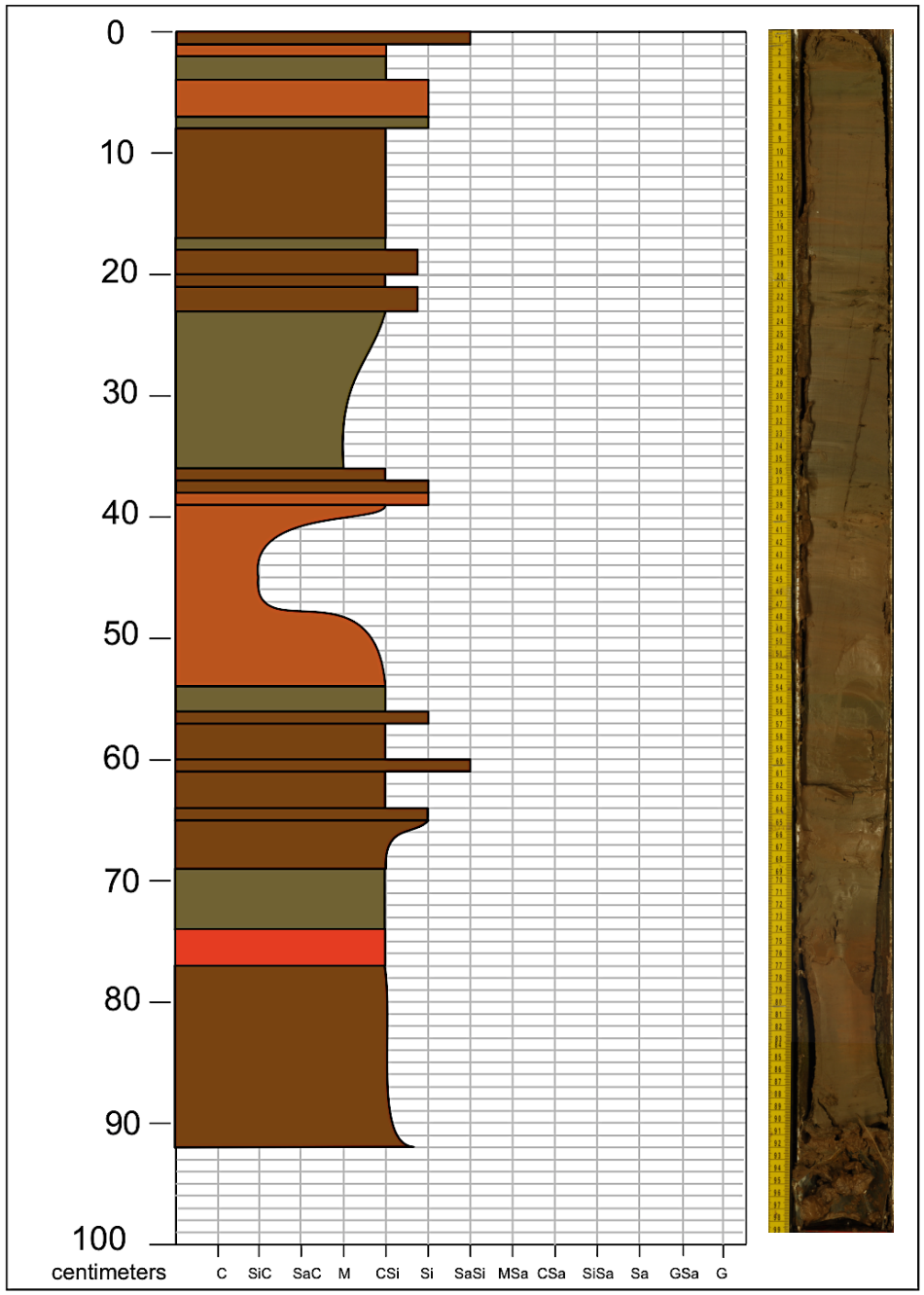

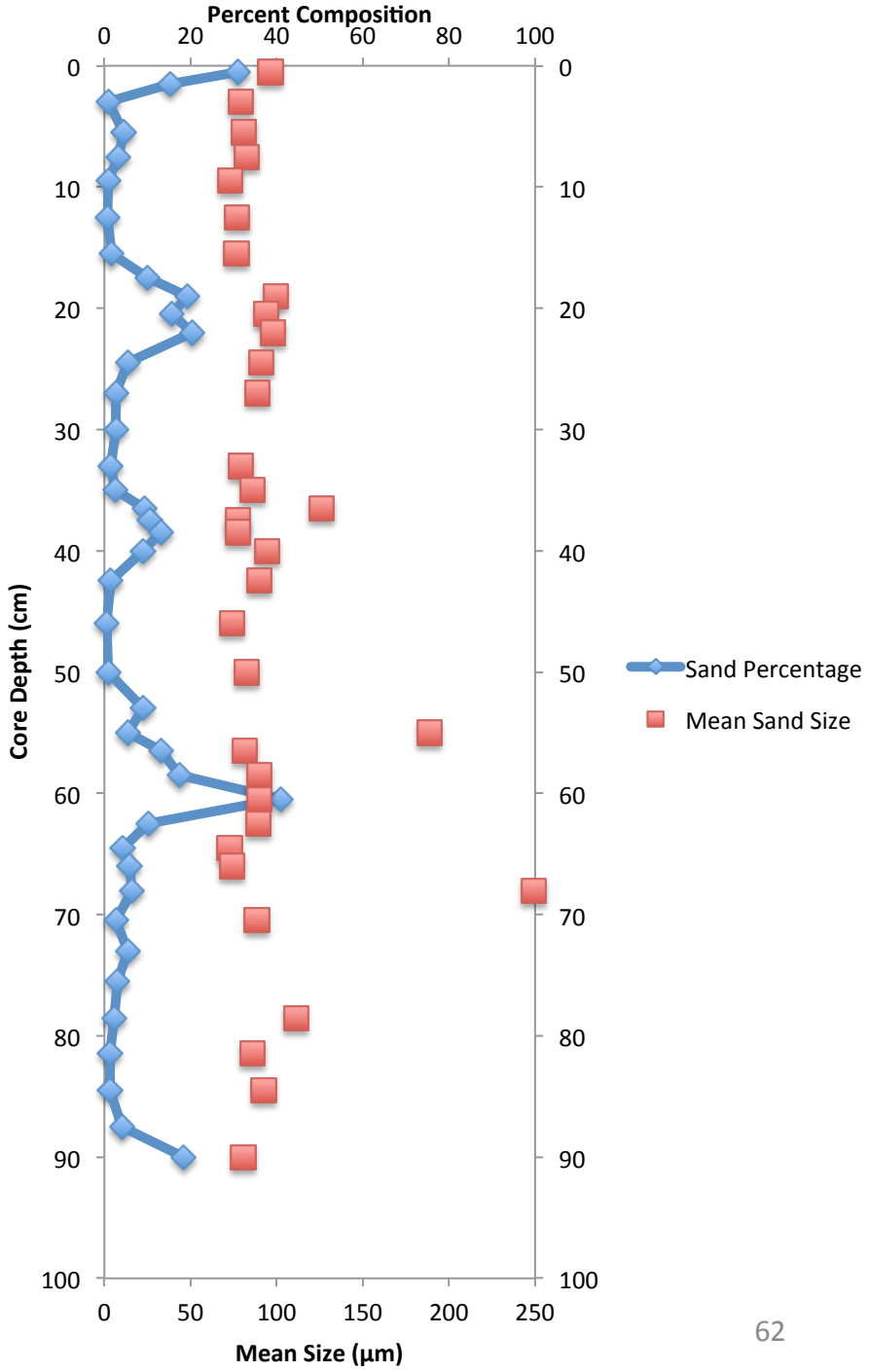

Brazos Delta Core: BDVC18

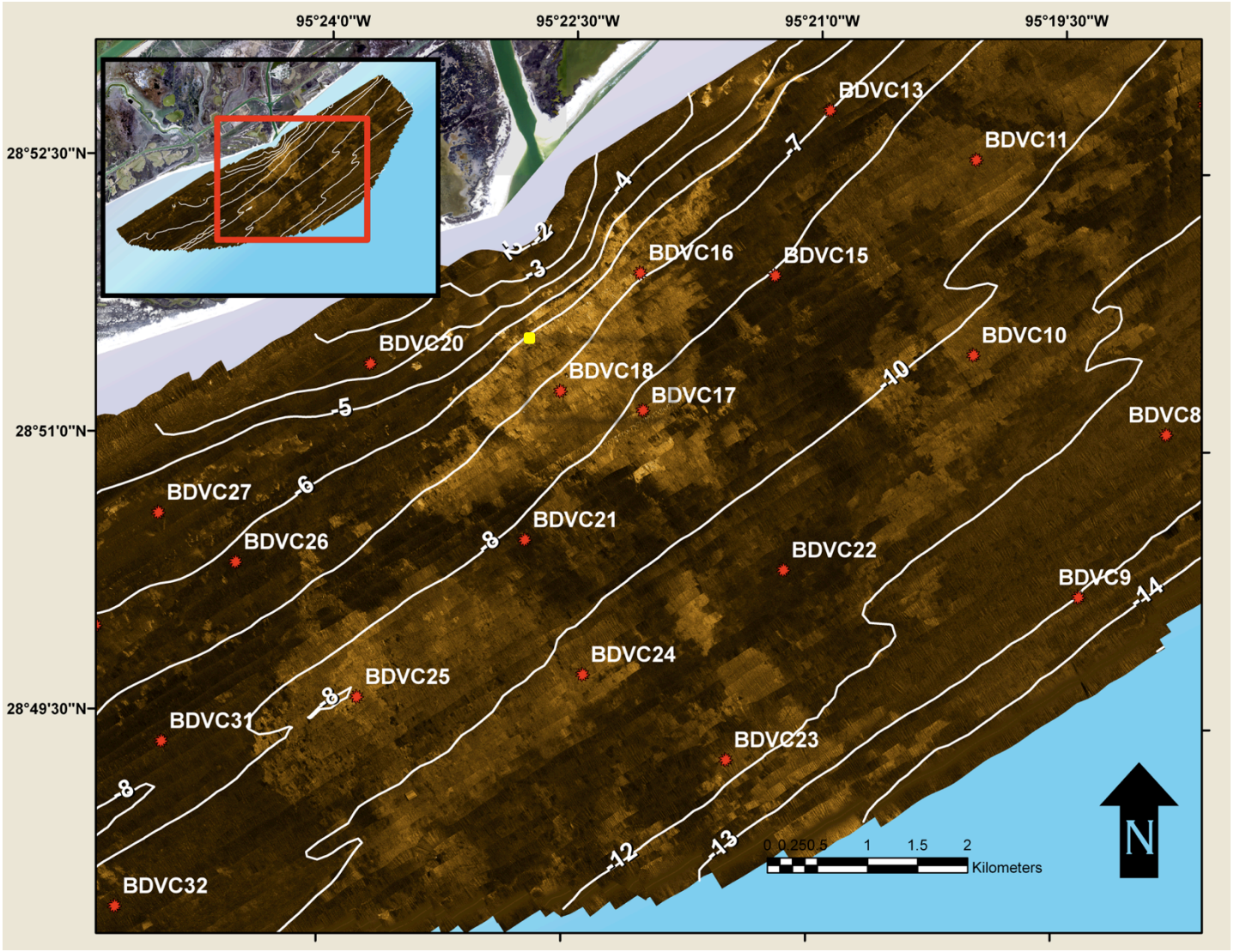

Project:_Brazos Delta Fall 2011___ Core: _BDVC18_____

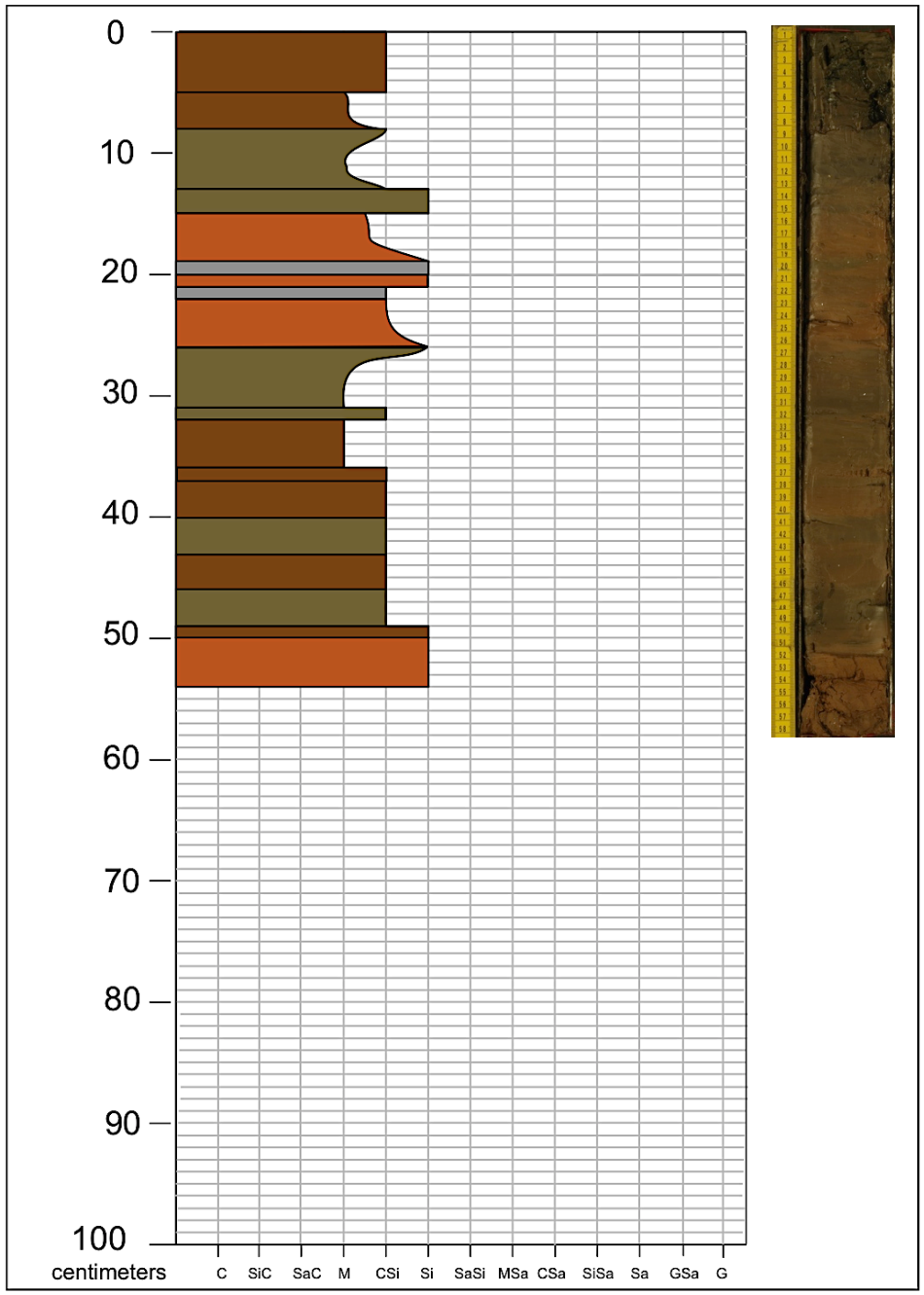

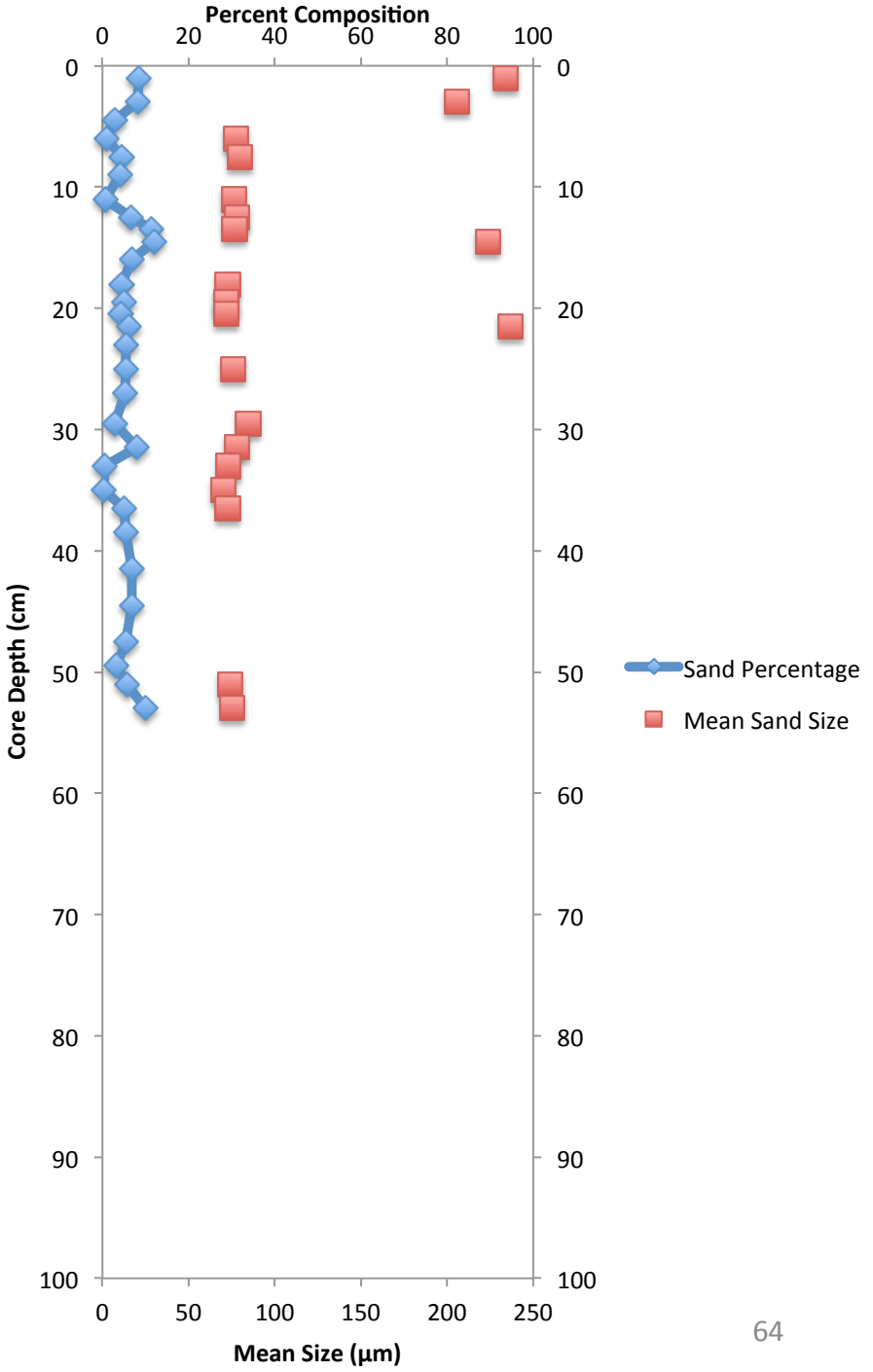

Brazos Delta Core: BDVC20

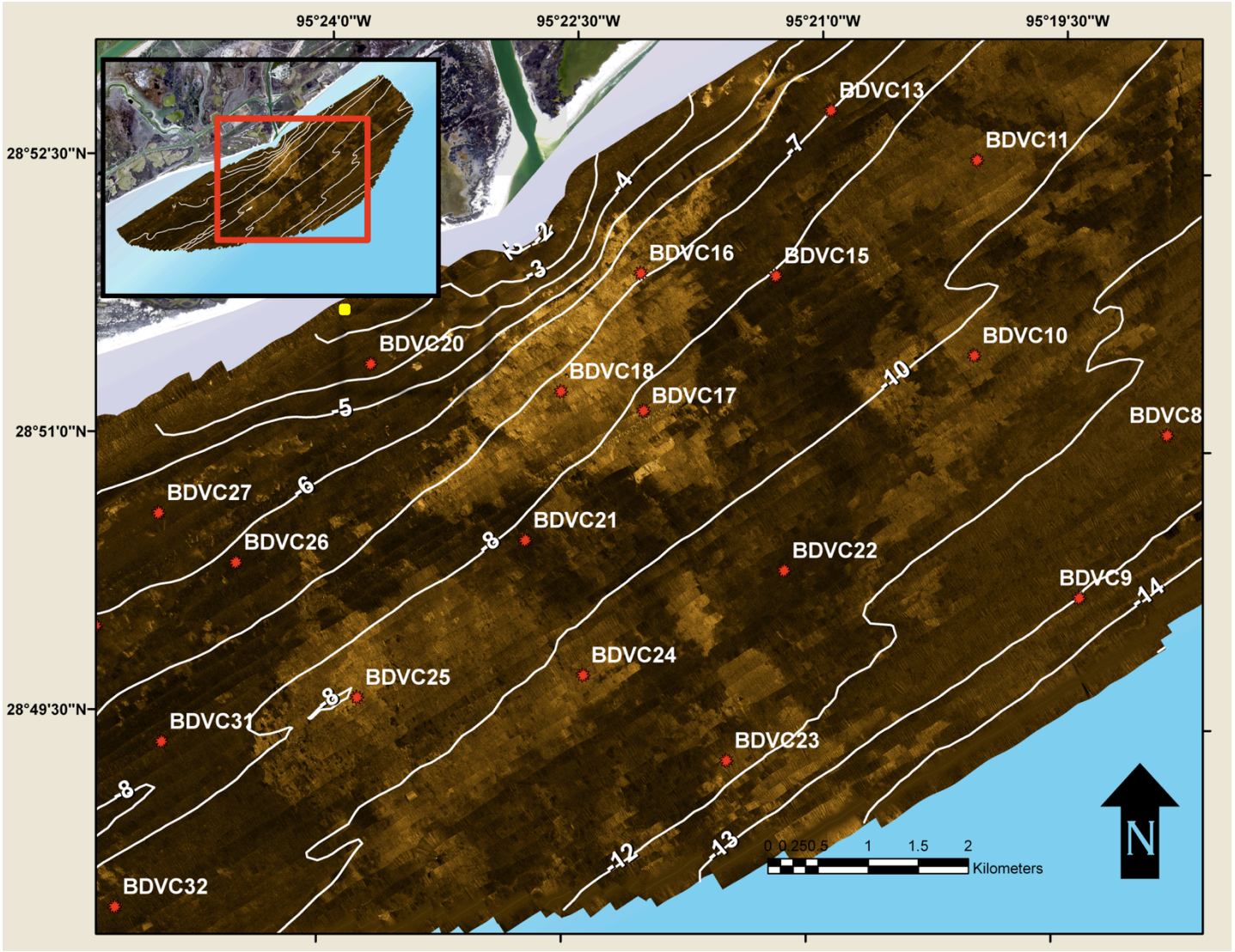

Project:_Brazos Delta Fall 2011___ Core: _BDVC20_____

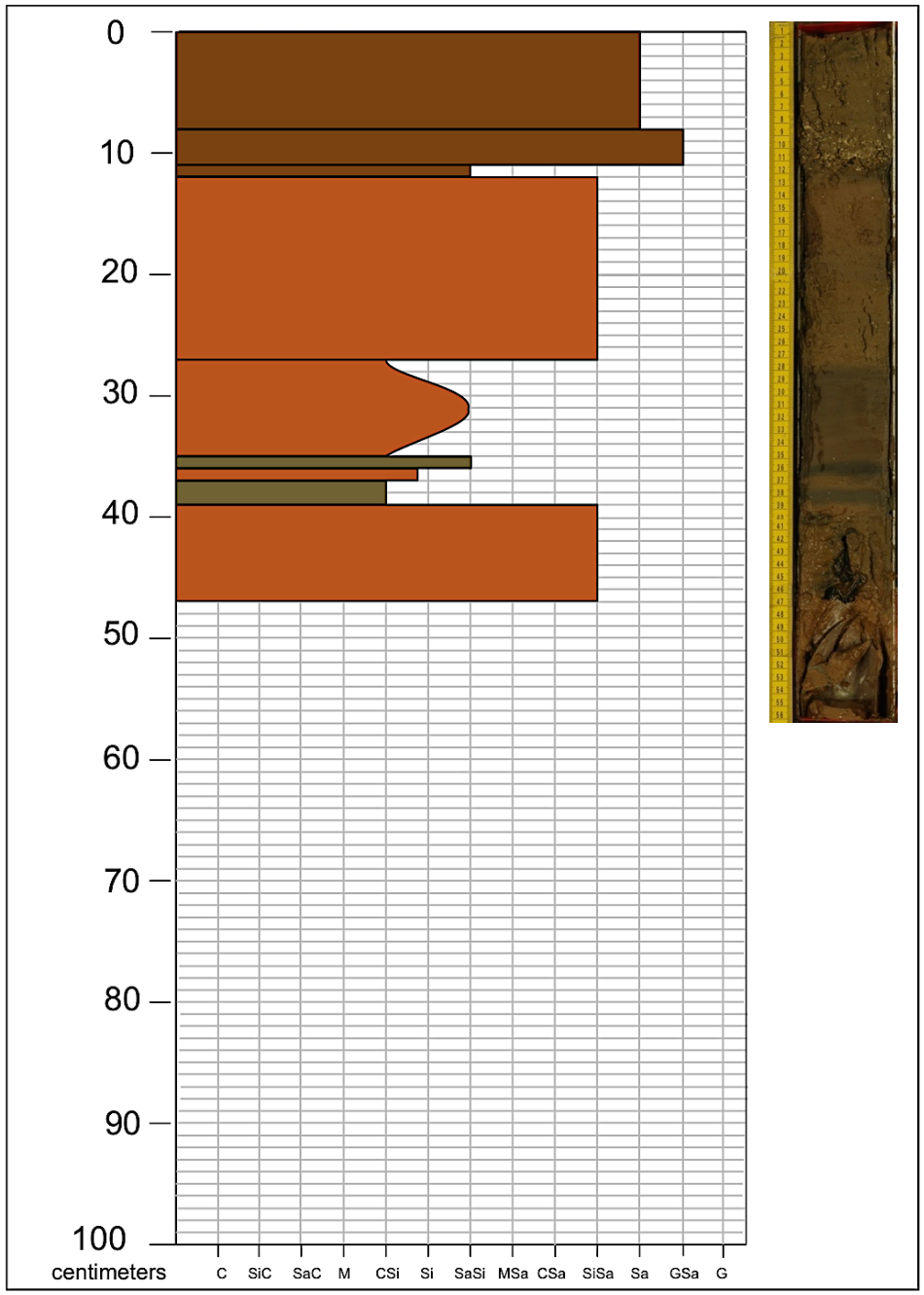

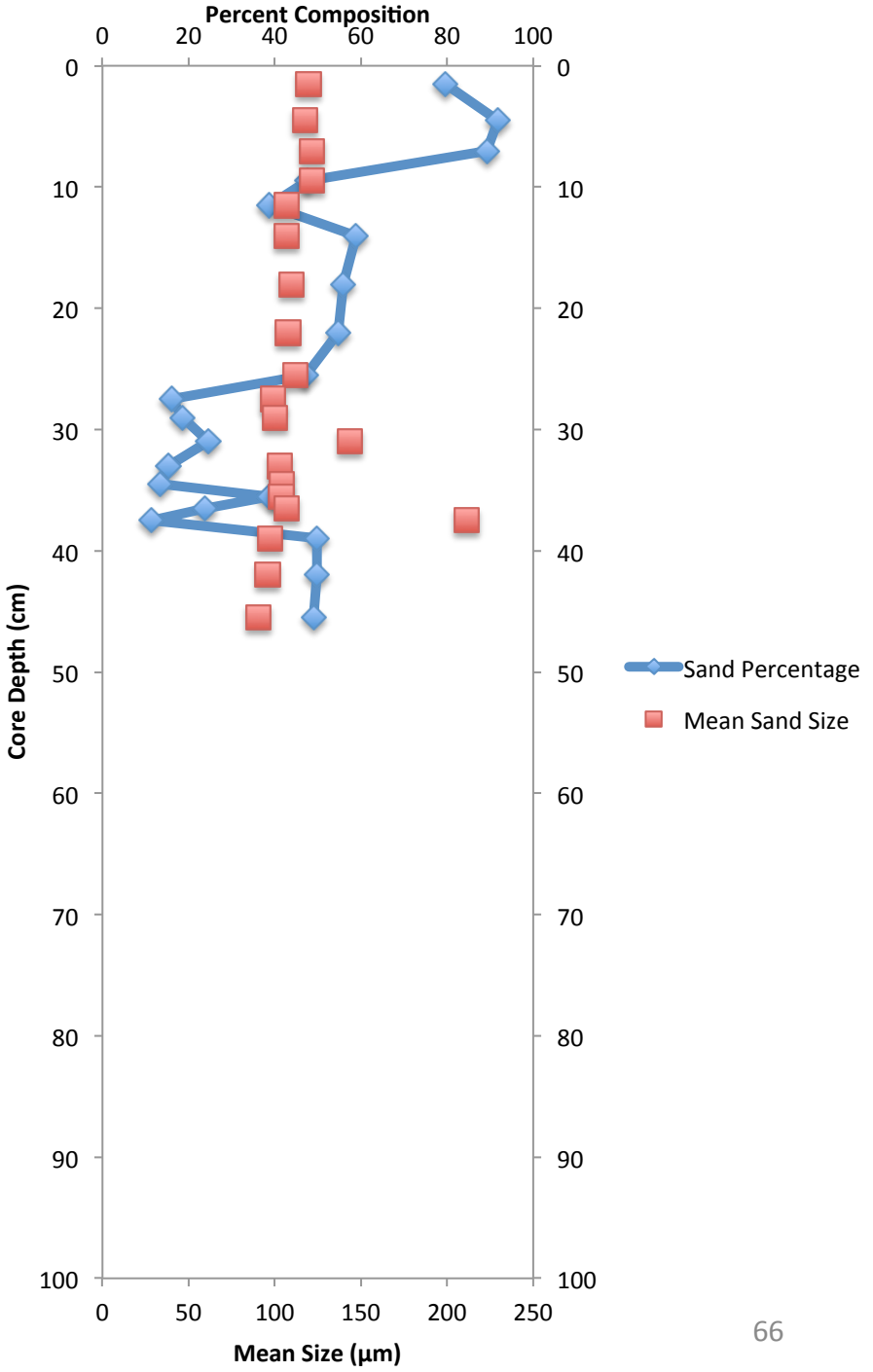

Brazos Delta Core: BDVC21

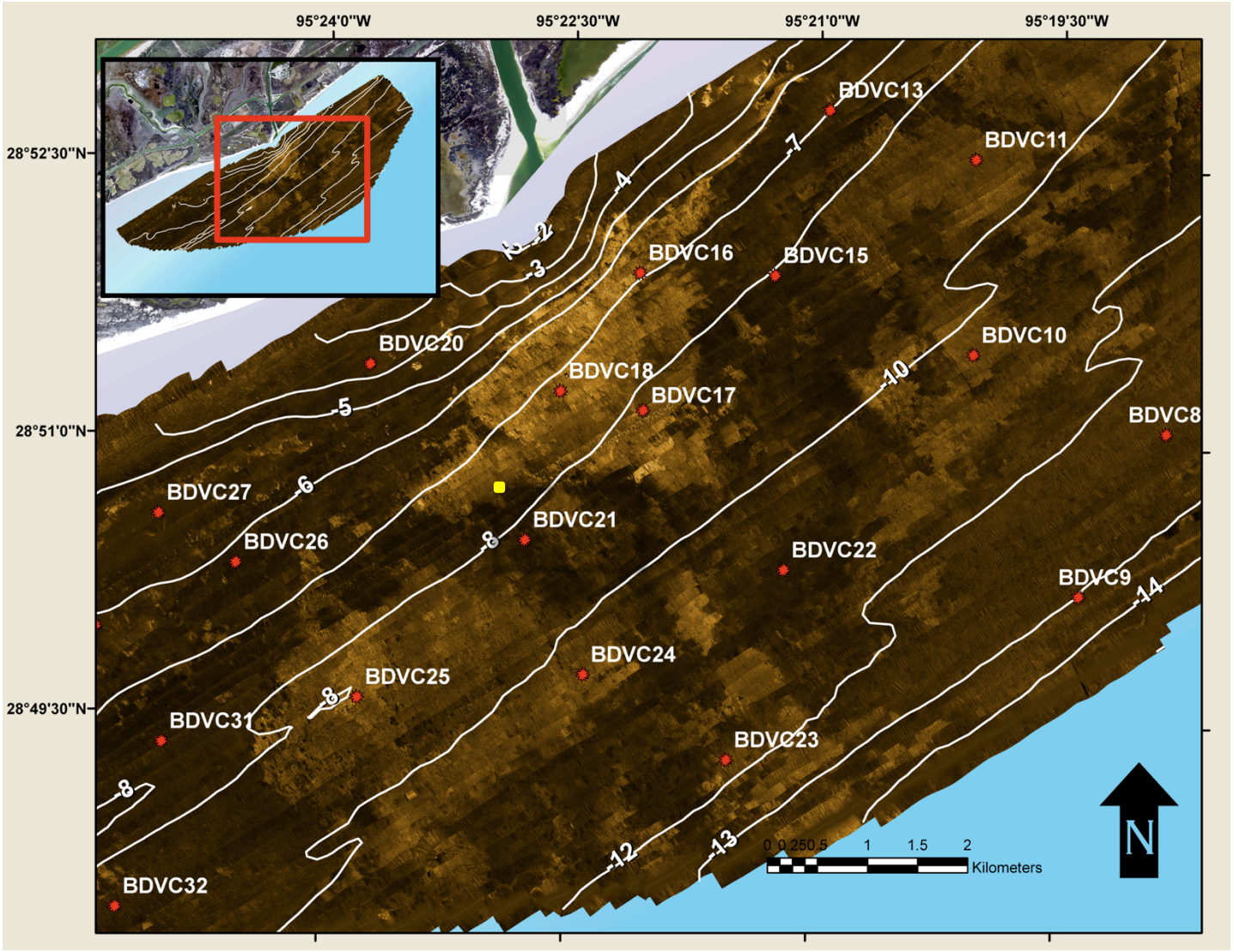

Project:_Brazos Delta Fall 2011___ Core: _BDVC21A_____

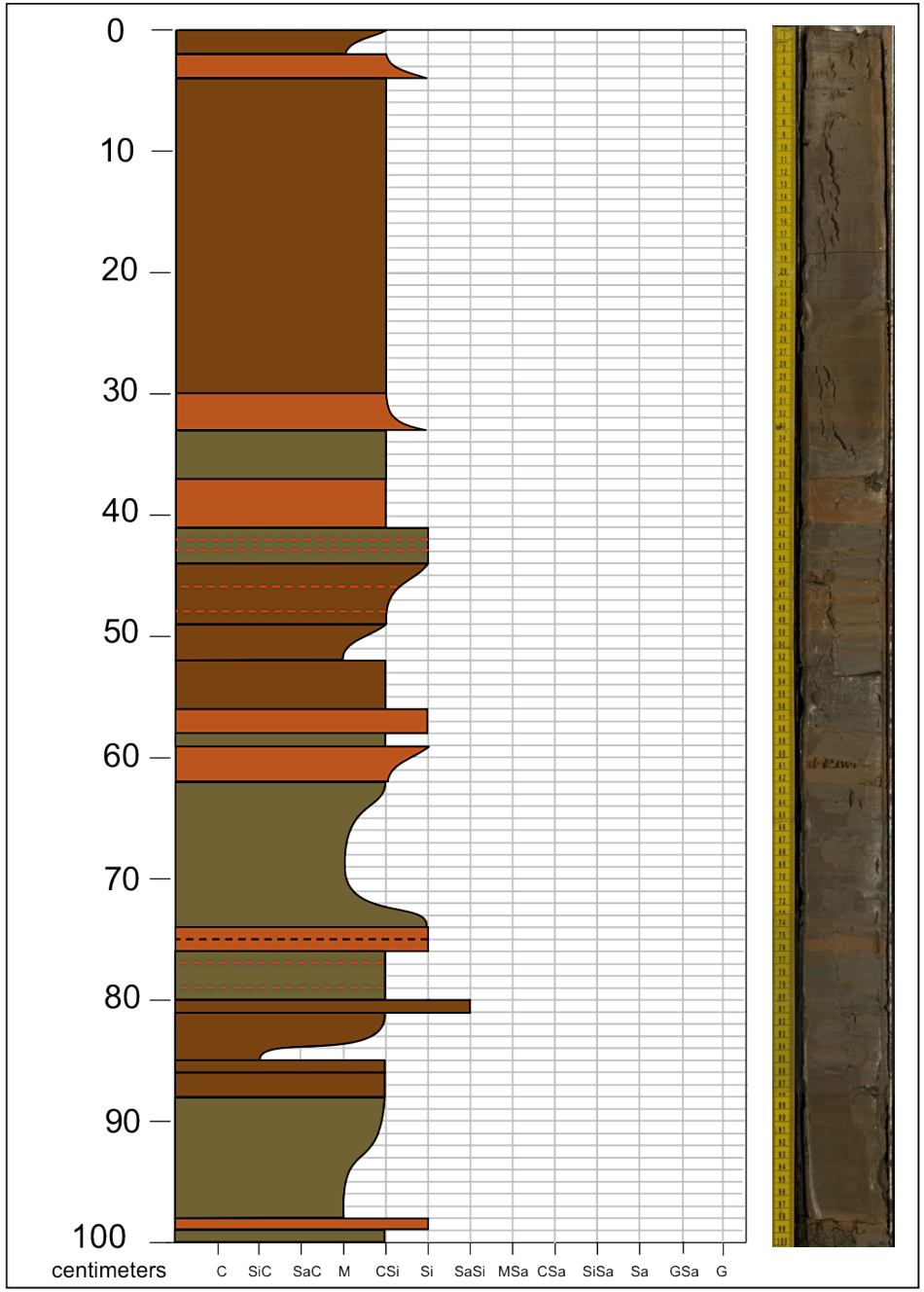

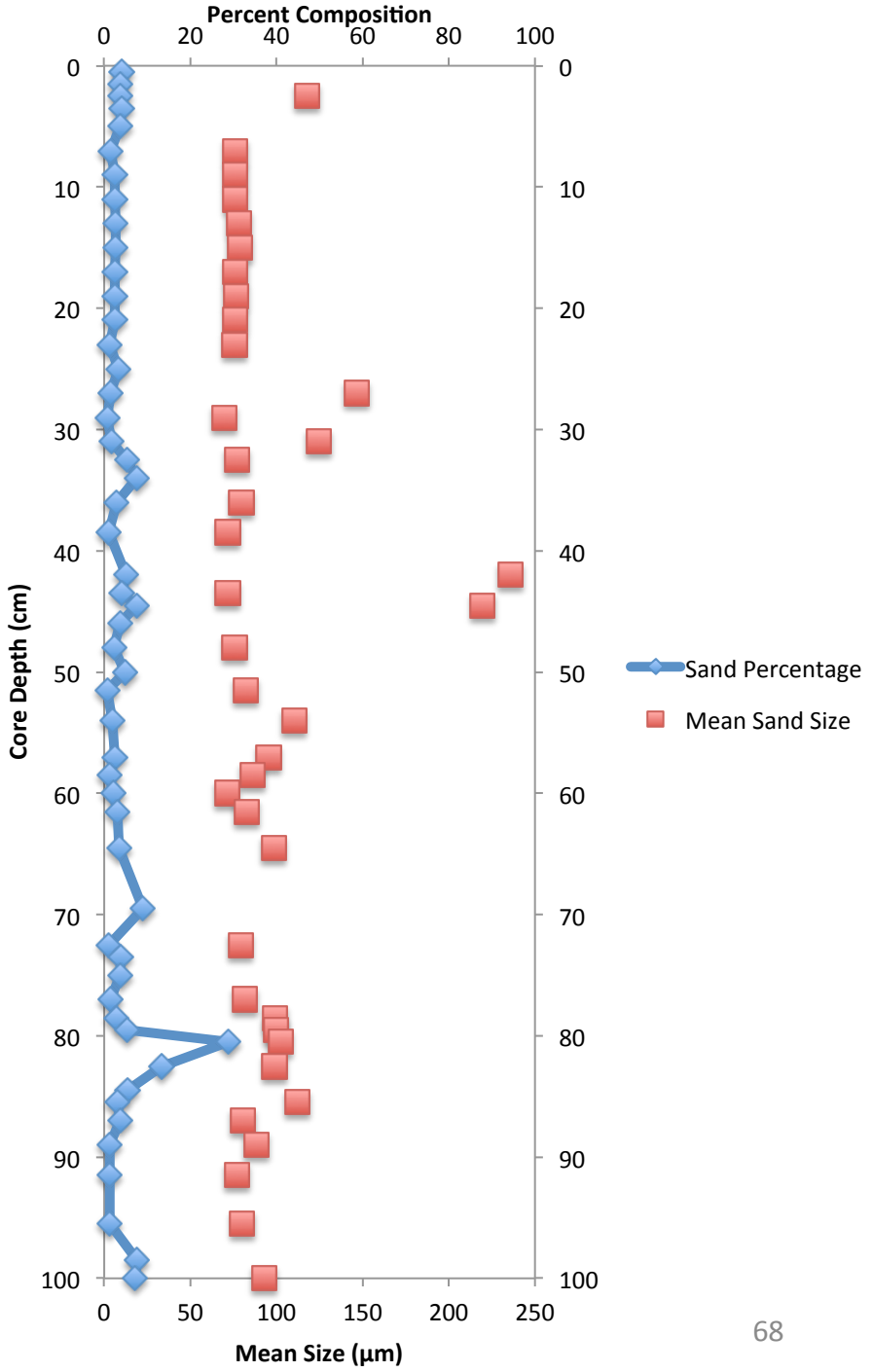

Project:_Brazos Delta Fall 2011___ Core: _BDVC21B_____

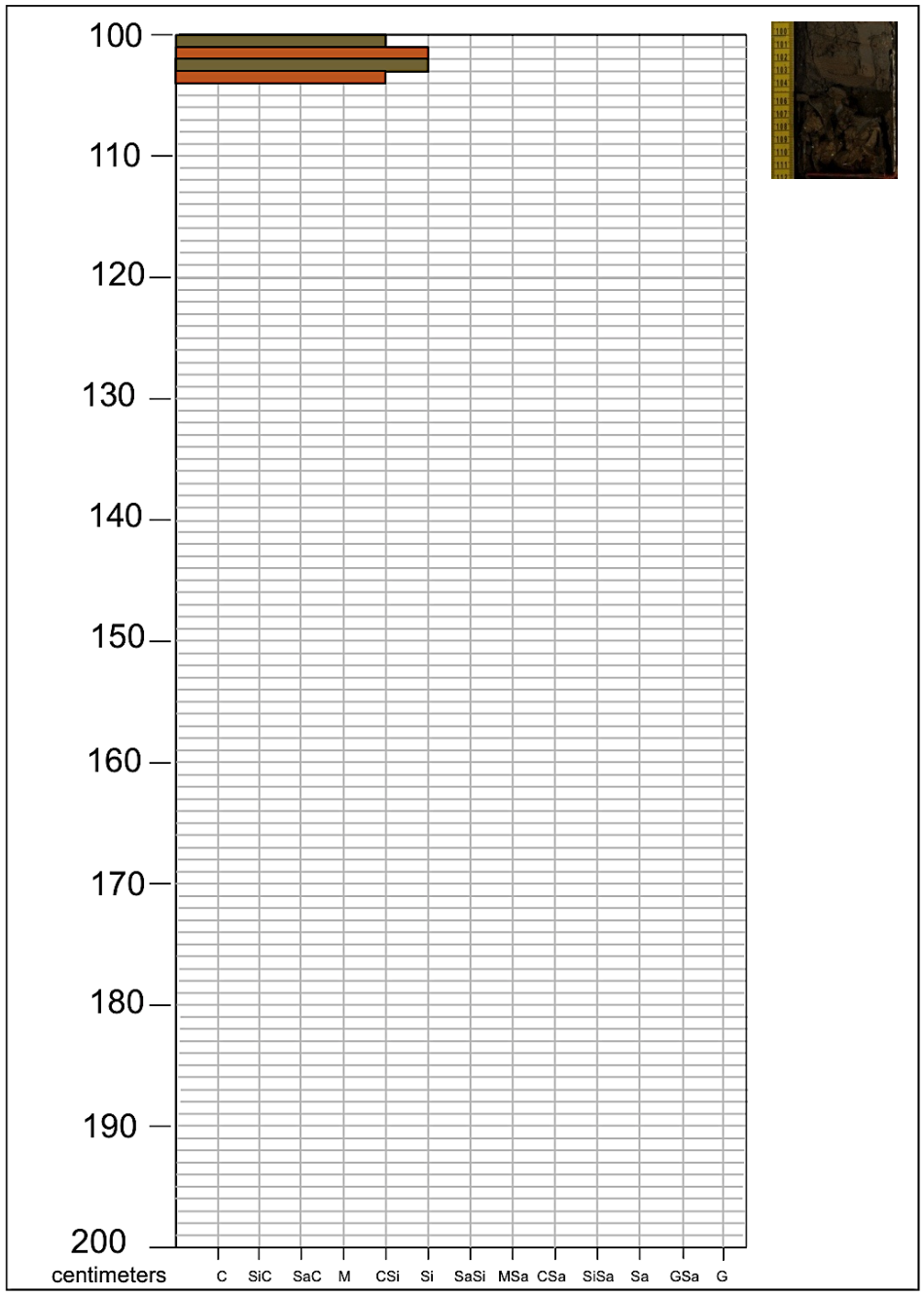

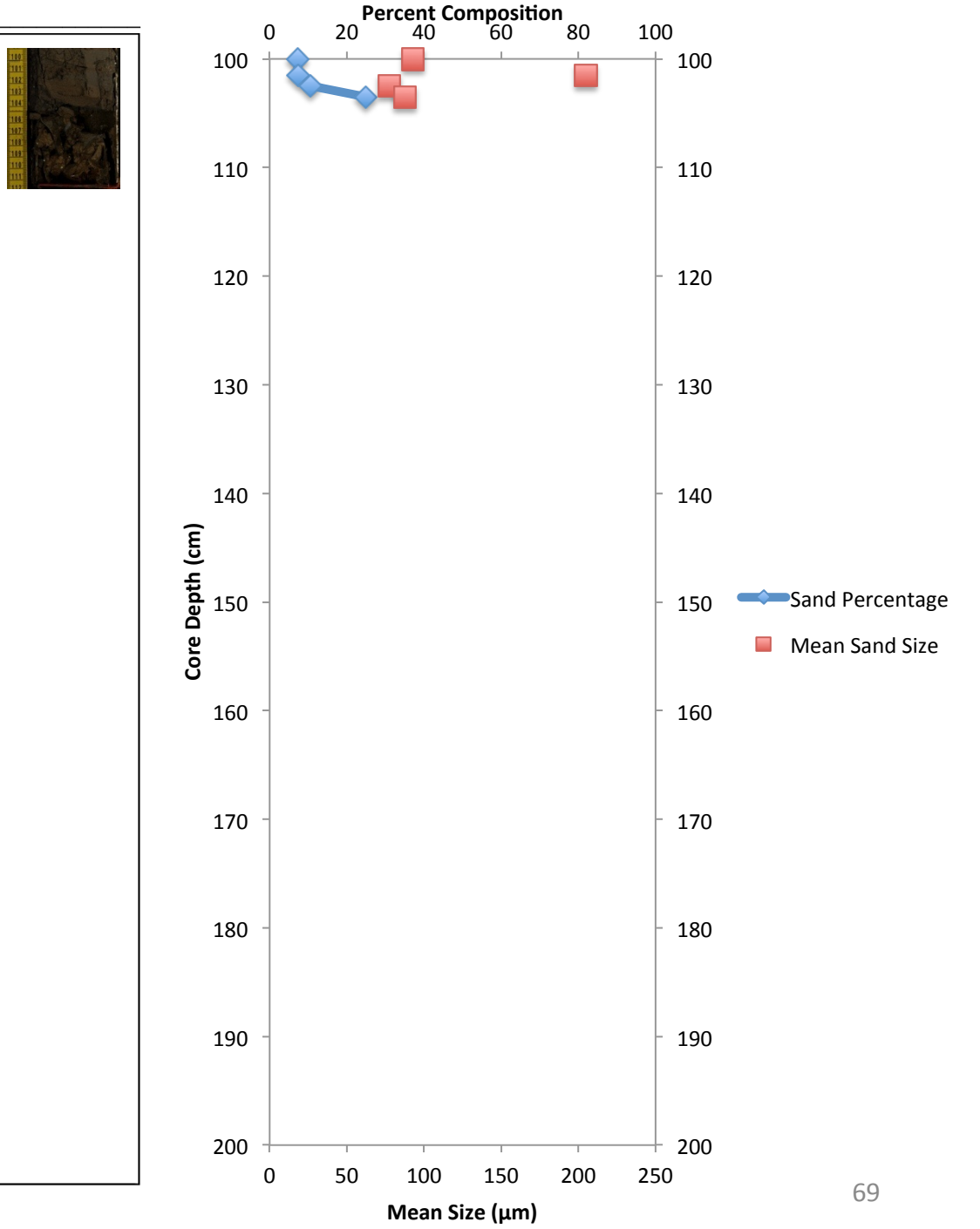

Brazos Delta Core: BDVC22

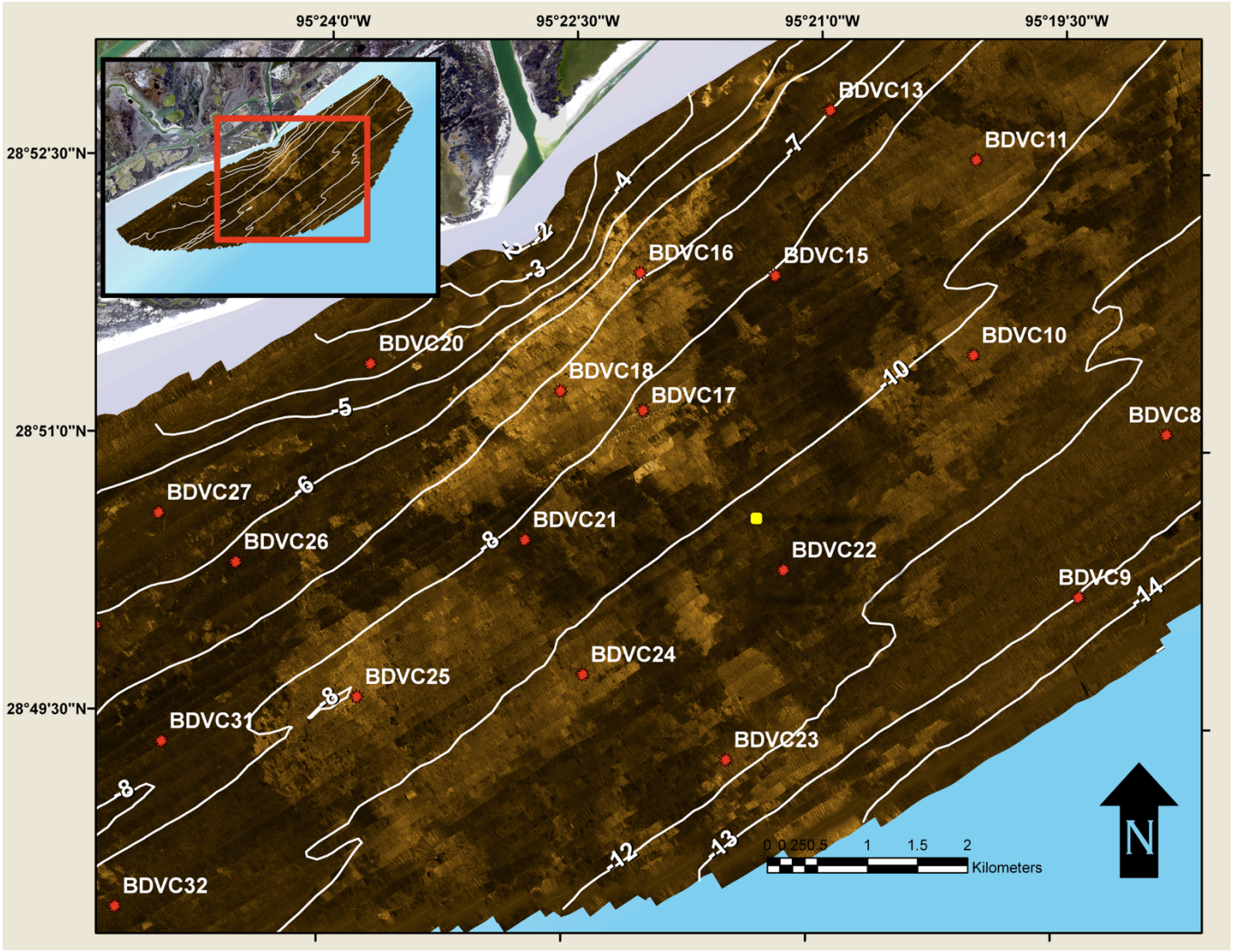

Project:_Brazos Delta Fall 2011___ Core: _BDVC22_____

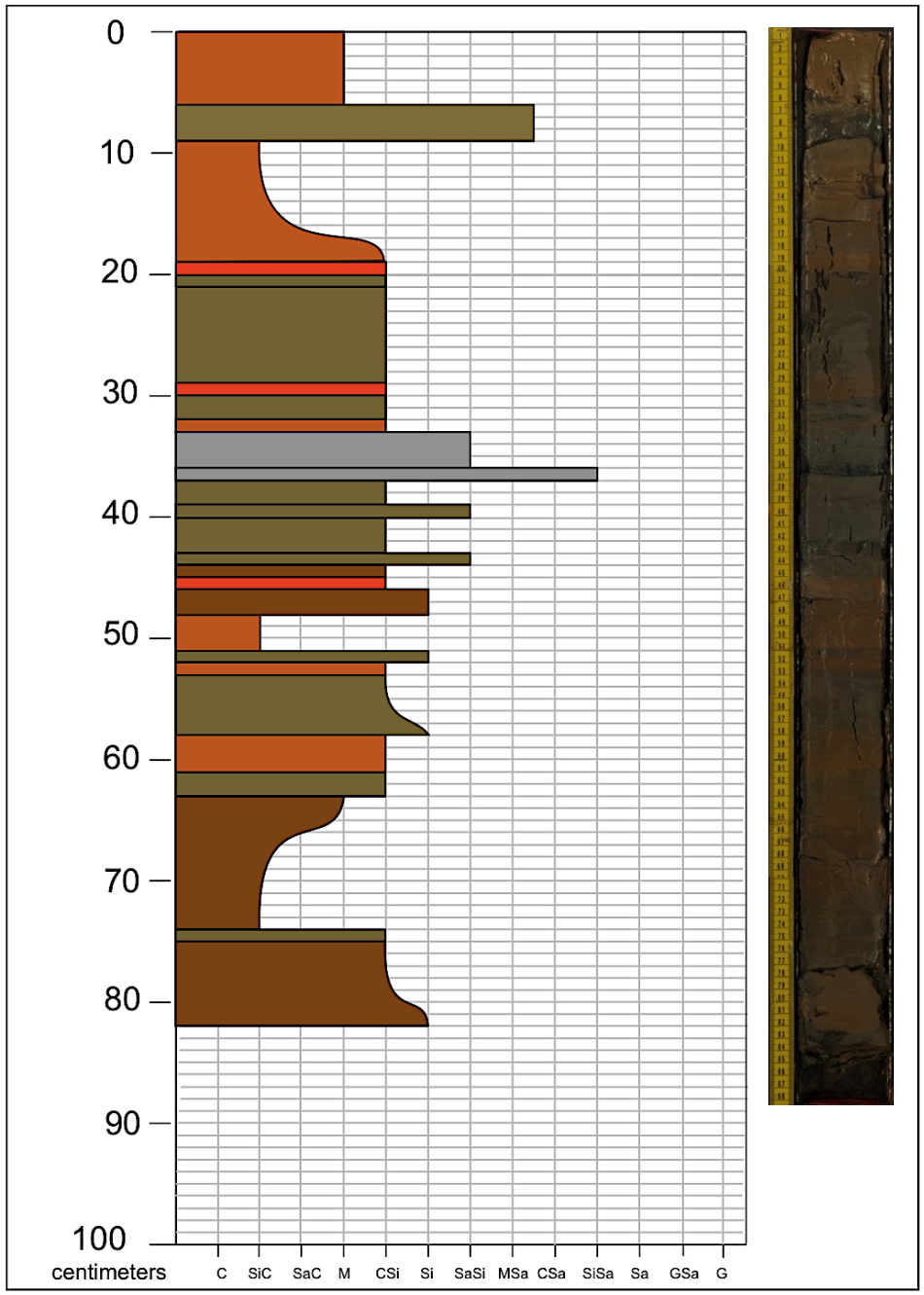

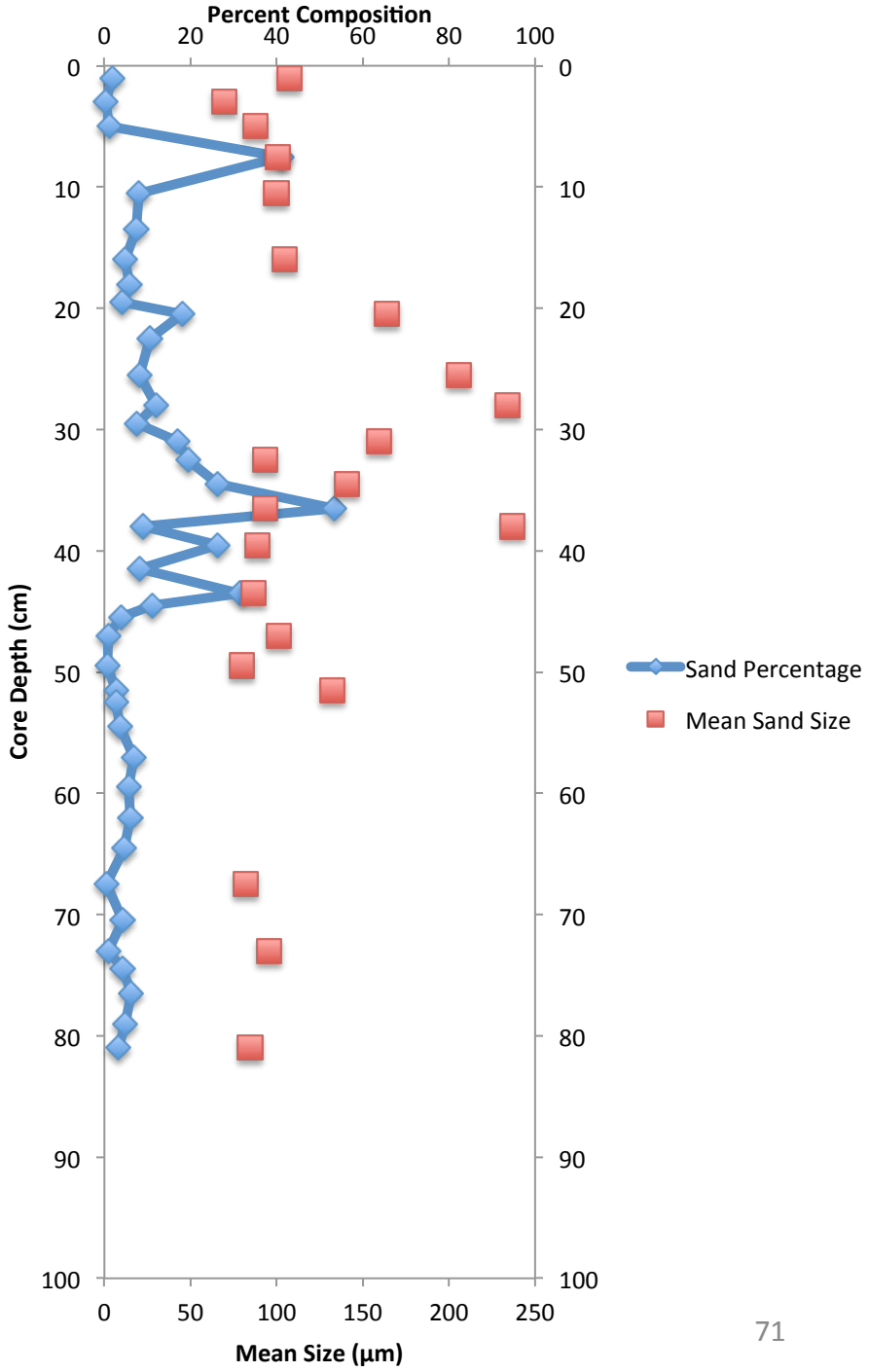

Brazos Delta Core: BDVC23

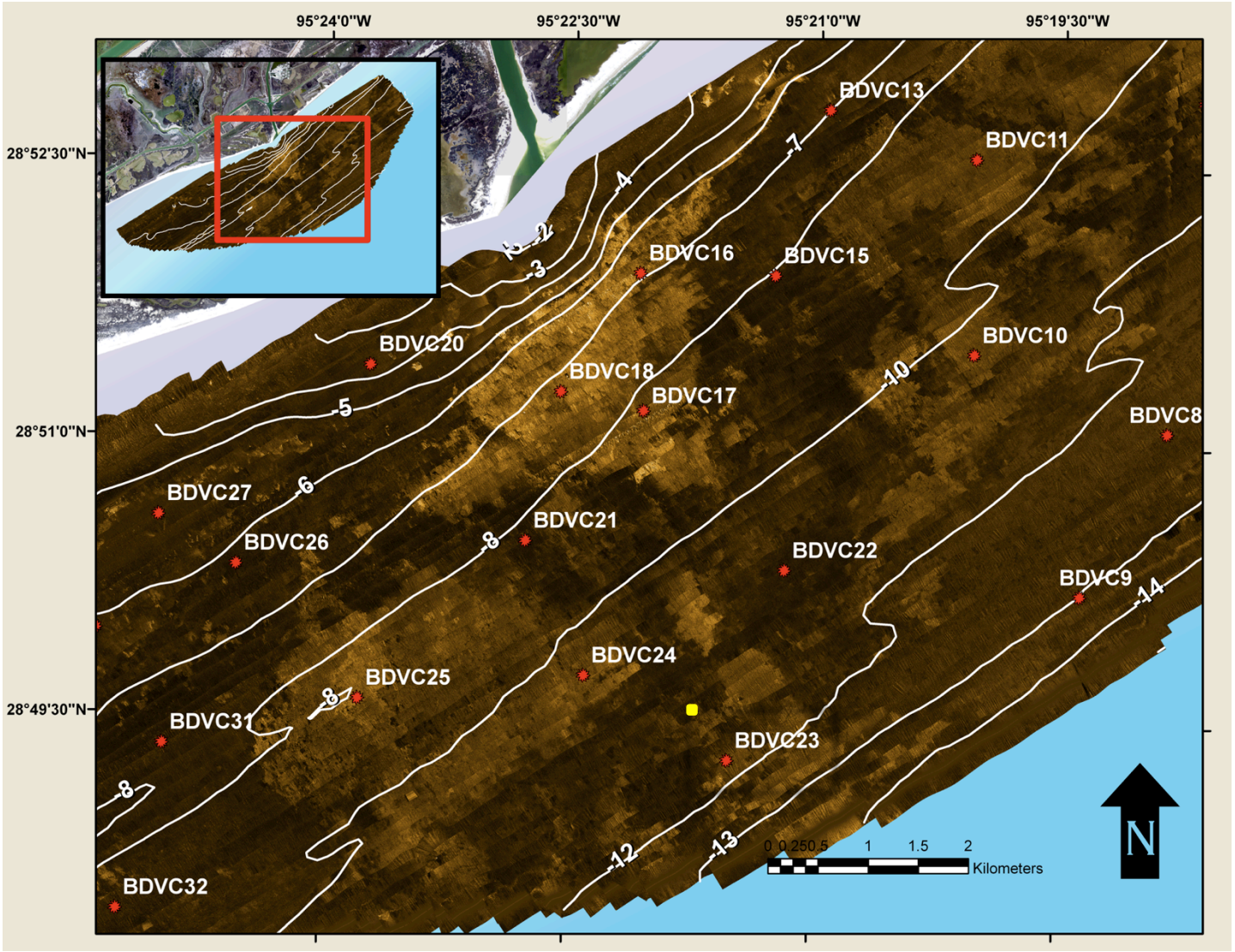

Project:_Brazos Delta Fall 2011___ Core: _BDVC23_____

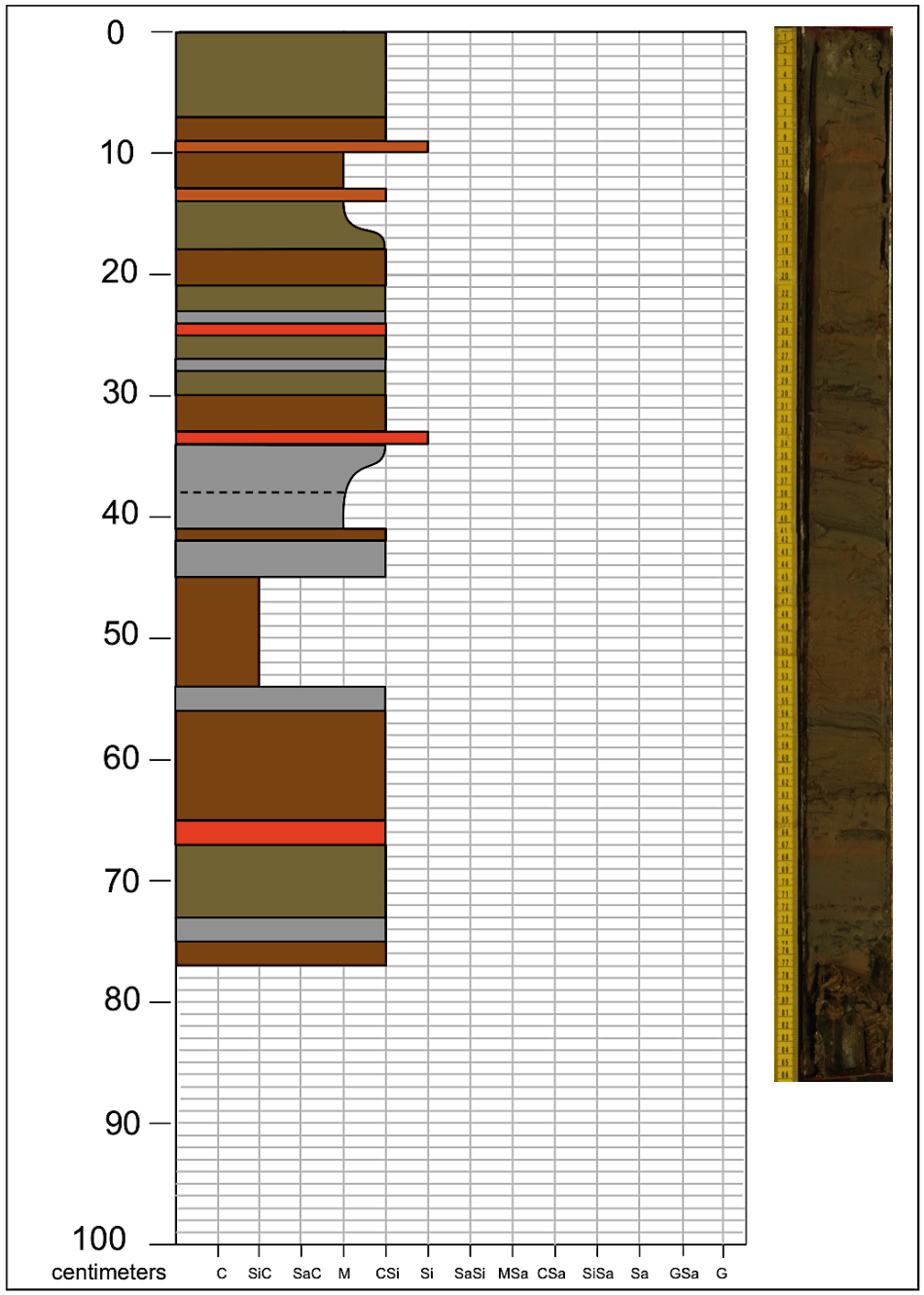

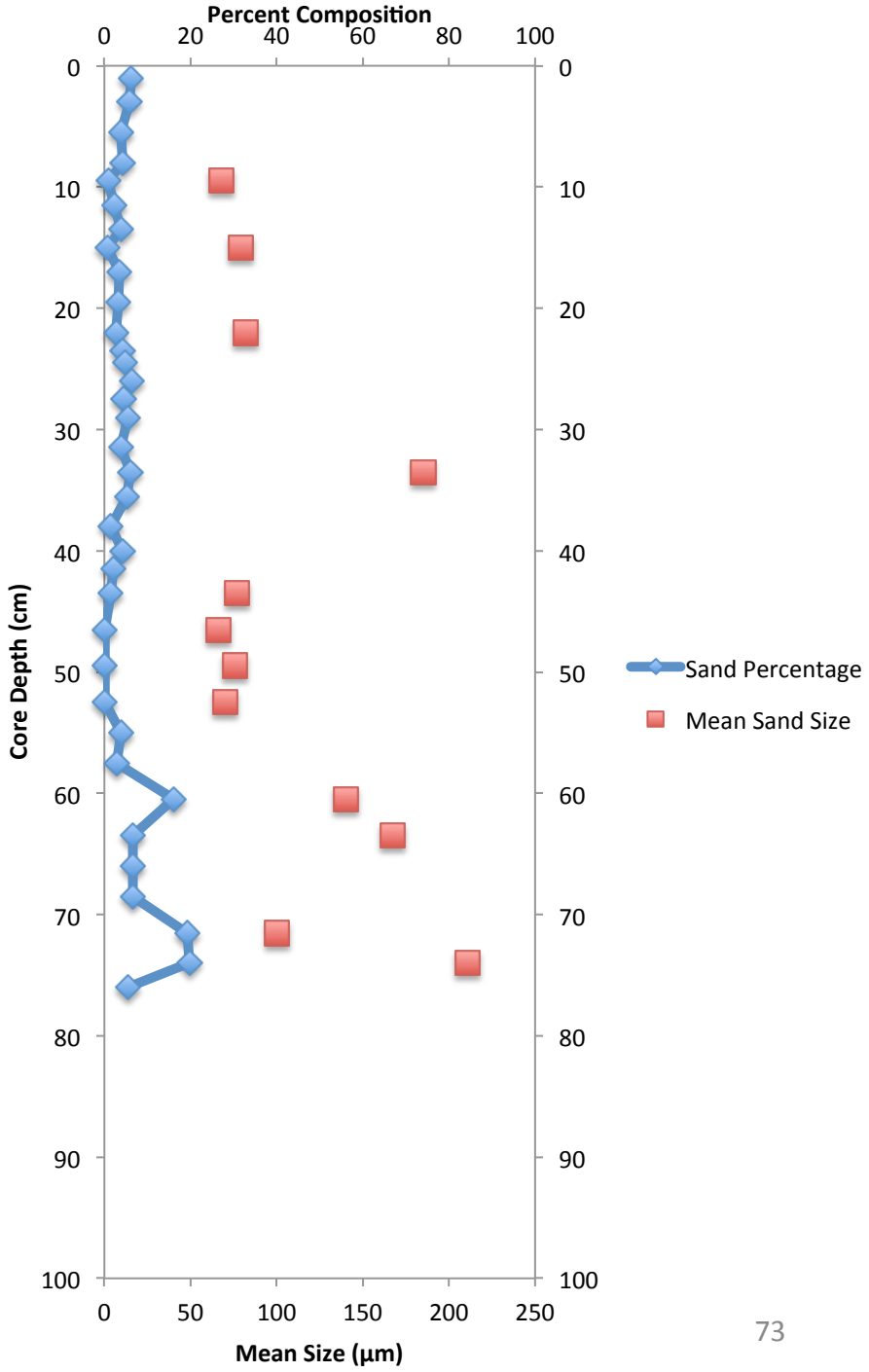

Brazos Delta Core: BDVC24

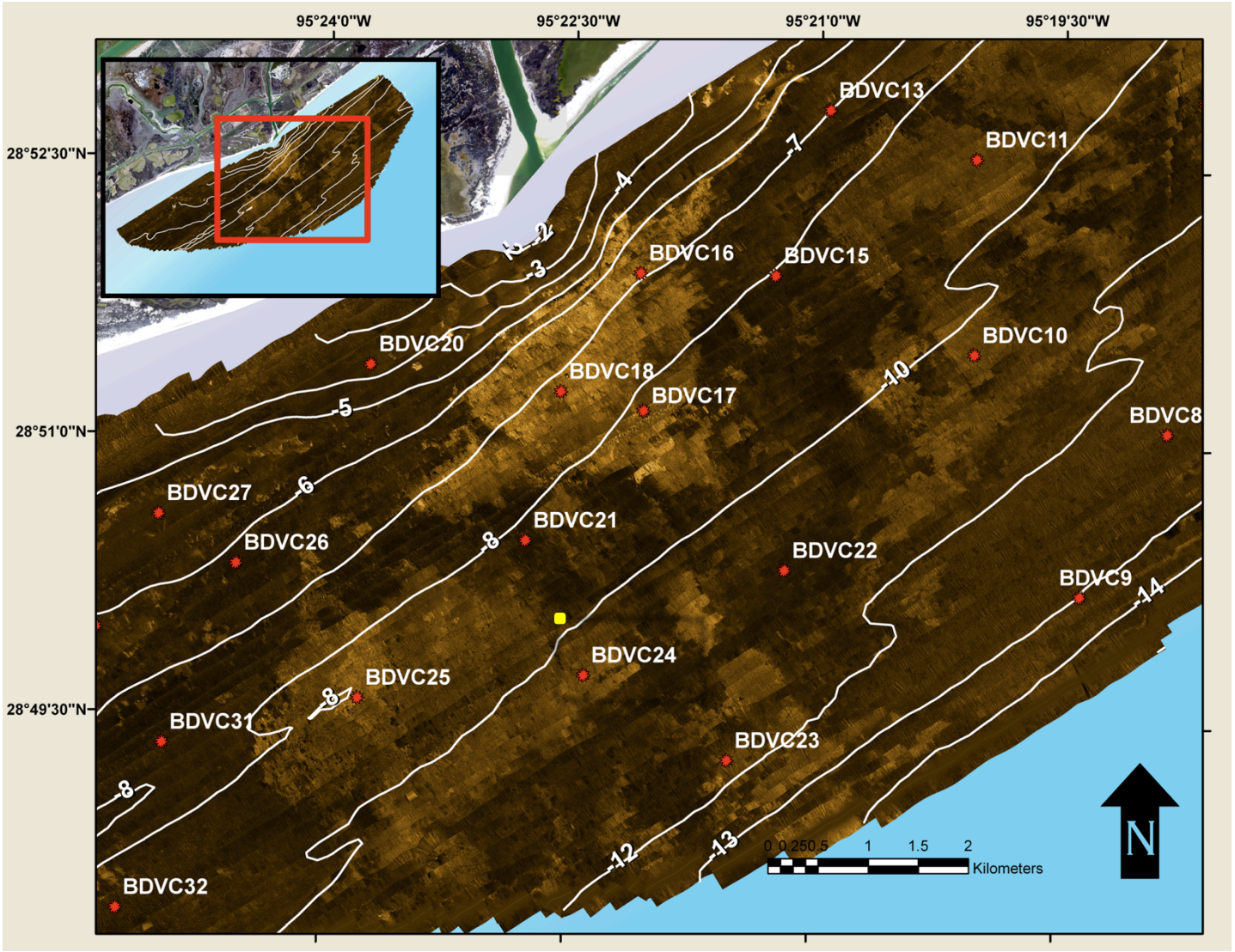

Project:_Brazos Delta Fall 2011___ Core: _BDVC24A_____

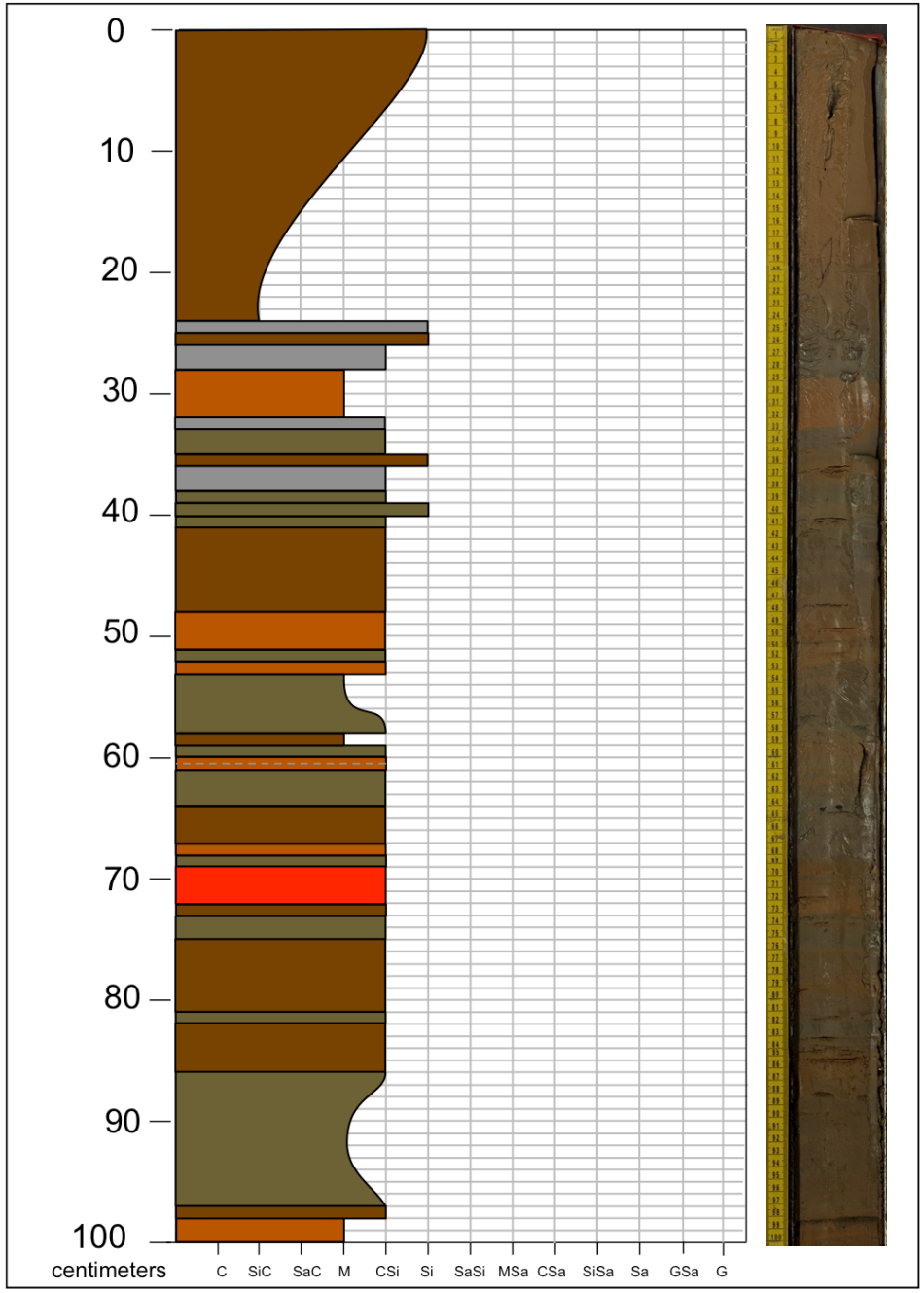

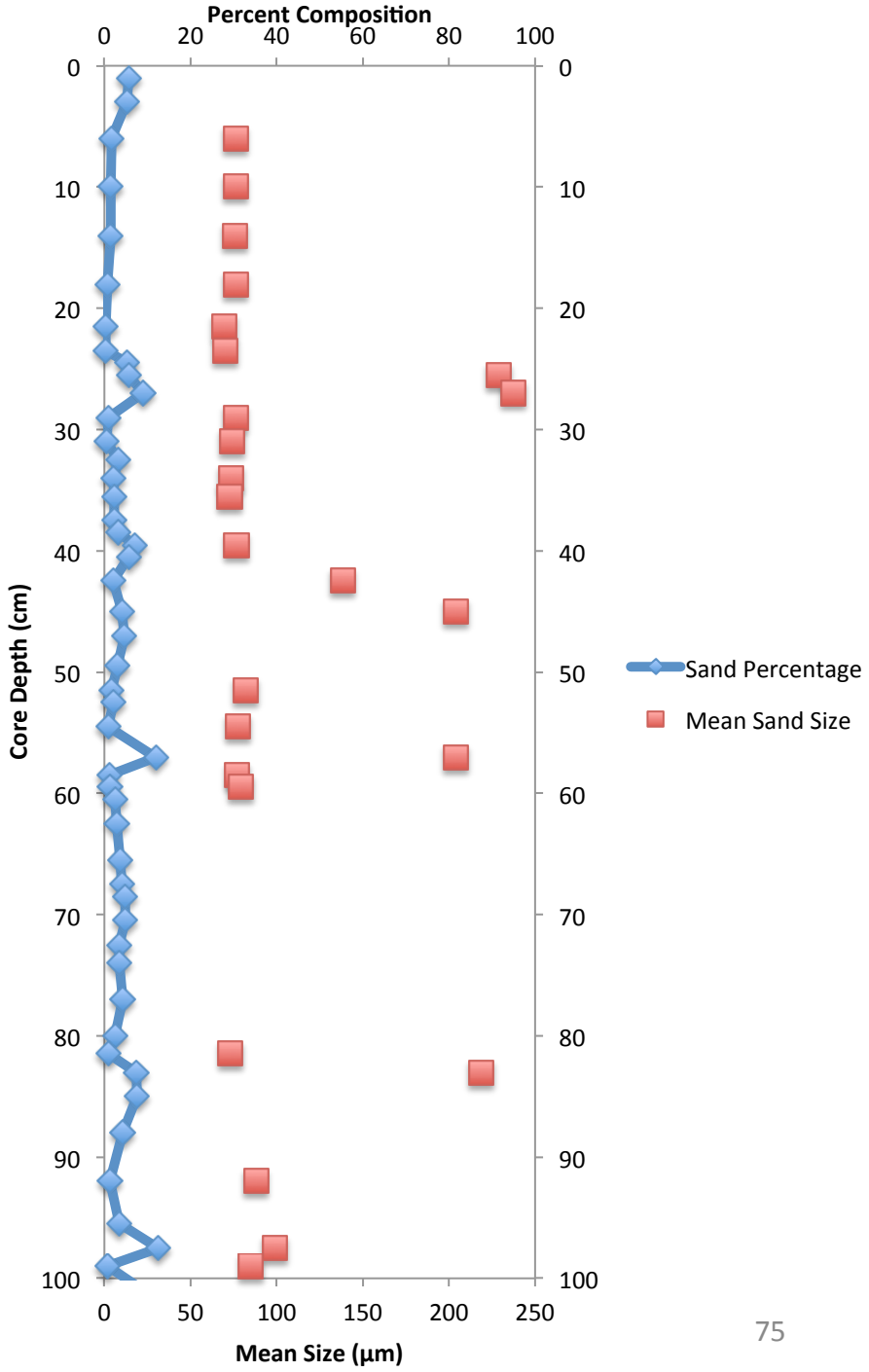

Project:_Brazos Delta Fall 2011___ Core: _BDVC24B_____

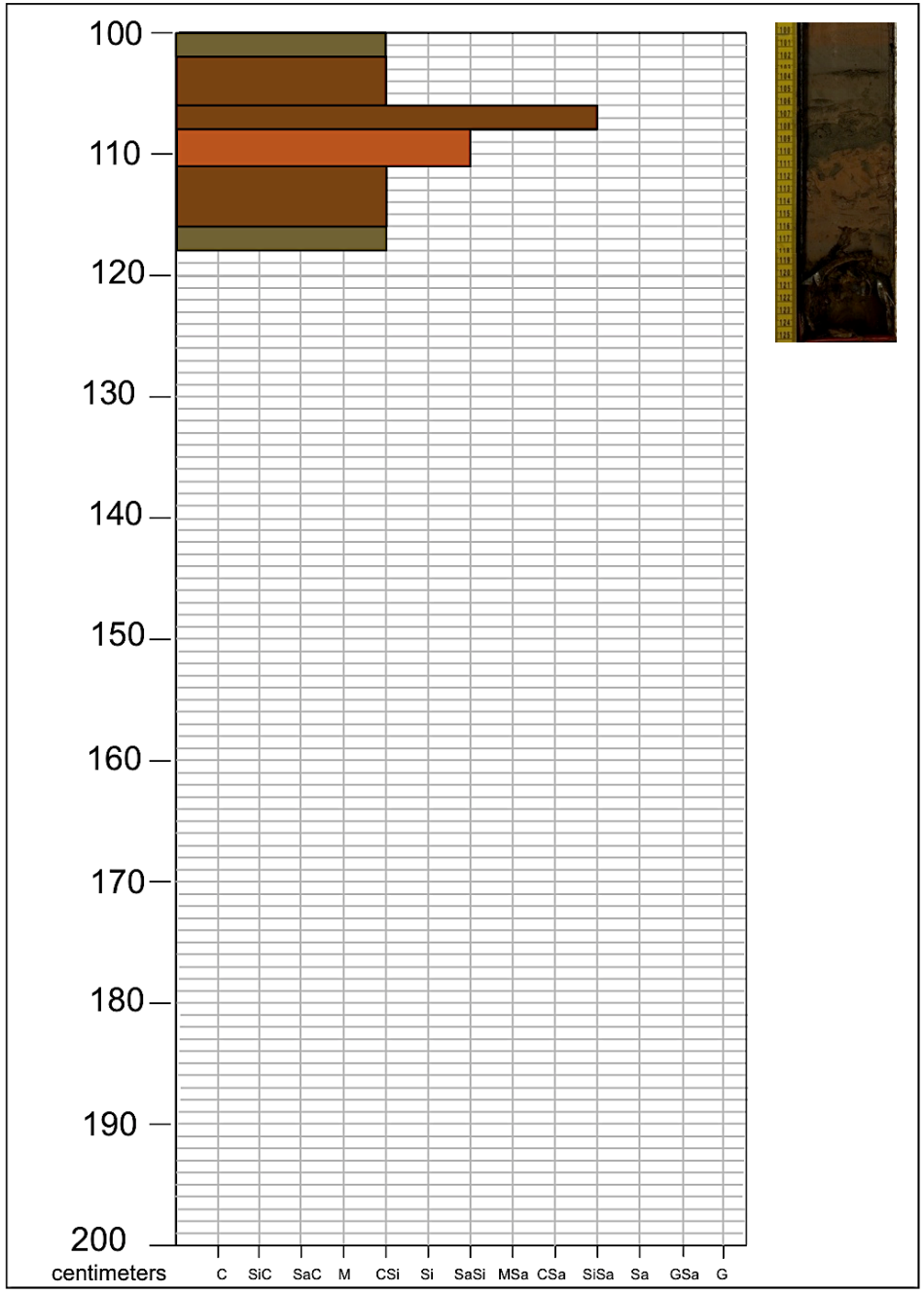

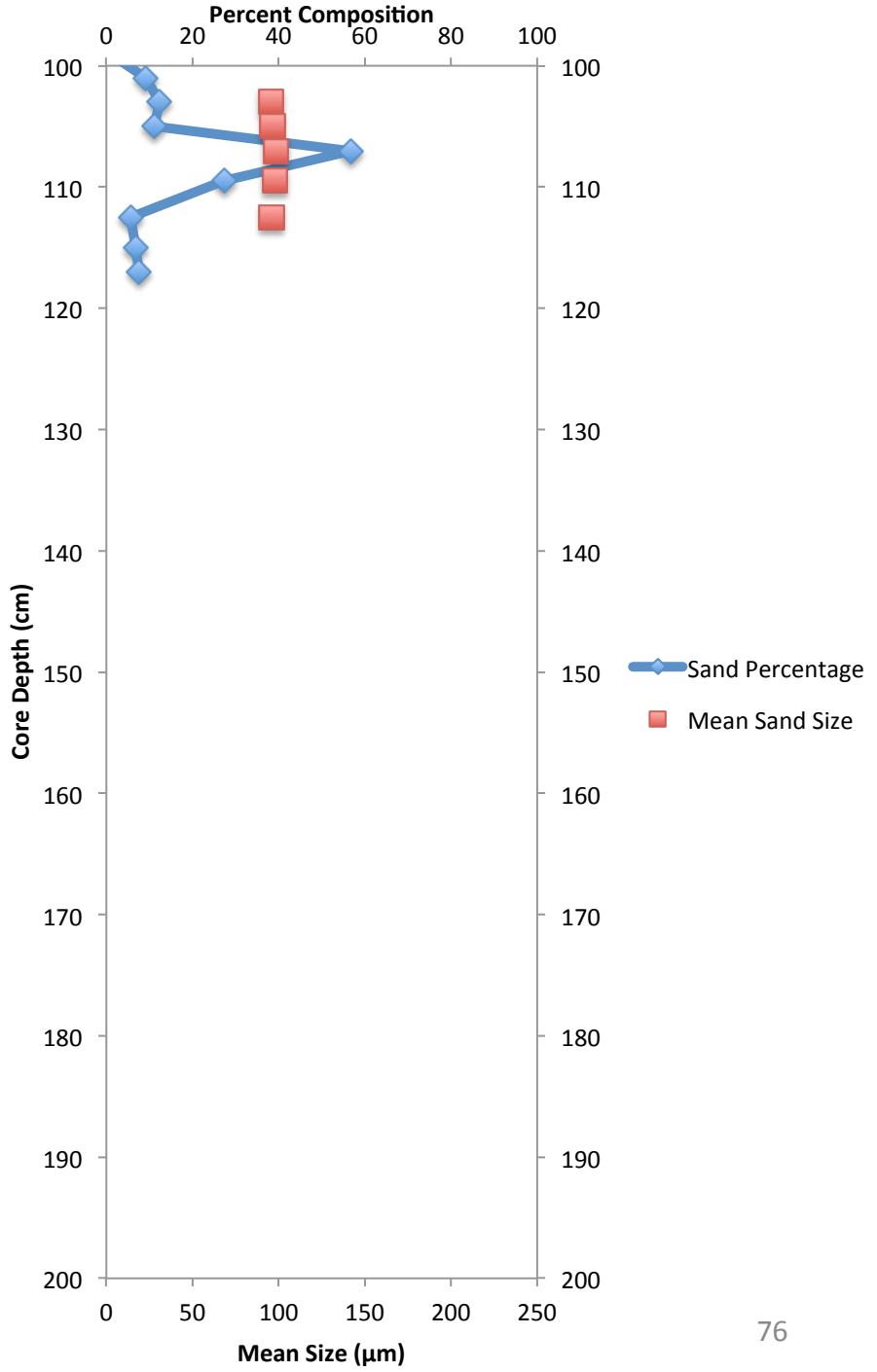

Brazos Delta Core: BDVC25

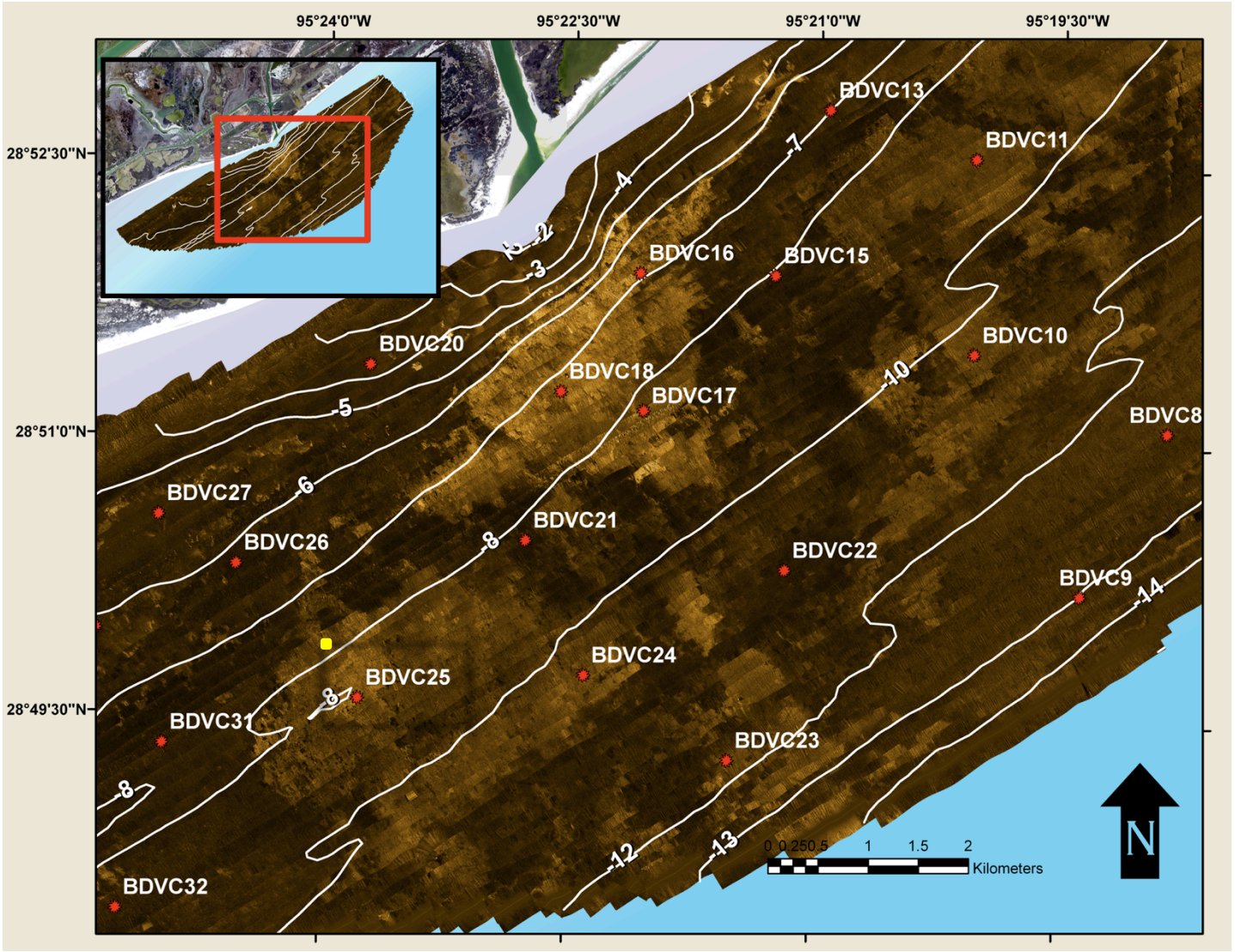

Project:_Brazos Delta Fall 2011___ Core: _BDVC25_____

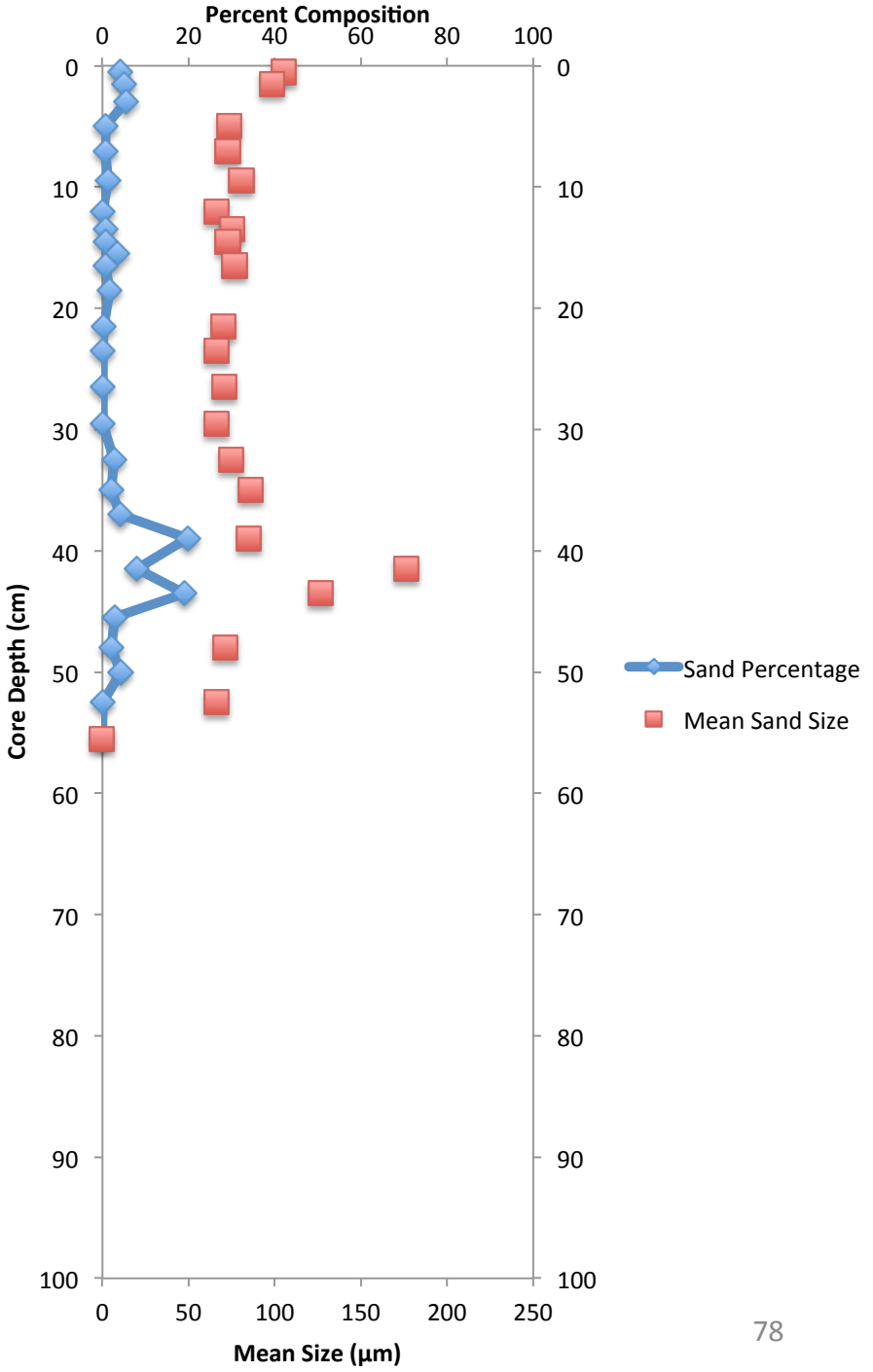

Brazos Delta Core: BDVC26

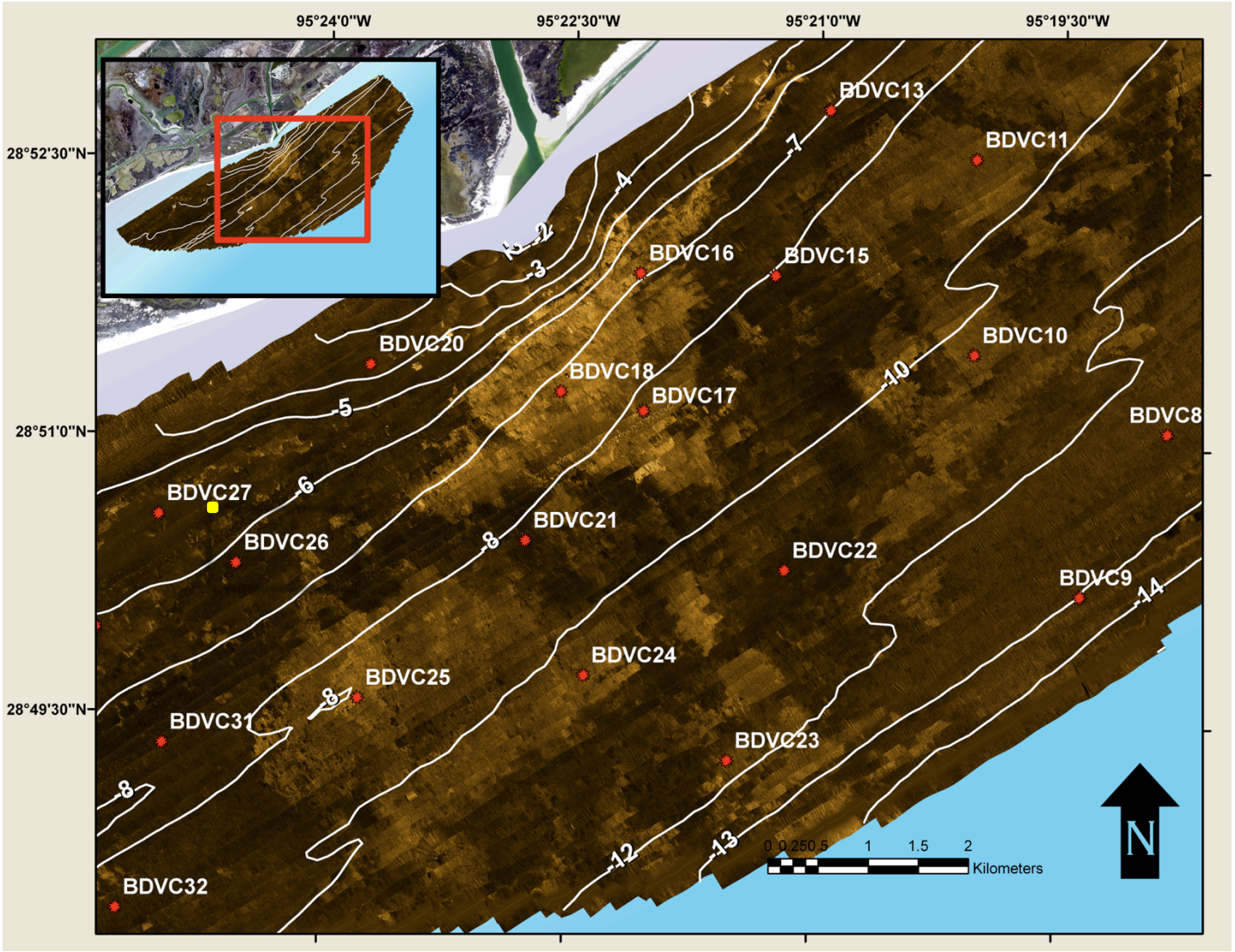

Project:_Brazos Delta Fall 2011___ Core: _BDVC26A_____

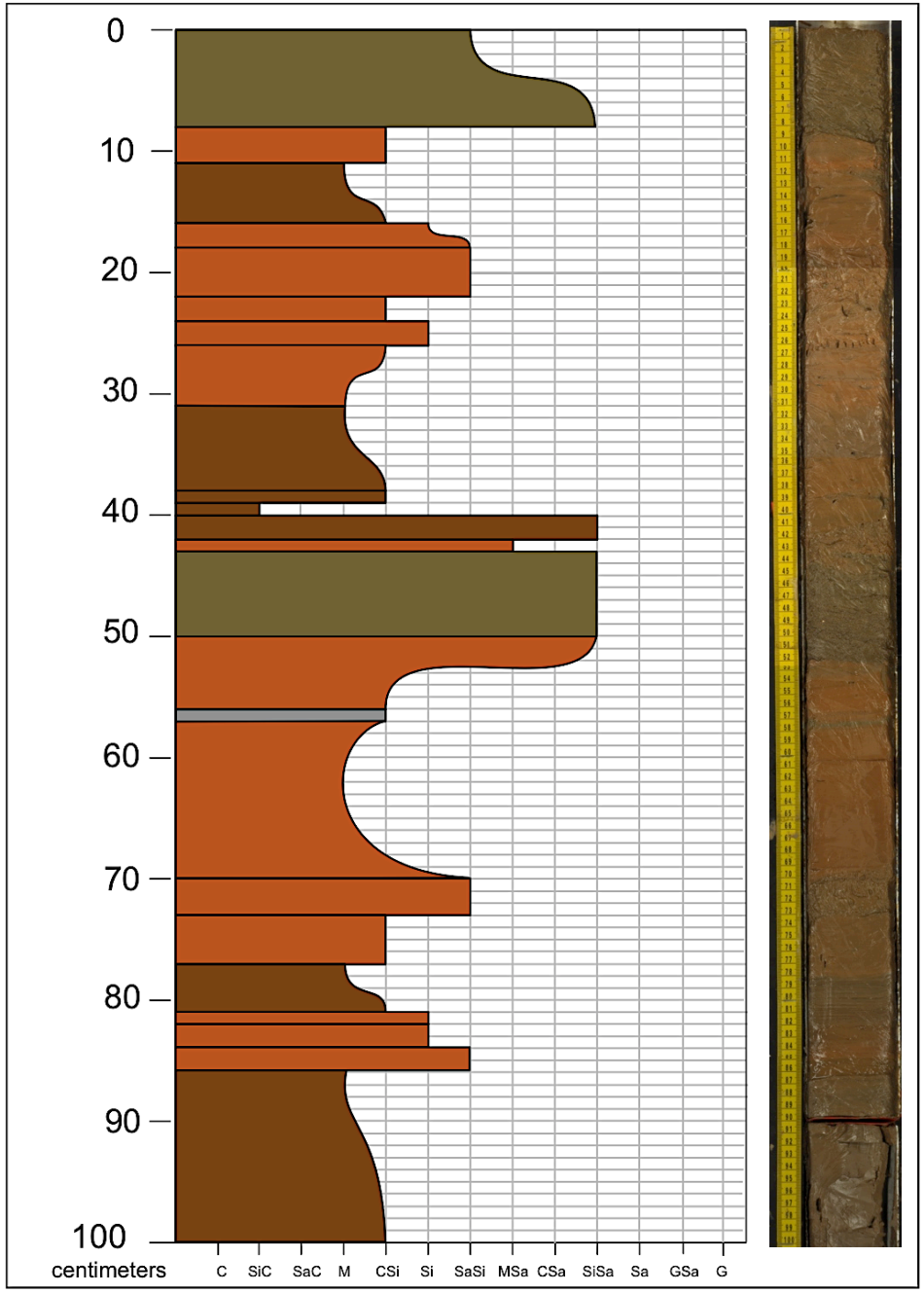

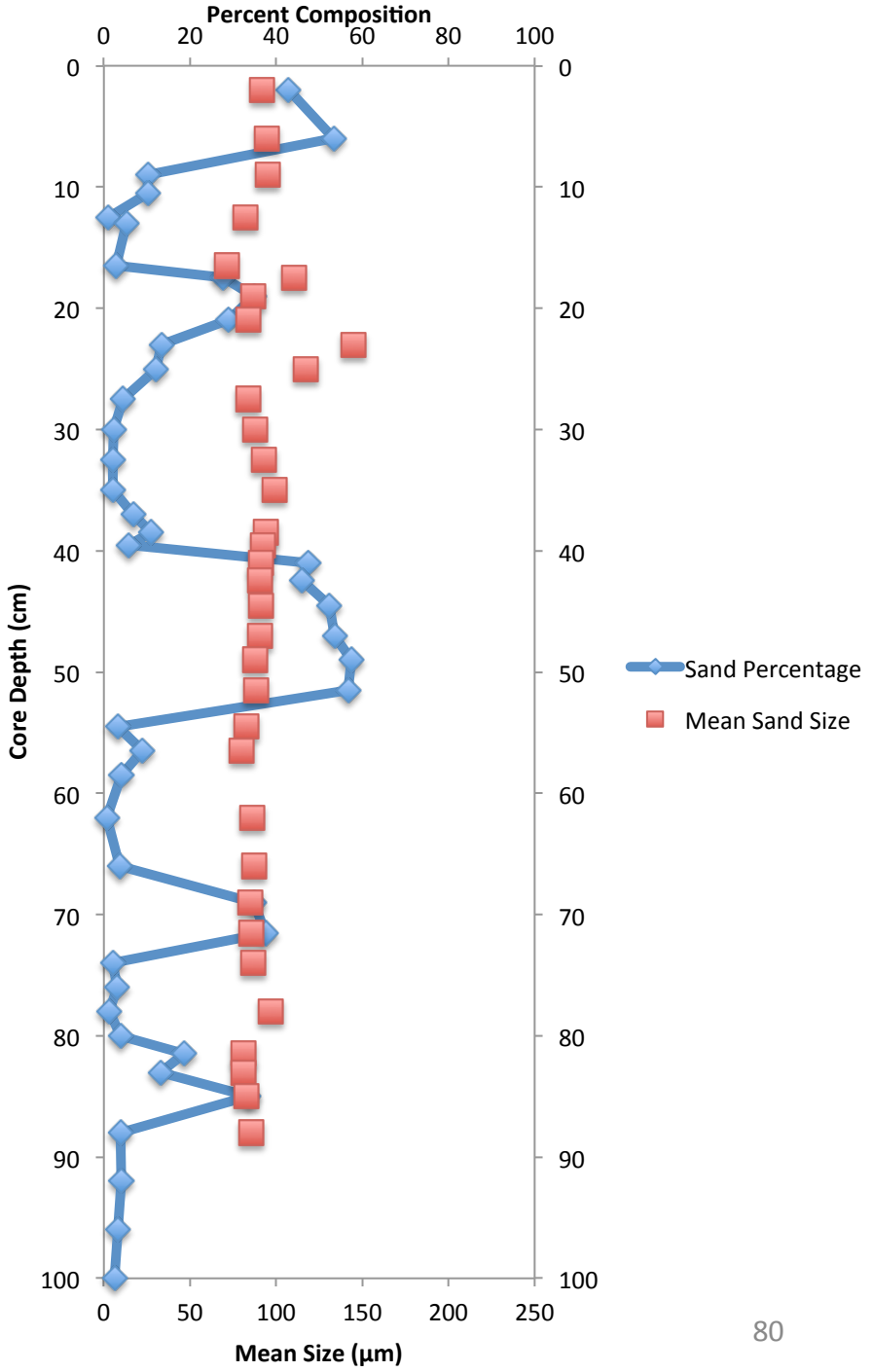

Project:_Brazos Delta Fall 2011___ Core: _BDVC26B_____

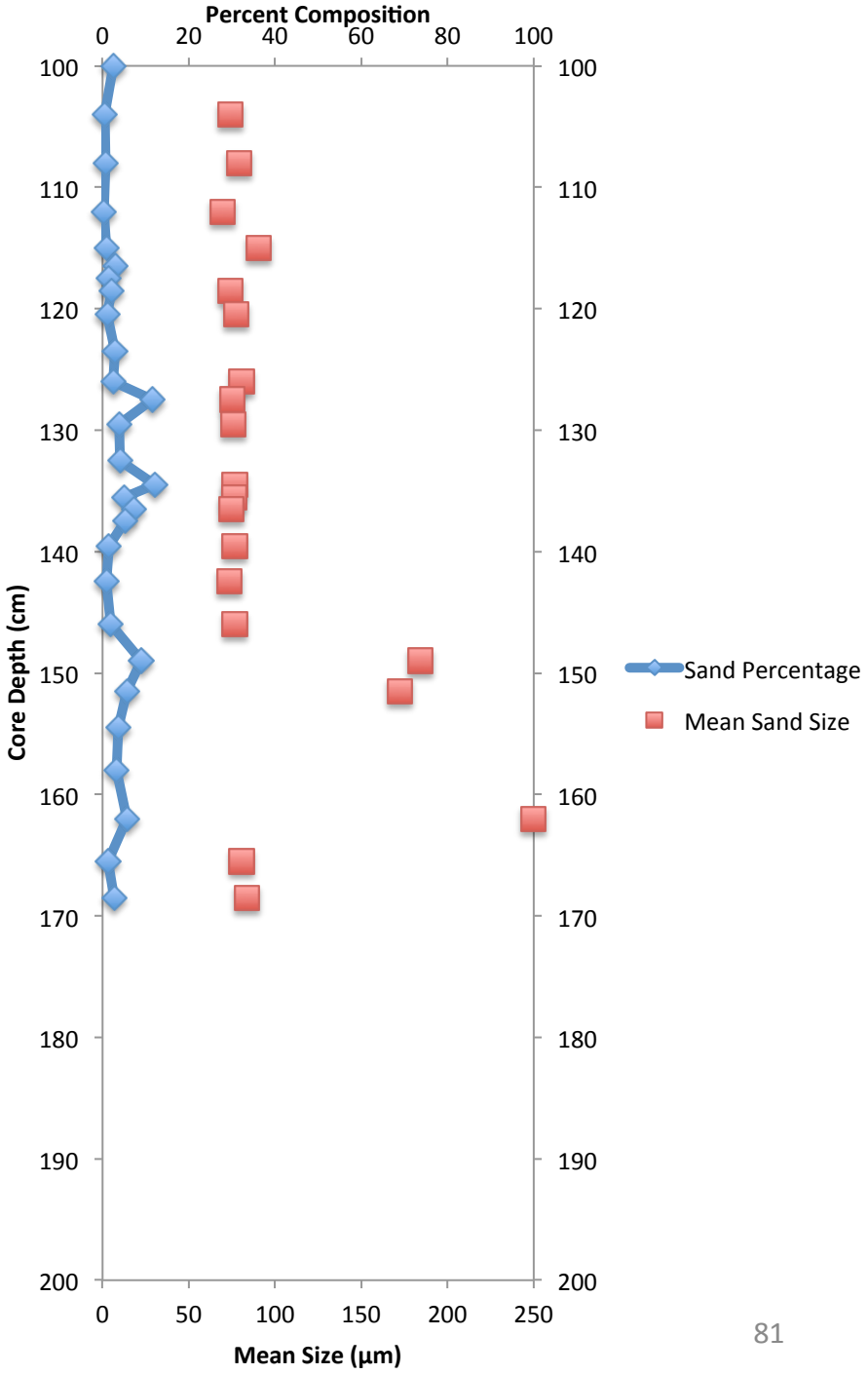

Brazos Delta Core: BDVC27

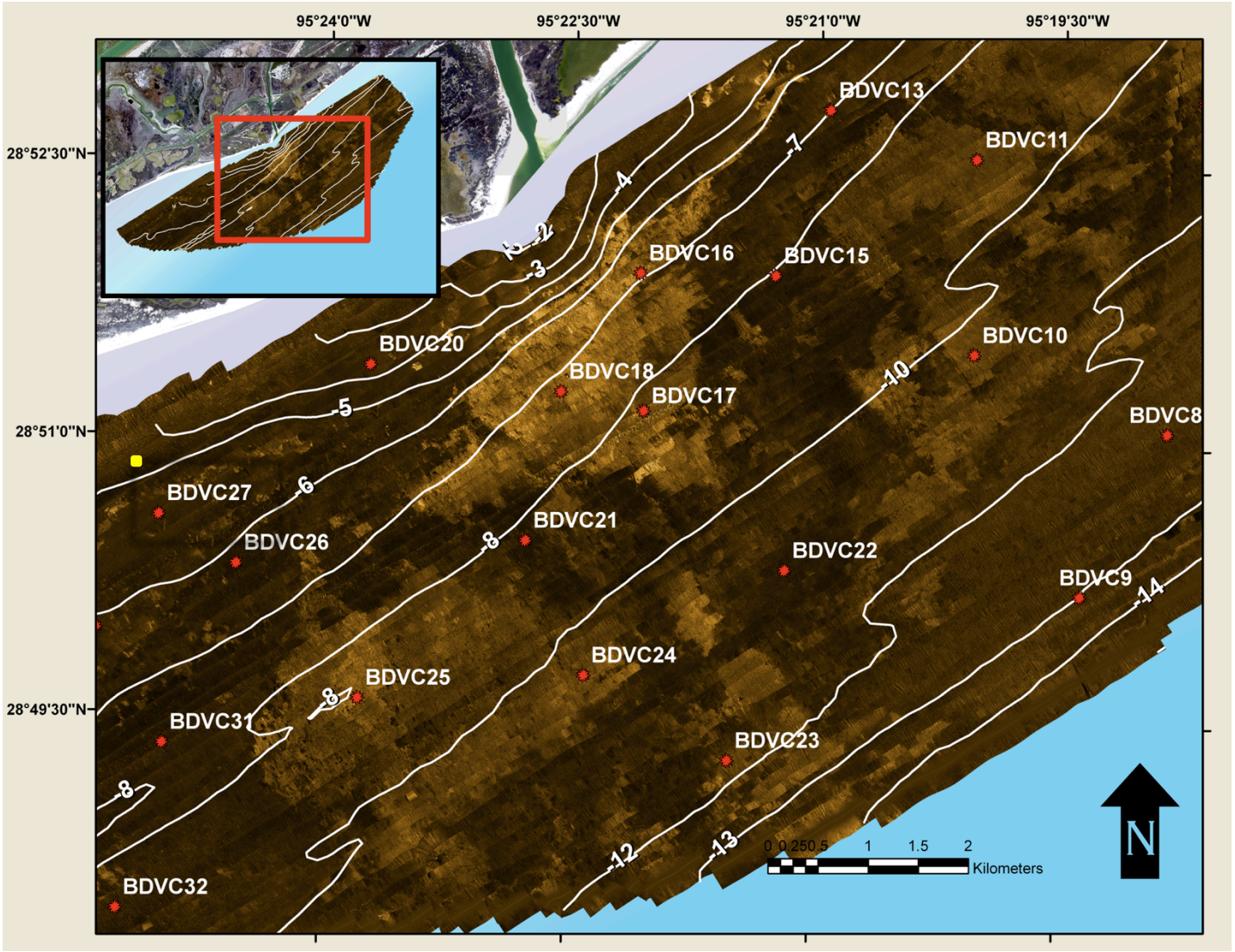

Project:_Brazos Delta Fall 2011___ Core: _BDVC27_____

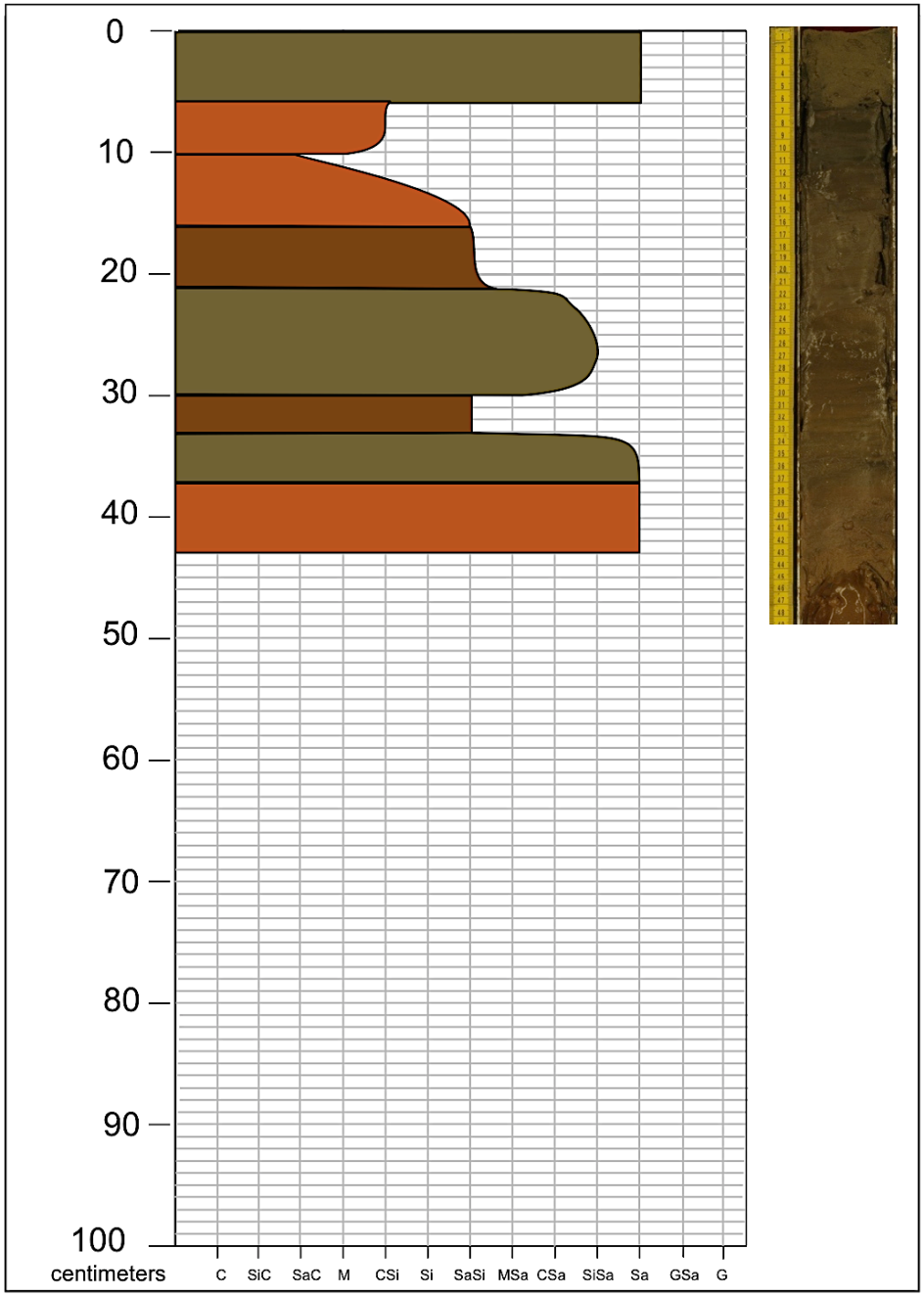

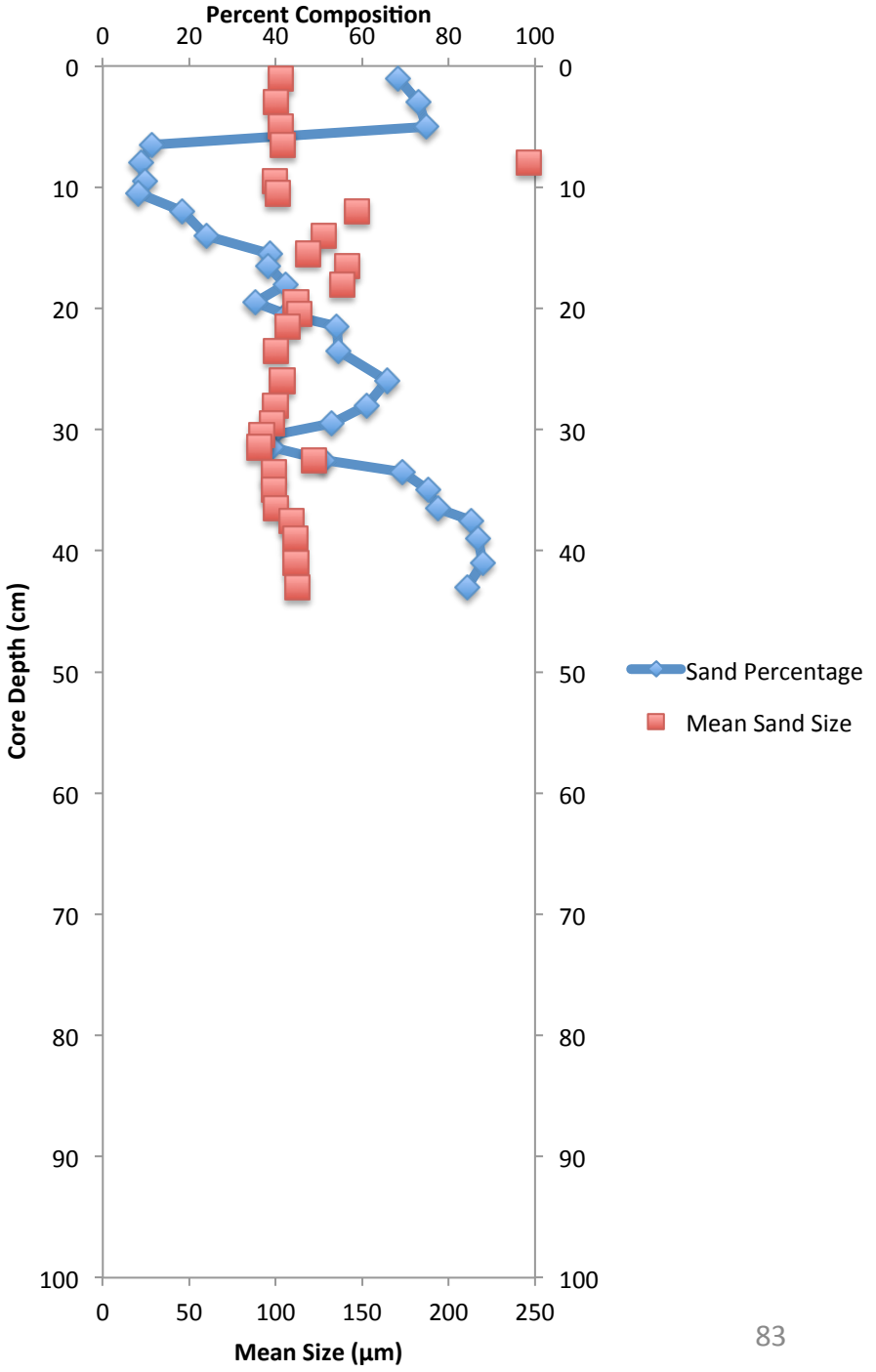

Brazos Delta Core: BDVC28

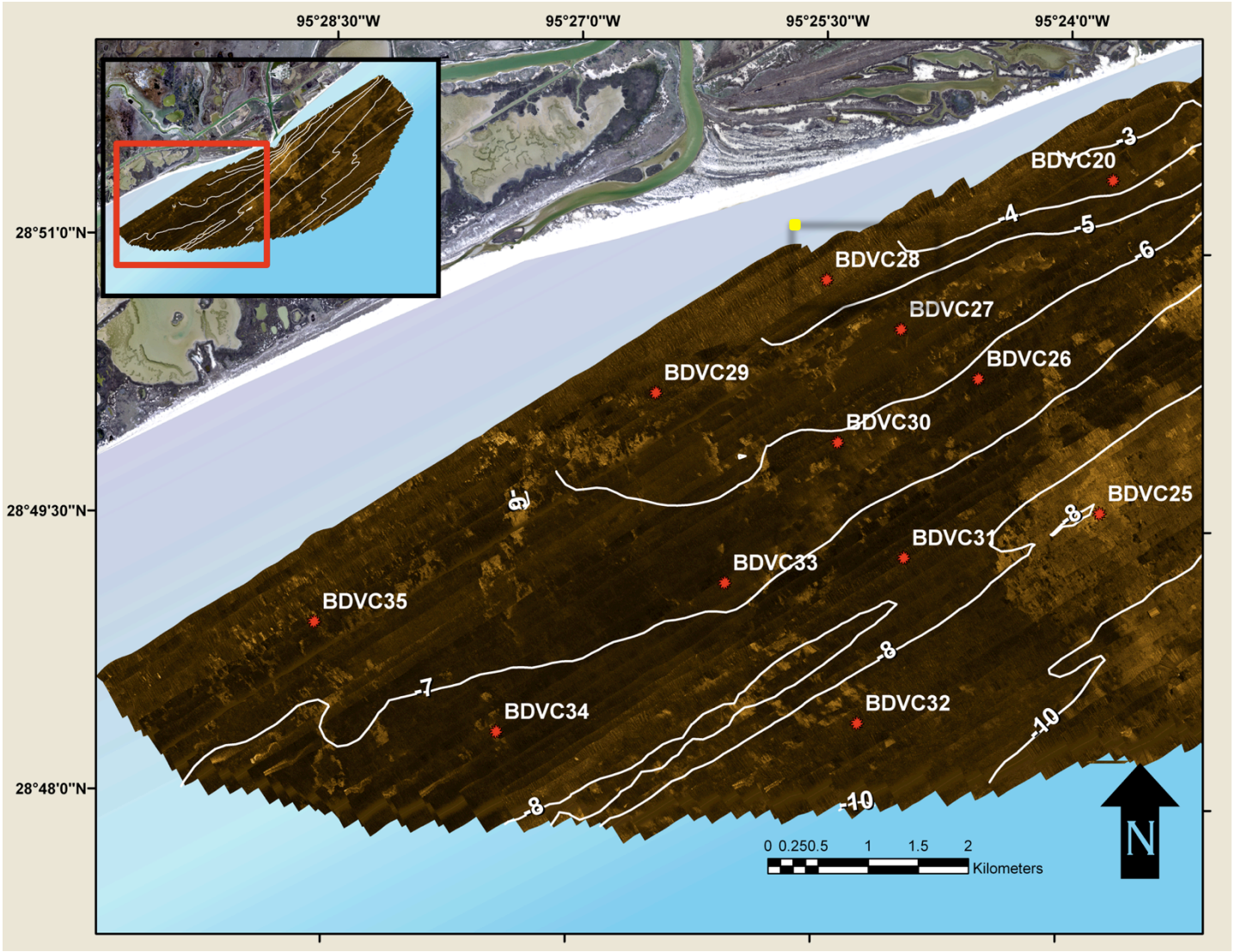

Project:_Brazos Delta Fall 2011___ Core: _BDVC28_____

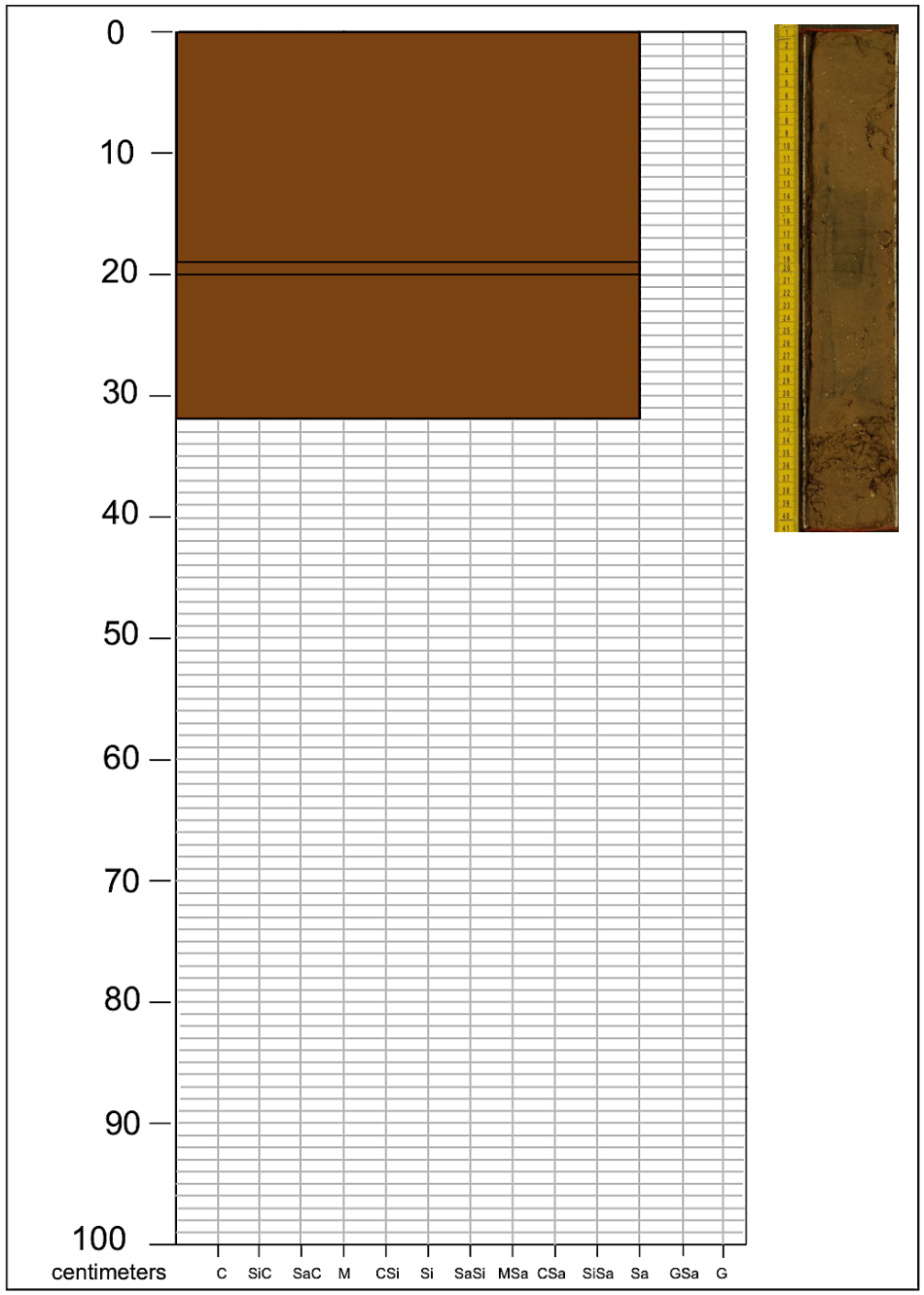

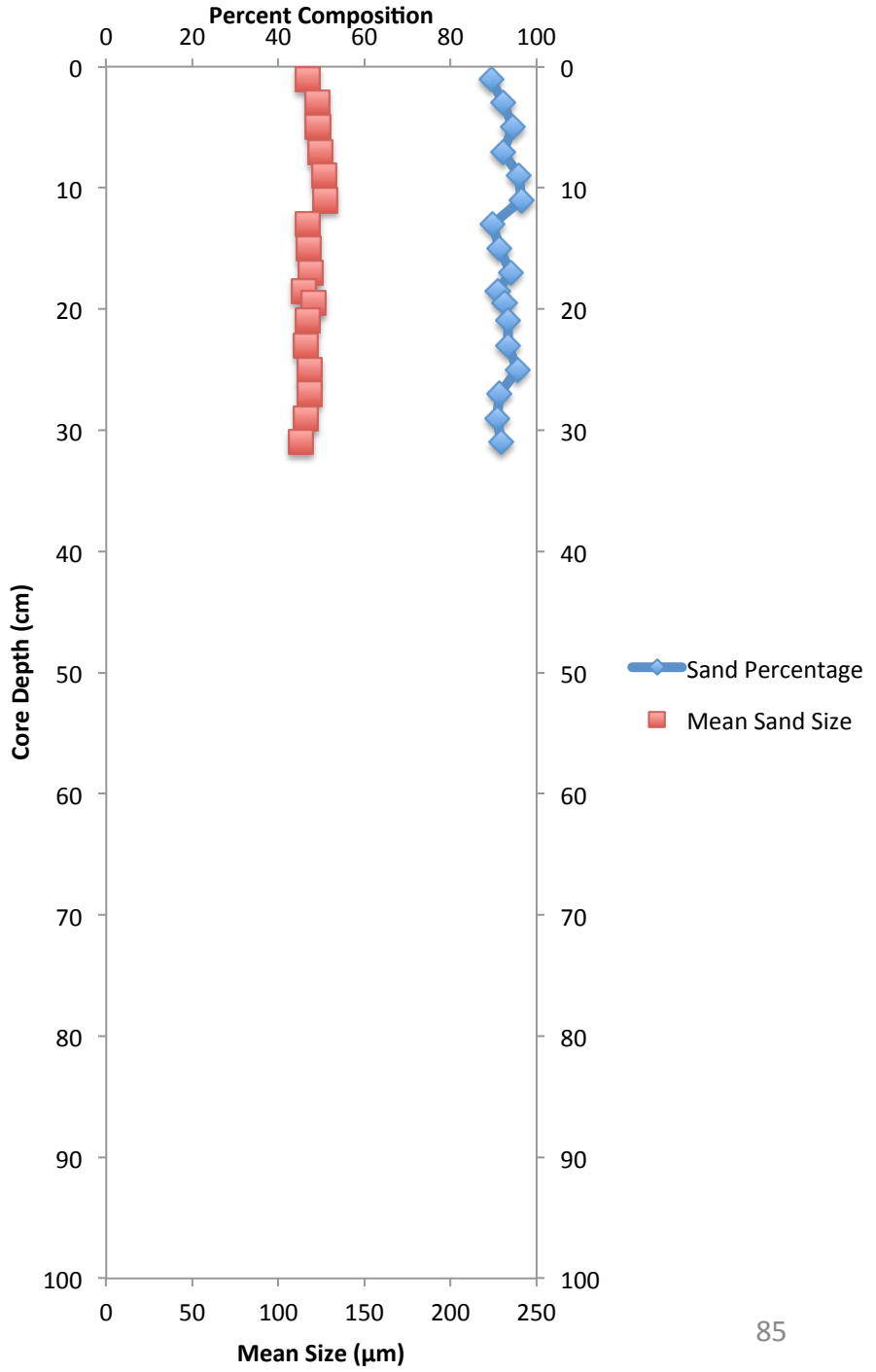

Brazos Delta Core: BDVC29

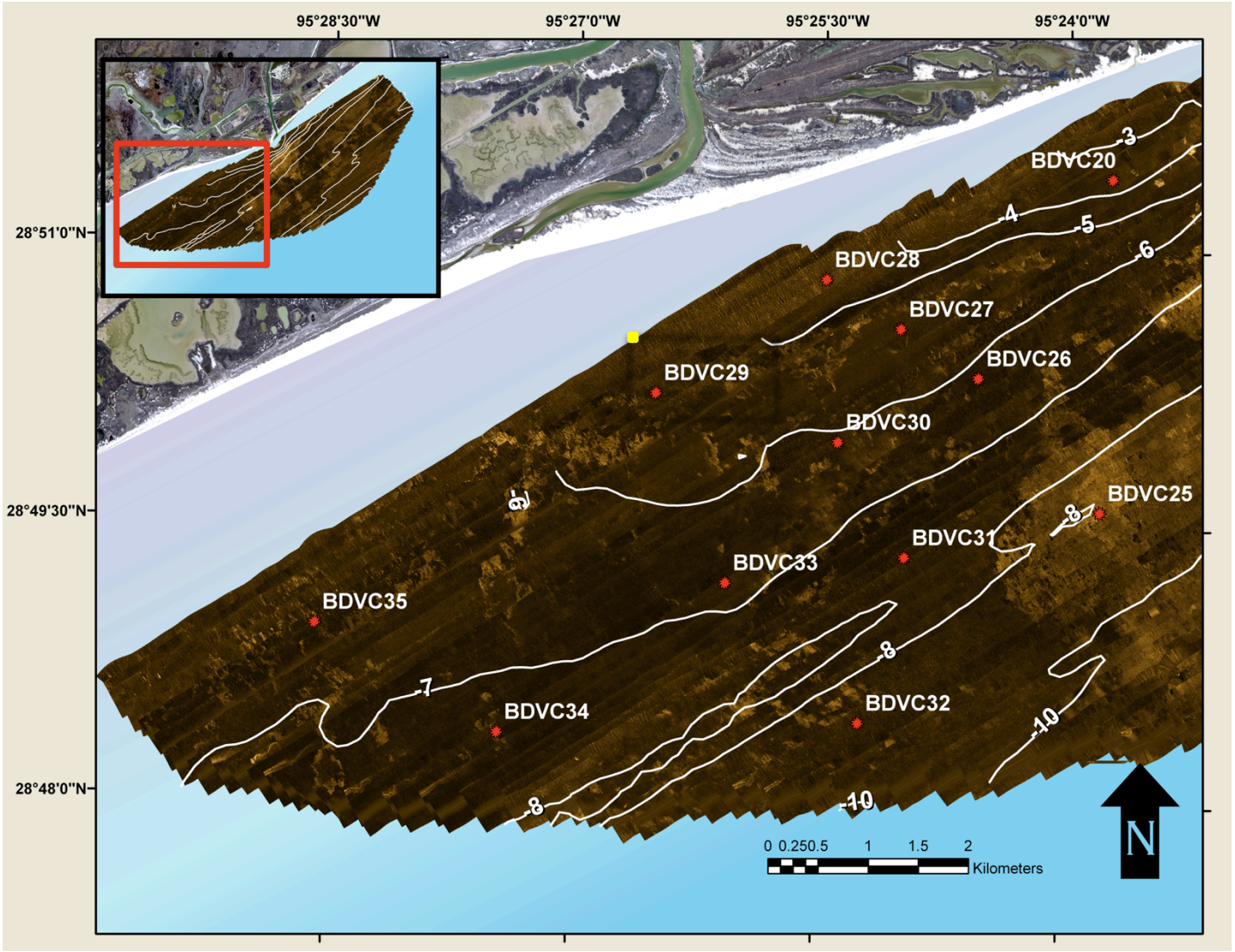

Project:_Brazos Delta Fall 2011___ Core: _BDVC29A_____

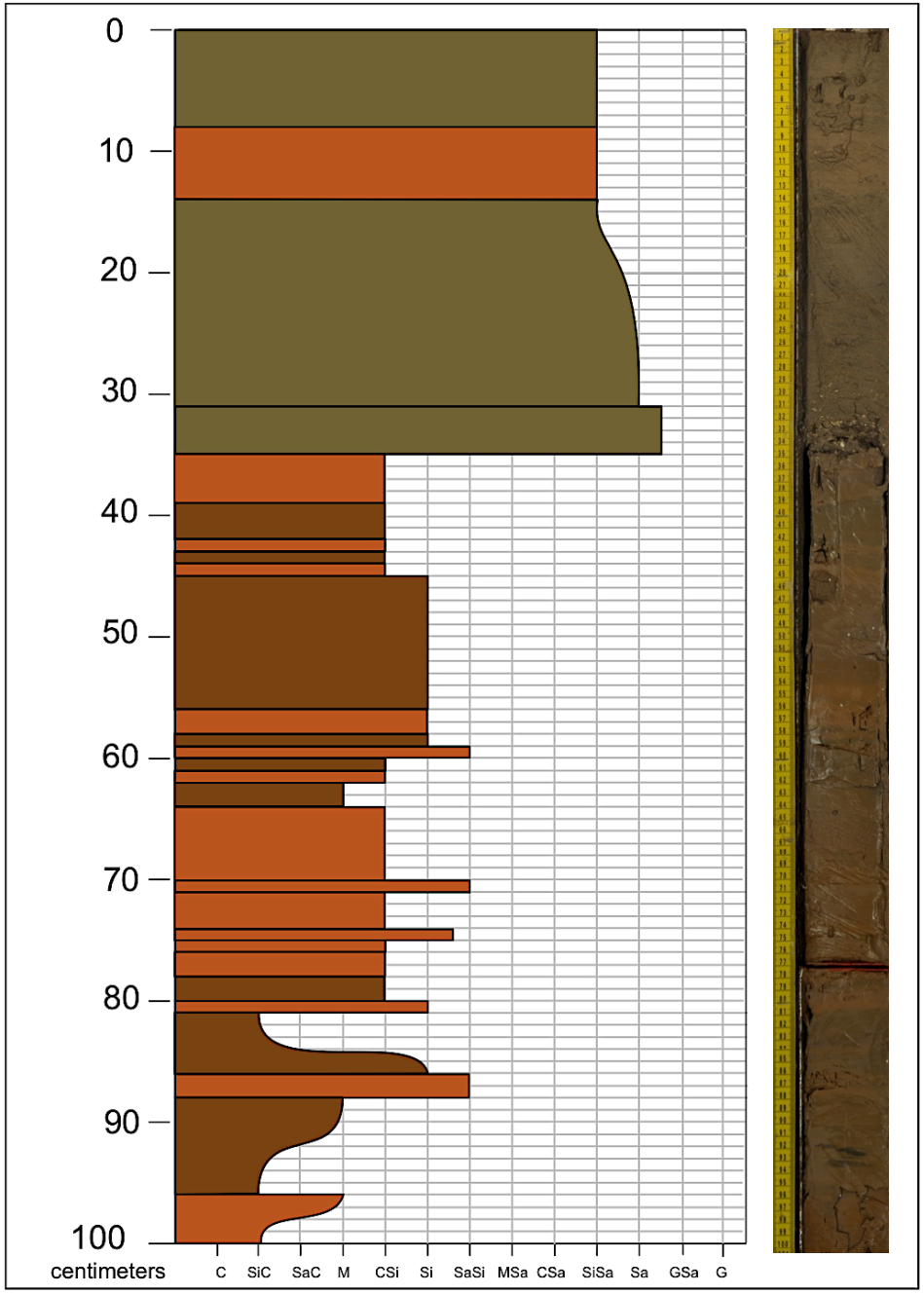

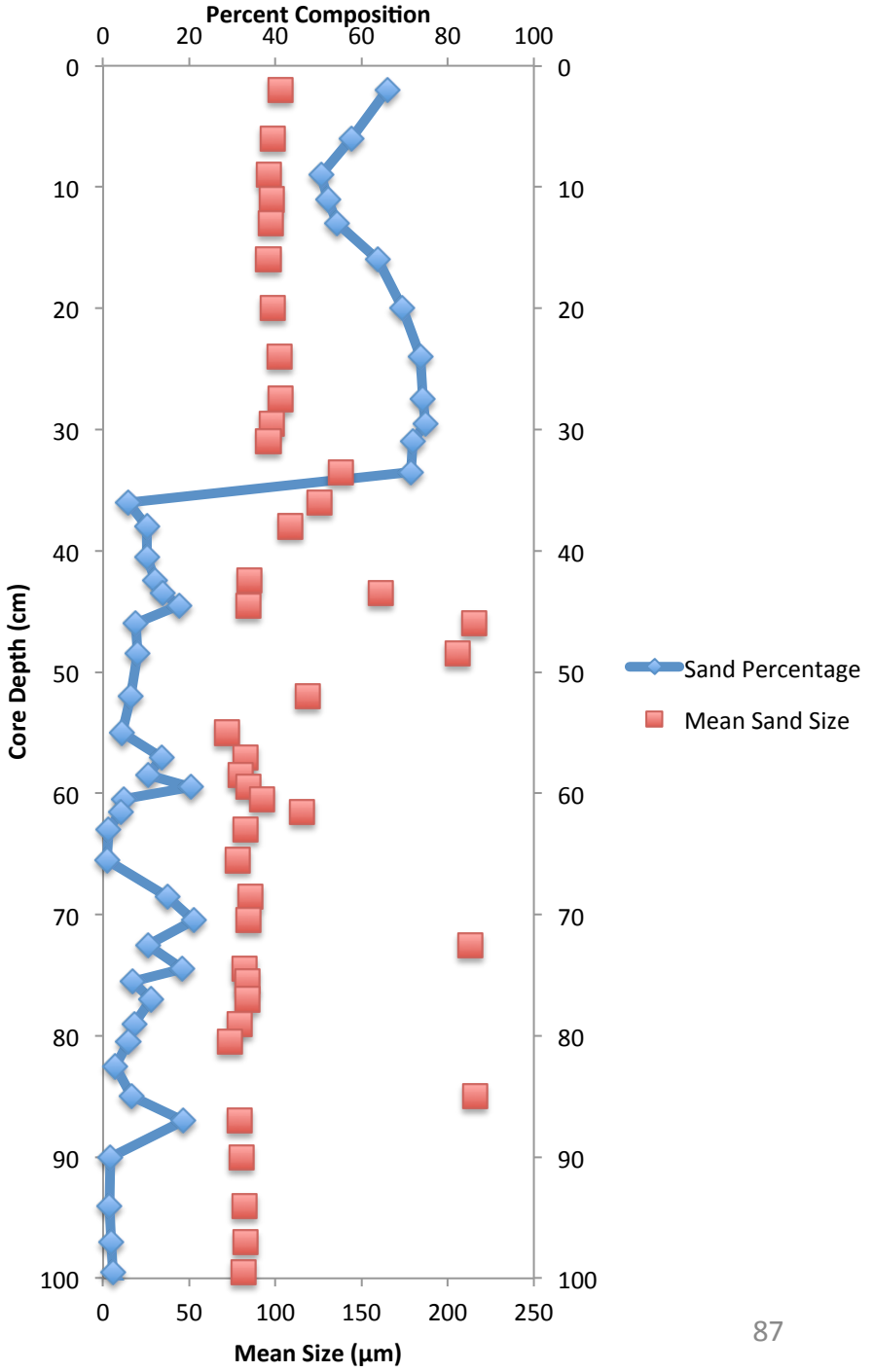

Project:_Brazos Delta Fall 2011___ Core: _BDVC29B_____

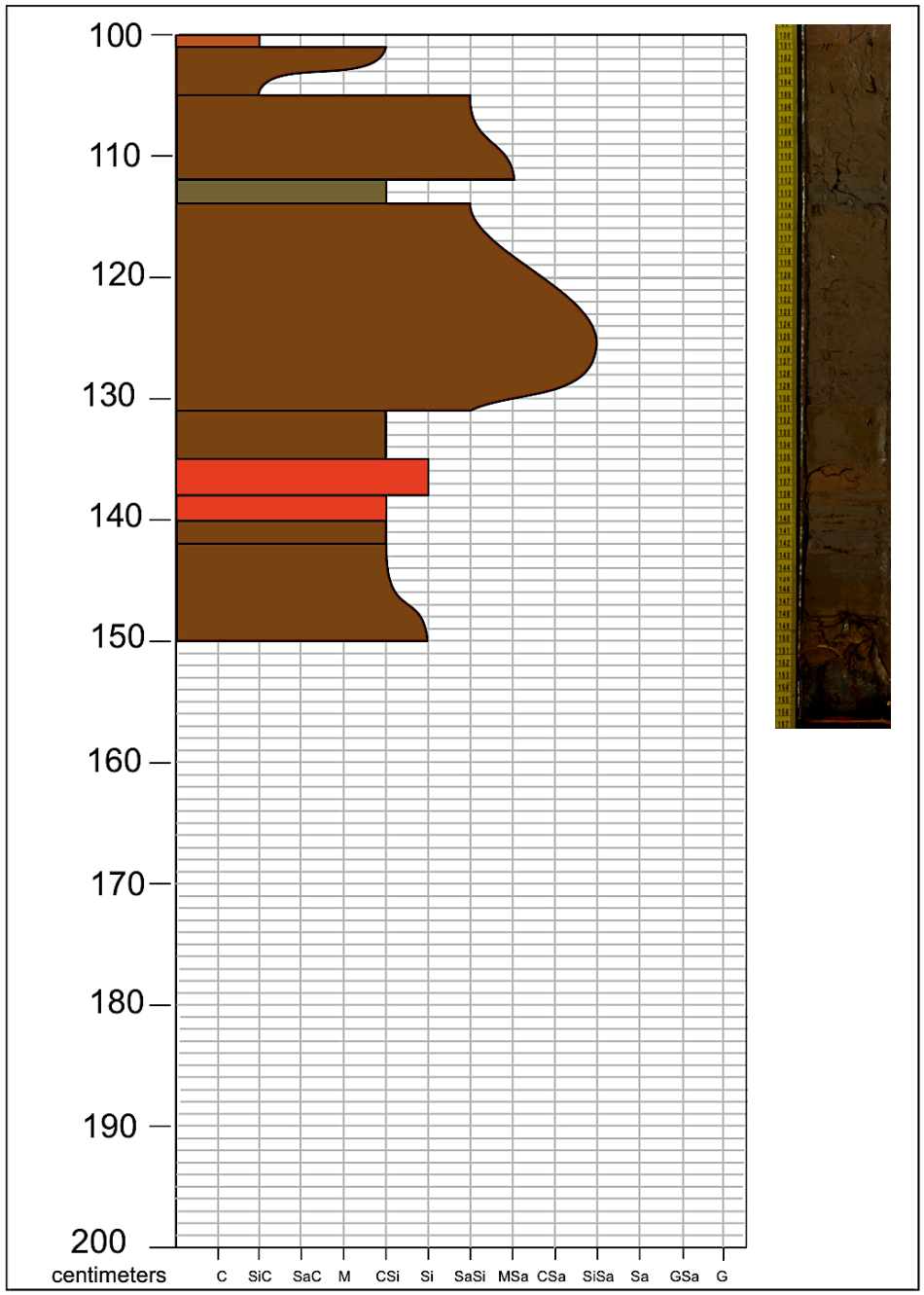

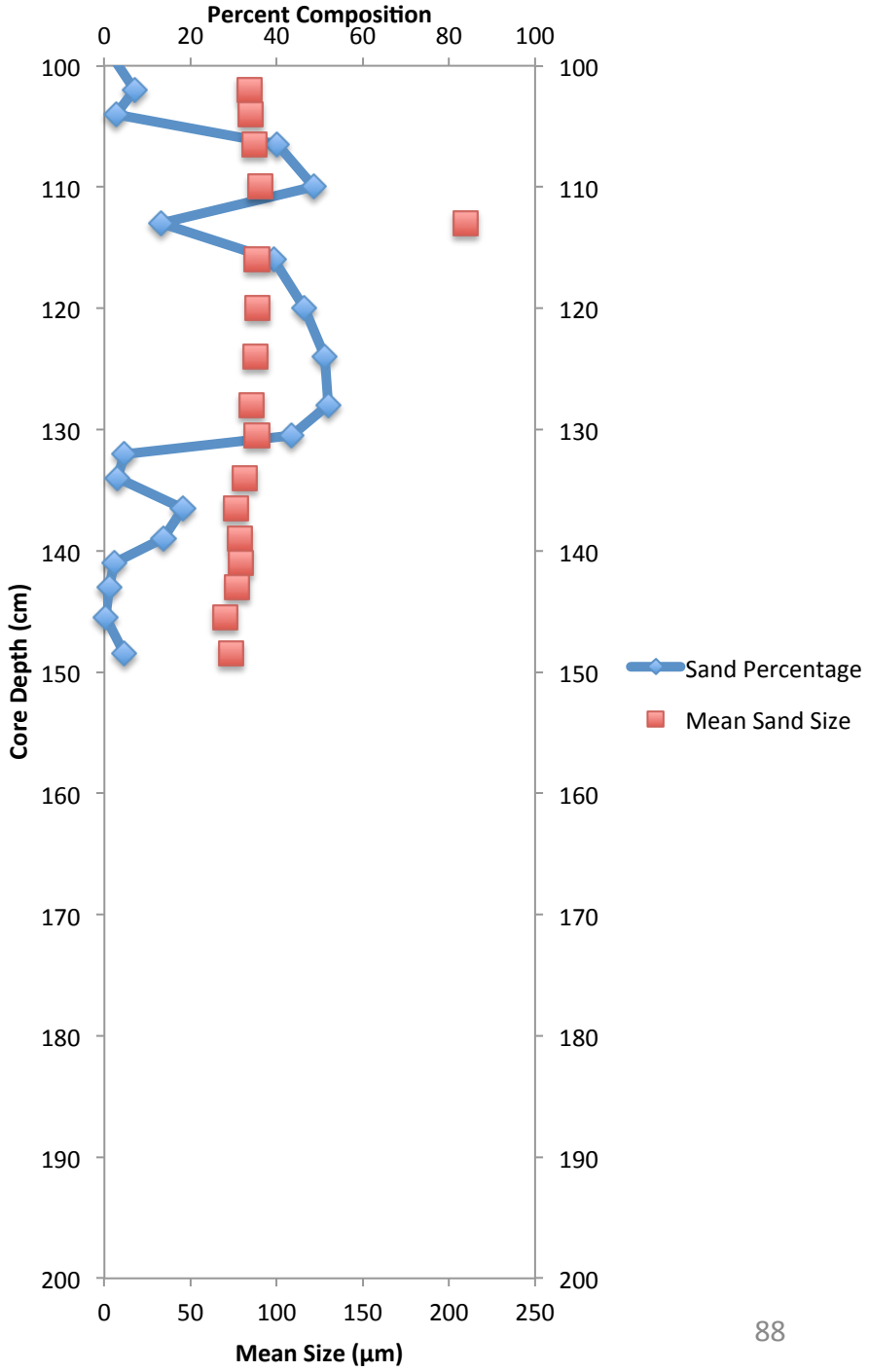

Brazos Delta Core: BDVC30

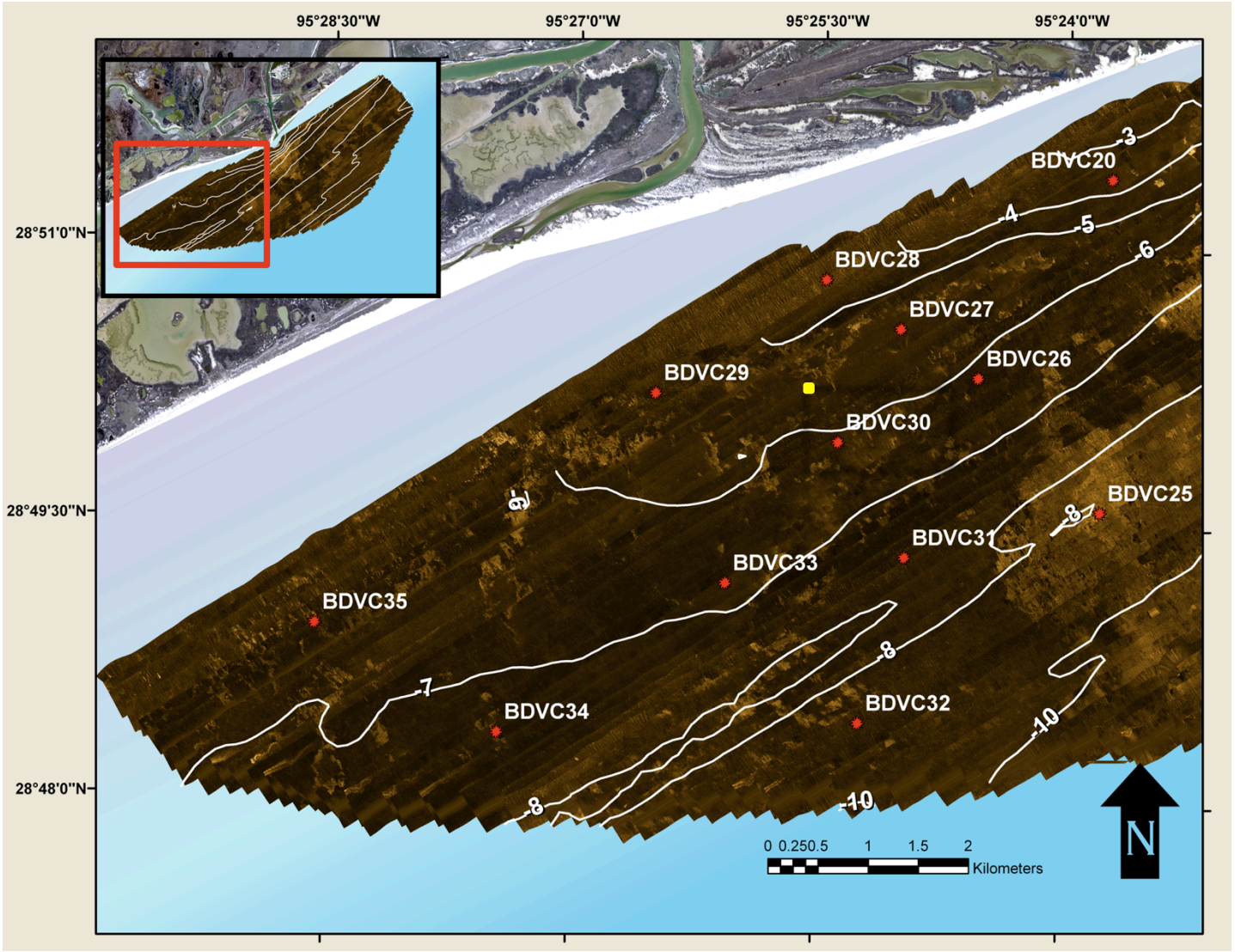

Project:_Brazos Delta Fall 2011___ Core: _BDVC30A_____

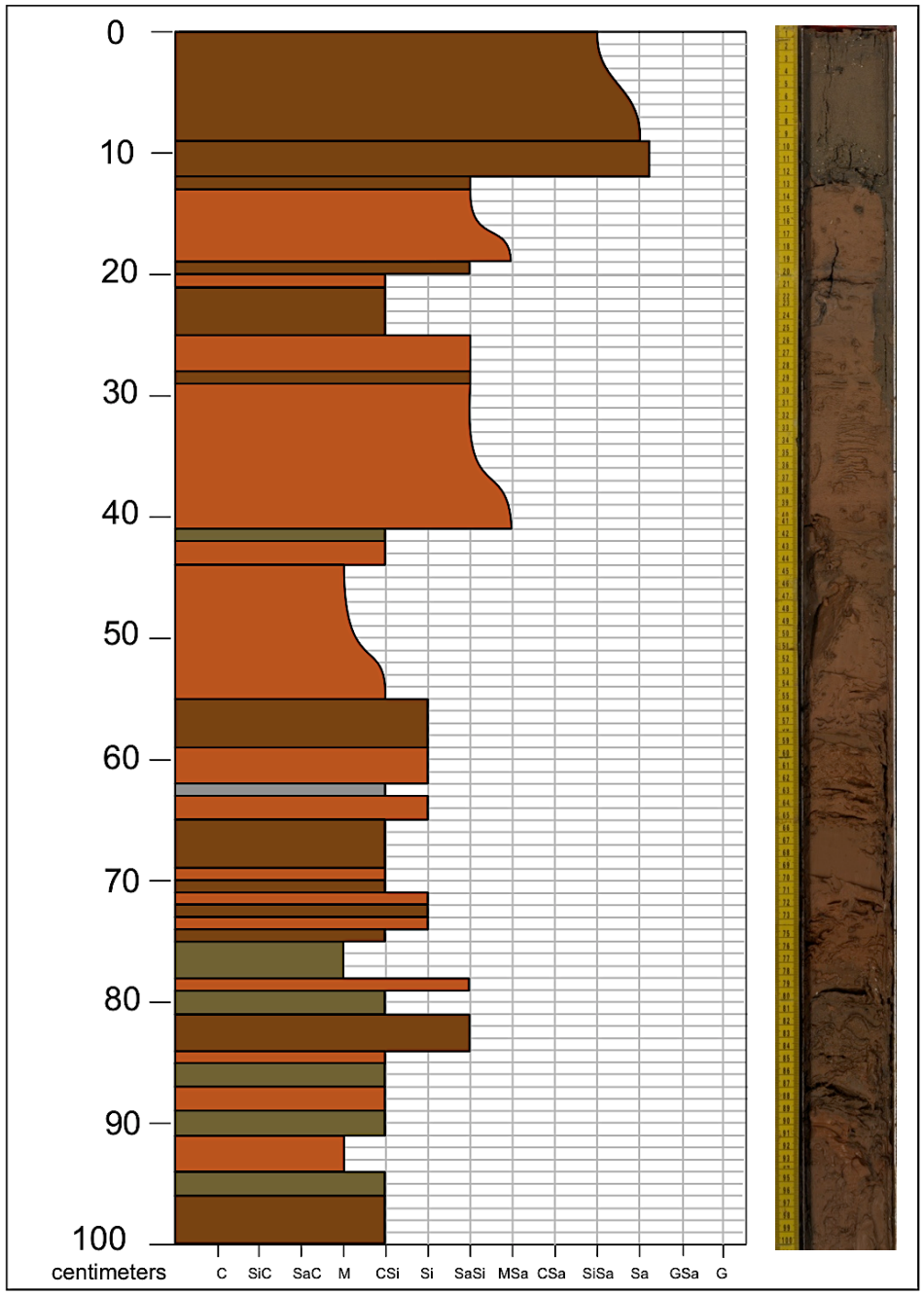

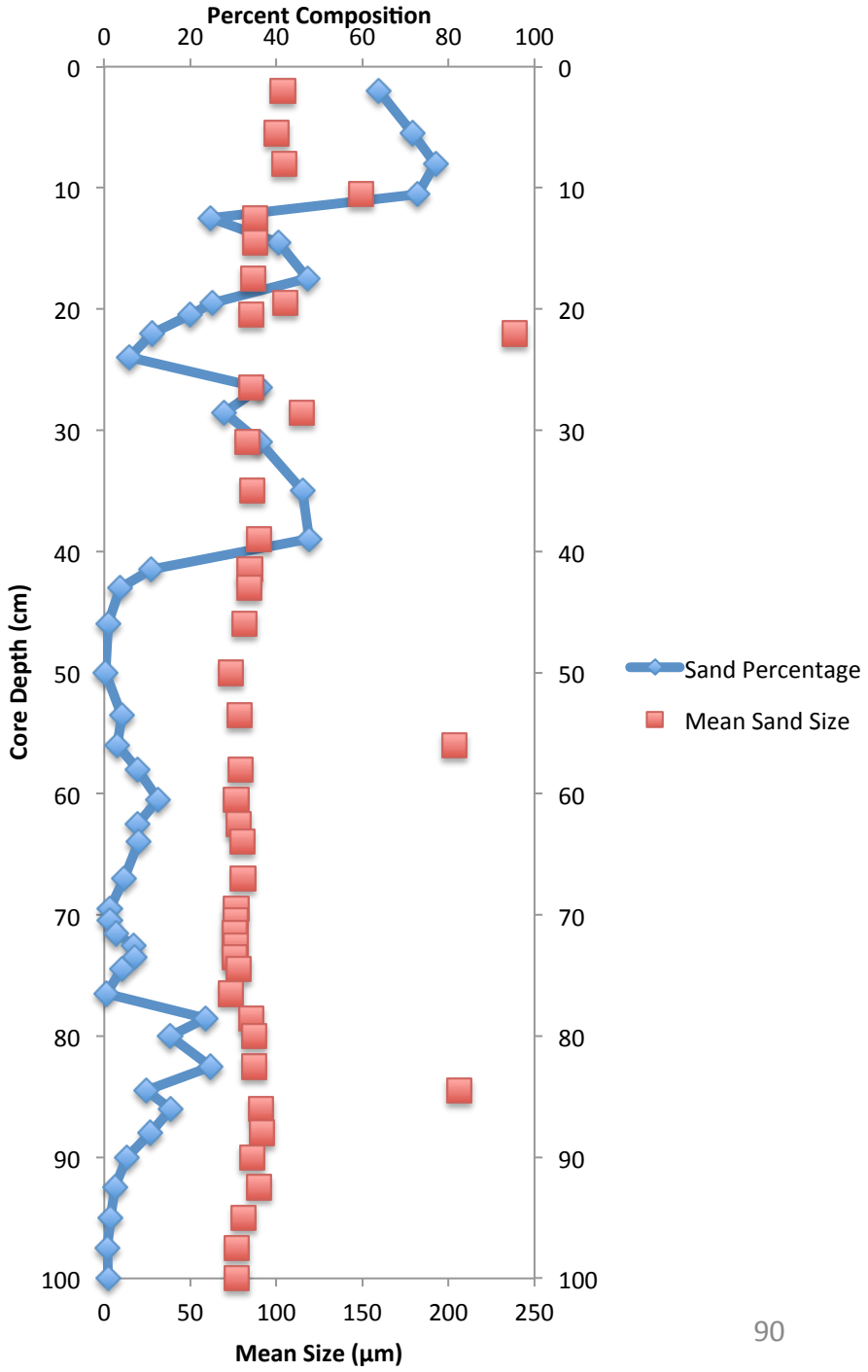

Project:_Brazos Delta Fall 2011___ Core: _BDVC30B_____

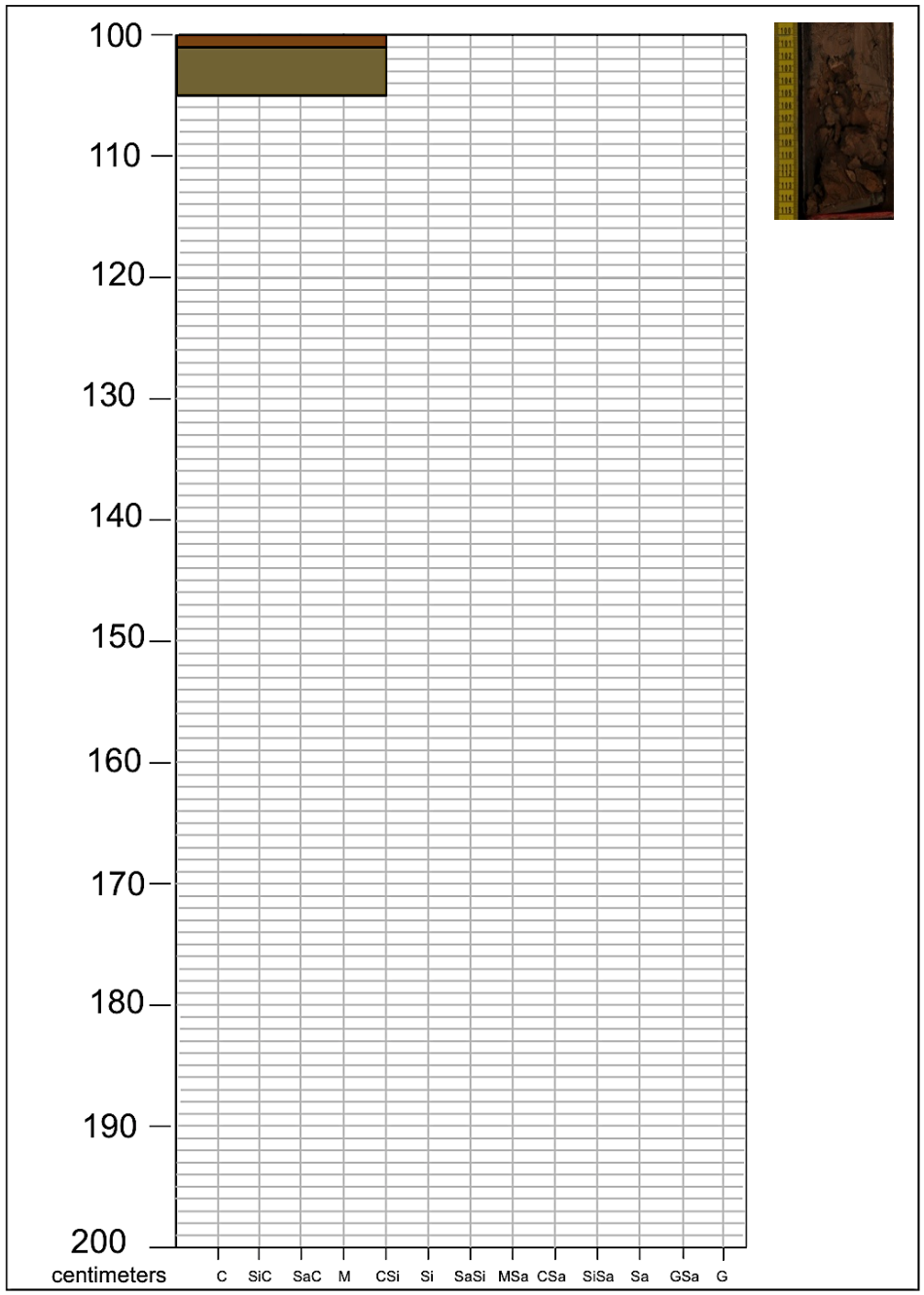

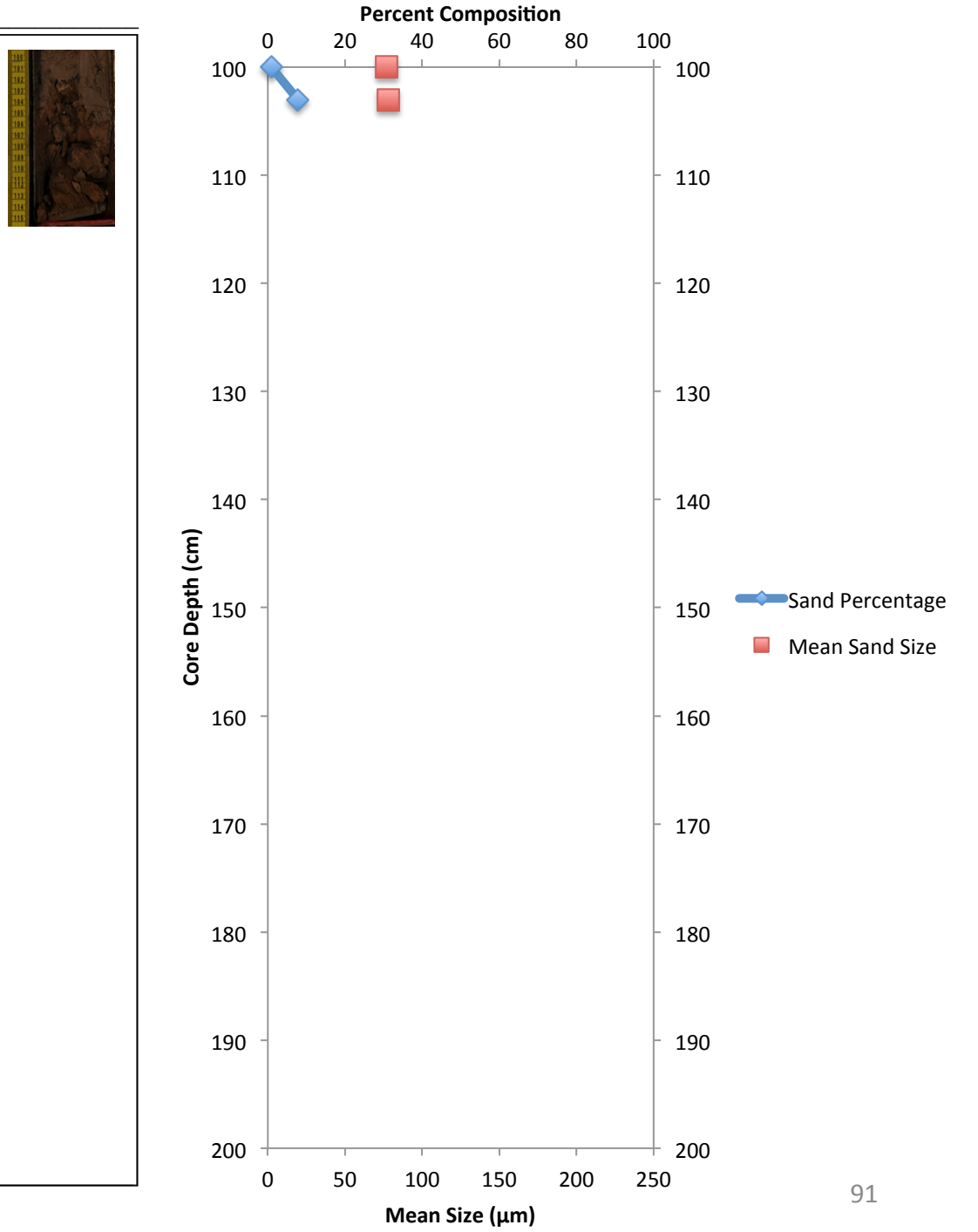

Brazos Delta Core: BDVC31

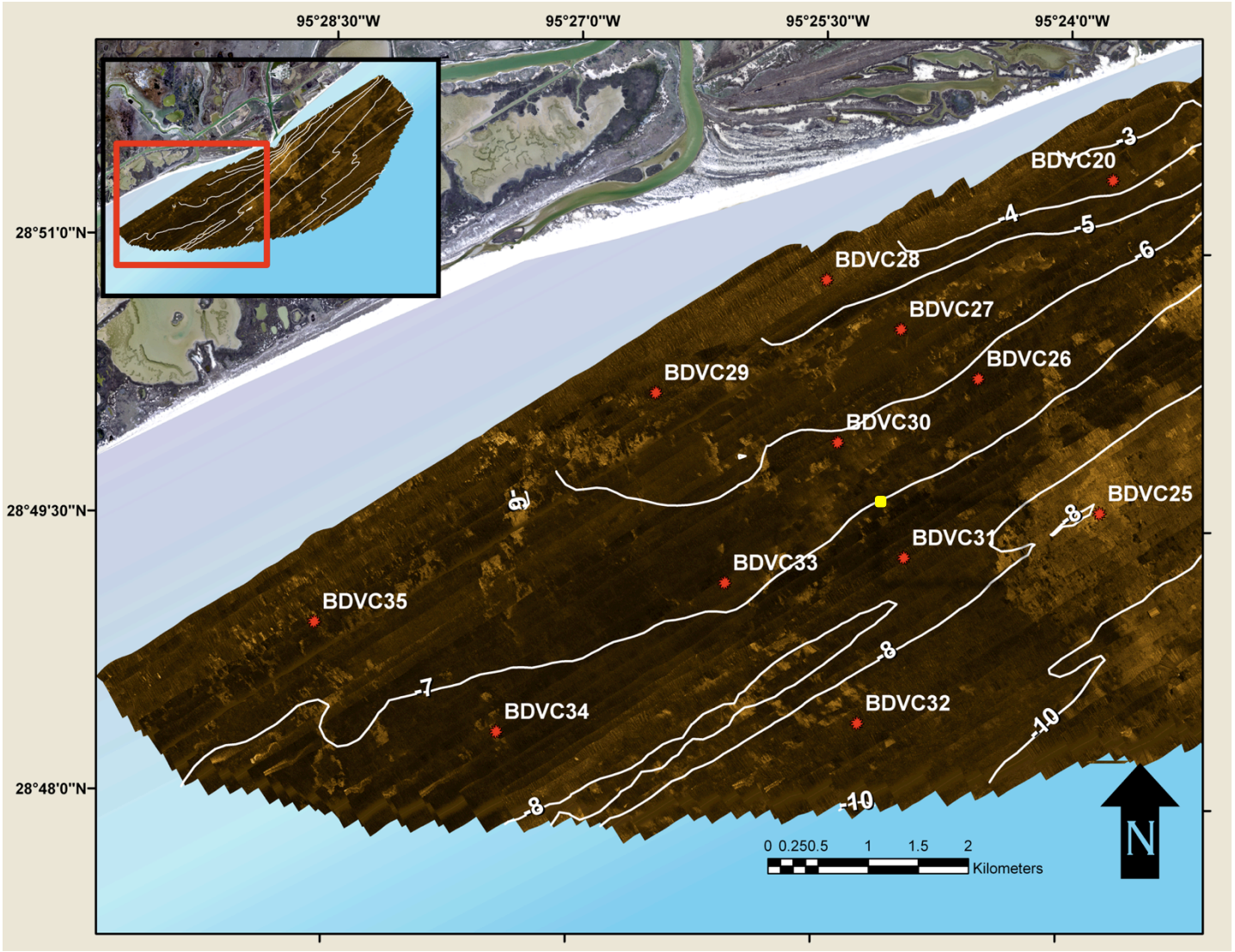

Project:_Brazos Delta Fall 2011___ Core: _BDVC31_____

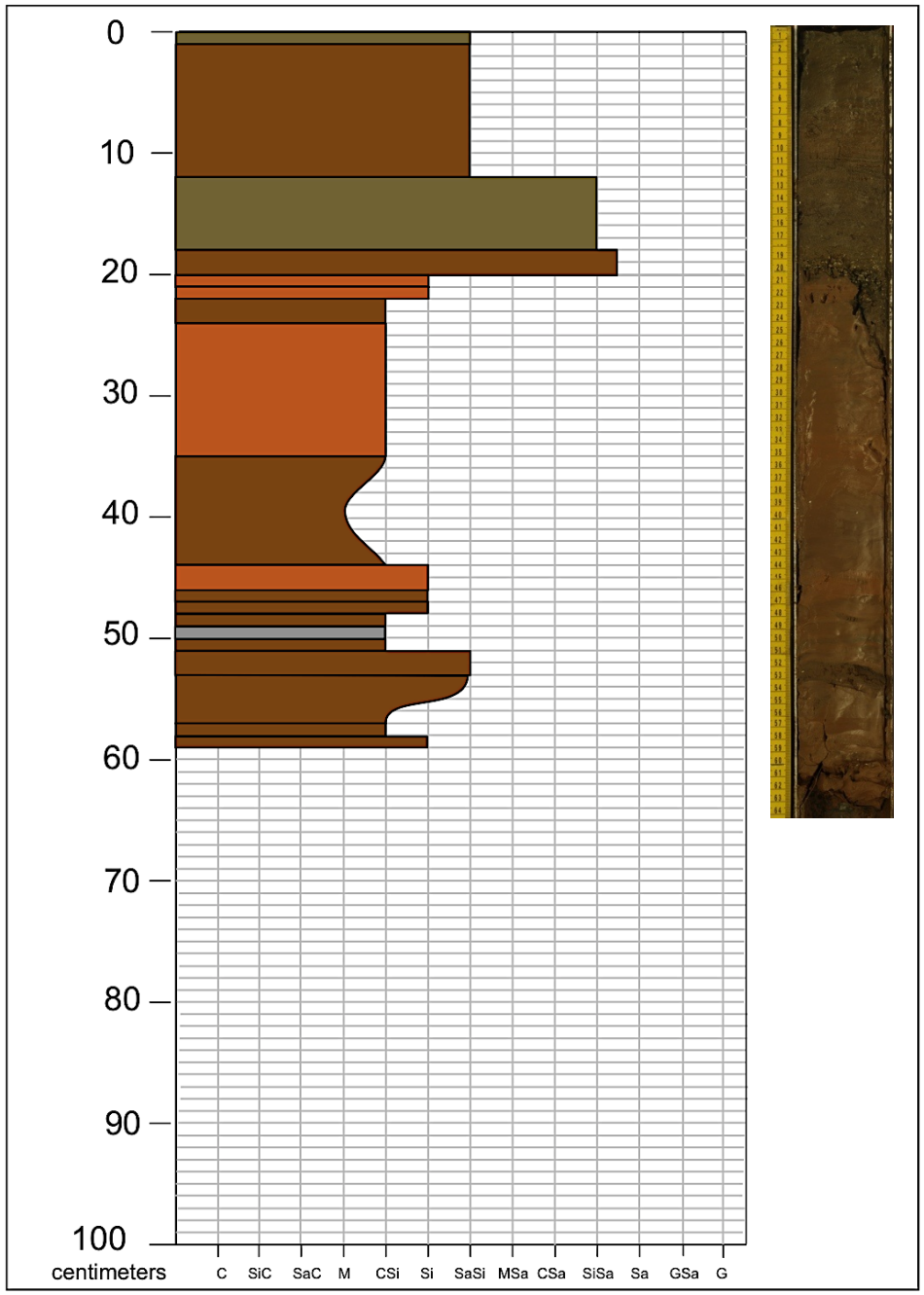

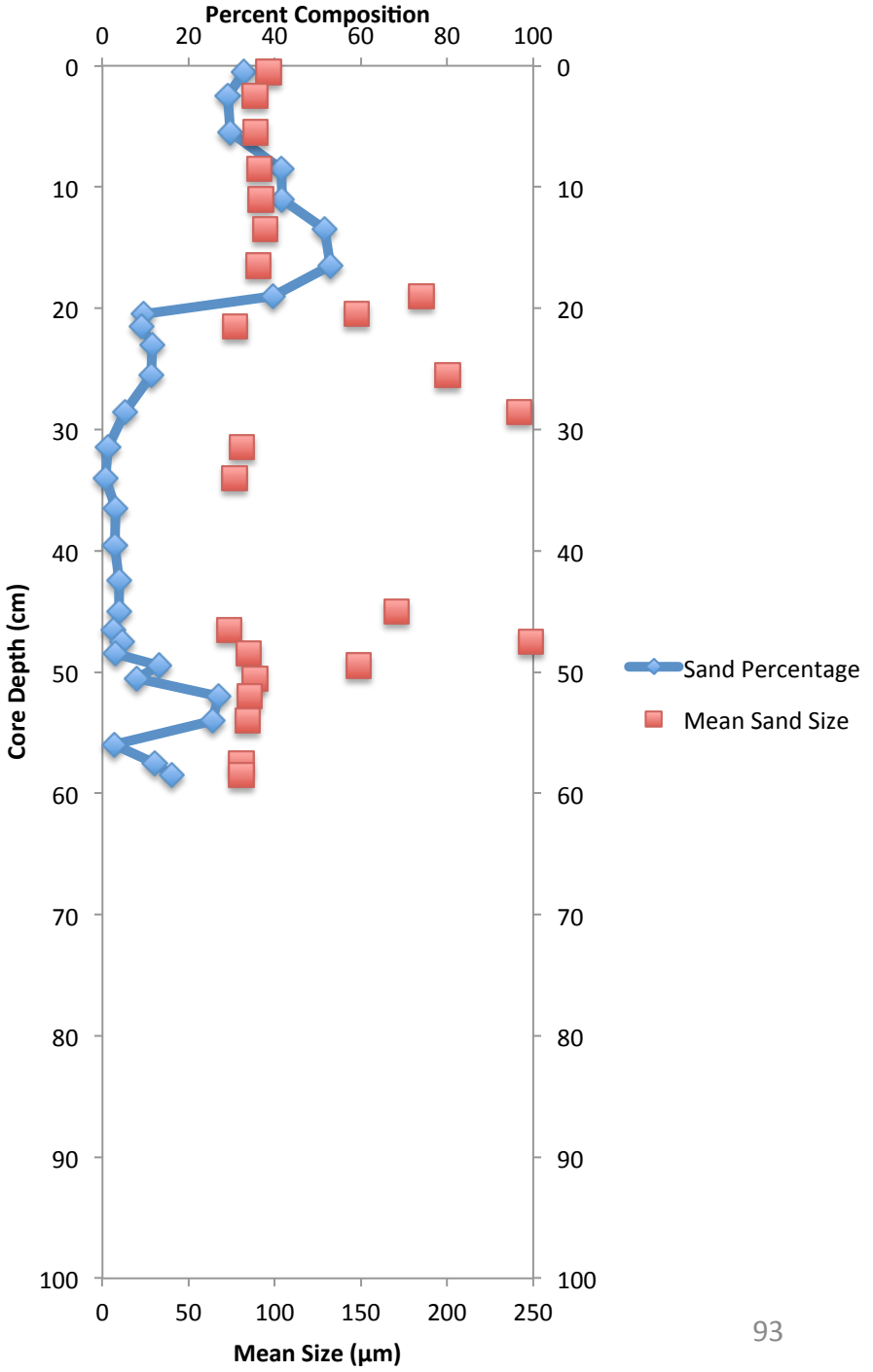

Brazos Delta Core: BDVC32

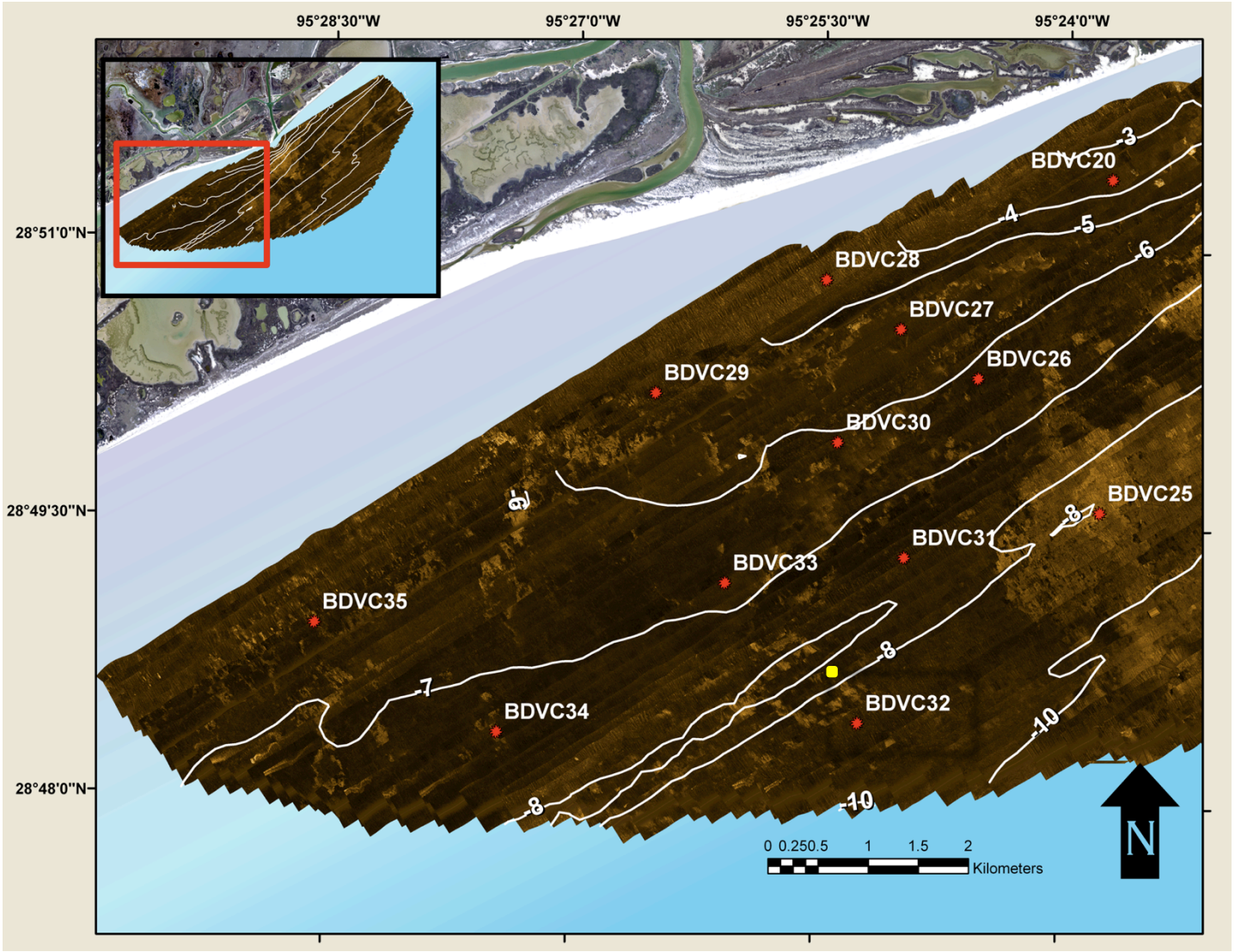

Project:_Brazos Delta Fall 2011___ Core: _BDVC32_____

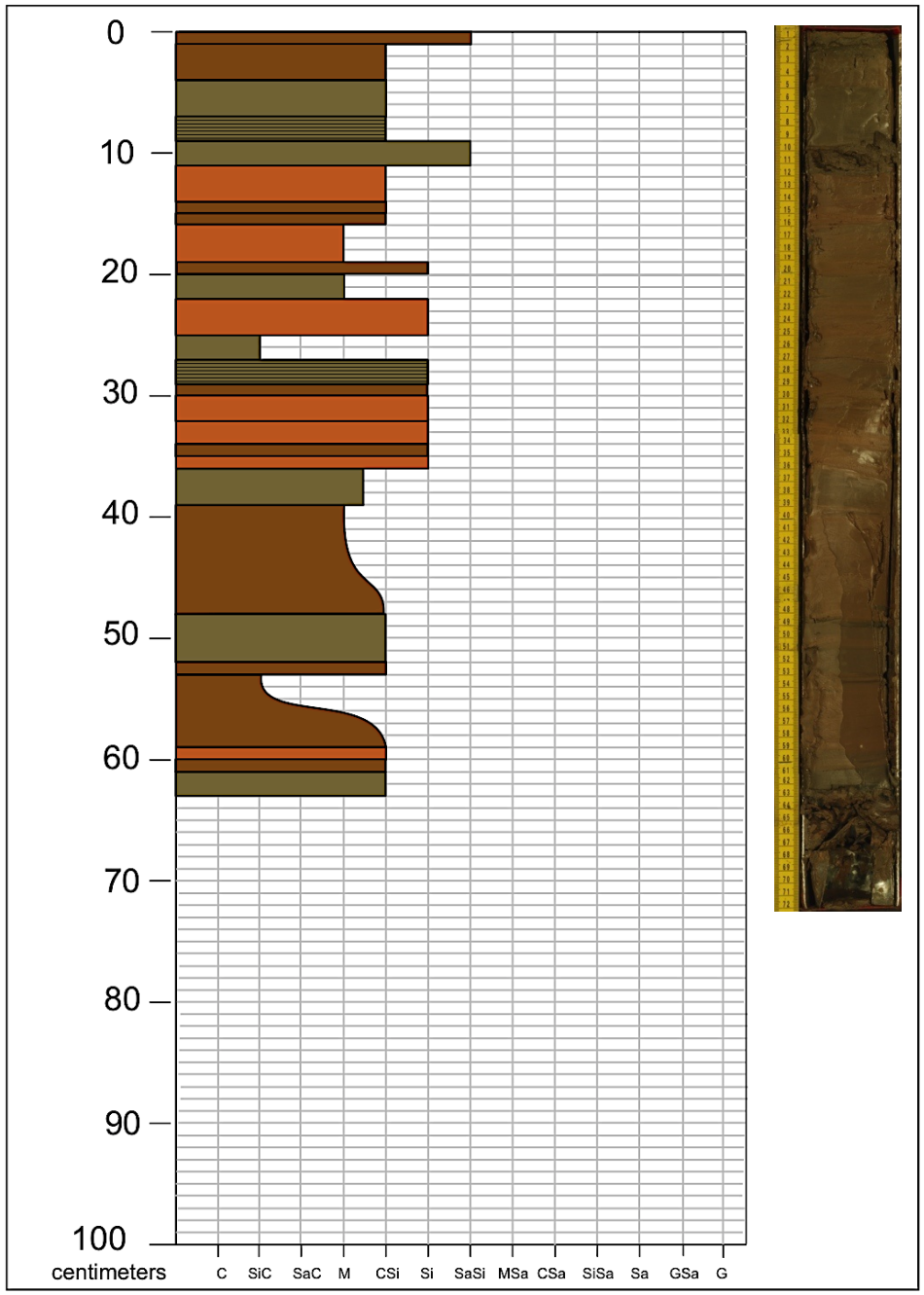

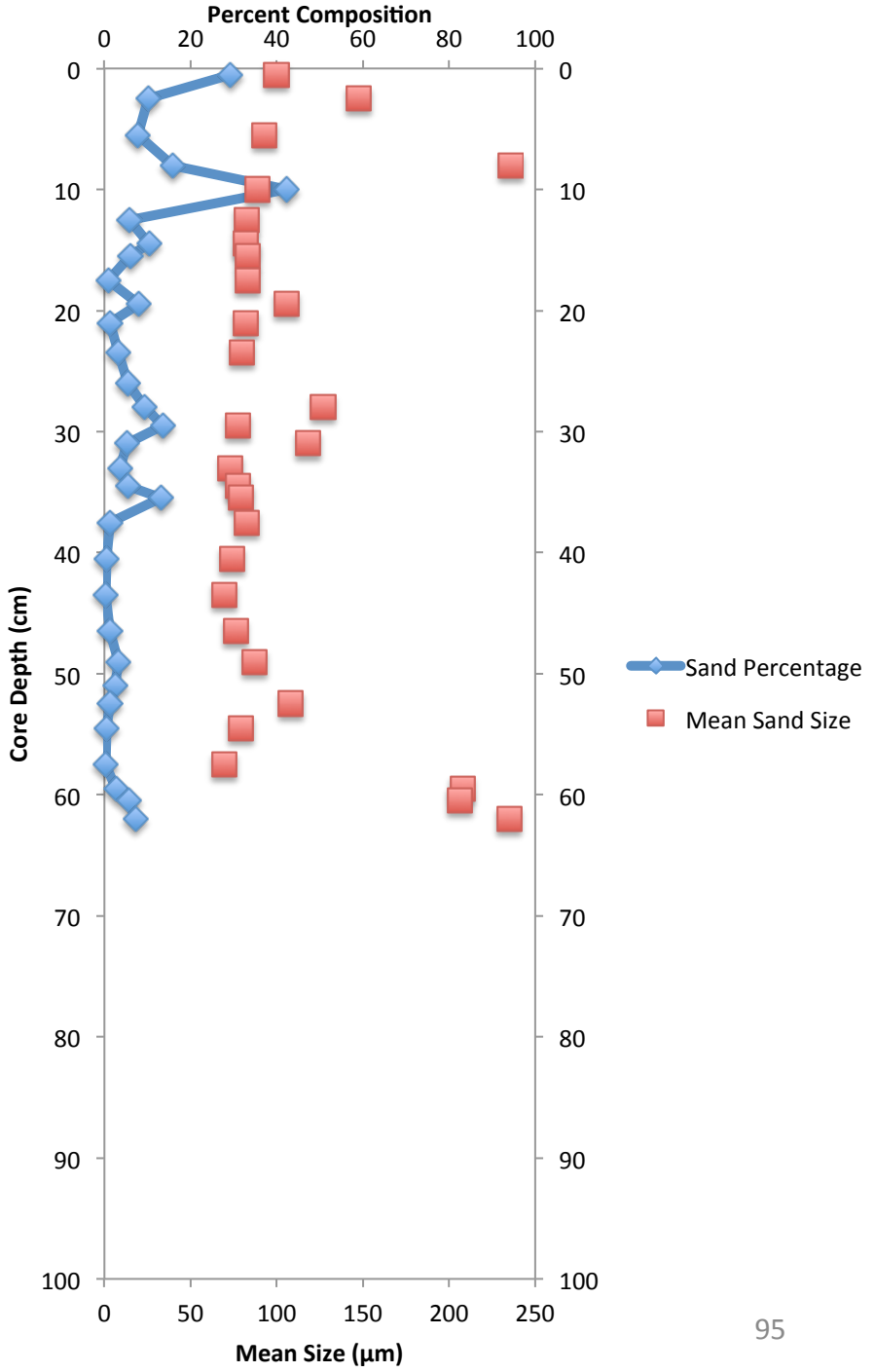

Brazos Delta Core: BDVC33

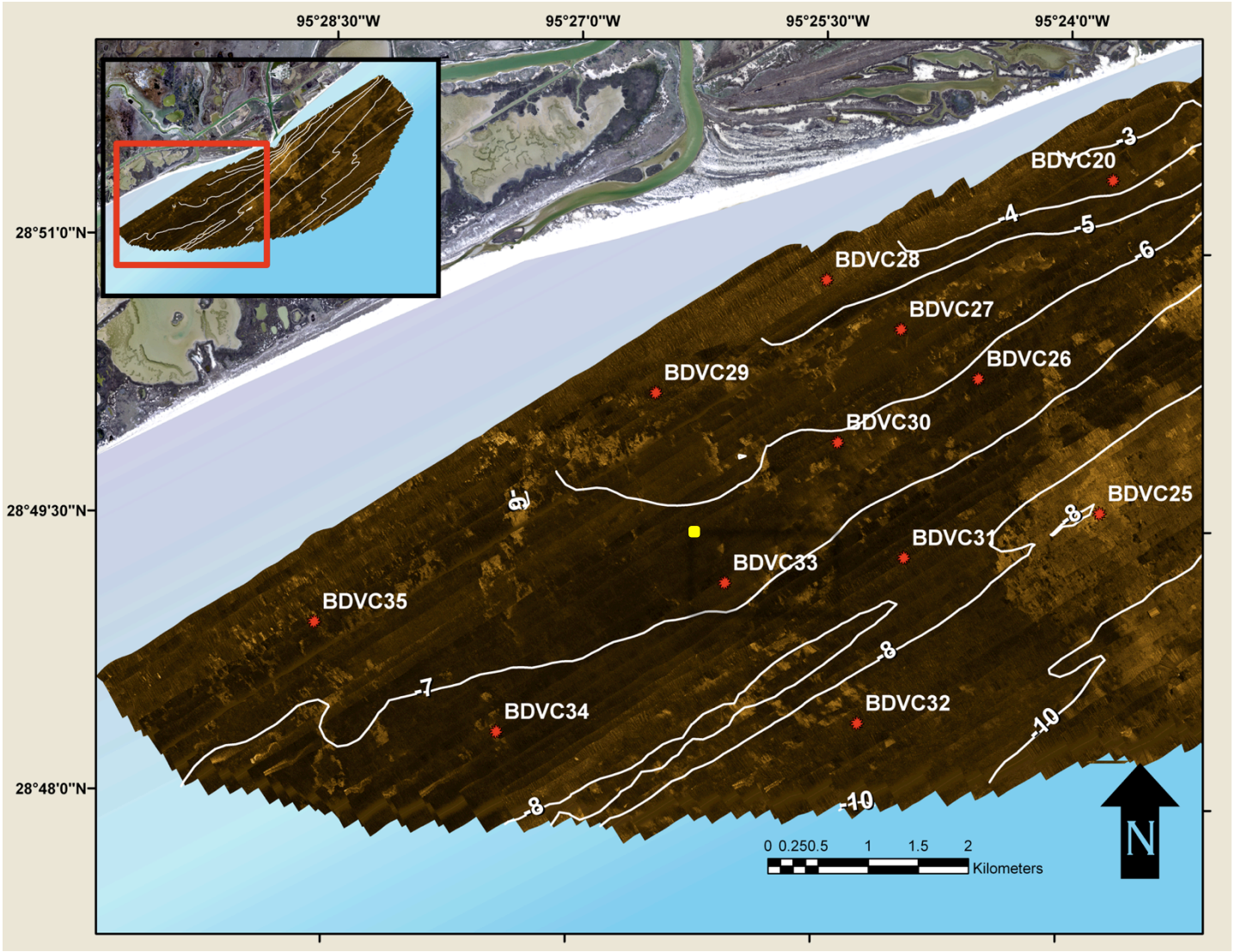

Project:_Brazos Delta Fall 2011___ Core: _BDVC33_____

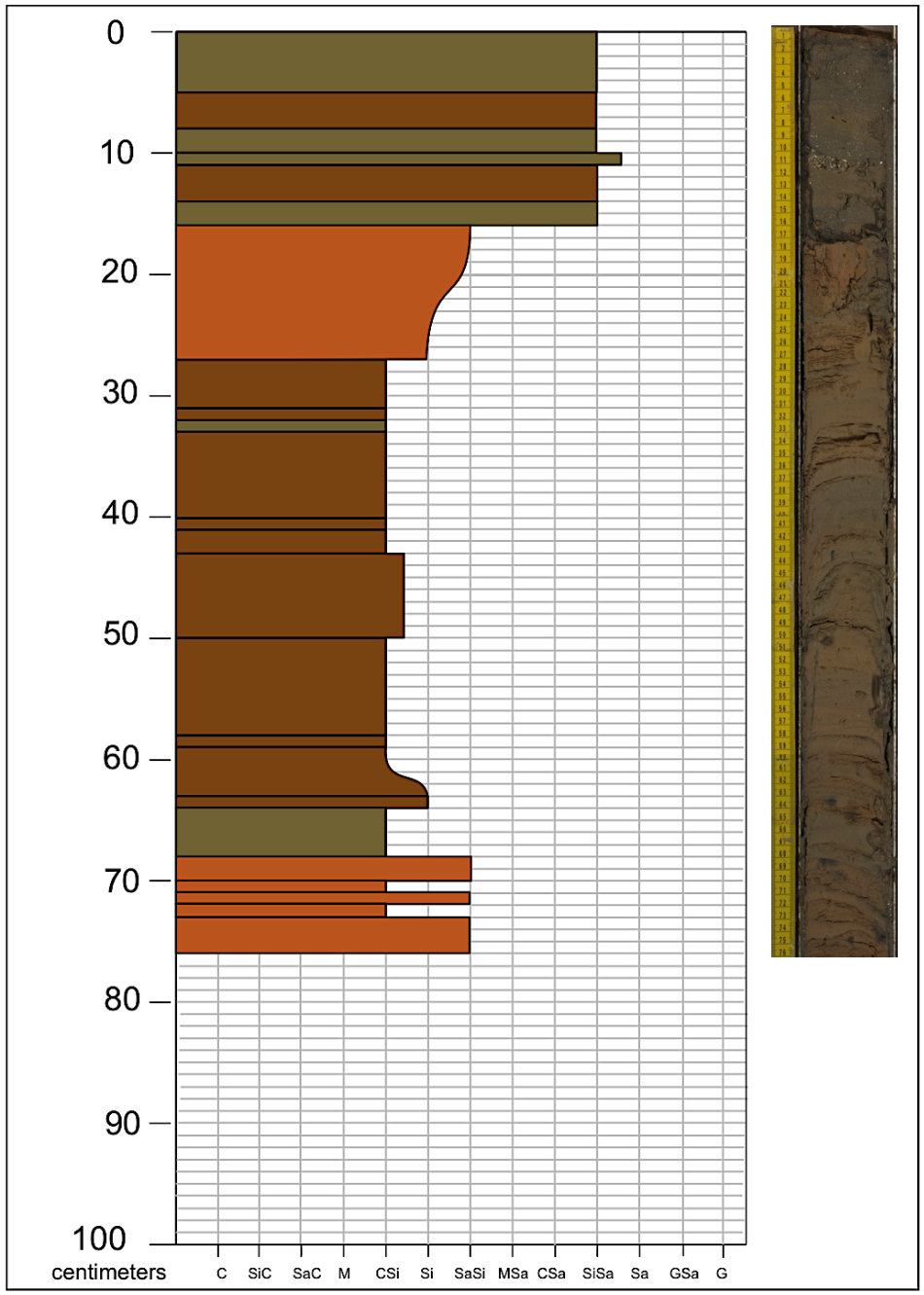

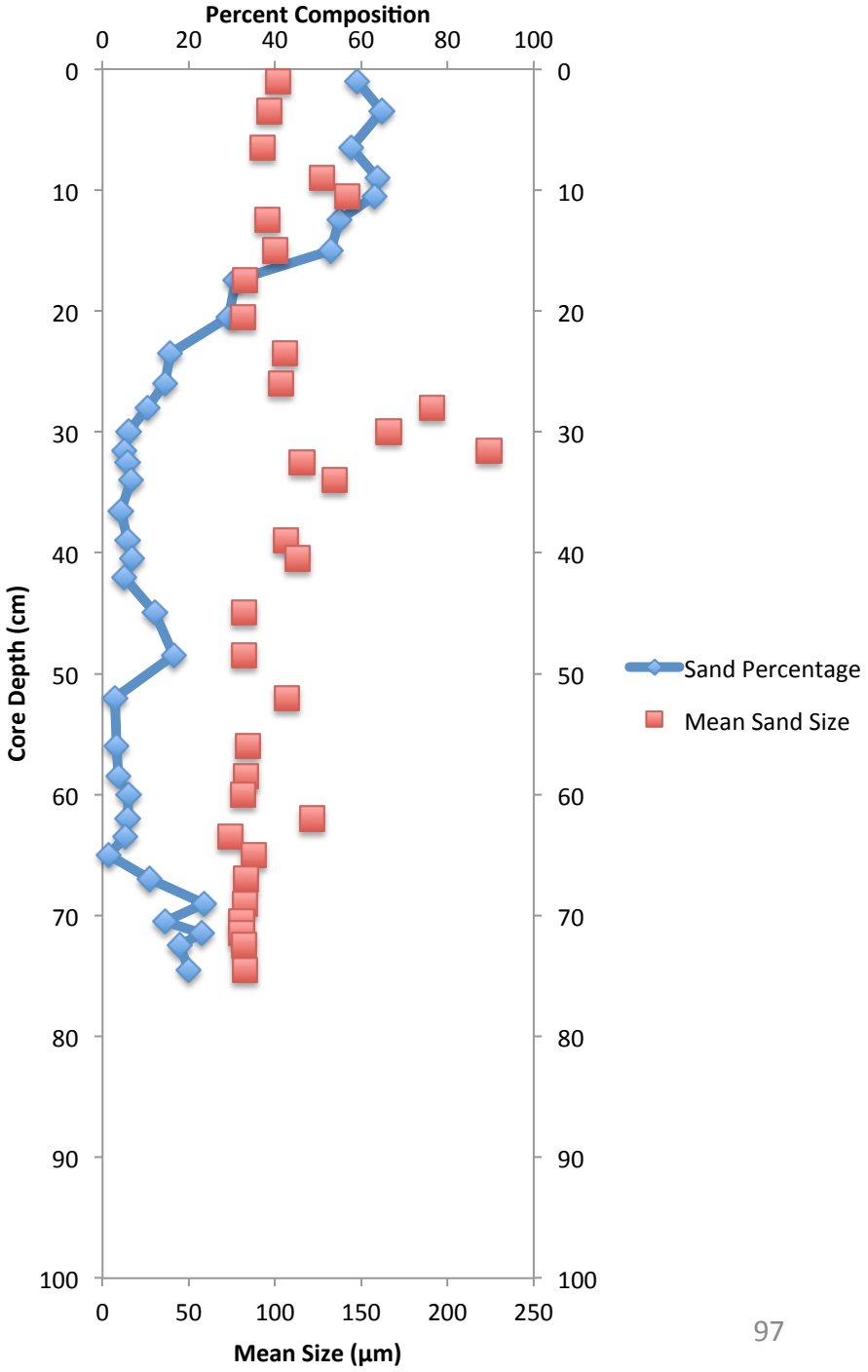

Brazos Delta Core: BDVC34

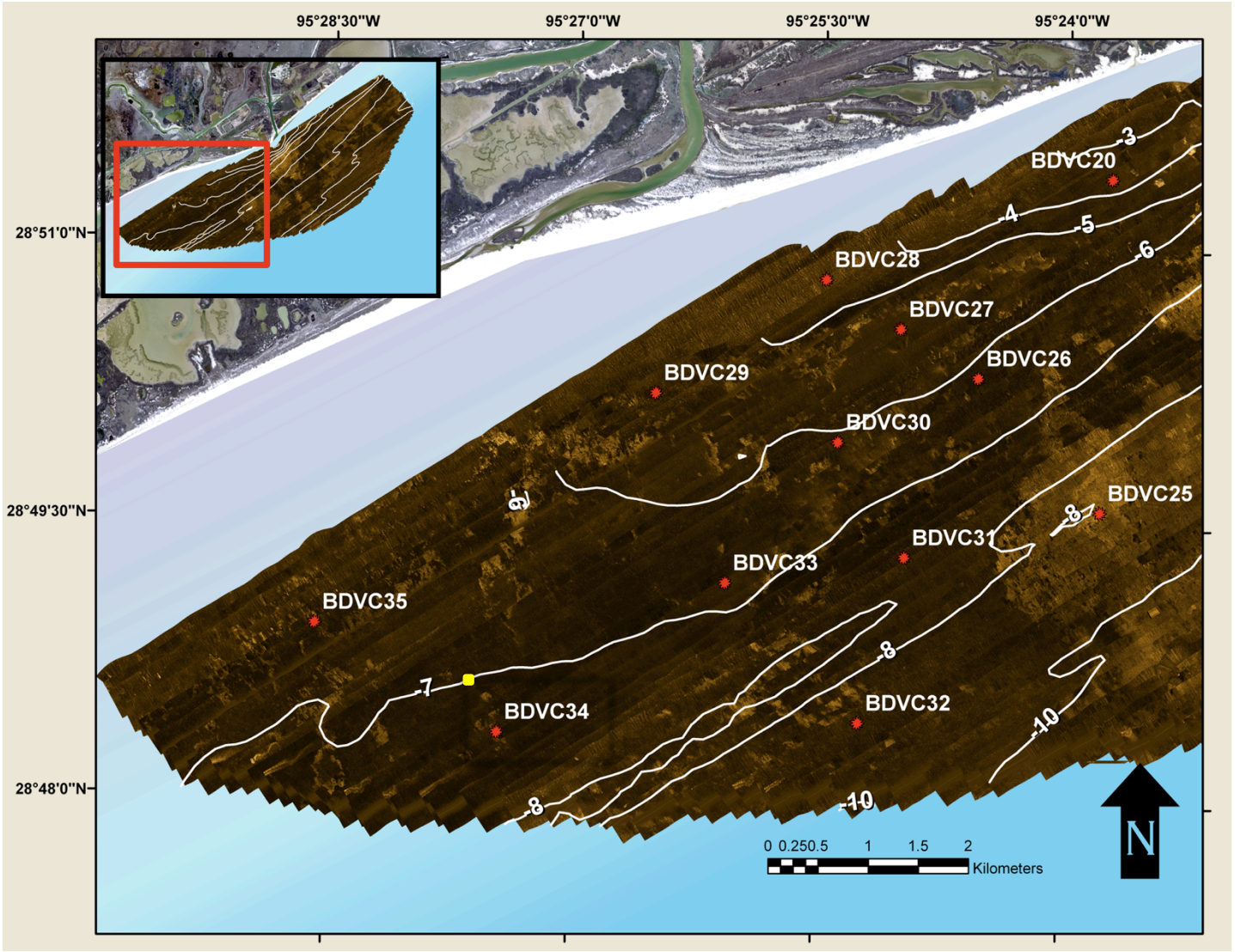

Project:_Brazos Delta Fall 2011___ Core: _BDVC34A_____

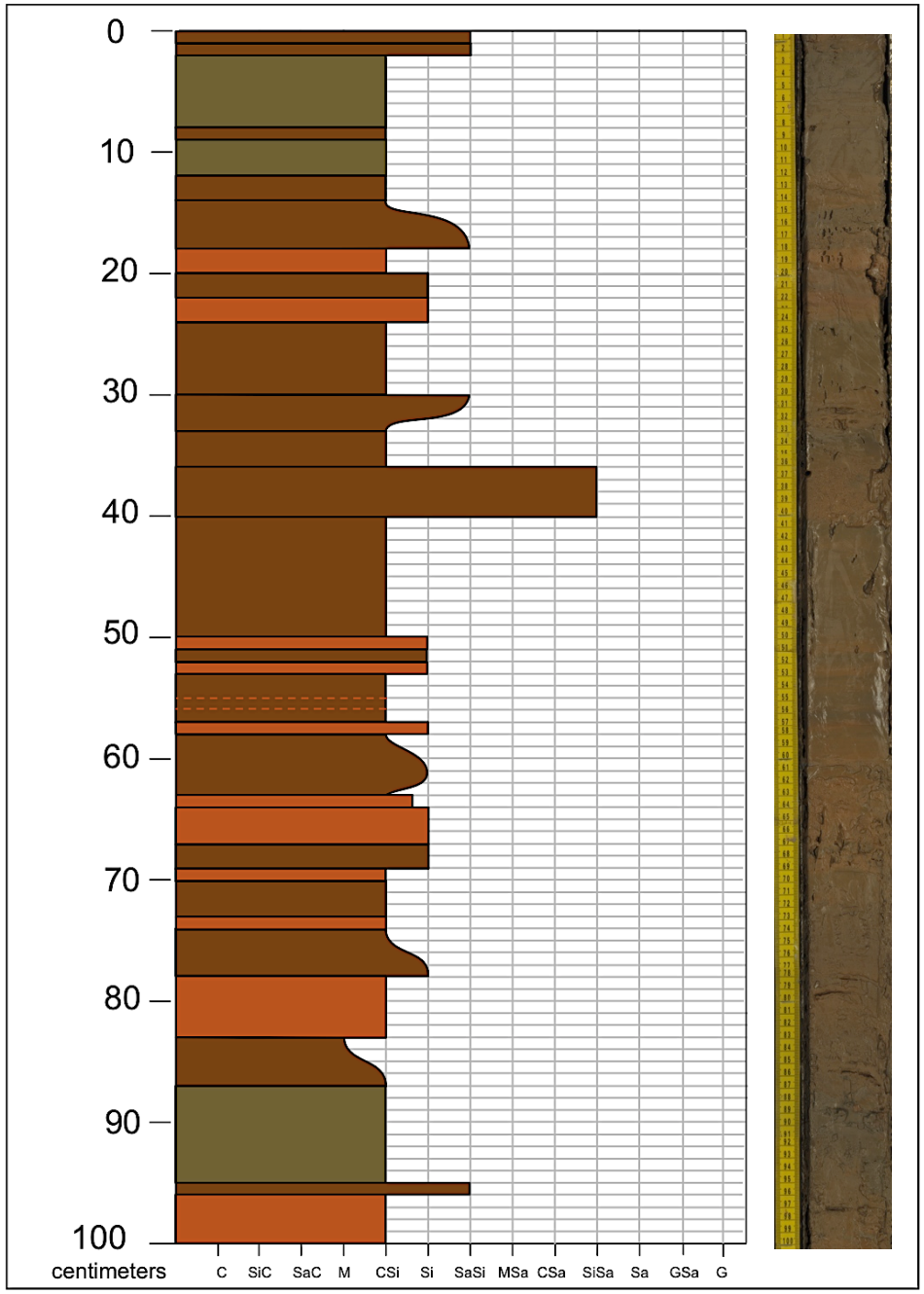

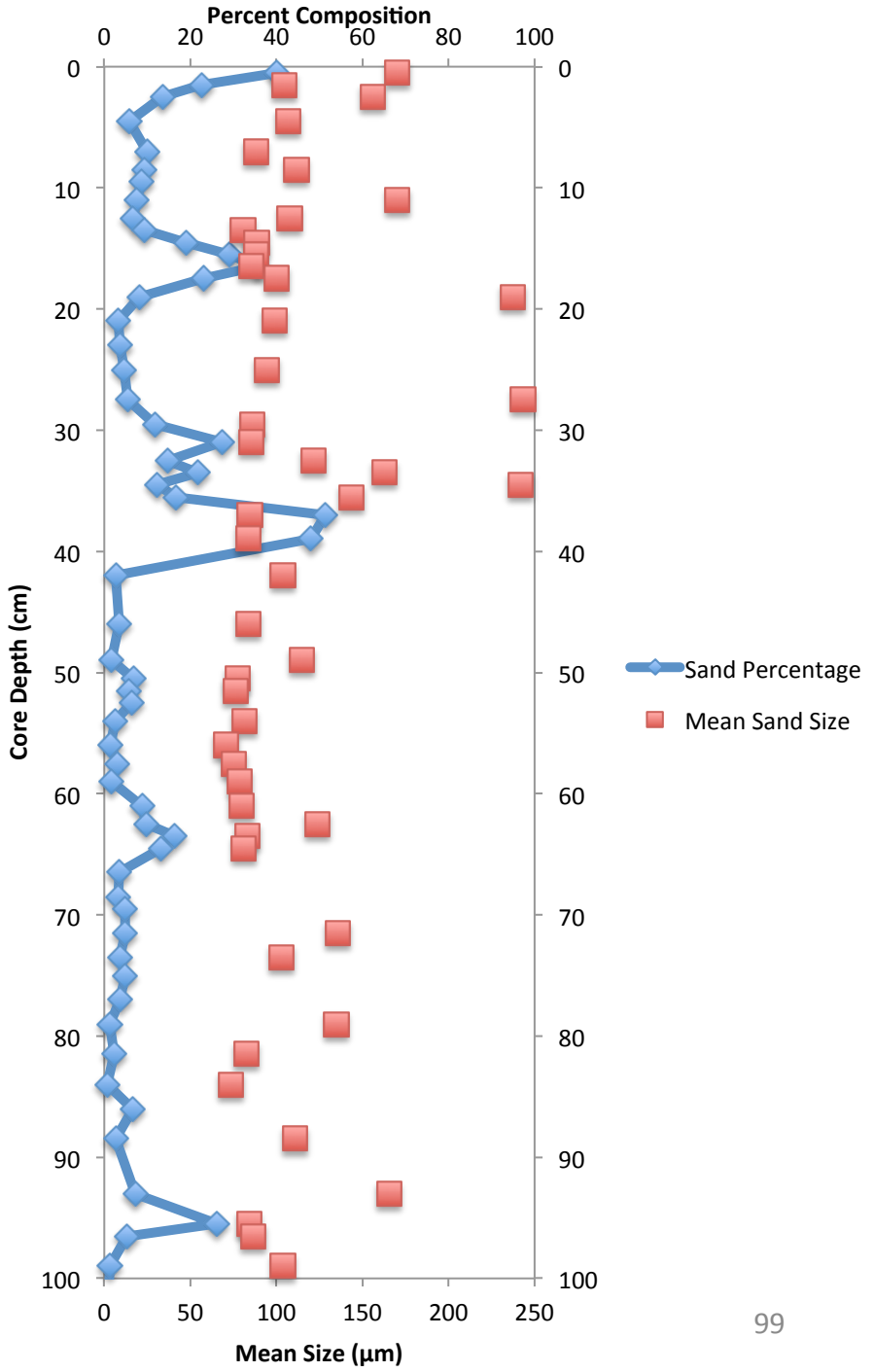

Project:_Brazos Delta Fall 2011___ Core: _BDVC34B_____

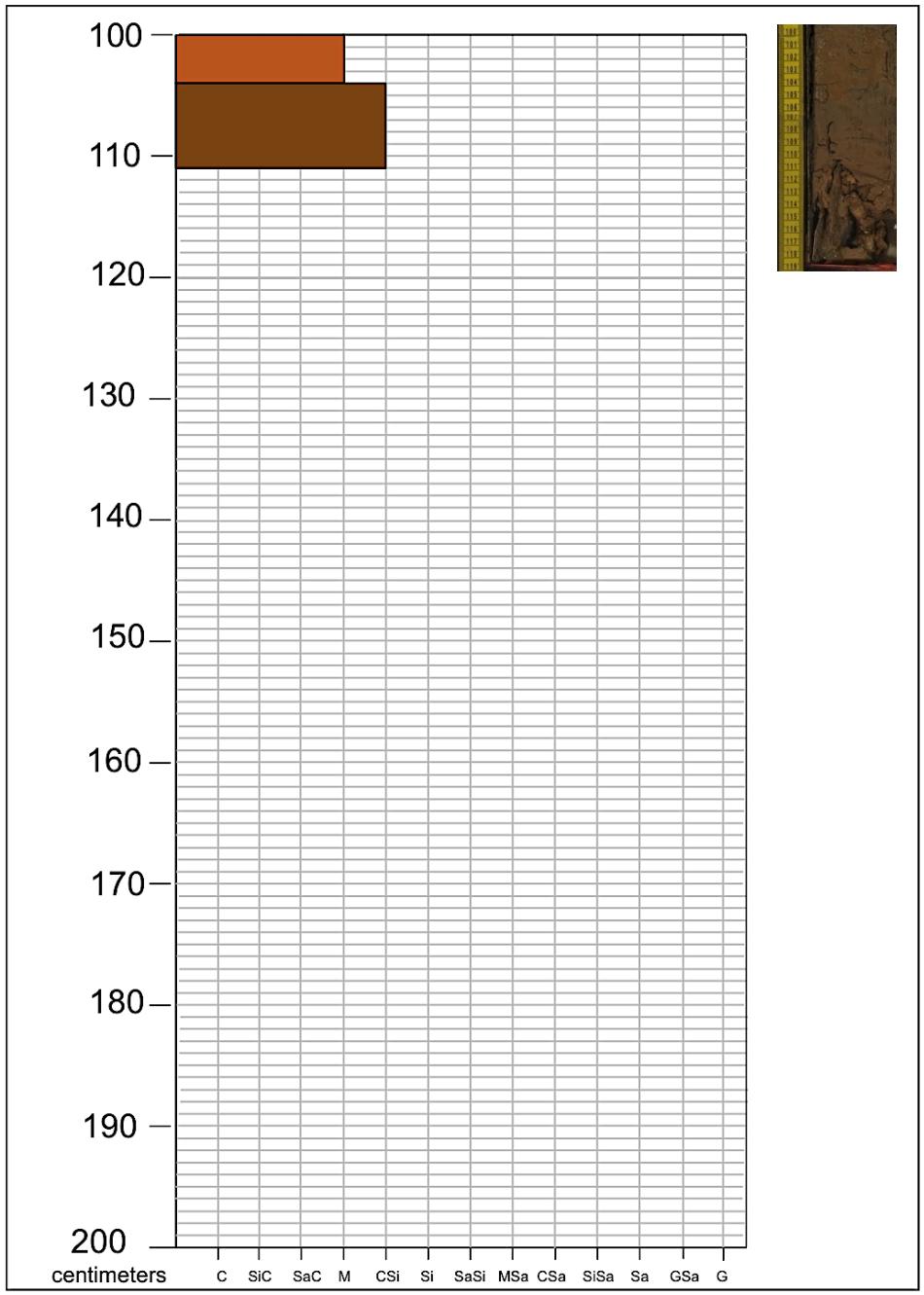

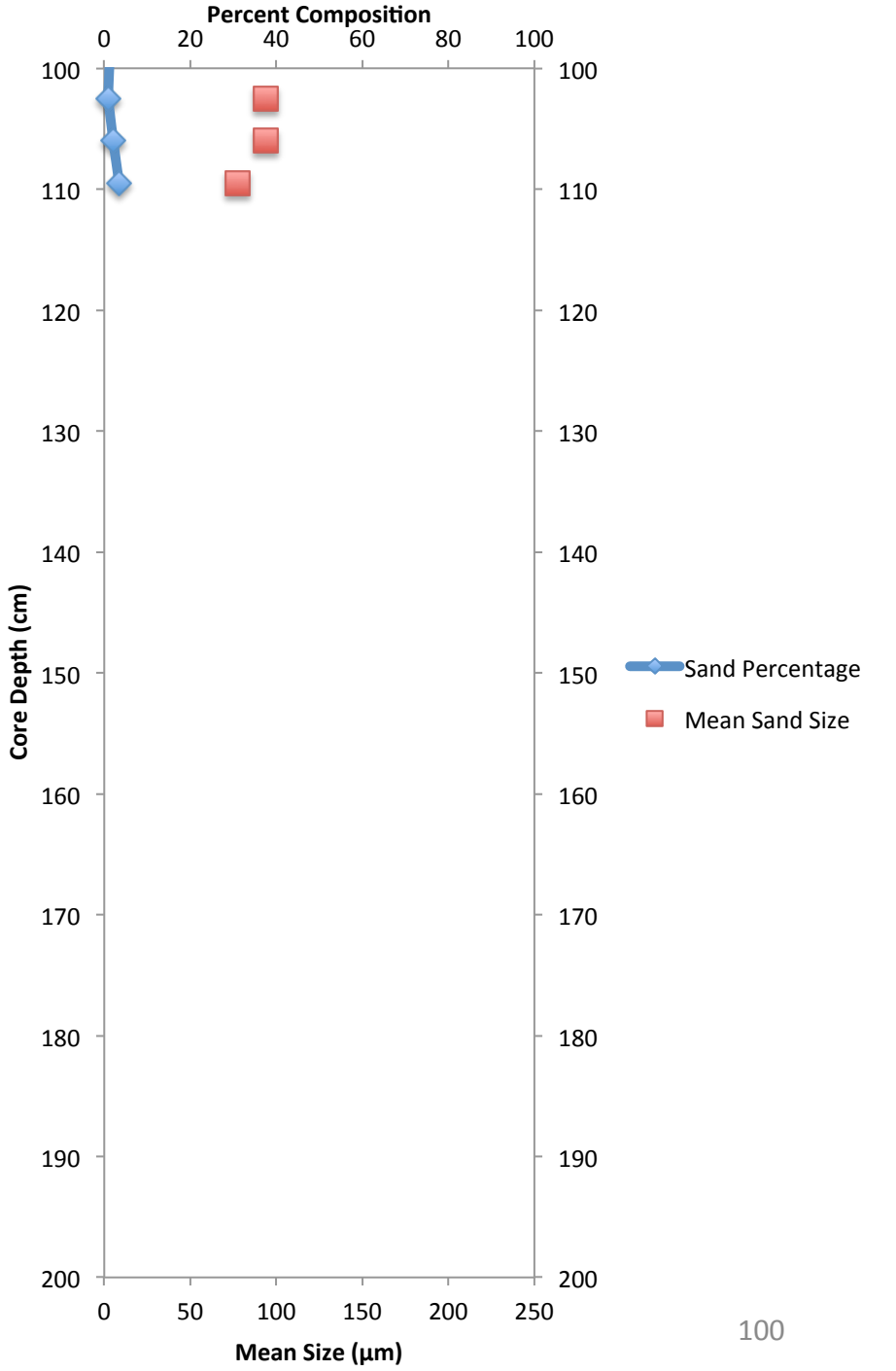

Brazos Delta Core: BDVC35

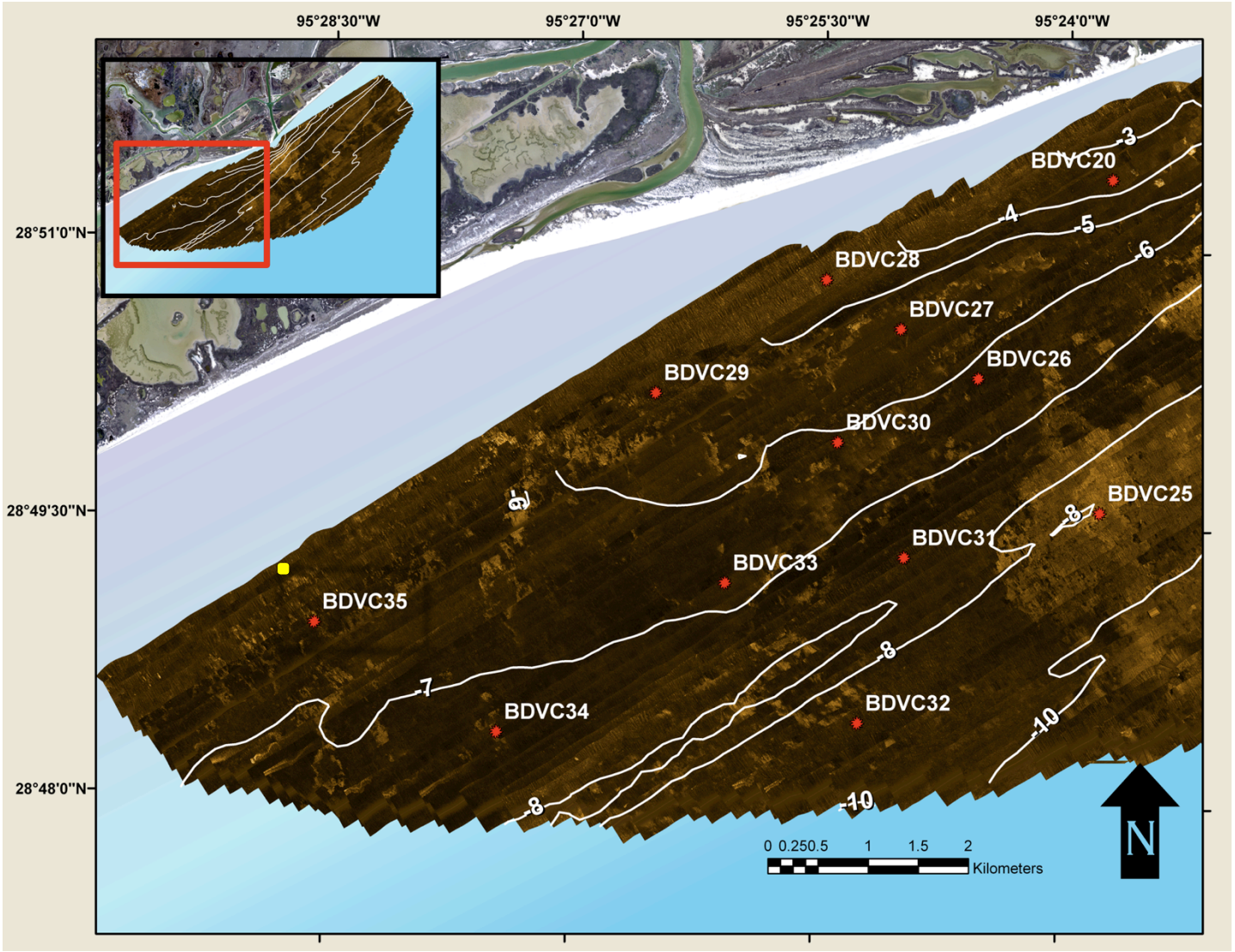

Project:_Brazos Delta Fall 2011___ Core: _BDVC35_____